

Award Number: W81XWH-11-1-0573

TITLE: Chemical Genetic Screens for TDP-43 Modifiers and ALS Drug Discovery

PRINCIPAL INVESTIGATOR: Pierre Drapeau

CONTRACTING ORGANIZATION: University of Montreal
Montreal, Canada H3C 3J7

REPORT DATE: March 2015

TYPE OF REPORT: Final

PREPARED FOR: U.S. Army Medical Research and Materiel Command
Fort Detrick, Maryland 21702-5012

DISTRIBUTION STATEMENT: Approved for Public Release;
Distribution Unlimited

The views, opinions and/or findings contained in this report are those of the author(s) and should not be construed as an official Department of the Army position, policy or decision unless so designated by other documentation.

REPORT DOCUMENTATION PAGE				Form Approved OMB No. 0704-0188	
Public reporting burden for this collection of information is estimated to average 1 hour per response, including the time for reviewing instructions, searching existing data sources, gathering and maintaining the data needed, and completing and reviewing this collection of information. Send comments regarding this burden estimate or any other aspect of this collection of information, including suggestions for reducing this burden to Department of Defense, Washington Headquarters Services, Directorate for Information Operations and Reports (0704-0188), 1215 Jefferson Davis Highway, Suite 1204, Arlington, VA 22202-4302. Respondents should be aware that notwithstanding any other provision of law, no person shall be subject to any penalty for failing to comply with a collection of information if it does not display a currently valid OMB control number. PLEASE DO NOT RETURN YOUR FORM TO THE ABOVE ADDRESS.					
1. REPORT DATE March 2015		2. REPORT TYPE Final		3. DATES COVERED 15 Sep 2011 – 31 Dec 2014	
4. TITLE AND SUBTITLE Chemical Genetic Screens for TDP-43 Modifiers and ALS Drug Discovery				5a. CONTRACT NUMBER W81XWH-11-1-0573	
				5b. GRANT NUMBER	
				5c. PROGRAM ELEMENT NUMBER	
6. AUTHOR(S) Pierre Drapeau, Alexandre Parker, Edor Kabashi, Jean-Pierre Julien email : p.drapeau@umontreal.ca				5d. PROJECT NUMBER	
				5e. TASK NUMBER	
				5f. WORK UNIT NUMBER	
7. PERFORMING ORGANIZATION NAME(S) AND ADDRESS(ES) Universite de Montreal, L' 2900 Boul. Edouard-Montpetit Montreal H3T 1J4				8. PERFORMING ORGANIZATION REPORT NUMBER	
9. SPONSORING / MONITORING AGENCY NAME(S) AND ADDRESS(ES) U.S. Army Medical Research and Materiel Command Fort Detrick, Maryland 21702-5012				10. SPONSOR/MONITOR'S ACRONYM(S)	
				11. SPONSOR/MONITOR'S REPORT NUMBER(S)	
12. DISTRIBUTION / AVAILABILITY STATEMENT Approved for Public Release; Distribution Unlimited					
13. SUPPLEMENTARY NOTES					
14. ABSTRACT Our objective was to screen libraries of several thousand compounds, including clinically approved drugs, for their ability to suppress the <i>in vivo</i> phenotypes observed in worm and fish models expressing mutant human TDP-43 related to ALS and validating hits in a mouse model. Our hypothesis was that chemical modifiers of TDP-43 <i>in vivo</i> function would provide new therapeutic approaches to ALS. Our screen of 3,750 FDA-approved compounds identified 20 active compounds, most of which were neuroleptics with the most potent being pimozide, as well as WithaferinA. In addition to the 4k FDA compounds, we screened 2k molecules that are structurally related to the neuroleptics as well as novel molecules. Also, we screened 4k novel derivatives of pimozide and identified several dozen active compounds. WithaferinA and pimozide were tested in TDP-43 and SOD1 mice. Results suggest that the beneficial effect of Withaferin A in mutant SOD1 mice may be due in part to an upregulation of heat shock proteins (Hsp27 and Hsp70) and to reduction in levels of misfolded SOD1 species. Motor behaviors were not significantly improved or possibly worsened by chronic treatment with pimozide. In addition, the spinal cord and brain of mice revealed and increase in TDP-43 aggregation, but no change in microgliosis, was noted. Neuromuscular transmission was improved acutely. Pimozide is being tested in an ALS clinical trial based on our neuromuscular biomarker.					
15. SUBJECT TERMS TDP-43, C. elegans, zebrafish, mice, motility screens, chemical libraries					
16. SECURITY CLASSIFICATION OF:			17. LIMITATION OF ABSTRACT Unclassified	18. NUMBER OF PAGES 93	19a. NAME OF RESPONSIBLE PERSON USAMRMC
a. REPORT Unclassified	b. ABSTRACT Unclassified	c. THIS PAGE Unclassified			19b. TELEPHONE NUMBER (include area code)

TABLE OF CONTENTS

	<u>Page</u>
Introduction.....	2
Body.....	2
Key Research Accomplishments.....	8
Reportable Outcomes.....	9
Conclusion.....	17
References.....	18
Appendices: 1- Vaccaro et al. (2012) PLoS One 7(2): e31321	19
2- Vaccaro et al. (2012) PLoS One 7(7): e42117	
3- Vaccaro et al. (2013) Neurobiol. Dis. 55:64-75.	
4- Audet JN et al. (2012) Neuroscience. 209:136-43	
5- Tauffenberger et al. (2013) Neurobiology of Aging. 9:2175-82.	
6- Therrien et al. (2014) Frontiers in Genetics, Apr 17;5:85	
7- Aggad et al. (2014) Journal of Neuroscience. 34(36): 12093-12103	

INTRODUCTION

Our project was to screen libraries of small chemicals, including clinically approved drugs, for their ability to suppress the pathogenic motor phenotypes in three unique *in vivo* genetic models of ALS that we had generated. Our functionally validated models are worms (*C. elegans*)^{1,2}, zebrafish (*D. rerio*)^{3,4}, and mice (*M. musculus*)⁵ expressing ALS-related mutations of the human *TARDBP* gene coding for TDP-43, a recently discovered major contributing factor in familial ALS and a major component of inclusions in many neurodegenerative diseases. We hypothesized that chemical genetic modifiers of TDP-43 *in vivo* function would provide new therapeutic approaches to ALS^{6,7}.

BODY

Study design.

Our department operates a platform for integrated robotic plating of libraries of small chemicals. We screened worms and fish expressing mutant human TDP-43 by video microscopy for the effects of these compounds on recovery of motility or survival and re-test hits for dose and time dependence and then test promising confirmed hits in mice.

We had the following specific aims according to our SOW:

Timeline	Year 1				Year 2				Year 3			
	Q1	2	3	4	Q1	2	3	4	Q1	2	3	4
Aim 1: Set-up motility assays for worms and fish												
1A) Semi-automated measurement of spontaneous activity in TDP-43 worms.												
1B) Semi-automated measurement of the motor response in TDP-43 zebrafish.												
Aim 2: Screen TDP-43 worms and zebrafish for restoration of motility with 3k+ approved compounds												
Aim 3: Screen TDP-43 worms and zebrafish for restoration of motility with 10k+ compounds												
Aim 4: Rescreen TDP-43 worms and zebrafish for specificity and potency of active compounds												
Aim 5: Screen TDP-43 worms and zebrafish for restoration of motility with \pm 10k other compounds												
Aim 6: Screen active compounds in TDP-43 mice.												

The screen set-up (Aims 1A,B) began immediately and proceed in parallel for worms and fish during the first 6 months (Y1Q1-Q2). This consisted of automating and quantifying the video microscopy screens for motility.

The first chemical screen (approved compounds, Aim 2) began immediately afterwards and was completed by the end of year 1 (Y1Q3-Q4).

The screen of representative molecules from the larger libraries (Aim 3) began in and required all of year 2 (Y2Q1-Q4).

As hits were identified during Y1Q3-Y2Q4, the active compounds were rescreened (Aim 4, Y1Q4-Y3Q1). Those that were confirmed were tested in our mouse model (Aim 6, Y2).

Finally, all members of the families of confirmed (rescreened) active compounds (Aim 5) were screened in worms and fish (Y3 Q1-Q4) and tested in mice (Aim 6, Y3).

AIM 1.

Previous screens with worms took two weeks to perform as that is the period it takes for them to develop adult-onset phenotypes such as for TDP-43 when grown on a solid substrate. We found a similar result for worms expressing human TDP-43 (see appendix 1¹, Figure 3) from a motoneuron promoter (see appendix 1¹, Figure 1). Further we found that by growing the worms in liquid suspension this accelerated the onset of the phenotype such that by 6 hours it was apparent (see appendix 1¹, Figure 10). This transformed our screening protocol as it permitted screening within the same working day and made it possible for one person to screen several hundred molecules per week. We also used our established transient zebrafish model^{4,8} to retest hits from the worm screen.

In preliminary tests we had found that methylene blue⁹ was effective in protecting against the TDP-43 phenotype in both worms (see appendix 2², Figure 1B&2A) and fish (see appendix 2², Figure 3) by protecting against cellular stress (see appendix 2², Figure 6). This compound was used as a positive control for setting up the larger screens and with structural analogs, was shown to promote the protective ER stress response¹².

AIM 2.

In year 1 we screened 3,750 clinically approved compounds in the Biomol Natural Products, Microsource Discovery Spectrum, Prestwick Commercial Products and Sigma Lopac sets at a concentration of 20 μ M. We identified 22 compounds (see Table 1), but 8 were excluded as being irrelevant (insecticides, tumour drugs – in blue in table 1).

We also tested ER stress compounds on longevity in *C. elegans* (see appendix 3¹³). The 13 neuroleptics were retested and confirmed in worms and zebrafish at concentrations ranging from 2-100 μ M. Almost all of the confirmed hits (in black, Table 1) were neuroleptics, the most potent of which was **pimozide**, acting at 0.5 μ M in zebrafish. We also found **withaferin A** to be a potent compound in our *C. elegans* assay.

AIM 3.

Our platform chemists examined the available libraries of nearly 100k novel compounds (Chembridge DriverSet, 60k molecules; Maybridge HitFinder, 16k; SPECS Selection, 16k) for structural homologs of the 13 neuroleptics identified in our first (FDA) screen of 3,750 FDA-approved compounds, including pimozide. They identified several dozen compounds present on plates containing a total of 1806 molecules. In year 2 we screened all 1806 molecules and identified 15 hits (see Table 2). As none of these were predicted structural homologs of the neuroleptics, they represent novel molecules that will require further characterization.

Given that pimozide proved to be the neuroleptic of highest potency in our assays, we learnt that Zalicus Pharmaceuticals Ltd. (Cambridge, MA) had prepared pimozide derivatives for testing in other disease models. With approval from the DoD, we entered into agreement with Zalicus for the testing of 3,658 pimozide derivatives in our ALS models. All 3,658 compounds were screened at 20 μ M in worms in years 2&3 and 24 hits were obtained.

Together, our screening of nearly four thousand FDA-approved molecules, close to two thousand novel compounds and about four thousand pimozide derivatives reached the goal of screening 10k molecules.

AIM 4.

In year 3 we rescreened the hits, including novel derivatives, for dose-response at 0.1-100 μ M in our worm and zebrafish models, though none appeared more potent than pimozide. We also tested paired combinations for 9 of the neuroleptics. All combinations were active at at least 5 μ M though some were deleterious at higher concentrations.

AIM 5.

As we had identified several interesting lead compounds, rather than screening 10k more novel molecules in year 3 we did more detailed phenotyping of our models in order to identify potential targets and biomarkers for the effects of neuroleptics and derivatives. Pimozide was initially designed as a dopamine antagonist but is now recognized to act also on calcium channels. In a neurophysiological analysis of mutant TDP zebrafish, we showed that calcium agonists could protect against development of the motor phenotype¹¹. We therefore hypothesized that pimozide may be acting in a similar manner to stabilise neuromuscular function. In preliminary work we indeed observed a decrement in neuromuscular transmission that was restored by pimozide, which reduced low-voltage-activated calcium currents.

This result provided a novel biomarker, the decremental response to repetitive nerve-muscle stimulation, and it is being used to test for the restorative effects of pimozide in an ALS clinical trial (see below) recently funded by collaborators as an offshoot of our project. The trial is underway and we are waiting for the results later this year before writing up our findings, including the results of the drug screen.

AIM 6.

The Julien lab generated transgenic mice with moderate and ubiquitous expression of TDP-43 species to mimic the human ALS disease. This was accomplished by generating transgenic mice harbouring an 18 kb genomic fragment coding for human *TARDBP*^{WT}, *TARDBP*^{A315T} or *TARDBP*^{G348C}. In year 1, the Julien lab tested methylene blue, our positive control for the drug screening, in their mutant TDP-43 mice¹⁰ (appendix 4).

Julien's lab reported previously that withaferin A, an inhibitor of NF- κ B activation, conferred beneficial effects in transgenic mice overexpressing WT TARDBP, a model of ALS, by reduction of inflammation and amelioration of motor impairment¹⁶. Recently, he further tested this compound in three other mouse models of ALS, transgenic mice expressing either *TARDBP*^{G348C} mice, *SOD1*^{G93A} or *SOD1*^{G37R}. Intraperitoneal injection of *TARDBP*^{G348C} mice with withaferin A (4mg/kg) twice a week starting at 30 weeks of age led to amelioration of motor dysfunction within 10 weeks of treatment (Fig.1, Appendix 4). Moreover, injection of withaferin A starting at P40 extended survival of *SOD1*^{G93A} and *SOD1*^{G37R} familial mice model of ALS (Fig. 2). His team examined the effect of withaferin A when intraperitoneally injected into the *SOD1*^{G93A} mice twice a week from the postnatal day 40 until death at a dose of 4 mg/kg body and into *SOD1*^{G37R} mice injected twice a week with the same dose starting at 9 months of age. Withaferin A treatment increased survival of *SOD1*^{G93A} by 8 days from 145 days (n=15) to 153 days (n=16, P<0.05) whereas this compound increased survival of *SOD1*^{G37R} mice by 18 days from 379 days (n=8) in controls to 397 days (n=8) in withaferin-treated mice, P<0.0001. Results suggest that the beneficial effect of Withaferin A in mutant *SOD1* mice may be due in part to an upregulation of heat shock proteins (Hsp27 and Hsp70) and to reduction in levels of misfolded *SOD1* species (Fig. 3). A manuscript describing these results is in preparation.

In the original plan, Julien was to test pimozide in adult *TARDBP*^{G348C} mice in year 2. However, this project was delayed due to the move of Julien's laboratory to a new institute (of the same university) during the spring of 2013. The *TARDBP*^{G348C} mice were re-derived into a new pathogen-free animal facility and a cohort of these mice at 8 months of age became available at the beginning of 2014. The *TARDBP*^{G348C} and *SOD1*^{G93A} mice were subjected to daily intraperitoneal injection of pimozide at 1mg/kg or saline for a period of two months, as described previously^{14,15}. The mice were subjected to learning tests (passive avoidance and Barnes maze) and a rotorod test before and after drug treatment as described¹⁶. These behaviors were not significantly improved or possibly worsened by pimozide. In addition, the spinal cord and brain of mice were analyzed for the effects of the drugs on pathological features (neuroinflammation, cytoplasmic ubiquitinated TDP-43 aggregates) and biochemical hallmarks (25 kd C-terminal cleavage fragment). An increase in TDP-43 aggregation, but no change in microgliosis, was noted. A manuscript describing these results is in preparation.

Parallel and future developments.

In parallel with the DoD project, we initiated two (now independently-funded) collaborations to help with our progress. In the first, Dr. Richard Robitaille of the Univ. Montreal, an expert on mouse neuromuscular transmission, has been testing the effects of pimozide on a mouse model of *SOD1*-related ALS. He determined synaptic strength of NMJs in the extensor-digitorum-lungus (EDL) nerve-muscle preparation in *SOD1*^{G37R} mice by measuring paired-pulse facilitation (PPF) and quantal content of each NMJ using a low Ca²⁺/high Mg²⁺ Ringer solution. Synaptic transmission was elicited by motor nerve stimulation using a suction electrode filled with extracellular saline and intracellular recordings of endplate potentials (EPPs) were performed using glass microelectrodes. Preliminary data reveal that the quantal content at *SOD1*^{G37R} mice was altered compared to wild type littermates while the frequency of miniature endplate potentials (mEPPs) was not different. Upon bath application of pimozide, the amplitude of the EPP doubled while the amplitude of the mEPP remained unaffected. As a whole and consistent with our data obtained using the zebrafish preparation in a TDP-43 background, these data indicate that the pimozide increased transmitter release at NMJs of a mammalian ALS model in an *SOD1* mutation background. We have provided Dr. Robitaille with our *TARDBP*^{G348C} mice so that he may test the effectiveness of pimozide in this model that is more closely related to our simpler screening models.

In addition, we have initiated a clinical collaboration with Dr. Lawrence Korngut, Director of the ALS Clinic at the Univ. Calgary and Director of the Canadian Neuromuscular Disease Registry. ALS patients show dysfunctional neuromuscular activity that can be easily assessed using repetitive nerve stimulation that reveals decremental responses of the trapezius as a novel biomarker. Given that pimozide is FDA-approved, Dr. Korngut has initiated a human pilot study in his clinic in Calgary that could potentially be expanded to his national network in Canada (Health Canada PIMOZIDE_ALS-001: *A registry-based randomized-controlled, double-blinded clinical trial of pimozide in patients with neuromuscular junction transmission dysfunction due to amyotrophic lateral sclerosis*). Discussion is underway to test withaferin A as well.

Table 1. Summary of FDA-approved compounds with hits in *C. elegans*.

Legend. Each compound was first tested at 20 μ M. Those showing restoration of motility in worms were retested in both worms and fish (**in black**), then once validated retested at 2,5, 5, 10, 20, 50 and 100 μ M. The most potent was pimozide, active at 0.5 μ M in zebrafish.

Source plate	Pick plate	Source well	Name / Action	
CCC0327CP1	P00017066	B010	Mianserine HCl	antidepressant/DA
CCC0327CP1	P00017066	C003	Amoxapine	antidep/tetracyclic/DA reuptake block
CCC0327CP1	P00017066	C004	Cyproheptadine HCl	antihistamine/5HT rec antag
CCC0327CP1	P00017066	G008	Nicergoline	senile dementia/vascular/alpha-1A adrenergic receptor antagonist
CCC0328CP1	P00017067	E008	Kawain	anticonvulsant/anxiolytic/many systems
CCC0329CP1	P00017068	F005	Pimethixene maleate	antihistamine/anxiety
CCC0329CP1	P00017068	G009	Pimozide	antipsychotic/Tourette/D2
CCC0330CP1	P00017069	B011	Flupentixol dihydrochloride cis-(Z)	antipsychotic/schizo/antidep/DA, 5-HT
CCC0330CP1	P00017069	C009	Chlorprothixene hydrochloride	antipsychotic/5HT, DA
CCC0330CP1	P00017069	C011	Clozapine	antipsychotic/5HT, DA
CCC0330CP1	P00017069	F006	Methiothepin maleate	antipsychotic/5HT, DA
CCC0346CP1	P00017085	G008	Chlorprothixene hydrochloride	antipsychotic/5HT, DA
CCC0352CP1	P00017091	E006	(\pm)-Octoclotheptin maleate	neuroleptic/many systems
			withaferin A	inhibitor of NF-kB
		H007	Ivermectin (Insecticide)	Glu (Cl)/GABAR
		F009	Fenbufen	inflammation, prostaglandins
		A003	Flavoxate hydrochloride	anticholinergic/bladder
		F009	Melatonin	diurnal/mito, DNA protection/natural
		F010	Menadione	Vit K/cancer/EGFR
		B011	Avermectin B1 (Insecticide)	insecticide, antihelmintic
		C011	hypericin	antibiotic/kinases /DA B-hydroxylase
		D007	deoxyphorbol	antitumour
		D011	mezeirein	antitumour/phorbol
		F003	genistein	antihelmintic/natural

Table 2. Novel compounds with hits.

Legend. Structural homologs of the neuroleptics (Table 1) were tested in worms at 20 μ M, along with novel compounds present on the same plates.

1. 4-bromo-N-[2,2,2-trichloro-1-(1-piperidiny)ethyl]benzamide;
2. 4-(4-methoxyphenyl)-1,6-dimethyl-5-nitro-3,4-dihydro-2(1H)-pyrimidinone
3. 2-(2-oxopropyl)phenyl 3-nitrobenzoate
4. 1-(phenylsulfonyl)cyclopropanecarboxylic acid
5. 4-bromobenzaldehyde O-(2-methylbenzoyl)oxime
6. N-(1-propylcyclohexyl)acrylamide
7. 2-hexyl-1-cyclopentanone semicarbazone
8. 3-nitro-N'-(1-phenylbutylidene)benzohydrazide
9. 2-(3,4-dimethoxyphenyl)-N-(2-phenylethyl)-4-quinolinecarboxamide
10. N-(4-chlorobenzyl)-3-(2,6-dichlorophenyl)-5-methyl-4-isoxazolecarboxamide
11. N-[2-chloro-5-(trifluoromethyl)phenyl]-3-(4-methoxyphenyl)propanamide
12. 3-([4-(4-bromophenyl)-1,3-thiazol-2-yl]amino)carbonylbicyclo[2.2.1]heptane-2-carboxylic acid;t
13. 4-(4-fluorophenyl)-3,4,5,6-tetrahydrobenzo[h]quinazoline-2(1H)-thione
14. 7-acetyl-3-(allylsulfanyl)-6-(4-ethoxy-3-methoxyphenyl)-6,7-dihydro[1,2,4]triazino[5,6-d][3,1]benzoxazepine
15. 4-(3-methylphenyl)-1'-phenyl-spiro[4-azatricyclo[5.2.1.0~2,6~]dec[8]ene-10,2'-cyclopropane]-3,5-dione

KEY RESEARCH ACCOMPLISHMENTS

- Validation of 13 neuroleptics in TDP-43 worms and zebrafish.
- Identification and validation of pimozide as the most potent compound.
- Screening of 1,806 new molecules, including some structurally-related to neuroleptics, with identification of 15 novel hits.
- Screening of 3,658 derivatives of pimozide and identification of 24 hits (for a total of nearly 10k molecules screened).
- Withaferin A testing in *TARDBP*^{G348C} mice, *SOD1*^{G93A} mice and *SOD1*^{G37R} mice revealed protective effects.
- Derivation and generation of *TARDBP*^{G348C} mouse cohort in a pathogen-free mouse facility. Pimozide testing in 8 months old mice revealed increased NMJ transmission when applied acutely but no motor behavior restoration and an increase in insoluble TDP-43 in the spinal cord when treated chronically (two months).
- New (parallel) collaborations on pimozide and neuromuscular function in mice and ALS patients, including a new biomarker (decremental response to repetitive nerve-muscle stimulation) being assessed, together with the effectiveness of pimozide, in an on-going ALS clinical trial.

REPORTABLE OUTCOMES

Manuscripts (see appendix).

Vaccaro et al. (2012) PLoS One 7(2): e31321

Vaccaro et al. (2012) PLoS One 7(7): e42117

Audet JN et al. (2012) Neuroscience. 209:136-43

Vaccaro et al. (2013) Neurobiol. Dis. 55:64-75.

Tauffenberger et al. (2013) Neurobiology of Aging. 9:2175-82

Therrien et al. (2014) Frontiers in Genetics, Apr 17;5:85

Aggad et al. (2014) Journal of Neuroscience. 34(36): 12093-12103

Abstracts.

Vaccaro A, Kabashi E, Patten K, Aggad D, Drapeau P, Parker JA, Drug Discovery for ALS, ALS Association USA, 2012, Washington, DC, USA.

Vaccaro A, Kabashi E, Patten K, Aggad D, Drapeau P, Parker JA. Chemical genetic screens for in vivo TDP-43 modifiers and ALS drug discovery. 22nd International symposium on ALS/MND, 2011. Sydney, Australia

Vaccaro A, Tauffenberger A, Parker JA. Development of *C. elegans* models for ALS. 22nd International symposium on ALS/MND, 2011. Sydney, Australia

Vaccaro A, Tauffenberger A, Parker JA. *C. elegans* models for ALS. International *C. elegans* Meeting 2011, University of California at Los Angeles, Los Angeles, California.

Patten SA, Vaccaro A, Kabashi E, Parker JA, Drapeau P. Pharmacological reduction of ER stress protects against TDP-43 neuronal toxicity in vivo. Society for Neuroscience, New Orleans, LO (2012)

Vaccaro A, Patten SA, Ciura S, Maios C, Therrien M, Drapeau P, Kabashi E, Parker JA. Methylene blue protects against TDP-43 and FUS neuronal toxicity in *C. elegans* and *D. rerio*. Pathology and Cellular Biology Department, University of Montreal, QC (2012)

P. Drapeau and A. Parker Chemical genetic screens of TARDBP and FUS modifiers in *C. elegans* and zebrafish. Alzheimer's Disease meeting, Cancun, Mexico (2012)

P. Drapeau and A. Parker Chemical genetic screens of TARDBP and FUS modifiers in *C. elegans* and zebrafish. Keystone Conference 'New Frontiers in Neurodegenerative Disease Research', Santa Fe NM (2013)

Patten SA, Vaccaro A, Aggad D, Maios C, Kabashi E, Parker JA, Drapeau P. Chemical genetic screens of TARDBP modifiers in *C. elegans* and zebrafish. 8th European Zebrafish meeting, Barcelona, Spain (2013)

Patten SA, Vaccaro A, Aggad D, Kabashi E, Parker JA, Drapeau P. Chemical genetic screens of TARDBP modifiers in *C. elegans* and zebrafish.. Canada Association for Neuroscience, Toronto, ON (2013)

Patten SA, Vaccaro A, Aggad D, Drapeau P, Kabashi E, Parker JA, Drapeau P. Chemical genetic screens of TARDBP modifiers in *C. elegans* and zebrafish. ALS Canada, Toronto, ON (2013)

Patel P, Swarup V, Phaneuf D, Kriz J, Julien J-P. Neuroprotective effects of Withaferin A in three mouse models of amyotrophic lateral sclerosis. The XI European meeting on Glial cell function, Berlin, Germany (2013).

Comparison of zebrafish models of ALS. Alexandra Lissouba, Gary Armstrong and Pierre Drapeau. 8th European zebrafish meeting (9-13 July 2013)

Comparison of gene expression patterns between different genetic models of ALS. Alexandra Lissouba, Gary Armstrong and Pierre Drapeau. 2014 Canadian zebrafish conference (16-17 March 2014)

Comparisons of different models of ALS using zebrafish. Alexandra Lissouba, Gary Armstrong, Kessen Patten, Edor Kabashi, Nathalie Champagne, and Pierre Drapeau. 25th international symposium on ALS/MND (5-7 December 2014)

Patten SA, Vaccaro A, Drapeau P, Kabashi E, Parker JA. Chemical genetic screens of TARDBP modifiers in *C. elegans* and zebrafish. 1th, Zebrafish Translational medicine conference, Toronto, Canada (2013)

Armstrong, G.A.B. and Drapeau, P. Aberrant glutamatergic synaptic connectivity with motoneurons in the spinal cord of zebrafish expressing mutant human TARDBP (TDP-43) with a mutation causing ALS and FTL. *Proceedings from the 8th Annual Canadian Neuroscience*. (2014).

Armstrong, G.A.B. and Drapeau, P. Synaptic transmission in a genetic model of ALS. 1st *Zebrafish for Personalized/Precision Medicine Conference program book*. (2013).

Armstrong, G.A.B. and Drapeau, P. Loss and gain of FUS function impair neuromuscular synaptic transmission in a genetic model of ALS. *Symposium sur SLA de la Fondation André-Delambre Programme livre*. P3 (2013).

Armstrong, G.A.B. and Drapeau, P. Loss and gain of FUS function impair neuromuscular synaptic transmission in a genetic model of ALS. *European Zebrafish Abstracts book*. P122 (2013)

Armstrong, G.A.B. and Drapeau, P. Defective synaptic transmission at the NMJ in a zebrafish model of the FUS gene in ALS. *Proceedings from the 7th Annual Canadian Neuroscience*. 1-C-98 (2013).

Presentations.

P. Drapeau

2012

- Israel-Canada Workshop in Medical Neuroscience, Jerusalem, Israel
- Brain Research Centre, UBC, Vancouver, CA
- Session on Clinical Research and Practice, ALS Canada, Toronto, ON
- Session speaker, first joint Canadian Human Genetics Conference and Canadian Genetic Epidemiology and Statistical Genetics Meeting, Niagara-on-the-Lake, ON.
- Neuroscience program, Queen's U., Kingston, ON
- Neuroscience Axis, Research Institute of the Univ. Montreal Hospital Centre, Montréal
- Motor Neuron Center, Columbia University, New York, NY
- Centre de recherche de l'Institut en santé mentale de Québec, Québec
- 8th Annual Symposium on ALS of the Fondation André-Delambre, Quebec
- Keynote speaker, 52nd Annual Meeting of the Canadian Association of Neuropathologists, Mt-Tremblant, Qc

2013

- Keystone Conference 'New Frontiers in Neurodegenerative Disease Research', Santa Fe, NM.
- Brain and Mind Institute, Univ. Sydney, AUS
- Concord Hospital/ANZAC Research, Institute, Sydney, AUS
- Motoneuron Disease Group, Australian School of Advanced Medicine, Macquarie U., Sydney, AUS
- Département des sciences biologiques et Centre de recherche BioMed, UQAM
- Zebrafish Functional Genomics Conference, St. Michael's Hospital, Toronto, ON
- France-Québec ALS/MS conference, Montréal, Qc
- Institut Fessard, Gif-sur-Yvette, France
- Institut du cerveau et de la moelle (ICM), Paris, FR
- Institut Curie, Paris, FR

2014

- Killam Research Seminar, Montreal Neurological Institute, McGill University
- 2nd Quebec-France ALS/FTD Workshop, Montreal Neurological Institute, McGill Univ.
- 10th ALS Canada meeting, Toronto, ON
- Gordon Research Conference, Neural Development: From Stem Cells to Circuits, Newport, RI, USA
- 10th Annual Symposium on ALS, Fondation André-Delambre, MNI, Montréal
- Conférence CRCHUM, Montréal
- Institut de Neurobiologie de la Méditerranée, Université de la Méditerranée, Marseille, FR
- 2nd France-Québec ALS/MS Conference, Montpellier, FR
- Keenan Research Centre, Li Ka Shing Knowledge Institute, St. Michael's Hospital, Toronto, ON

2015

- 11th Annual Bellairs Research Workshop in "Systems Biology and Neuroscience", Bellairs, Barbados
- Pharmacology Dept., Univ. Vermont, Burlington, VT

E. Kabashi

- Breakthroughs in Motor Neuron Diseases (2013) Strasbourg France.
- Institute of Neuroscience, Montpellier, France
- Annual meeting of Packard Center at Johns Hopkins. Baltimore, 2013.
- 2nd Quebec-France ALS/FTD Workshop, MNI, McGill Univ. 2014
- Institute of Genetics and Molecular and Cellular Biology Strasbourg, France
- Annual meeting of Packard Center at Johns Hopkins. Baltimore, 2014.
- Annual meeting of Packard Center at Johns Hopkins. Baltimore, February 2015.

JA. Parker

2012

- Chemical genetic screens for *in vivo* TDP-43 and FUS modifiers in *C. elegans*. ALS/MND Meeting, Chicago, December, 2012.
- Amyotrophic Lateral Sclerosis: Two *in vivo* screening platforms and service offer. BioTransfert, Montreal, May, 2012
- Chemical genetic screens for *in vivo* TDP-43 and FUS modifiers in *C. elegans*. ALS Society of Canada's Eighth Annual ALS Research Forum, May, 2012
- High throughput *in vivo* drug screening in *C. elegans*. ALS Canada, Bench 2 Bedside, Université de Montréal (host: D. Figlewicz) January, 2012
- Development of TDP-43 and FUS motor neuron toxicity models in *C. elegans*. ICM, Paris, France (host: E. Kabashi) January, 2012

2013

- Worming forward: Amyotrophic lateral sclerosis toxicity mechanisms and drug discovery in *C. elegans*. Ninth Annual ALS Canada Research Forum, Toronto, May, 2013.
- Worming forward: Amyotrophic lateral sclerosis toxicity mechanisms and drug discovery in *C. elegans*. McGill Centre for Research in Neuroscience Seminar Series, Montreal, January, 2013.
- Chemical genetic screens for *in vivo* TDP-43 and FUS modifiers in *C. elegans*. 23rd International Symposium on ALS/MND, Chicago, December, 2013.
- Les « vers », vers le traitement des maladies neurodégénératives. Association canadienne-française pour l'avancement des sciences, Quebec City, May 2013
- Worming forward: Amyotrophic lateral sclerosis toxicity mechanisms and drug discovery in *C. elegans*. Ninth Annual ALS Canada Research Forum, Toronto, May, 2013.
- Worming forward: Amyotrophic lateral sclerosis toxicity mechanisms and drug discovery in *C. elegans*. McGill Centre for Research in Neuroscience Seminar Series, Montreal, January, 2013.

2014

- Role of the innate immune system in motor neuron degeneration in *C. elegans* ALS models. 10th annual symposium, Fondation Andre-Delambre. McGill University, Montreal, September 2014.
- Identification of neuroleptics as novel therapeutics from chemical genetic screens in simple models of TDP-43 mutations in ALS. 10th Annual ALS Canada Research Forum, Toronto, May 2014.
- *C. elegans* and ALS toxicity mechanisms, 2nd France-Quebec ALS FTD Workshop, Montreal, March 2014.
- Worming forward: Amyotrophic lateral sclerosis toxicity mechanisms and drug discovery

in *C. elegans*, University of Ottawa, March, 2014.

- Rise to the bait: Using *C. elegans* to find causes and cures for neurodegenerative disorders. Department of Anatomy and Cell Biology, University of Western Ontario, London, Ontario, November 2015.
- Rise to the bait: Using *C. elegans* to find causes and cures for neurodegenerative disorders. TGIF Seminar Series, Child & Family Research Institute, University of British Columbia, Vancouver, October, 2014.
- Using *C. elegans* to model neurodegenerative diseases. Neurodegenerative Disease Awareness Symposium, McGill University, Montreal, October, 2014.

JP. Julien

2012

- ECNP Congress Vienna, 13-17 October 2012.
- Symposium of Global Centre of Excellence University of Nagoya, NF-kB as a new therapeutic target. 15-16 November 2012.
- Symposium on ALS, University of Kyoto. NF-kB as a new therapeutic target. 17 November 2012.
- Columbia University, New York. TDP-43 drives NF-kB activation in ALS, 4 December 2012.

2013

- Annual meeting of Packard Center at Johns Hopkins. Development of therapeutic antibodies. Baltimore, 28 February – 2 March 2013.
- Invited speaker at third conference on Neurodegenerative disorders:immunotherapy and biomarkers. Therapeutic nanobodies for ALS. Uppsala, Sweden 23-24 May 2013.
- Speaker at Annual Meeting of ALS Society in Toronto. Therapeutic nanobodies for ALS. 4-5 May 2013.
- Meeting on Giant axonal neuropathy organized by Hannah's Foundation USA. A mouse model of GAN with humanized neurofilaments. Boston, 8 and 9 August 2013.
- Conférencier au Symposium Annuel de la Fondation André-Delambre. Role of chromogranin B variants in ALS. Québec 20 and 21 Septembre 2013.

2014

- Speaker at the Annual meeting of Packard Center at Johns Hopkins. Development of single chain therapeutic antibodies. Baltimore, 10-12 March 2014.
- Speaker at Glow brain workshop at University of Zagreb. My talk was about development of therapeutic antibodies for ALS. 27-29 March 2014.
- Speaker at Annual Meeting of ALS Society in Toronto. Therapeutic nanobodies for ALS. 3-5 May 2014.
- Speaker at Gordon Research Conference on IFs. IFs as targets of neuronal signaling.Mount Snow Resort. 15-20 June 2014.
- Symposium on glia and neurons in Health and disease organized by the Croatian academy of Sciences and arts. Talk on NF-kB activation in ALS. Rijeka, Croatia 7 July 2014.
- Conférencier au Symposium Annuel de la Fondation André-Delambre. Single chain antibodies for ALS treatment.Québec 19 and 20 Septembre 2014 at MNI, Montreal.
- Invited speaker at ALS Quebec-France meeting. Recombinant single chain antibodies for ALS. 23 – 26 October 2014, Montpellier France.
- Speaker at mini-symposium at Society of Neuroscience meeting: Trafficking dysfunction in

neurodegenerative diseases. Washington 18 November 2014.

- Invited speaker at Canadian-German Workshop on Neurodegeneration. NF- κ B as therapeutic target. Berlin 15-17 October 2014.

Licenses/patents applied for:

JP Julien

WITHANOLIDES USEFUL FOR THE TREATMENT OF NEURODEGENERATIVE DISEASES U.S Application No.: 61/908,455

Seed IP Reference No.: 480314.401P1

TDP-43 BINDING POLYPEPTIDES USEFUL FOR THE TREATMENT OF NEURODEGENERATIVE DISEASES U.S. Patent Application N° 62/088.012 filed on December 5, 2014 O/Ref. : 000819-0273; Canadian Patent Application N° 2.874.083 filed on December 5, 2014

Development of repositories. None.

Degrees obtained. None.

Animal models.

Development of a new liquid suspension *C. elegans* model for ALS drug screening:

Vaccaro, A. Tauffenberger, D. Aggad, GA Rouleau, P Drapeau and J.A Parker.

Mutant TDP-43 and FUS Cause Age-Dependent Paralysis and Neurodegeneration in *C. elegans*. *Plos One* 7, e31321 (2012). (see appendix)

Funding obtained.

- Synaptic targets for therapeutic protection of motor function in a genetic model of ALS. P Drapeau, Canadian Institutes for Health Research CAN\$664,370, 04/2013-03/2018.
- Investigating the ER stress response in TDP-43/FUS motor neuron toxicity. JA Parker, Muscular Dystrophy Association (USA), \$231,000, 08/2012-07/2015.
- Development of automated zebrafish high throughput screening technology platforms to accelerate in vivo screening of small molecules in disease models. Xiao-Yan Wen (PI), with P. Drapeau and C. Barden / Treventis Inc. Ontario Centres of Excellence-Québec Consortium for Drug Discovery (CQDM), CAN\$900 000, 08/2014-07/2017.
- Development of a treatment of ALS that targets the synapse. G. Armstrong (PI), with P. Drapeau and R. Robitaille, Weston Brain Institute 'Rapid Response: Neurodegenerative Diseases of Aging' Program, 09/2014-03/2016, CAN\$150,000.
- Z-BRAIN: A Zebrafish Drug Screening Platform Targeting Brain Disorders. Xiao-Yan Wen (PI), with P. Drapeau and 8 others, Brain Canada Platform Support Grant, 01/2015-12/2017, CAN\$2,620,000
- Nanobodies to disrupt TDP-43 interaction. JP Julien, FRSQ-Pfizer \$200,000, 07/2013-06/2015
- Nanobodies for ALS treatment. JP Julien, CIHR/ALS Society of Canada. \$220,000, 09/2013-08/2015
- Development of C9orf72 zebrafish models. E. Kabashi AFM/Telethon, France \$200,000, 06/2015-08/2017

- Chemical-genetics approaches using *in vivo* models of age-dependent neurodegeneration. JA Parker, Canadian Institutes for Health Research CAN\$602,000, 04/2014-03-2019

Also, our clinical collaborators L. Komgut and L. Zinman obtained an ALS Canada Arthur J. Hudson Translational Team Grant “A randomized controlled trial of pimozide in subjects with ALS”, CAN\$500,000, 01/21014-12/2016.

Funding applied for in the past year

P Drapeau, A Parker and others

Weston Brain Institute, *CAN-ADAPT-ALS: The CANAdian DynAmic Program of Translational research in ALS*, \$1,500,000 for 3 years.

ALS Association TREAT ALS Drug Development Contract, *Screening neuroleptic derivatives in genetic models of ALS*, \$500,000 for 2 years.

Brain Canada Multi Investigator Research Initiative Application, *CAN-ADAPT-ALS: The CANAdian DynAmic Program of Translational research for ALS*, \$1,500,000 for 3 years.

ALS Canada/Brain Canada ARTHUR J. HUDSON TRANSLATIONAL TEAM GRANT PROGRAM, *Correcting connections: Synaptic defects and novel therapeutic targets in ALS*, \$2,500,000 for 5 years.

ALS Canada/Brain Canada ARTHUR J. HUDSON TRANSLATIONAL TEAM GRANT, Pipeline for ALS drug discovery and treatment, \$2,500,000 for 5 years.

JP Julien

CIHR Foundation program, *From pathogenic pathways to novel therapeutic strategies in amyotrophic lateral sclerosis*, \$3,500,000 for 7 years.

ALS Association USA, *Development of the new chemical entity IMS-088 for treatment of amyotrophic lateral sclerosis*, \$500,000 for 18 months.

Weston Foundation, *Nanobodies to target TDP-43 interactions for treatment of neurodegenerative diseases*, \$1,200,000 for 3 years.

ALS Canada-Brain Canada Hudson grant, *Preclinical and clinical studies with withanolides: Therapeutic effects, molecular signatures and biomarkers*, \$3,000,000 for 3 years.

ALS Association USA CLINICAL RESEARCH GRANT APPLICATION, *Nuclear Factor Kappa Beta Inhibition in ALS: A Phase II Randomized Placebo Controlled Trial*, PI Lorne Zinman (University of Toronto), co-PI JP Julien, \$500,000

E Kabashi

Testing drugs that target connexin channels, E. Kabashi and three other partners, ALSA \$500,000

Employment/research opportunities.

- E Kabashi, Group Leader, ICM institute, Paris, France.
- J Gomez, Research Assistant, Kabashi lab, ICM, Paris.
- D Agad, postdoctoral fellow, France.
- A Vaccaro, Ph.D student, France
- S. Patten, Group Leader (formerly Canadian CIHR and Quebec RMGA Fellow), Armand-Frappier Institute, Montreal, Canada
- G Armstrong, Postdoctoral Fellow (Canada NSERC, CIHR, Weston Brain Institute and U. Montreal Jasper Fellow), Univ. Montreal.
- A. Lissouba, Ph.D. Student, U. Montreal, Canada (Canada CIHR Banting & Best MSc award, CIHR-ALS Canada PhD award, Quebec FRQS award, U. Montreal GRSNC, FESP Excellence, CRCHUM Excellence awards).
- S. Dzieciolowska, M.Sc. student, McGill University, Montreal, Canada
- S. Ciruna, Research Assistant, ICM Intsitute, Paris, France.
- S. Pozzi, Postdoctoral Fellow, Univ. Laval.

CONCLUSION

Our screen has identified neuroleptics, of which pimozide is the most potent, as well as withaferin A, an NFkB inhibitor, as being protective in worm and zebrafish models, with withaferin A confirmed in several mouse models and pimozide in acute though not chronic mouse models and with pimozide being tested clinically. We have identified several new molecules as well as pimozide derivatives in our worm screen. We have tested combinations of compounds to test for synergistic effects at low doses. Based on related observations with calcium channels agonists that proved to be neuroprotective in zebrafish, we found that pimozide acts off-target on calcium channels and may be acting to help maintain neuromuscular function, offering a readily accessible peripheral target. Pimozide is being tested clinically with neuromuscular stimulation as a novel biomarker.

So what?

Because pimozide is an FDA-approved compound, it is now being tested in patients through an outside collaboration in parallel to this project. From our analysis of the effects of pimozide on neuromuscular activity in our models, we have developed a new clinical biomarker to help evaluate the usefulness of neuroleptics to treat ALS.

REFERENCES

- 1 Vaccaro, A. *et al.* Mutant TDP-43 and FUS Cause Age-Dependent Paralysis and Neurodegeneration in *C. elegans*. *Plos One* **7**, e31321 (2012).
- 2 Vaccaro et al. Methylene Blue Protects against TDP-43 and FUS Neuronal Toxicity in *C. elegans* and *D. rerio*. *PLoS ONE* **7**(7): e42117 (2012).
- 3 Kabashi, E. *et al.* Gain and loss of function of ALS-related mutations of TARDBP (TDP-43) cause motor deficits in vivo. *Hum Mol Genet* **19**, 671-683 (2010).
- 4 Kabashi, E. *et al.* FUS and TARDBP but Not SOD1 Interact in Genetic Models of Amyotrophic Lateral Sclerosis. *Plos Genetics* **7**, e1002214 (2011).
- 5 Swarup, V. *et al.* Pathological hallmarks of amyotrophic lateral sclerosis/frontotemporal lobar degeneration in transgenic mice produced with TDP-43 genomic fragments. *Brain* **134**, 2610-2626 (2011).
- 6 Kabashi, E., Champagne, N., Brustein, E. & Drapeau, P. In the swim of things: recent insights to neurogenetic disorders from zebrafish. *Trends Genet* **26**, 373-381 (2010).
- 7 Kabashi, E., Brustein, E., Champagne, N. & Drapeau, P. Zebrafish models for the functional genomics of neurogenetic disorders. *Biochim Biophys Acta* **3**, 335-345 (2011).
- 8 Kabashi, E. *et al.* Gain and loss of function of ALS-related mutations of TARDBP (TDP-43) cause motor deficits in vivo. *Hum Mol Genet* **19**, 3102-3102 (2010).
- 9 Vaccaro, A. *et al.* Methylene Blue Protects against TDP-43 and FUS Neuronal Toxicity in *C. elegans* and *D. rerio*. *Plos One* **7**, e42117 (2012).
- 10 Audet JN, Soucy G, Julien JP. (2012) Methylene blue administration fails to confer neuroprotection in two amyotrophic lateral sclerosis mouse models. *Neuroscience*. 209:136-43.
- 11 Armstrong, GAB and Drapeau, P. (2013) Calcium channel agonists protect against neuromuscular dysfunction in a genetic model of TDP-43 mutation in ALS. *J. Neurosci.* 33(4):1741–1752.
12. Vaccaro, A; S.A. Patten; D. Aggad; C. Julien; C. Maios; E. Kabashi; P.Drapeau; JA Parker (2013) Pharmacological reduction of ER stress protects against TDP-43 neuronal toxicity in vivo. *Neurobiol. Dis.* 55:64-75.
13. Tauffenberger A, Julien C, Parker JA. Evaluation of longevity enhancing compounds against transactive response DNA-binding protein-43 neuronal toxicity. *Neurobiology of Aging*. 2013 (9):2175-82.
14. Dawe GS 2010 *Neuroscience* 171, 162-172;
15. Navarro JF et al. *Prog Neuropsychopharmacol Biol Psychiatry*. 2000 Jan;24(1):131-42)
16. Swarup V., Phaneuf D., Dupré N., Petri S., Strong M., Kriz J. and Julien J.-P. (2011) Deregulation of TDP-43 in ALS triggers nuclear factor-κB-mediated pathogenic pathways. *J Exp Med*, 208(12):2429-2447

- Appendices:**
- 1- Vaccaro et al. (2012) PLoS One 7(2): e31321
 - 2- Vaccaro et al. (2012) PLoS One 7(7): e42117
 - 3- Vaccaro et al. (2013) Neurobiol. Dis. 55:64-75.
 - 4- Audet JN et al. (2012) Neuroscience. 209:136-43
 - 5- Tauffenberger et al. (2013) Neurobiology of Aging. 9:2175-82.
 - 6- Therrien et al. (2014) Frontiers in Genetics, Apr 17;5:85
 - 7- Aggad et al. (2014) Journal of Neuroscience. 34(36): 12093-12103

Mutant TDP-43 and FUS Cause Age-Dependent Paralysis and Neurodegeneration in *C. elegans*

Alexandra Vaccaro^{1,2,3}, Arnaud Tauffenberger^{1,2,3}, Dina Aggad^{1,2,3}, Guy Rouleau^{1,2,4}, Pierre Drapeau^{2,3}, J. Alex Parker^{1,2,3*}

1 The Research Centre of the University of Montreal Hospital Centre, Université de Montréal, Montréal, Québec, Canada, **2** Centre of Excellence in Neuromics, Université de Montréal, Montréal, Québec, Canada, **3** Département de Pathologie et Biologie Cellulaire, Université de Montréal, Montréal, Québec, Canada, **4** Département de Médecine, Université de Montréal, Montréal, Québec, Canada

Abstract

Mutations in the DNA/RNA binding proteins TDP-43 and FUS are associated with Amyotrophic Lateral Sclerosis and Frontotemporal Lobar Degeneration. Intracellular accumulations of wild type TDP-43 and FUS are observed in a growing number of late-onset diseases suggesting that TDP-43 and FUS proteinopathies may contribute to multiple neurodegenerative diseases. To better understand the mechanisms of TDP-43 and FUS toxicity we have created transgenic *Caenorhabditis elegans* strains that express full-length, untagged human TDP-43 and FUS in the worm's GABAergic motor neurons. Transgenic worms expressing mutant TDP-43 and FUS display adult-onset, age-dependent loss of motility, progressive paralysis and neuronal degeneration that is distinct from wild type alleles. Additionally, mutant TDP-43 and FUS proteins are highly insoluble while wild type proteins remain soluble suggesting that protein misfolding may contribute to toxicity. Populations of mutant TDP-43 and FUS transgenics grown on solid media become paralyzed over 7 to 12 days. We have developed a liquid culture assay where the paralysis phenotype evolves over several hours. We introduce *C. elegans* transgenics for mutant TDP-43 and FUS motor neuron toxicity that may be used for rapid genetic and pharmacological suppressor screening.

Citation: Vaccaro A, Tauffenberger A, Aggad D, Rouleau G, Drapeau P, et al. (2012) Mutant TDP-43 and FUS Cause Age-Dependent Paralysis and Neurodegeneration in *C. elegans*. PLoS ONE 7(2): e31321. doi:10.1371/journal.pone.0031321

Editor: Leonard Petrucelli, Mayo Clinic, United States of America

Received: October 11, 2011; **Accepted:** January 5, 2012; **Published:** February 21, 2012

Copyright: © 2012 Vaccaro et al. This is an open-access article distributed under the terms of the Creative Commons Attribution License, which permits unrestricted use, distribution, and reproduction in any medium, provided the original author and source are credited.

Funding: This research was supported by: Montreal University Hospital Foundation (<http://fondationduchum.com/fr>) to JAP, Natural Sciences and Engineering Research Council Discovery Grant (<http://www.nserc-crsng.gc.ca>) to JAP, Canadian Institutes of Health Research New Investigator (<http://www.cihr-irsc.gc.ca>) to JAP, Frick Foundation for ALS Research (<http://frick-foundation.ch>) to PD and JAP and a Bernice Ramsay Discovery Grant from the ALS Society of Canada (<http://www.als.ca/>) to JAP. The funders had no role in study design, data collection and analysis, decision to publish, or preparation of the manuscript.

Competing Interests: The authors have declared that no competing interests exist.

* E-mail: ja.parker@umontreal.ca

Introduction

Amyotrophic Lateral Sclerosis (ALS) is a late-onset progressive disease affecting motor neurons ultimately causing fatal paralysis [1,2]. Most cases are sporadic, but ~10% of patients have an inherited familial form of the disease. Dominant mutations in SOD1 (copper/zinc superoxide dismutase 1) account for ~20% of familial ALS cases and ~1% of sporadic cases [1]. The recent discovery of mutations in TAR DNA-binding protein-43 (TDP-43) and Fused in sarcoma (FUS, also named TLS) in both familial ALS and frontotemporal dementia (FTD) has shifted research into disease mechanisms and potential therapeutics [3–9].

TDP-43 and FUS are evolutionarily conserved DNA/RNA binding proteins that shuttle between the nucleus and cytoplasm having multiple roles including DNA transcription and RNA processing [3,9–12]. Mutant TDP-43 and FUS (mTDP-43 and mFUS) are found in cytoplasmic inclusions in the disease state while the accumulation of wild type TDP-43 and FUS (wtTDP-43 and wtFUS) are observed in an increasing number of disorders including Alzheimer's Disease, Parkinson's Disease and the polyglutamine diseases (reviewed in [10]). The pathogenic mechanisms for mutant TDP-43 and FUS age-dependent neuronal toxicity remain unclear. As of now there is no consensus whether mutant TDP-43 and FUS employ a loss-of-function, a gain-of-function, or both in motor neuron cell death.

Since TDP-43 and FUS are evolutionarily conserved we used the nematode *Caenorhabditis elegans* to investigate mutant TDP-43 and FUS age-dependent neurodegeneration. We created transgenic nematodes that express full-length wild type or mutant TDP-43 and FUS in the worm's GABAergic motor neurons. Transgenic TDP-43 and FUS worms recapitulate a salient feature of ALS; they display adult-onset, age-dependent, progressive paralysis and degeneration of motor neurons. Importantly, mTDP-43 and mFUS, but not wtTDP-43 and wtFUS, strains show the presence of insoluble proteins in extracts from whole animals suggesting that protein misfolding may be a primary cause of toxicity. We introduce a genetically tractable platform to investigate motor neuron toxicity caused by mutant TDP-43 and FUS that can be used for suppressor screening.

Results

Transgenic worms expressing full-length human TDP-43 or FUS in motor neurons display age-dependent paralysis

Since ALS is a motor neuron disease we expressed wild type and mutant human TDP-43 and FUS proteins in the worm's 26 GABAergic motor neurons with the vesicular GABA transporter (*unc-47*) promoter (Figures 1A, B) [13]. Multiple transgenic strains carrying extrachromosomal arrays were obtained by microinjection and stable lines with chromosomally-integrated transgenes

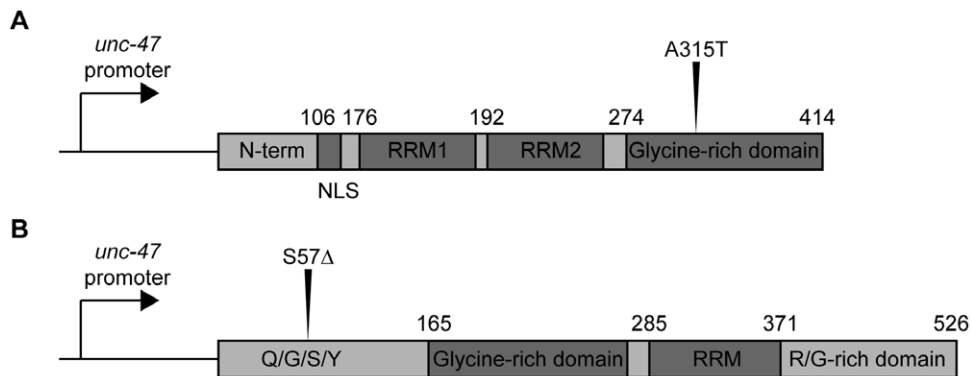


Figure 1. TDP-43 and FUS transgene constructs. (A) Full-length wild type human TDP-43 and the clinical mutation A315T were cloned into a vector for expression in motor neurons by the *unc-47* promoter and injected into *C. elegans*. (B) Full-length wild type human FUS and the clinical mutation S57Δ were cloned into the *unc-47* expression vector and injected into *C. elegans*. RRM (RNA Recognition Motif), Q/G/S/Y (Glutamine-Glycine-Serine-Tyrosine-rich region), R/G (Arginine-Glycine-rich region), NLS (Nuclear localization signal).
doi:10.1371/journal.pone.0031321.g001

were isolated after UV-irradiation [14]. Both wild type TDP-43 and the ALS-associated A315T mutant proteins were expressed in transgenic worms as detected by immunoblotting of worm protein extracts with a human specific TDP-43 antibody (Figure 2A) [4]. Similarly, using a FUS antibody we confirmed the expression of wild type and the ALS-linked S57Δ mutant proteins by western blotting (Figure 2B) [15].

All strains were morphologically normal and showed no adverse phenotypes during development. However, during adulthood the transgenic strains begin to display uncoordinated motility phenotypes that progressed to paralysis. Paralysis was age-dependent and occurred at higher rate for mTDP-43 and mFUS worms compared to wtTDP-43 and wtFUS transgenics (Figures 3 A, B). Typically, after 12–13 days on plates 100% of the mTDP-43 and mFUS worms were paralysed while only 20% of the wtTDP-43 and wtFUS worms were affected. The low rate of paralysis for wtTDP-43 and wtFUS strains is comparable to what is observed in transgenics expressing GFP from the same *unc-47* promoter (Figure 3C). Additionally, the paralysis assay is widely used to study age-dependent degenerative phenotypes and is not observed in wild type non-transgenic worms until they reach advanced age (approximately 20 days) [16–18]. Finally, motility defects and

adult onset paralysis have been previously observed in worms with degenerating GABAergic motor neurons suggesting that mTDP-43 and mFUS may negatively affect GABAergic neuronal function and survival [19].

TDP-43 and FUS transgenics have normal lifespans

One of the signs of aging in worms is decreased motility [18,20]. Thus the progressive paralysis phenotypes observed in the TDP-43 and FUS transgenics may be due to overall decreased health from the expression of toxic non-native proteins leading to accelerated mortality, a part of which is a decline in motility. We conducted lifespan analyses and observed that all of the transgenics had lifespans indistinguishable from non-transgenic wild type N2 worms (Figures 4A, B and Table S1). These observations suggest that the paralysis observed in our models is specific to the expression of TDP-43 and FUS in motor neurons and not due to secondary effects from general sickness and reduced lifespan.

TDP-43 and FUS cause neuronal dysfunction

The progressive paralysis phenotypes caused by mTDP-43 and mFUS suggest there may be motor neuron dysfunction and/or

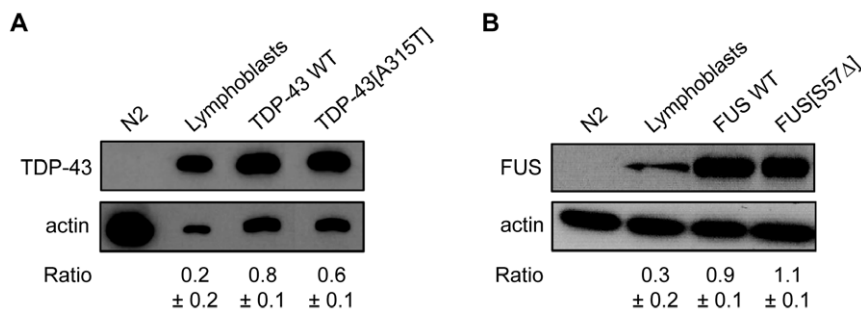


Figure 2. Expression of human TDP-43 and FUS proteins in *C. elegans* transgenics. (A) Total protein levels from non-transgenic worms, human lymphoblast cells and transgenic worms expressing wtTDP-43 or mTDP-43. Staining with a human TDP-43 antibody showed no signal for non-transgenic worms but a signal corresponding to full-length human TDP-43 at ~45 kDa in size was observed in extracts from human cells and the two transgenic TDP-43 worm strains. wtTDP-43 and mTDP-43 strains showed comparable protein expression levels. (B) Total protein levels from non-transgenic worms, human lymphoblast cells and transgenic worms expressing wtFUS or mFUS. Using a human FUS antibody, no signal was detected in non-transgenic worms, but a signal corresponding to full-length human FUS at ~75 kDa in size was observed in extracts from lymphoblast cells and the transgenic FUS worm strains. wtFUS and mFUS worms showed identical levels of protein expression. For all experiments actin staining was used as a loading control and expression ratios \pm SEM of TDP-43 or FUS to actin was determined from 3 independent experiments. Representative western blots are shown.
doi:10.1371/journal.pone.0031321.g002

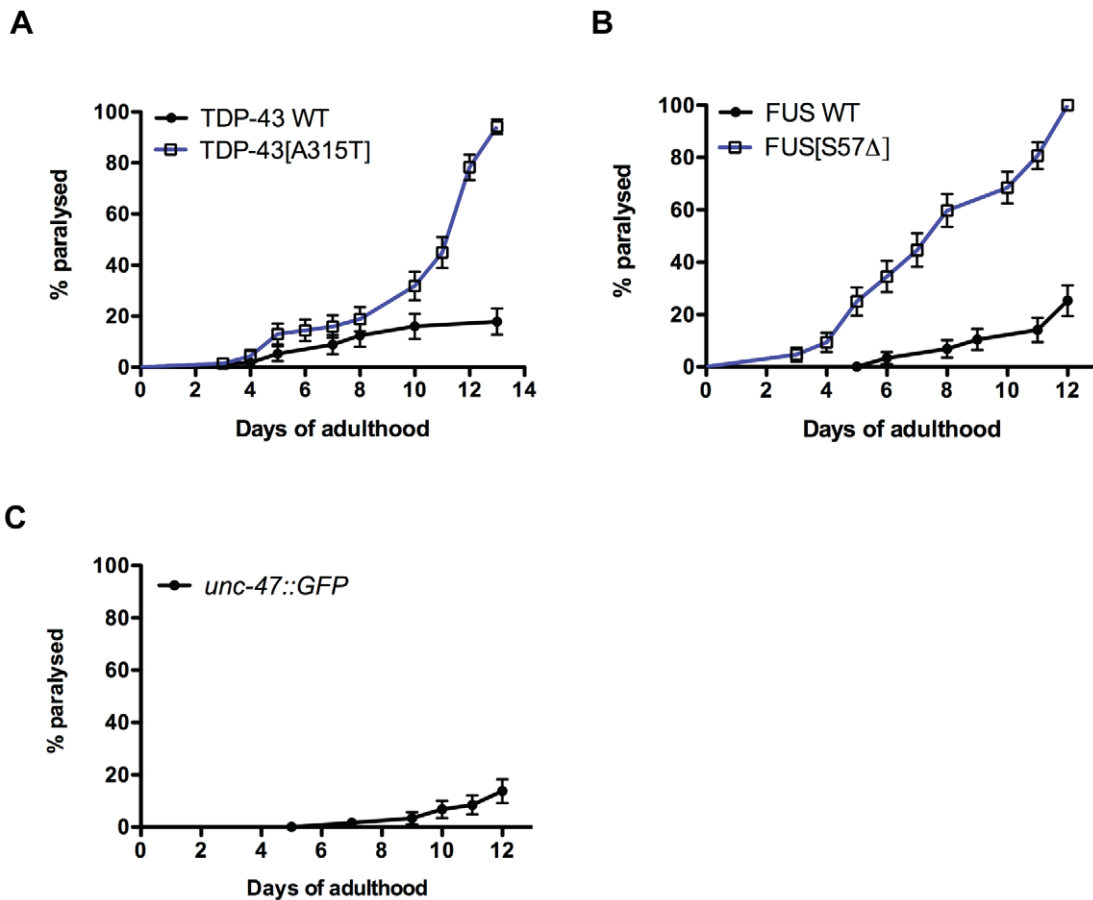


Figure 3. Mutant TDP-43 and FUS cause adult-onset, age-dependent paralysis in *C. elegans*. Transgenics were monitored from the adult stage and scored daily for paralysis. (A) mTDP-43 worms show a rate of progressive paralysis that is greater than transgenics expressing wtTDP-43 ($P < 0.001$). (B) Transgenics expressing mFUS become paralyzed significantly sooner than wtFUS control transgenics ($P < 0.001$). (C) Transgenic worms expressing GFP in motor neurons show low levels of paralysis. doi:10.1371/journal.pone.0031321.g003

degeneration in these animals. *C. elegans* body wall muscle cells receive excitatory (acetylcholine) and inhibitory (GABA) inputs to coordinate muscle contraction/relaxation and facilitate movement [21,22]. Body wall muscle activity can be measured indirectly with

the acetylcholinesterase inhibitor aldicarb [23]. Exposure to aldicarb causes accumulation of acetylcholine at neuromuscular junctions resulting in hyperactive cholinergic synapses, muscle hypercontraction, and acute paralysis [23]. Hypersensitivity to

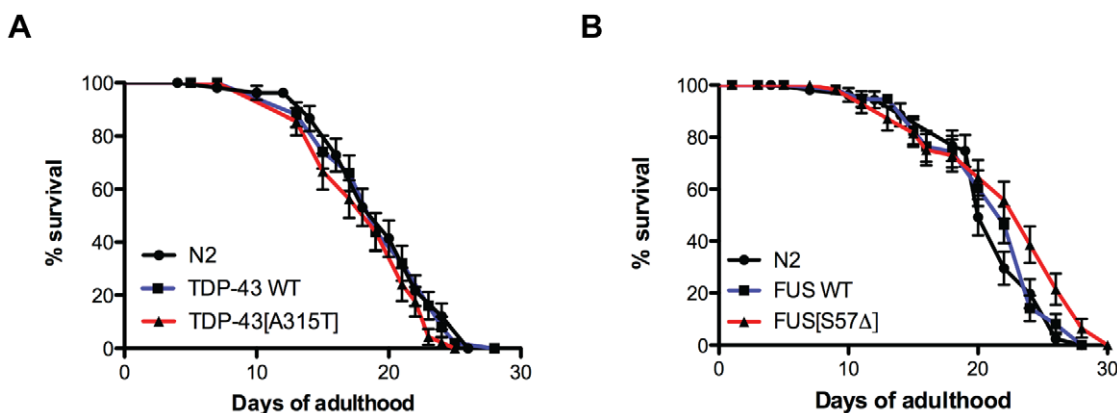


Figure 4. TDP-43 and FUS transgenes do not affect lifespan. Beginning at Day 1 of adulthood we tested the lifespans of wild type non-transgenic N2 worms and transgenics expressing (A) wtTDP-43 and mTDP-43 as well as (B) animals expressing wtFUS and mFUS. Animals expressing TDP-43 or FUS transgenes had lifespans indistinguishable from N2 worms. doi:10.1371/journal.pone.0031321.g004

aldicarb-induced paralysis has been used to identify genes that increase acetylcholine secretion or decrease inhibitory GABA signalling [24]. For example mutants lacking genes required for GABA transmission like the vesicular GABA transporter *unc-47* are hypersensitive to aldicarb-induced paralysis [25]. To investigate if our TDP-43 and FUS transgenics had abnormal activity at the neuromuscular junction we exposed the animals to aldicarb. We observed that, like *unc-47* mutants, mTDP-43 and mFUS animals were hypersensitive to aldicarb-induced paralysis, while wtTDP-43 and wtFUS transgenics showed a rate paralysis identical to non-transgenic N2 worms (Figures 5A, B). These data suggest that the inhibitory GABA signalling is impaired in mTDP-43 and mFUS transgenics. *unc-47* mutants are classically described as having a “shrinker” phenotype, where in response to touch the worm does not move away but instead the whole body undergoes longitudinal shortening [21], and we observed that the shrinker phenotype was weakly penetrant in adult mTDP-43 and mFUS worms. To determine if impaired GABAergic neurotransmission contributed to the paralysis phenotype we examined two *unc-47* loss-of-function mutants and they both showed age-dependent paralysis, a phenotype not previously reported for *unc-47* (Figure 5C) [21]. Thus, mTDP-43 and mFUS cause neuronal dysfunction in GABA neurons leading to progressive motility

defects culminating in paralysis, a phenotype similar to animals deficient in GABAergic signalling.

TDP-43 and FUS cause progressive degeneration of motor neurons

Many neurodegenerative diseases are characterized by neuronal dysfunction prior to degeneration [26]. To investigate if the progressive paralysis phenotypes in our TDP-43 and FUS transgenics were accompanied by neurodegeneration we crossed all of the transgenics with an integrated reporter (*unc-47p::GFP*) that expresses GFP in the same GABAergic motor neurons [13] (Figures 6A, B). Similar to reports from another *C. elegans* TDP-43 toxicity model [27], we observed gaps/breaks in motor neuron processes in TDP-43 and FUS animals compared to animals expressing *unc-47p::GFP* alone (Figures 6 C–F). We extended our analysis by scoring degeneration in living GFP, wtTDP-43, mTDP-43, wtFUS and mFUS transgenics at days 1, 5 and 9 of adulthood. We observed that degeneration was age-dependent and occurred at higher rate for the mTDP-43 and mFUS animals compared to the wtTDP-43 and wtFUS transgenics (Figure 6G). Thus our TDP-43 and FUS transgenics mimic the adult-onset, gradual decline of neuronal function ultimately resulting in age-dependent motor neuron degeneration seen in diseases like ALS.

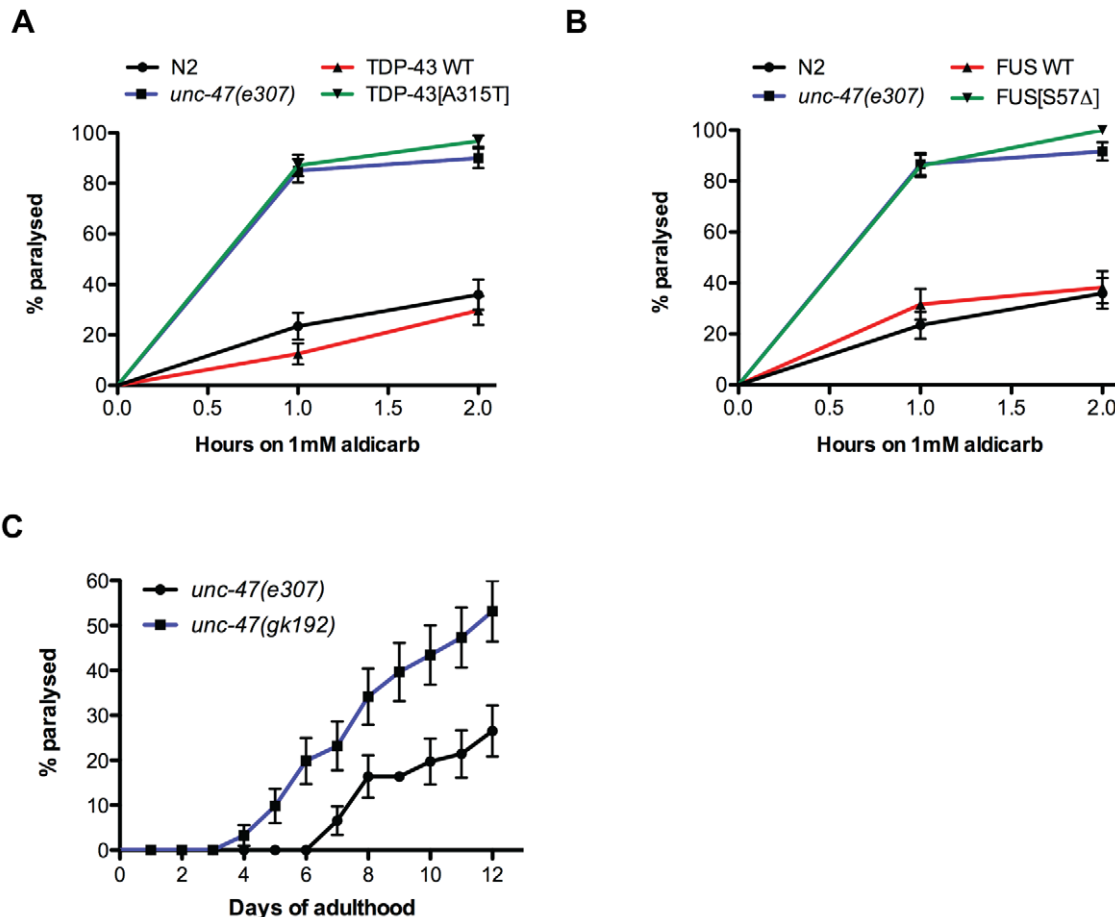


Figure 5. Mutant TDP-43 and FUS impair synaptic transmission. (A) Cholinergic neuronal transmission was measured by determining the onset of paralysis induced by the cholinesterase inhibitor aldicarb. *unc-47(e307)* mutants and mTDP-43 transgenics were hypersensitive to aldicarb-induced paralysis compared to either wtTDP-43 transgenics or N2 worms ($P < 0.001$ for *unc-47* or mTDP-43 compared to N2 or wtTDP-43 worms). (B) mFUS transgenics and *unc-47(e307)* mutants were more sensitive to aldicarb induced paralysis compared to either wtFUS transgenics or N2 controls ($P < 0.001$). (C) *unc-47* mutants grown on regular worm plates showed age-dependent progressive paralysis. doi:10.1371/journal.pone.0031321.g005

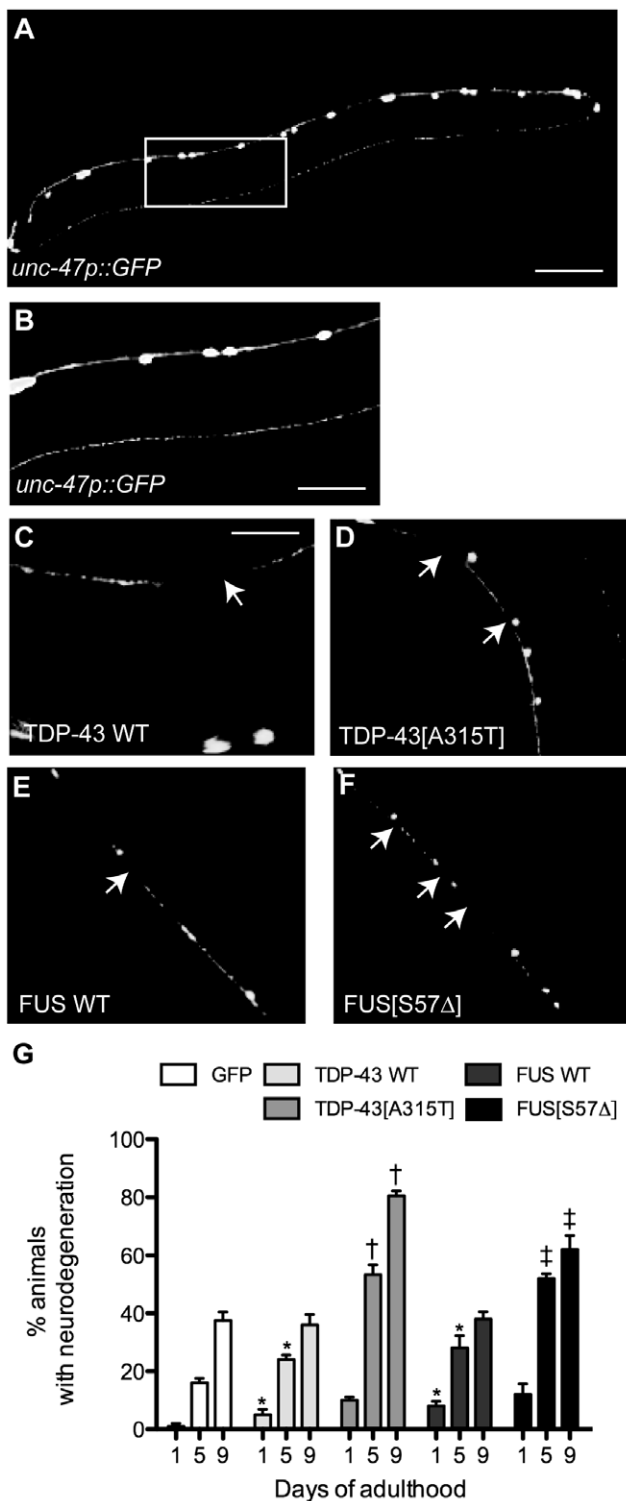


Figure 6. Mutant TDP-43 causes motor neuron degeneration. Shown are representative photos of living, adult *unc-47p::GFP*, *unc-47p::GFP*;TDP-43, and *unc-47p::GFP*;FUS transgenics. (A) Image of an entire *unc-47p::GFP* worm showing the GABAergic motor neurons. Scale bar represents 50 μ m. (B) High-magnification of the framed area from (A) showing wild type morphology of motor neurons. Scale bar represents 20 μ m. High magnification of motor neurons labelled with *unc-47p::GFP* in (C) wtTDP-43, (D) mTDP-43, (E) wtFUS and (F) mFUS transgenics showing gaps along neuronal processes (arrows). Scale bar represents 10 μ m for photos (C) to (F). (G) Quantification of neurodegeneration in transgenic worms at days 1, 5 and 9 of adulthood. * wtTDP-43 and wtFUS

have a higher rate of neurodegeneration compared to *unc-47p::GFP* controls at days 1 and 5 of adulthood ($P < 0.05$). †mTDP-43 transgenics have a higher rate of neurodegeneration at days 5 and 9 compared to wtTDP-43 transgenics ($P < 0.001$). ‡mFUS transgenics show an enhanced rate of neurodegeneration at days 5 and 9 of adulthood in compared to wtFUS transgenics ($P < 0.001$).
doi:10.1371/journal.pone.0031321.g006

Mutant TDP-43 and FUS are highly insoluble

Since TDP-43 and FUS are prone to aggregation in several model systems including *C. elegans*, we tested if the same was true for our transgenics [27–33]. To examine if protein misfolding is more pronounced for strains expressing mTDP-43 and mFUS, we used a biochemical assay to detect protein aggregation. Homogenized protein extracts from transgenic worms were separated into supernatant (detergent-soluble) and pellet (detergent-insoluble) fractions [30]. Immunoblotting the TDP-43 transgenics with a human TDP-43 antibody revealed the accumulation of mTDP-43 in the pelleted, insoluble fraction, while wtTDP-43 proteins were predominantly detected in the supernatant, or soluble fractions (Figure 7A). Similar results were obtained for the FUS transgenics where immunoblotting with a human FUS antibody showed that mFUS accumulated in the insoluble pellet fraction while wtFUS proteins remained soluble (Figure 7B). These data suggest that mTDP-43 and mFUS proteins are susceptible to misfolding leading to insolubility and aggregation that may contribute to motor neuron dysfunction and degeneration.

Next focusing on the mTDP-43 and mFUS transgenics we fixed whole *unc-47p::GFP*;mTDP-43 and *unc-47p::GFP*;mFUS worms and respectively stained them with human TDP-43 and human FUS antibodies. We detected mTDP-43 and mFUS in both the nuclei and cytoplasm of motor neurons (Figure 8). The cytoplasmic accumulation of mTDP-43 and mFUS in our transgenics is consistent with findings in patients suggesting that these proteins misfold leading to intracellular build-up and aggregation [10].

Finally, we noticed that the fixed mTDP-43 and mFUS showed gaps or breaks along the GFP labelled neuronal processes similar to what was observed in living animals (Figures 6D, F). To confirm that neurodegeneration was not simply due to loss of GFP signals, we stained whole *unc-47p::GFP*;mTDP-43 and *unc-47p::GFP*;mFUS worms for GABA [22]. We observed that the gaps along the processes as visualized by a loss of GFP signal likewise corresponded to a loss of GABA staining (Figure 9). Altogether these data suggest that the expression of TDP-43 and FUS lead to degeneration of motor neurons as has been observed for TDP-43 in other worm models [27].

Paralysis phenotypes are enhanced in liquid culture

One goal in developing these transgenics is for use in genetic and pharmacological suppressor screens. TDP-43 and FUS transgenics may have decreased inhibitory GABA signalling ultimately causing muscle hypercontraction leading to paralysis. When grown on solid media the mTDP-43 and mFUS paralysis phenotypes manifest over a period of 5 to 13 days (Figure 3). Worms grown in liquid culture exhibit a stereotypical swimming motion that is considerably more vigorous than worms crawling on solid media [34]. We hypothesized that placing worms in liquid culture would increase activity at the neuromuscular junction and precipitate paralysis phenotypes much earlier than worms grown on solid media.

Using age-synchronized worms we transferred young adult TDP-43 and FUS transgenics to 96-well plates with liquid media and scored their motility every 2 hours. We observed a rapid

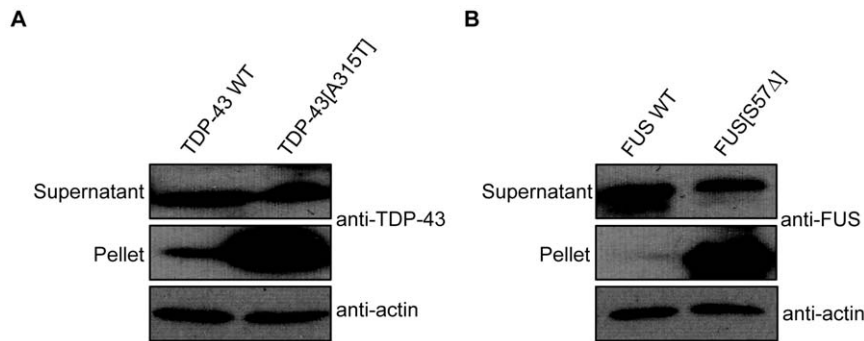


Figure 7. Mutant TDP-43 and FUS are highly insoluble. Shown are representative images from western blotting of the soluble supernatant and insoluble pellet fractions of protein extracts from transgenic TDP-43 and FUS strains. (A) Blotting against TDP-43 shows that a large proportion of the TDP-43 signal resides in the insoluble fraction for mTDP-43 worms, while the signal is largely soluble for the wtTDP-43 samples. (B) Immunoblotting with a human FUS antibody revealed that mFUS proteins primarily resided in the insoluble fractions while wtFUS proteins were exclusively soluble. Immunoblotting for actin was used as the loading control.
doi:10.1371/journal.pone.0031321.g007

onset of paralysis for the mTDP-43 and mFUS lines with approximately 80% of the population becoming immobile after 6 hours progressing to 100% paralysis after 12 hours (Figure 10A, B Videos S1, S2, S3, S4). wtTDP-43 and wtFUS animals also showed increased paralysis but at a much lower rate, with approximately 20% of the animals immobile after 6 hours moving to 80% paralysis after 12 hours (Figure 10, Videos S5, S6, S7, S8). Non-transgenic N2 animals showed a very low rate of paralysis of approximately 15% after 12 hours (Figure 10C, Videos S9, S10). In comparison, approximately 50% of transgenic *unc-47p::GFP* control animals were paralysed after 12 hours, a rate intermediate between non-transgenic N2 worms and transgenic wtTDP-43 and wtFUS animals (Figure 10C, Videos S11, S12). The difference between wild type and mutant transgenic lines is easy to distinguish, particularly at 6 hours, and suggests that this phenotype may be used for rapid genetic and chemical screening.

Discussion

Here we introduce a novel *C. elegans* platform for investigating mechanisms of motor neuron toxicity caused by mTDP-43 and mFUS. To more closely model human disease we chose to express full-length human TDP-43 and FUS without additional tags since the inclusion of tags like GFP can mask or enhance the phenotypes of wild type and mutant proteins [35,36]. Additionally, we reasoned that restricting expression to a smaller set of neurons might produce phenotypes less severe, or later, than observed in other *C. elegans* models [27,29,30,33]. Since ALS is characterized by degeneration of the motor neurons we engineered strains expressing human TDP-43 and FUS in the animal's 26 GABAergic neurons [13,22]. Additionally, ALS patients show cortical hyperexcitability that may be due to reduced inhibitory signalling from the GABAergic system [37,38]. We believe our transgenic mTDP-43 and mFUS worms recapitulate this patho-

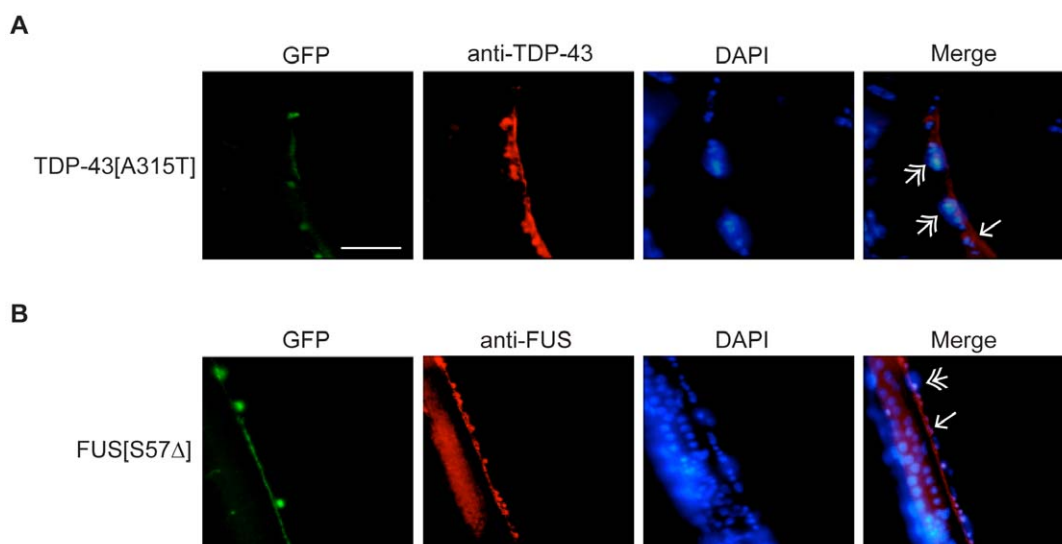


Figure 8. Mutant TDP-43 and FUS aggregate in vivo. (A) Representative image of a fixed *unc-47p::GFP;mTDP-43* worm stained with a human TDP-43 antibody. The green channel shows GFP labelled motor neurons. Antibody staining (red signal) revealed aggregation of TDP-43 signals in motor neurons. Staining of motor neuron nuclei with DAPI (blue signal) revealed that TDP-43 is both cytoplasmic (single arrowhead) and nuclear (double arrowhead). Scale bar represents 10 μ m for all photos. (B) Staining of *unc-47p::GFP;mFUS* worms with a human FUS antibody (red signal) and DAPI (blue signal) revealed cytoplasmic (single arrowhead) and nuclear (double arrowhead) accumulations in motor neurons.
doi:10.1371/journal.pone.0031321.g008

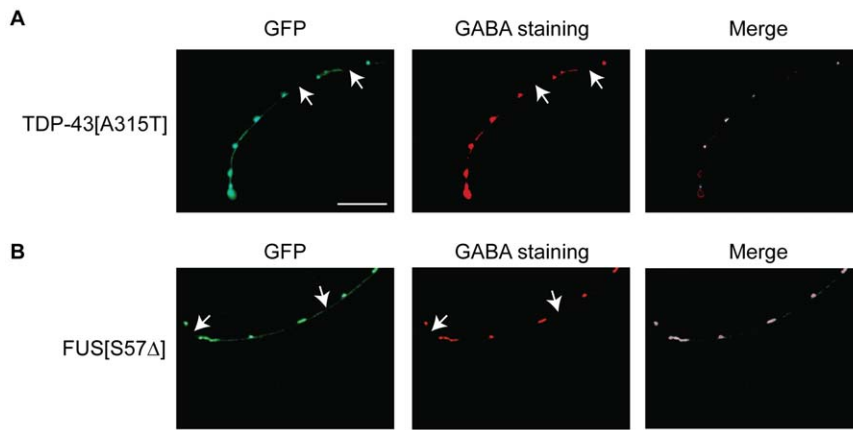


Figure 9. Decreased GABA staining in mutant TDP-43 and FUS worms. (A) Fluorescent micrograph of a fixed *unc-47p::GFP;mTDP-43* worm stained with a GABA antibody revealed neurodegeneration in motor neurons that mirrors the loss of GFP signals. Scale bar represents 10 μ m for all photos. (B) Staining of *unc-47p::GFP;mFUS* worms also showed loss of GABA signals similar to the loss of GFP in the motor neurons.
doi:10.1371/journal.pone.0031321.g009

physiological mechanism; they show decreased GABA staining and are hypersensitive to the acetylcholinesterase inhibitor aldicarb, suggesting a reduction of inhibitory GABA input at neuromuscular junctions [24,25]. In our models sensitivity to aldicarb can be detected in day 1 adult worms, while paralysis and motor neuron degeneration can first be detected starting at day 5

of adulthood demonstrating that similar to ALS, neuronal dysfunction occurs prior to neurodegeneration [39].

Importantly, our transgenic TDP-43 and FUS animals only begin to show motility defects once they have reached adulthood a feature absent from other models [27,29,30,33]. Thus our models mirror a prominent clinical feature of ALS, they display adult-

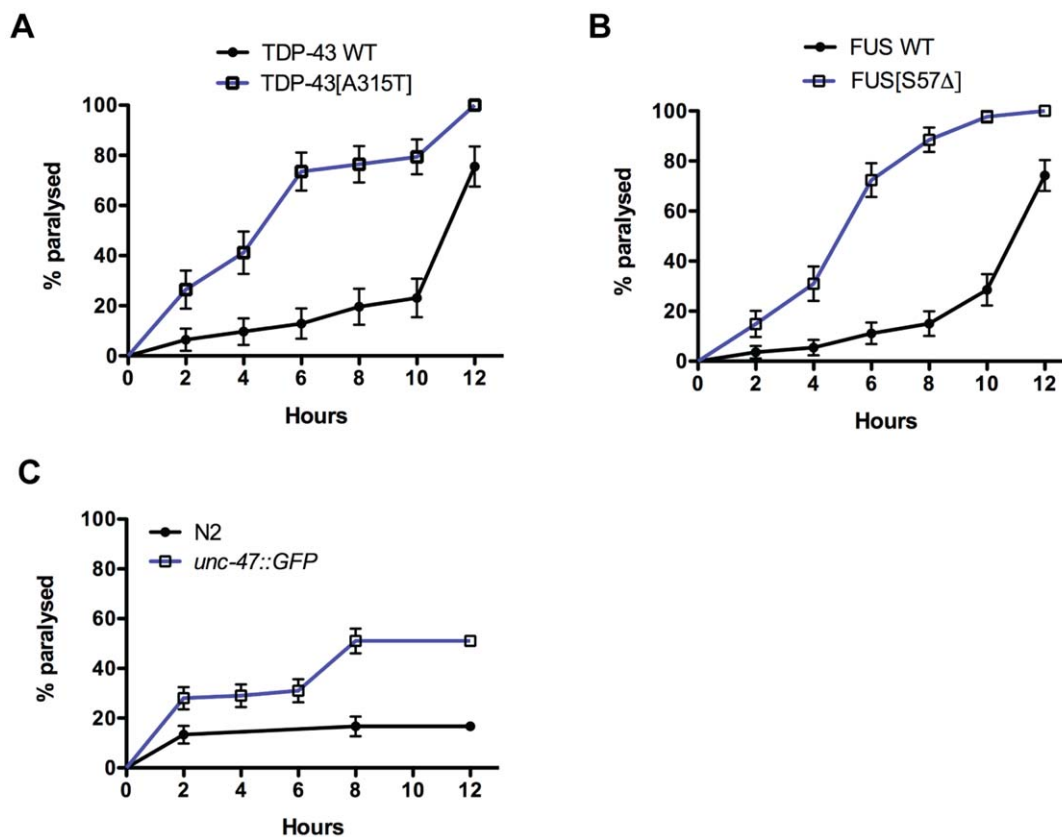


Figure 10. Accelerated paralysis phenotypes for TDP-43 and FUS transgenics in liquid culture. (A) Paralysis phenotypes resolve over a number of hours for wtTDP-43 and mTDP-43 worms grown in liquid culture. mTDP-43 worms have a faster rate of paralysis compared to wtTDP-43 transgenics ($P < 0.001$). (B) Transgenic mFUS worms show motility defects and become paralysed at a rate faster than wtFUS controls ($P < 0.001$). (C) *unc-47p::GFP* transgenics have an increased rate of paralysis compared to non-transgenic N2 worms ($P < 0.001$).
doi:10.1371/journal.pone.0031321.g010

onset, age-dependent, progressive paralysis [40,41]. Additionally, unlike previously described TDP-43 and FUS models based on pan-neuronal expression [27,30,33] our transgenics do not show reduced lifespan suggesting the behavioural phenotypes observed in our transgenics are not influenced by general sickness. Our transgenics do share many features with other neuronal-based models, notably the aggregation and insolubility of mutant TDP-43 and FUS as well as degeneration of motor neurons suggesting there may be common mechanisms of toxicity amongst the models [27,29,30,32,33,42–45]. However, cytoplasmic aggregation of TDP-43 and FUS is a prominent feature of the human pathologies and this is seen in a recently described worm FUS model [33], but is absent from previously reported TDP-43 models [27,29,30]. We detect TDP-43 and FUS in both the nucleus and the cytoplasm of motor neurons from young adult (Day 1) transgenics. The preferential toxicity of mutant TDP-43 and FUS alleles along with their cytoplasmic accumulation suggests our models may recapitulate aspects of neurotoxicity relevant to the disease state.

With no clear mechanism for TDP-43 and FUS neuronal toxicity it is currently not possible to design *in vitro* assays for high-throughput drug screening. Thus the further development and characterization of *in vivo* models for neurodegeneration will guide studies in mammalian systems. We believe our models strike an optimal balance between strong, age-dependent phenotypes and the expression of mutant proteins in relatively few neurons and may be useful for modifier screening. In terms of sensitivity, genetic mechanisms and/or small molecules need only to work on 26 neurons to achieve suppression. In terms of speed, our transgenics offer the possibility of medium-throughput suppressor screening based on the accelerated paralysis phenotype of mTDP-43 and mFUS worms grown in liquid culture. mTDP-43 and mFUS cause neuronal dysfunction in advance of motor neuron degeneration. The path from protein misfolding to neuronal dysfunction and cell death takes many decades in humans and it may be more efficient to target therapies to early pathogenic stages. Thus using simple systems to screen for suppression of neuronal dysfunction may be useful to prevent subsequent neurodegeneration.

A number of models for TDP-43 and FUS toxicity in various systems have been described, but there is still no clear answer whether TDP-43 and FUS neuronal toxicity are due to a loss/gain of function of these proteins individually or together in some common genetic pathway [44–46]. Furthermore it is still unclear if all TDP-43 and FUS mutations share similar pathogenic mechanisms but having similarly constructed models for each may address this question. Now that we have validated the *unc-47* motor neuron approach for modelling toxicity, future work will focus on the development of new transgenics with additional TDP-43 and FUS mutations.

We present here novel transgenics for investigating age-dependent motor neuron toxicity caused by mutant TDP-43 and FUS. We expect these strains will be useful for identifying genetic and chemical suppressors to give insights into disease mechanisms and support the development of new therapies for age-dependent neurodegeneration.

Materials and Methods

Nematode strains

Standard methods of culturing and handling worms were used [47]. Worms were maintained on standard NGM plates streaked with OP50 *E. coli*. Strains used in this study were obtained from the *C. elegans* Genetics Center (University of Minnesota, Minne-

apolis) and include: N2, *oxIs12[unc-47p::GFP+lin-15]*, *unc-47(e307)*, *unc-47(gk192)* and *unc-119(ed3)*.

Transgenic TDP-43 and FUS worms

Human cDNAs for wild type and mutant TDP-43[A315T], and wild type and mutant FUS-TLS[S57Δ] were obtained from Dr. Guy Rouleau (CRCHUM, Université de Montréal). The cDNAs were amplified by PCR and cloned into the Gateway vector pDONR221 following the manufacturer's protocol (Invitrogen). Multisite Gateway recombination was performed with the pDONR TDP-43 and FUS clones along with clones containing the *unc-47* promoter (kind gift from Dr. Erik Jorgensen, University of Utah), the *unc-54* 3'UTR plasmid pCM5.37 (Dr. Geraldine Seydoux, Johns Hopkins, Addgene plasmid 17253) and the destination vector pCFJ150 to create *unc-47::TDP-43* and *unc-47::FUS* expression vectors. Transgenic lines were created by microinjection of *unc-119(ed3)* worms, multiple lines were generated and strains behaving similarly were kept for further analysis. Transgenes were integrated by UV irradiation and lines were outcrossed to wild type N2 worms 5 times before use. The main strains used in this study include: *xqIs132[unc-47::TDP-43-WT;unc-119(+)]*, *xqIs133[unc-47::TDP-43[A315T];unc-119(+)]*, *xqIs173[unc-47::FUS-WT;unc-119(+)]*, and *xqIs98[unc-47::FUS[S57Δ];unc-119(+)]*.

Paralysis assays on plates

For worms expressing TDP-43 or FUS, 20–30 adult day 1 animals were picked to NGM plates and scored daily for movement. Animals were counted as paralyzed if they failed to move upon prodding with a worm pick. Worms were scored as dead if they failed to move their head after being prodded in the nose and showed no pharyngeal pumping. All experiments were conducted at 20°C.

Lifespan assays

Worms were grown on NGM-FUDR plates to prevent progeny from hatching. 20 animals/plate by triplicates were tested at 20°C from adult day 1 until death. Worms were declared dead if they did not respond to tactile or heat stimulus. Survival curves were produced and compared using the Log-rank (Mantel-Cox) test.

Aldicarb test

To evaluate synaptic transmission, worms were grown on NGM and transferred to NGM plates +1 mM aldicarb at adult day 1. Paralysis was scored after 1 and 2 hours on aldicarb plates. Animals were counted as paralyzed if they failed to move upon prodding with a worm pick. All tests were performed at 20°C.

Liquid culture protocol

Synchronized populations of worms were obtained by hypochlorite extraction. Young adult worms were distributed in 96-wells plate (20 µl per well; 20–30 worms per well), containing DMSO or test compounds and incubated for up to 6 h at 20°C on a shaker. The motility test was assessed by stereomicroscopy. Videos of worms were taken with on an Olympus S7x7 stereomicroscope equipped with a Grasshopper GRAS-03K2M camera using Flycap software (Point Grey Research) at a rate of 300 frames per second.

Immunostaining of whole worms

Age synchronized, adult day 1, whole worms were fixed and stained as described in WormBook [48]. Antibodies used include:

rabbit anti-TDP-43 (1:50, Proteintech), rabbit anti-FUS/TLS (1:50, AbCam), and rabbit anti-GABA (1:50, Proteintech).

Fluorescence microscopy

For scoring gaps/breaks from TDP-43 and FUS transgenics, synchronized animals were selected at days 1, 5 and 9 of adulthood for visualization of motor neurons *in vivo*. Animals were immobilized in M9 with 5 mM levamisole and mounted on slides with 2% agarose pads. Motor neurons were visualized with a Leica 6000 microscope and a Leica DFC 480 camera. A minimum of 100 animals was scored per treatment over 4–6 trials. The mean and SEM were calculated for each trial and two-tailed t-tests were used for statistical analysis.

Worm lysates

Worms were collected in M9 buffer, washed 3 times with M9 and pellets were placed at -80°C overnight. Pellets were lysed in RIPA buffer (150 mM NaCl, 50 mM Tris pH 7.4, 1% Triton X-100, 0.1% SDS, 1% sodium deoxycholate)+0.1% protease inhibitors (10 mg/ml leupeptin, 10 mg/ml pepstatin A, 10 mg/ml chymostatin LPC; 1/1000). Pellets were passed through a 27_{1/2} G syringe 10 times, sonicated and centrifuged at 16000g. Supernatants were collected.

Protein quantification

All supernatants were quantified with the BCA Protein Assay Kit (Thermo Scientific) following the manufacturer instructions.

Protein solubility

For TDP-43 and FUS transgenics soluble/insoluble fractions, worms were lysed in Extraction Buffer (1 M Tris-HCl pH 8, 0.5 M EDTA, 1 M NaCl, 10% NP40+protease inhibitors (LPC; 1/1000)). Pellets were passed through a 27_{1/2} G syringe 10 times, sonicated and centrifuged at 10000g for 5 min. The soluble supernatant was saved and the remaining pellet was resuspended in extraction buffer, sonicated and centrifuged at 10000g for 5 min. The remaining pellet was resuspended into 100 μl of RIPA buffer, sonicated until the pellet was resuspended in solution and saved.

Immunoblots

Worm RIPA samples (175 μg /well) were resuspended directly in 1 \times Laemmli sample buffer, migrated in 12.5% or 10% polyacrylamide gels, transferred to nitrocellulose membranes (BioRad) and immunoblotted. Antibodies used: rabbit anti-human-TDP-43 (1:200, Proteintech), rabbit anti-human-FUS/TLS (1:200, AbCam), and mouse anti-actin (1:10000, MP Biomedical). Blots were visualized with peroxidase-conjugated secondary antibodies and ECL Western Blotting Substrate (Thermo Scientific). Densitometry was performed with Photoshop (Adobe).

Statistics

For paralysis and stress-resistance tests, survival curves were generated and compared using the Log-rank (Mantel-Cox) test,

and 60–100 animals were tested per genotype and repeated at least three times. For image analysis statistical significance was determined by Student's t-test and the results shown as mean \pm standard error. Prism 5 (GraphPad Software) was used for all statistical analyses.

Supporting Information

Table S1 Lifespan analysis for all experiments.
(PDF)

Video S1 mTDP-43 worms in liquid culture at time 0.
(MOV)

Video S2 mTDP-43 worms after 6 hours in liquid culture.
(MOV)

Video S3 mFUS worms in liquid culture at time 0.
(MOV)

Video S4 mFUS worms after 6 hours in liquid culture.
(MOV)

Video S5 wtTDP-43 worms in liquid culture at time 0.
(MOV)

Video S6 wtTDP-43 worms after 6 hours in liquid culture.
(MOV)

Video S7 wtFUS worms in liquid culture at time 0.
(MOV)

Video S8 wtFUS worms after 6 hours in liquid culture.
(MOV)

Video S9 N2 worms in liquid culture at time 0.
(MOV)

Video S10 N2 worms after 6 hours in liquid culture.
(MOV)

Video S11 *unc-47p::GFP* worms in liquid culture at time 0.
(MOV)

Video S12 *unc-47p::GFP* worms after 6 hours in liquid culture.
(MOV)

Acknowledgments

We thank S. Peyrard, E. Bourgeois and S. Al Ameri for technical support, H. Catoire for critical reading of the manuscript, and Dr. E. Jorgensen for the *unc-47* plasmid.

Author Contributions

Conceived and designed the experiments: JAP. Performed the experiments: AV AT DA. Analyzed the data: AV JAP. Contributed reagents/materials/analysis tools: GAR PD. Wrote the paper: AV JAP.

References

- Boillee S, Vande Velde C, Cleveland DW (2006) ALS: a disease of motor neurons and their nonneuronal neighbors. *Neuron* 52: 39–59.
- Lomen-Hoerth C (2008) Amyotrophic lateral sclerosis from bench to bedside. *Semin Neurol* 28: 205–211.
- Neumann M, Sampathu DM, Kwong LK, Truax AC, Micsenyi MC, et al. (2006) Ubiquitinated TDP-43 in frontotemporal lobar degeneration and amyotrophic lateral sclerosis. *Science* 314: 130–133.
- Gitcho MA, Baloh RH, Chakraverty S, Mayo K, Norton JB, et al. (2008) TDP-43 A315T mutation in familial motor neuron disease. *Ann Neurol*.
- Kabashi E, Valdmanis PN, Dion P, Spiegelman D, McConkey BJ, et al. (2008) TARDBP mutations in individuals with sporadic and familial amyotrophic lateral sclerosis. *Nat Genet*.
- Sreedharan J, Blair IP, Tripathi VB, Hu X, Vance C, et al. (2008) TDP-43 mutations in familial and sporadic amyotrophic lateral sclerosis. *Science* 319: 1668–1672.
- Vance C, Rogelj B, Hortobagyi T, De Vos KJ, Nishimura AL, et al. (2009) Mutations in FUS, an RNA processing protein, cause familial amyotrophic lateral sclerosis type 6. *Science* 323: 1208–1211.

8. Deng HX, Chen W, Hong ST, Boycott KM, Gorrie GH, et al. (2011) Mutations in UBQLN2 cause dominant X-linked juvenile and adult-onset ALS and ALS/dementia. *Nature*.
9. Mackenzie IR, Rademakers R, Neumann M (2010) TDP-43 and FUS in amyotrophic lateral sclerosis and frontotemporal dementia. *Lancet Neurol* 9: 995–1007.
10. Lagier-Tourenne C, Polymenidou M, Cleveland DW (2010) TDP-43 and FUS/TLS: emerging roles in RNA processing and neurodegeneration. *Hum Mol Genet* 19: R46–64.
11. Kim SH, Shanware NP, Bowler MJ, Tibbetts RS (2010) Amyotrophic lateral sclerosis-associated proteins TDP-43 and FUS/TLS function in a common biochemical complex to co-regulate HDAC6 mRNA. *J Biol Chem* 285: 34097–34105.
12. Ling SC, Albuquerque CP, Han JS, Lagier-Tourenne C, Tokunaga S, et al. (2010) ALS-associated mutations in TDP-43 increase its stability and promote TDP-43 complexes with FUS/TLS. *Proc Natl Acad Sci U S A* 107: 13318–13323.
13. McIntire SL, Reimer RJ, Schuske K, Edwards RH, Jorgensen EM (1997) Identification and characterization of the vesicular GABA transporter. *Nature* 389: 870–876.
14. Evans TC (2006) Transformation and microinjection. *WormBook*. pp 1–15.
15. Belzil VV, Valdmanis PN, Dion PA, Daoud H, Kabashi E, et al. (2009) Mutations in FUS cause FALS and SALS in French and French Canadian populations. *Neurology* 73: 1176–1179.
16. Cohen E, Bieschke J, Perciavalle RM, Kelly JW, Dillin A (2006) Opposing activities protect against age-onset proteotoxicity. *Science* 313: 1604–1610.
17. Steinkraus KA, Smith ED, Davis C, Carr D, Pendergrass WR, et al. (2008) Dietary restriction suppresses proteotoxicity and enhances longevity by an hsf-1-dependent mechanism in *Caenorhabditis elegans*. *Aging Cell* 7: 394–404.
18. Collins JJ, Huang C, Hughes S, Kornfeld K (2008) The measurement and analysis of age-related changes in *Caenorhabditis elegans*. *WormBook*. pp 1–21.
19. Earls LR, Hacker ML, Watson JD, Miller DM, 3rd (2010) Coenzyme Q protects *Caenorhabditis elegans* GABA neurons from calcium-dependent degeneration. *Proc Natl Acad Sci U S A* 107: 14460–14465.
20. Herndon LA, Schmeissner PJ, Dudaronek JM, Brown PA, Listner KM, et al. (2002) Stochastic and genetic factors influence tissue-specific decline in ageing *C. elegans*. *Nature* 419: 808–814.
21. Jorgensen EM (2005) Gaba. *WormBook*. pp 1–13.
22. McIntire SL, Jorgensen E, Kaplan J, Horvitz HR (1993) The GABAergic nervous system of *Caenorhabditis elegans*. *Nature* 364: 337–341.
23. Mahoney TR, Luo S, Nonet ML (2006) Analysis of synaptic transmission in *Caenorhabditis elegans* using an aldicarb-sensitivity assay. *Nat Protoc* 1: 1772–1777.
24. Loria PM, Hodgkin J, Hobert O (2004) A conserved postsynaptic transmembrane protein affecting neuromuscular signaling in *Caenorhabditis elegans*. *J Neurosci* 24: 2191–2201.
25. Vashlishan AB, Madison JM, Dybbs M, Bai J, Sieburth D, et al. (2008) An RNAi screen identifies genes that regulate GABA synapses. *Neuron* 58: 346–361.
26. Saxena S, Caroni P (2011) Selective neuronal vulnerability in neurodegenerative diseases: from stressor thresholds to degeneration. *Neuron* 71: 35–48.
27. Liachko NF, Guthrie CR, Kraemer BC (2010) Phosphorylation Promotes Neurotoxicity in a *Caenorhabditis elegans* Model of TDP-43 Proteinopathy. *J Neurosci* 30: 16208–16219.
28. Johnson BS, McCaffery JM, Lindquist S, Gitler AD (2008) A yeast TDP-43 proteinopathy model: Exploring the molecular determinants of TDP-43 aggregation and cellular toxicity. *Proc Natl Acad Sci U S A*.
29. Ash PE, Zhang YJ, Roberts CM, Saldi T, Hutter H, et al. (2010) Neurotoxic effects of TDP-43 overexpression in *C. elegans*. *Hum Mol Genet*.
30. Zhang T, Mullane PC, Periz G, Wang J (2011) TDP-43 neurotoxicity and protein aggregation modulated by heat shock factor and insulin/IGF-1 signaling. *Hum Mol Genet*.
31. Swarup V, Phaneuf D, Bareil C, Robertson J, Rouleau GA, et al. (2011) Pathological hallmarks of amyotrophic lateral sclerosis/frontotemporal lobar degeneration in transgenic mice produced with TDP-43 genomic fragments. *Brain*.
32. Li Y, Ray P, Rao EJ, Shi C, Guo W, et al. (2010) A *Drosophila* model for TDP-43 proteinopathy. *Proc Natl Acad Sci U S A* 107: 3169–3174.
33. Murakami T, Yang SP, Xie L, Kawano T, Fu D, et al. (2011) ALS mutations in FUS causes neuronal dysfunction and death in *C. elegans* by a dominant gain-of-function mechanism. *Hum Mol Genet*.
34. McDonald PW, Hardie SL, Jessen TN, Carvelli L, Matthies DS, et al. (2007) Vigorous motor activity in *Caenorhabditis elegans* requires efficient clearance of dopamine mediated by synaptic localization of the dopamine transporter DAT-1. *J Neurosci* 27: 14216–14227.
35. Catoire H, Pasco MY, Abu-Baker A, Holbert S, Tourette C, et al. (2008) Sirtuin Inhibition Protects from the Polyalanine Muscular Dystrophy Protein PABPN1. *Hum Mol Genet*.
36. Wang J, Farr GW, Hall DH, Li F, Furtak K, et al. (2009) An ALS-linked mutant SOD1 produces a locomotor defect associated with aggregation and synaptic dysfunction when expressed in neurons of *Caenorhabditis elegans*. *PLoS Genet* 5: e1000350.
37. Caramia MD, Palmieri MG, Desiato MT, Iani C, Scalise A, et al. (2000) Pharmacologic reversal of cortical hyperexcitability in patients with ALS. *Neurology* 54: 58–64.
38. Vucic S, Nicholson GA, Kiernan MC (2008) Cortical hyperexcitability may precede the onset of familial amyotrophic lateral sclerosis. *Brain* 131: 1540–1550.
39. Kiernan MC, Vucic S, Cheah BC, Turner MR, Eisen A, et al. (2011) Amyotrophic lateral sclerosis. *Lancet* 377: 942–955.
40. Pasinelli P, Brown RH (2006) Molecular biology of amyotrophic lateral sclerosis: insights from genetics. *Nat Rev Neurosci* 7: 710–723.
41. Dion PA, Daoud H, Rouleau GA (2009) Genetics of motor neuron disorders: new insights into pathogenic mechanisms. *Nat Rev Genet* 10: 769–782.
42. Ju S, Tardiff DF, Han H, Divya K, Zhong Q, et al. (2011) A yeast model of FUS/TLS-dependent cytotoxicity. *PLoS Biol* 9: e1001052.
43. Lanson NA, Jr., Maltre A, King H, Smith R, Kim JH, et al. (2011) A *Drosophila* model of FUS-related neurodegeneration reveals genetic interaction between FUS and TDP-43. *Hum Mol Genet* 20: 2510–2523.
44. Kabashi E, Bercier V, Lissouba A, Liao M, Brustein E, et al. (2011) FUS and TARDBP but not SOD1 interact in genetic models of Amyotrophic Lateral Sclerosis. *PLoS Genet*; in press.
45. Kabashi E, Lin L, Tradewell ML, Dion PA, Bercier V, et al. (2009) Gain and loss of function of ALS-related mutations of TARDBP (TDP-43) cause motor deficits in vivo. *Hum Mol Genet* 19: 671–683.
46. Wang JW, Brent JR, Tomlinson A, Shneider NA, McCabe BD (2011) The ALS-associated proteins FUS and TDP-43 function together to affect *Drosophila* locomotion and life span. *J Clin Invest*.
47. Stiernagle T (2006) Maintenance of *C. elegans*. *WormBook*. pp 1–11.
48. Duerr JS (2006) Immunohistochemistry. *WormBook*. pp 1–61.

Methylene Blue Protects against TDP-43 and FUS Neuronal Toxicity in *C. elegans* and *D. rerio*

Alexandra Vaccaro^{1,2,3}, Shunmoogum A. Patten^{2,3}, Sorana Ciura^{2,3}, Claudia Maios², Martine Therrien^{1,2,3}, Pierre Drapeau^{2,3}, Edor Kabashi^{2*α}, J. Alex Parker^{1,2,3*}

1 Université de Montréal Hospital Research Centre, Montréal, Québec, Canada, **2** Département de pathologie et biologie cellulaire and Groupe de recherche sur le système nerveux central, Université de Montréal, Montréal, Canada, **3** Centre of Excellence in Neuromics, Université de Montréal, Montréal, Canada

Abstract

The DNA/RNA-binding proteins TDP-43 and FUS are found in protein aggregates in a growing number of neurodegenerative diseases, including amyotrophic lateral sclerosis (ALS) and related dementia, but little is known about the neurotoxic mechanisms. We have generated *Caenorhabditis elegans* and zebrafish animal models expressing mutant human TDP-43 (A315T or G348C) or FUS (S57Δ or R521H) that reflect certain aspects of ALS including motor neuron degeneration, axonal deficits, and progressive paralysis. To explore the potential of our humanized transgenic *C. elegans* and zebrafish in identifying chemical suppressors of mutant TDP-43 and FUS neuronal toxicity, we tested three compounds with potential neuroprotective properties: lithium chloride, methylene blue and riluzole. We identified methylene blue as a potent suppressor of TDP-43 and FUS toxicity in both our models. Our results indicate that methylene blue can rescue toxic phenotypes associated with mutant TDP-43 and FUS including neuronal dysfunction and oxidative stress.

Citation: Vaccaro A, Patten SA, Ciura S, Maios C, Therrien M, et al. (2012) Methylene Blue Protects against TDP-43 and FUS Neuronal Toxicity in *C. elegans* and *D. rerio*. PLoS ONE 7(7): e42117. doi:10.1371/journal.pone.0042117

Editor: Weidong Le, Baylor College of Medicine, Jiao Tong University School of Medicine, United States of America

Received: March 9, 2012; **Accepted:** July 2, 2012; **Published:** July 27, 2012

Copyright: © 2012 Vaccaro et al. This is an open-access article distributed under the terms of the Creative Commons Attribution License, which permits unrestricted use, distribution, and reproduction in any medium, provided the original author and source are credited.

Funding: This research was supported by: Montreal University Hospital Foundation (<http://fondationduchum.com/fr>) to JAP, Canadian Institutes of Health Research New Investigator Award (<http://www.cihr-irsc.gc.ca>) to JAP, Frick Foundation for ALS Research (<http://frick-foundation.ch>) to JAP, EK, PD, and a Bernice Ramsay Discovery Grant from the ALS Society of Canada (<http://www.als.ca/>) to JAP. Genome Québec to EK and PD. The funders had no role in study design, data collection and analysis, decision to publish, or preparation of the manuscript.

Competing Interests: The authors have declared that no competing interests exist.

* E-mail: edor.kabashi@icm-institute.org (EK); or ja.parker@umontreal.ca (JAP)

α Current address: Institut du Cerveau et de la Moelle épinière, Centre de Recherche, CHU Pitié-Salpêtrière, Paris, France.

Introduction

ALS is a late-onset progressive neurodegenerative disease affecting motor neurons and ultimately resulting in fatal paralysis [1,2]. The majority of cases are sporadic but ~10% of patients have an inherited familial form of the disease. Dominant mutations in SOD1 (copper/zinc superoxide dismutase 1) account for ~20% of familial ALS cases and ~1% of sporadic cases [1]. A recent biochemical approach identified cytosolic aggregates of TDP-43 in ALS and frontotemporal lobar dementia pathological tissue [3]. This breakthrough discovery was quickly followed by the identification of TDP-43 mutations in ALS patients by numerous groups [3–6]. TDP-43 is a multifunctional RNA/DNA binding protein and mutations in the related protein FUS have also been found in ALS patients [7] though the molecular pathology induced by mutant TDP-43 and FUS is not understood. The mislocalization and subsequent aggregation of TDP-43 has been observed in pathological tissue obtained from a number of neurological disorders including frontotemporal lobar dementia, Parkinson's disease, polyglutamine diseases and several myopathies [8]. Similarly, FUS inclusions have been observed in clinically distinct forms of frontotemporal lobar dementia and the polyglutamine diseases [8] suggesting that TDP-43 and FUS may be a common pathogenic factor in neurodegeneration. Furthermore, TDP-43 and FUS interact genetically (though not with SOD1) in zebrafish [9] and *Drosophila* [10] indicating that

they may act in a common pathway. In the absence of knowledge concerning the biochemical defects caused by these ALS-related mutations in TDP-43 and FUS, the use of *in vivo* models is currently the most promising approach available to further our understanding of pathogenic mechanisms as well as for therapeutic discovery for ALS.

Indeed a number of chemical and drug screens have been published using *in vivo* models such as *C. elegans* and zebrafish [11–14]. These model organisms offer several advantages over mouse models for cheaper, faster and large-scale initial drug screening and target characterization. For instance, it is possible to rapidly produce large numbers of mutant offspring that can be assayed in liquid culture in multiwell plates and treated with various compounds to determine if disease phenotypes are rescued. Moreover, these organisms have relatively short reproductive cycles, they are easy to manipulate genetically, and their transparency permits visual assessment of developing cells and organs. Also, biochemical pathways are highly conserved between *C. elegans*, zebrafish and humans. We developed novel *in vivo* genetic models of mutant human TDP-43 and FUS in *C. elegans* [15] and zebrafish [9,16,17]. Our models exhibit several aspects of ALS including motor neuron degeneration, axonal deficits and progressive paralysis. The goal of this study was to test the ability of our *in vivo* models to identify neuroprotective compounds and determine their suitability as a platform for pre-clinical drug discovery in ALS. We focused on three compounds with known

neuroprotective properties in an attempt to identify small molecules that might rescue disease phenotypes observed in our models. Here, we show that methylene blue (MB) restores normal motor phenotypes in *C. elegans* and zebrafish ALS models.

Results

Methylene blue rescues mutant TDP-43 and FUS behavioral phenotypes in *C. elegans*

Using *C. elegans* transgenics that express mutant TDP-43 or FUS (TDP-43[A315T] or FUS[S57Δ], referred to herein as mTDP-43 and mFUS respectively) in motor neurons [15] we evaluated the efficacy of these models as drug discovery tools by testing three compounds with known clinically neuroprotective properties: lithium chloride, MB and riluzole [18,19]. The mTDP-43 and mFUS transgenic worms show adult-onset, progressive motility defects leading to paralysis when grown under standard laboratory conditions on solid agar plates over the course of 10 to 12 days [15]. However, worms grown in liquid culture exhibit a swimming behavior that is more vigorous than crawling on plates and accelerates neuronal dysfunction in the TDP-43 and FUS transgenics [15]. As a result, paralysis phenotypes manifest in a matter of hours instead of days. We took advantage of this phenomenon to develop a chemical screening assay to identify compounds that suppress the acute paralysis of mTDP-43 and mFUS transgenic worms grown in liquid culture. With this assay we tested if lithium chloride, MB or riluzole could suppress the paralysis caused by mTDP-43 and mFUS (**Figure 1**). Of the three compounds tested, we observed that MB reduced the rate of paralysis for mTDP-43 and mFUS transgenics with no effect on wild type TDP-43 (wtTDP-43) or wild type FUS (wtFUS) control strains (**Figures 1B, 1E**). Furthermore MB had no significant effect on movement phenotypes for wild type, non-transgenic N2 worms (**Figure S1A**).

To ensure that suppression of paralysis was not an artifact of the liquid culture assay and to confirm that MB retained its rescuing activity in the context of aging we retested it at two doses (6 and 60 μ M) for mTDP-43 and mFUS worms grown on plates and observed a reduction in the rates of paralysis for treated animals compared to untreated controls (**Figures 2A, B**). The paralysis phenotype likely results from impaired synaptic transmission at the neuromuscular junction as shown by the hypersensitivity of the mTDP-43 worms to the acetylcholine esterase inhibitor aldicarb. mTDP-43 animals treated with MB showed reduced sensitivity to aldicarb, matching the response from control strains, suggesting that MB restores synaptic function in animals expressing mutant proteins (**Figure 2C**). Transgenic *C. elegans* expressing ALS-related mutations mTDP-43 or mFUS in motor neurons also show age-dependent degeneration most frequently observed as gaps or breaks along neuronal processes [15]. These neurodegenerative phenotypes were significantly reduced by treatment with MB (**Figures 2D, E, F**) and did not change mTDP-43 or mFUS transgene expression (**Figures 2G, H**).

Methylene blue rescues motor phenotypes in mutant TDP-43 and FUS zebrafish

To test if MB had protective effects beyond *C. elegans* we turned to zebrafish. First, as in worms, we observed that MB had no effect on the movement phenotypes of wild type non-transgenic fish (**Figure S1B, C, D, E**). Zebrafish expressing mTDP-43[G348C] or mFUS[R521H] have impaired swimming as assessed by their ability to produce a touch-evoked escape response (TEER) [9,16]. mTDP-43 fish showed a greatly reduced TEER compared to non-transgenic or wtTDP-43 fish (**Figure 3A**). mTDP-43 fish treated

with 60 μ M MB showed improved swimming response including swim duration, distance swam and maximum swim velocity (**Figures 3A, B, C, D**). Zebrafish expressing mFUS also show greatly reduced swimming activity compared to wild type or wtFUS fish and the swimming phenotype of mFUS fish was greatly improved when treated with 60 μ M MB (**Figures 3E, F, G, H**). Besides behavioral defects, immunohistochemical analyses show that transgenic zebrafish expressing mTDP-43 or mFUS also displayed abnormally shortened and branched motor neuron axonal processes as observed by the unbranched axonal length (UAL) quantification [9,16] and this phenotype was rescued by incubation with either 30 or 60 μ M MB (**Figures 4A, B**). These results demonstrate that MB can significantly reduce the motor neuron phenotypes elicited by expression of mTDP-43 and mFUS both in *C. elegans* and zebrafish genetic models of disease.

Methylene blue protects against oxidative stress in *C. elegans* and zebrafish

Since we observed that MB rescued paralysis in transgenic models of mTDP-43 or mFUS, we sought to further examine the protective effects of MB in an aging and stress context. First, MB treatment had no effect on the lifespan of wild type N2 worms suggesting that its cellular protection mechanisms are not due to non-specific effects from extended longevity (**Figure 5A, Table S1**). To test for protective effects against environmental stress we tested wild type N2 worms for their ability to withstand lethal exposure to thermal, hyperosmotic or oxidative stresses. We observed that MB offered no protection to worms subjected to elevated temperature or hyperosmotic stress from treatment with NaCl as their survival rate was indistinguishable from untreated control animals (**Figures 5B, C**). Juglone is a natural aromatic compound found in the black walnut tree that induces high levels of oxidative stress within cells [20]. Juglone is highly toxic to wild type N2 worms and causes complete mortality after approximately 4 hours in our assay. We observed that MB provided significant protection against oxidative stress since wild type N2 worms were resistant to juglone in a dose dependent manner (**Figure 5D**). These data suggest that MB is specific in its cell protection capabilities and helps overcome oxidative stress conditions in *C. elegans*.

Since we showed that MB confers protection to wild type N2 worms under oxidative stress in a dose dependent manner we hypothesized that MB may help reduce oxidative damage in mTDP-43 worms. To test this hypothesis we stained our TDP-43 transgenic strain with dihydrofluorescein diacetate (DHF), a compound known to fluoresce when exposed to intracellular peroxides associated with oxidative stress [21]. We observed no DHF signal from wtTDP-43 transgenics but strong fluorescence from mTDP-43 worms (**Figure 6A**). The fluorescence observed in the mTDP-43 transgenics was reduced when treated with 60 μ M MB (**Figure 6A**). We observed a similar effect with our FUS transgenics, with no DHF signal from wtFUS animals, but strong fluorescence from mFUS worms that was reduced upon MB treatment (**Figure 6B**). Extending our findings we examined oxidative stress with DHF in mTDP-43 and mFUS fish. Similar to worms, we observed a strong fluorescent signal in mTDP-43 fish compared to non-transgenic or wtTDP-43 fish and that this signal was reduced by treatment with MB (**Figures 6C, D**). MB also reduced the fluorescent signal in mFUS fish stained with DHF (**Figure 6E**). These data suggest that MB reduces the general level of oxidative status generated by the expression of mutant proteins *in vivo*.

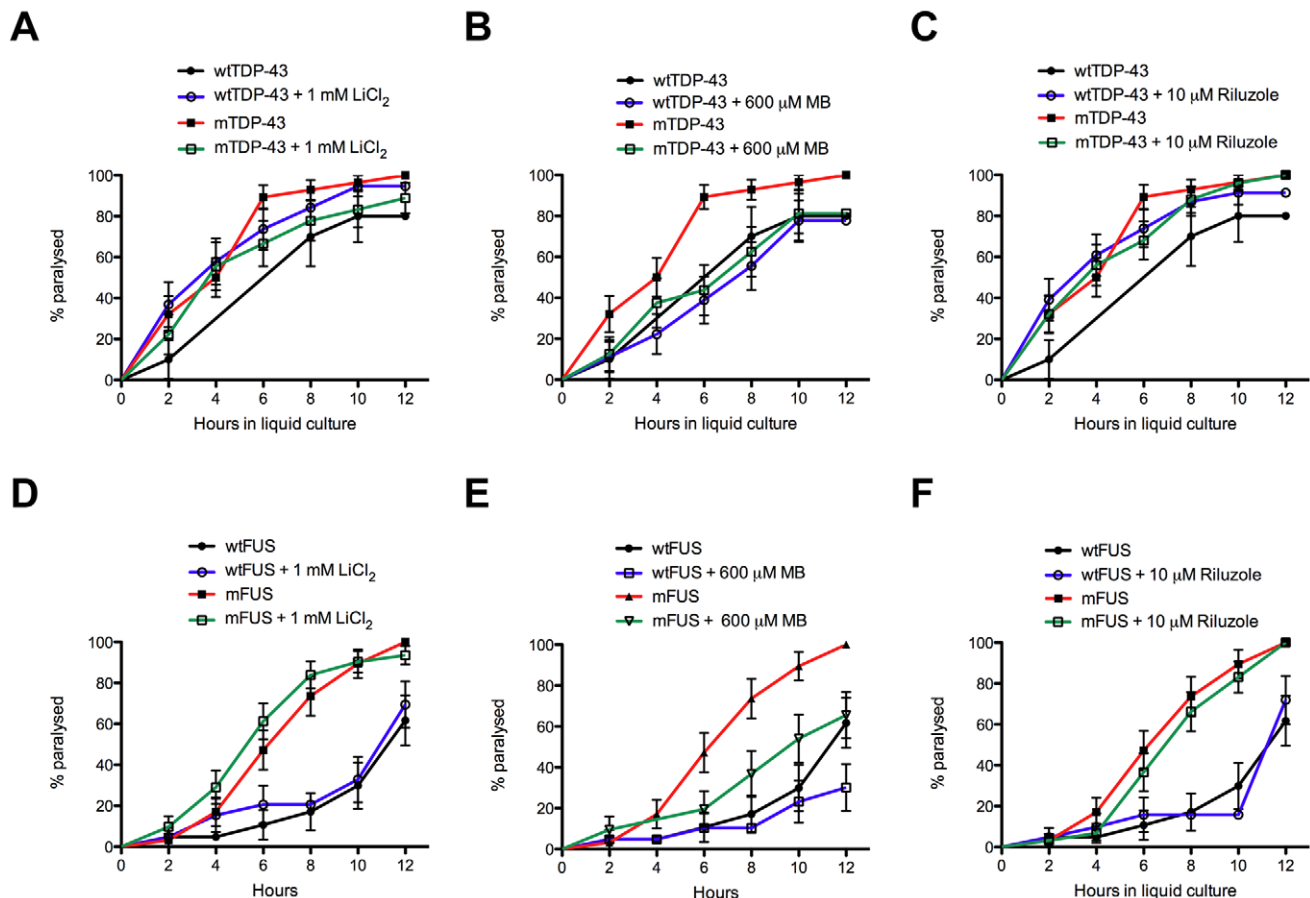


Figure 1. Methylene blue suppresses mTDP-43 and mFUS associated paralysis in *C. elegans*. We screened for suppression of TDP-43 (A–C) and FUS (B–D) induced paralysis in liquid culture by lithium chloride (LiCl₂), methylene blue (MB) or riluzole. MB significantly reduced the rate of paralysis in (B) mTDP-43 and (D) mFUS transgenics compared to untreated mutant transgenic worms ($P < 0.05$) with no effect on wild type transgenic controls.

doi:10.1371/journal.pone.0042117.g001

Reduced neuroprotection from late administration of methylene blue

In the previous experiments worms and fish were treated with MB from hatching. We tested whether the timing of treatment had an effect on the magnitude of neuroprotection by growing mTDP-43 worms on normal plates and transferring them at day 5 of adulthood to plates supplemented with MB. We observed that late administration of MB reduced paralysis with approximately 55% of treated animals becoming paralysed at day 12 of adulthood compared to a paralysis rate of approximately 80% for untreated animals (Figure 7). However the extent of rescue by late MB administration was far less than the approximate 10% paralysis rate observed for mTDP-43 animals grown on MB plates from hatching (Figure 2A). These data suggest that early administration of MB is more effective at reducing mTDP-43 toxicity than intervention in older animals.

Discussion

In this study we demonstrated that our *C. elegans* and zebrafish ALS models can be used to identify neuroprotective molecules which represents the first *in vivo* chemical genetic screening platform for ALS. With this platform we discovered that MB is a potent suppressor of mTDP-43 and mFUS motor neuron toxicity *in vivo*. In both worms and fish MB corrected motor deficits and

reduced the level of oxidative stress associated with the expression of mutant proteins.

MB is a pleiotropic molecule with a long and varied history of medical use [18] but in the context of neurodegeneration MB has been reported to prevent amyloid- β and tau aggregation *in vitro* [22,23]. A previous study also showed that the treatment of cells with MB inhibited the formation of TDP-43 aggregates [24] suggesting this compound might be appropriate for the treatment of ALS and other dementias. The efficacy of MB as a neuroprotective compound has been examined in Alzheimer's disease and ALS models where in some studies it is protective while in others it has no effect [24–28]. We decided to include this compound in our assay from which we identified MB as a potent suppressor of mTDP-43 and mFUS toxicity in both *C. elegans* and zebrafish. However, our data do not agree with a recent study examining the effects of MB in a TDP-43 mouse model [26]. Mutant TDP-43[G348C] mice treated with MB showed no improvement in motor phenotypes as determined by the rotarod assay. Furthermore no difference in the cytoplasmic localization of TDP-43 was observed in treated mice.

Worms and fish live in aqueous media and a simple explanation for their greater susceptibility may be that they are more permeable to MB. We further hypothesize that the differences in MB efficacy might also be due to variations in timing for delivery of the compound. Specifically, our worms and fish were treated

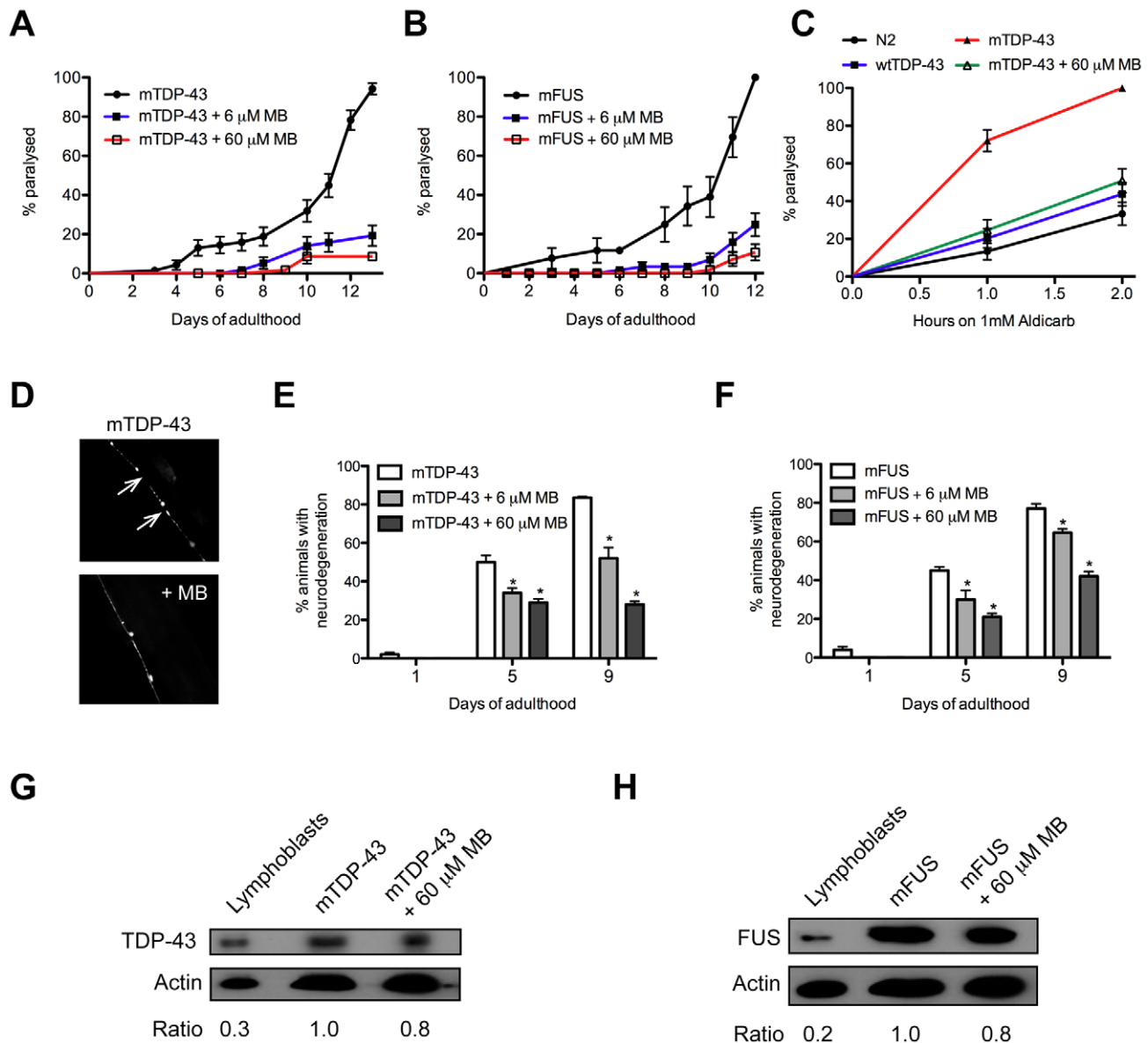


Figure 2. Methylene blue reduces TDP-43 and FUS neuronal toxicity. mTDP-43 and mFUS transgenics were grown on plates and assayed for various phenotypes. (A) MB reduced mTDP-43 induced paralysis in worms at two doses compared to untreated controls ($P < 0.001$). (B) MB at two doses reduced mFUS induced paralysis in worms compared to untreated controls ($P < 0.001$). (C) Aldicarb induced paralysis for mTDP-43 worms is significantly higher for mTDP-43 worms compared to non-transgenic N2 worms or transgenic wtTDP-43 controls ($P < 0.001$). MB reduced aldicarb induced paralysis of mTDP-43 worms back to non-transgenic N2 and wtTDP-43 levels. (D) Representative photos of motor neuron degeneration phenotypes observed in mTDP-43 transgenic worms. Similar phenotypes were observed for mFUS transgenics. Degeneration is most frequently seen as gaps (white arrows) along neuronal processes. MB reduced the age-dependent degeneration of motor neurons in (E) mTDP-43 and (F) mFUS transgenic worms ($*P < 0.001$ compared to untreated transgenics). MB did not affect the expression of mutant proteins in (G) mTDP-43 or (H) mFUS strains as determined by western blotting of protein extracts from transgenic worms grown with or without MB. Immunoblotting of human lymphoblasts was used as a size control.
doi:10.1371/journal.pone.0042117.g002

with MB from hatching whereas the TDP-43 mice were treated at 6 months. To confirm this hypothesis we treated mTDP-43 worms with MB at day 5 of adulthood and observed that late administration of the compound was significantly less effective at reducing paralysis. Thus, perhaps earlier (pre-clinical) treatment with MB may have greater effects in mouse models for ALS. Additionally there may be differences between the models since our worm and fish models capture a clinical aspect of ALS, namely progressive paralysis in animals expressing mTDP-43 that is absent from the TDP-43 mouse model.

Aging is a risk factor common to a number of neurodegenerative disorders including ALS, and oxidative stress is suspected to play a key role in the development of the disease by contributing to aging [29,30]. Indeed, interactions between genetic, environmental, and age-dependent risk factors have been hypothesized to trigger disease onset [31]. Consequently, we investigated the impact of MB treatment focusing on aging and stress response. Our *C. elegans* data are in agreement with the survival data from the mouse studies where we observed no effect on lifespan in MB treated worms even though there was a positive effect on multiple

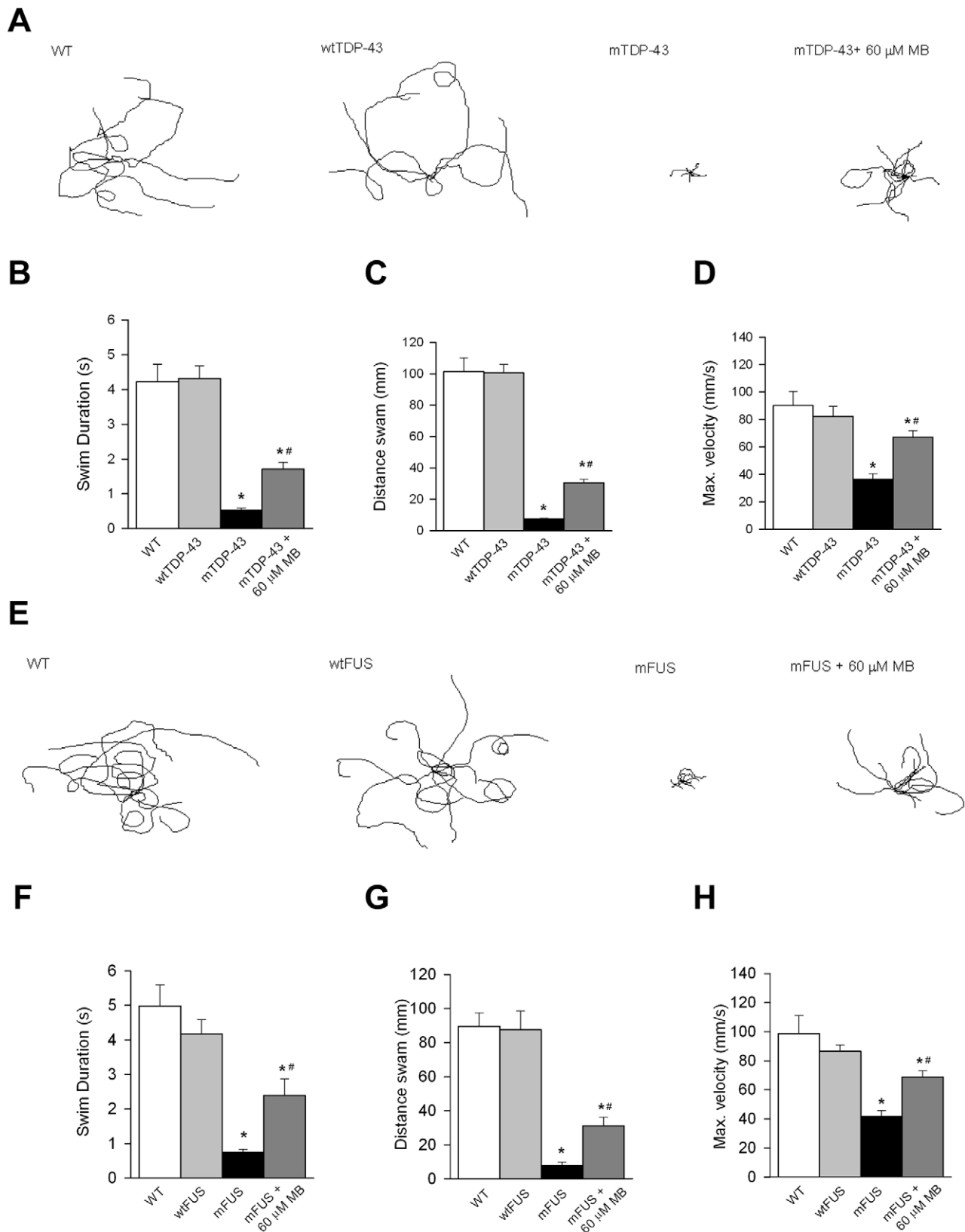


Figure 3. Methylene blue reduces motor deficits in zebrafish expressing mutant TDP-43 or FUS. (A) Representative traces of TEER phenotypes in wild type (WT), wtTDP-43, mTDP-43 and mTDP-43+MB. MB improved the swim duration (B), distance swam (C) and maximum swimming velocity (D) of mTDP-43 fish. (E) Representative traces of TEER phenotypes in WT, wtFUS, mFUS and mFUS+MB. Application of MB led to a significant improvement in the swim duration (F), distance swam (G) and maximum swimming velocity (H) of mTDP-43 fish. * denotes significant difference from WT, $P < 0.001$; # significantly different from mutant fish $P < 0.05$. doi:10.1371/journal.pone.0042117.g003

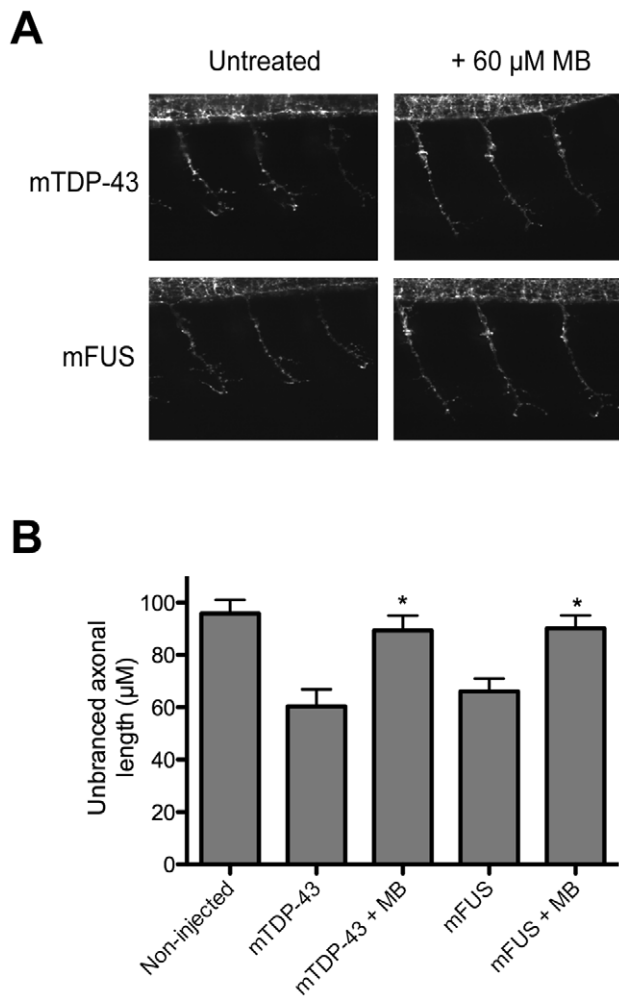


Figure 4. Methylene blue reduces axon defects in zebrafish expressing mutant TDP-43 or FUS. (A) Appearance of motor neurons in mTDP-43 and mFUS transgenic zebrafish with and without MB treatment. (B) MB reduced the unbranched axon length phenotype of motor neurons in mTDP-43 and mFUS transgenic zebrafish (* $P < 0.01$ compared to untreated transgenics). doi:10.1371/journal.pone.0042117.g004

phenotypes associated with mTDP-43 or mFUS. Thus, at least in simple systems lifespan effects can be uncoupled from neuroprotection but it remains to be seen if the same is true for mouse models of neurodegeneration.

In our previous work we showed that our TDP-43 and FUS transgenic *C. elegans* models exhibited no difference in lifespan compared to non-transgenic worms [15]. Thus, the paralysis phenotypes observed in our models specifically reflect the consequences of the expression of TDP-43 and FUS in motor neurons and are not due to secondary effects from general sickness and reduced lifespan. Therefore, it may be difficult to detect significant improvement on motor function or reflex phenotypes after MB treatment in mice showing generalized defects instead of treating problems resulting from TDP-43 or FUS proteotoxicity alone.

Finally, the TDP-43 mouse study did not examine the effects of MB on synaptic function or oxidative stress where we see clear effects in the worm and zebrafish models. MB can interact with nitric oxide synthase and also has an antioxidant potential by decreasing the generation of reactive oxygen species [32]. Using *C.*

elegans we showed that MB specifically decreased the sensitivity of wild type worms to oxidative stress. We also investigated the impact of MB treatment in the formation of reactive oxygen species in both *C. elegans* and *D. rerio* and have observed a significant reduction in the generation of reactive oxygen species. Consistent with the literature [33], our data suggest that MB counteracts oxidative stress to provide protection against proteotoxicity in both our *in vivo* models. Synaptic function was also restored after treatment with MB in transgenic mTDP-43 worms suggesting that this compound might also have an effect on synaptic transmission.

In summary, we present novel *in vivo* chemical genetic screening assays that may be useful for ALS drug discovery. Using two genetic models for ALS we report here that MB acts through reduction of oxidative stress and also restoration of normal synaptic function in genetic models of ALS. In addition, an important issue here is that in simple systems like *C. elegans*, lifespan effects can be uncoupled from neuroprotection. The next step will be to unravel MB's exact target and mechanism of action to develop compounds with more specific activities and also to capitalize on the strength of our assays to screen additional compounds as potential therapeutics in ALS.

Materials and Methods

C. elegans experiments

***C. elegans* strains.** Strains used in this study include: N2, *gas-1(fc21)*, *let-60(ga89)*, *oxIs12[unc-47p::GFP;lin-15(+)]*, *xqIs98[unc-47::FUS[S57Δ];unc-119(+)]*, *xqIs132[unc-47::TDP-43-WT;unc-119(+)]*, *xqIs133[unc-47::TDP-43[A315T];unc-119(+)]* and *xqIs173[unc-47::FUS-WT;unc-119(+)]*.

***C. elegans* liquid culture assay.** Young adult TDP-43 or FUS transgenic worms were distributed in 96-wells plate (20 μl per well; 20–30 worms per well), containing DMSO or test compounds and incubated for up to 12 hours at 20°C on a shaker. Compounds and final concentrations tested were 1 mM lithium chloride, 600 μM methylene blue, and 10 μM riluzole. The motility test was assessed by microscopy every 2 hours. Compounds were purchased from Sigma-Aldrich (St-Louis, MO).

***C. elegans* drug testing on plates.** Worms were grown on standard NGM plates with or without compounds. For worms expressing mFUS or mTDP-43, animals were counted as paralyzed if they failed to move upon prodding with a worm pick. Worms were scored as dead if they were immotile, showed no pharyngeal pumping and failed to move their head after being prodded in the nose. The final concentrations of methylene blue tested in plates either 6 or 60 μM.

Fluorescence microscopy. For scoring axons from transgenic mFUS and mTDP-43 worms, synchronized animals were selected at days 1, 5 and 9 of adulthood for visualization of motor neurons *in vivo* with the *unc-47p::GFP* transgenic reporter. Animals were immobilized in M9 with 5 mM levamisole and mounted on slides with 2% agarose pads. Motor neurons were visualized with a Leica CTR 6000 and a Leica DFC 480 camera. A minimum of 100 animals was scored per treatment over 4–6 trials. Animals showing gaps or breaks along motor neuron processes were scored as positive for the degeneration phenotype. The mean and SEM were calculated for each trial and two-tailed *t*-tests were used for statistical analysis. For visualization of fluorescence after treatment with dihydrofluorescein diacetate, L4 animals were grown on NGM plates or NGM plates with methylene blue and examined for fluorescence with the Leica system described above.

Lifespan assays. Worms were grown on NGM or NGM+60 μM methylene blue and transferred on NGM-FUDR or NGM-FUDR+60 μM methylene blue. 20 animals/plate by

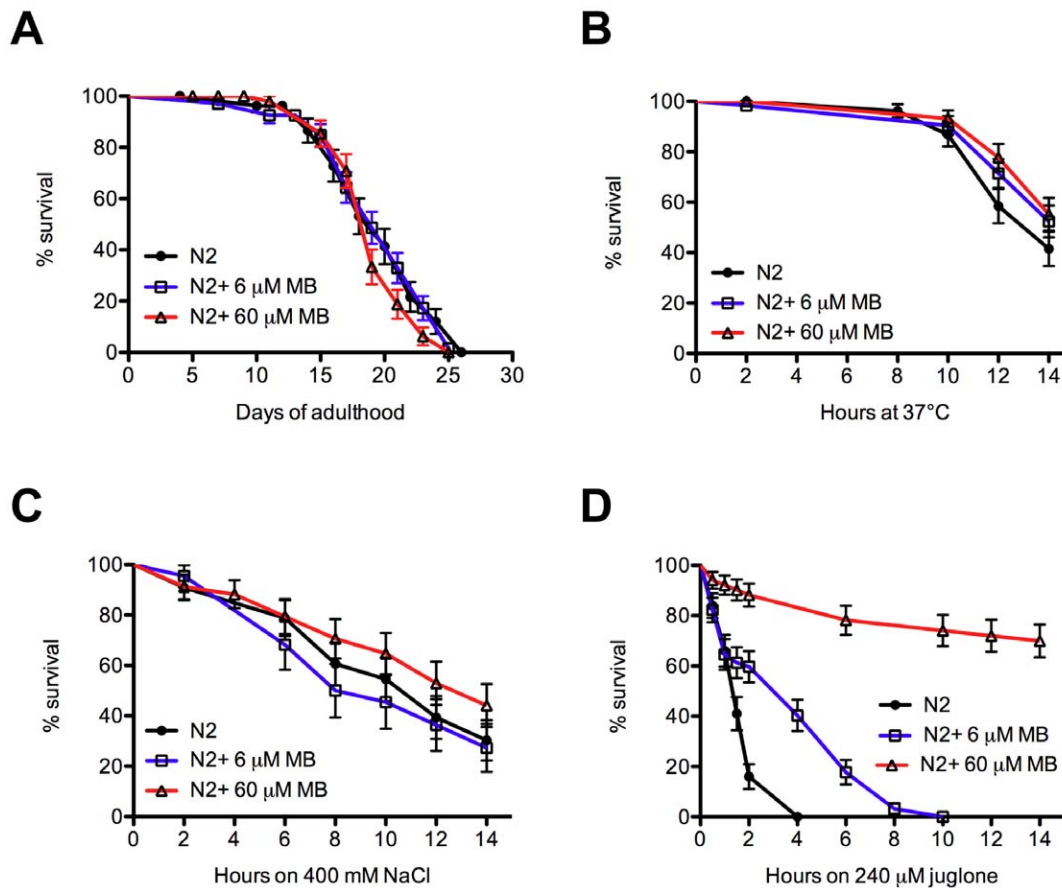


Figure 5. Methylene blue protects against oxidative stress in *C. elegans*. (A) N2 worms grown on plates with MB had lifespans indistinguishable from untreated worms (see also Table S1). (B) Worms grown on MB and subjected to thermal stress showed similar survival rates compared to untreated N2 worms. (C) N2 worms treated with MB showed similar rates of survival compared to untreated worms when subjected to hyperosmolarity. (D) MB had a dose-dependent protective effect on N2 worms against oxidative stress and mortality when grown on plates containing juglone ($P < 0.001$ for MB treated N2 worms compared to untreated worms). doi:10.1371/journal.pone.0042117.g005

triplicates were tested at 20°C from adult day 1 until death. Worms were declared dead if they were immotile and did not respond to tactile or heat stimulus.

Stress assays. For oxidative stress tests, worms were grown on NGM or NGM+60 μM methylene blue and transferred to NGM plates +240 μM juglone at adult day 1. For thermal resistance worms were grown on NGM or NGM 60 μM methylene blue and put at 37°C at adult day 1. For osmotic resistance worms were grown on NGM or NGM+60 μM methylene blue and put on 400 mM NaCl plates at adult day 1. For all assays, worms were evaluated for survival every 30 min for the first 2 hours and every 2 hours after up to 14 hours. Nematodes were scored as dead if they were immotile and unable to move in response to heat or tactile stimuli. For all tests worms, 20 animals/plate by triplicates were scored.

Dihydrofluorescein diacetate assay. For visualization of oxidative damage in the transgenic strains the worms were incubated on a slide for 30 min with 5 μM dihydrofluorescein diacetate dye and then washed with 1× PBS three times. After the slide was fixed, fluorescence was observed with the Leica system described above.

Worm lysates. Worms were collected in M9 buffer, washed 3 times with M9 and pellets were placed at −80°C overnight. Pellets were lysed in RIPA buffer (150 mM NaCl, 50 mM Tris pH 7.4, 1% Triton X-100, 0.1% SDS, 1% sodium deoxycholate)+protease

inhibitors (10 mg/ml leupeptin, 10 mg/ml pepstatin A, 10 mg/ml chymostatin LPC;1/1000). Pellets were passed through a 27_{1/2} G syringe 10 times, sonicated and centrifuged at 16,000× *g*. Supernatants were collected.

Immunoblot. Worm RIPA samples (175 μg/well), lymphoblast cell RIPA samples (15 μg/well) were resuspended directly in 1× Laemmli sample buffer, migrated in 12.5% polyacrylamide gels, transferred to nitrocellulose membranes (BioRad) and immunoblotted. Antibodies used: rabbit anti-TDP-43 (1:200; Proteintech), rabbit anti-FUS/TLS (1:200; AbCam), and mouse anti-actin (1:10000 for worms, MP Biomedicals). Blots were visualized with peroxidase-conjugated secondary antibodies and ECL Western Blotting Substrate (Thermo Scientific).

Statistical analysis. For paralysis and stress-resistance tests, survival curves were generated and compared using the Log-rank (Mantel-Cox) test, and a 60–100 animals were tested per genotype and repeated at least three times.

Zebrafish experiments

Zebrafish maintenance. Zebrafish (*Danio rerio*) embryos were raised at 28.5°C, and collected and staged using standard methods [34]. The Comité de Déontologie de l'Expérimentation sur les Animaux (CDEA), the local animal care committee at the Université de Montréal, having received the protocol relevant to

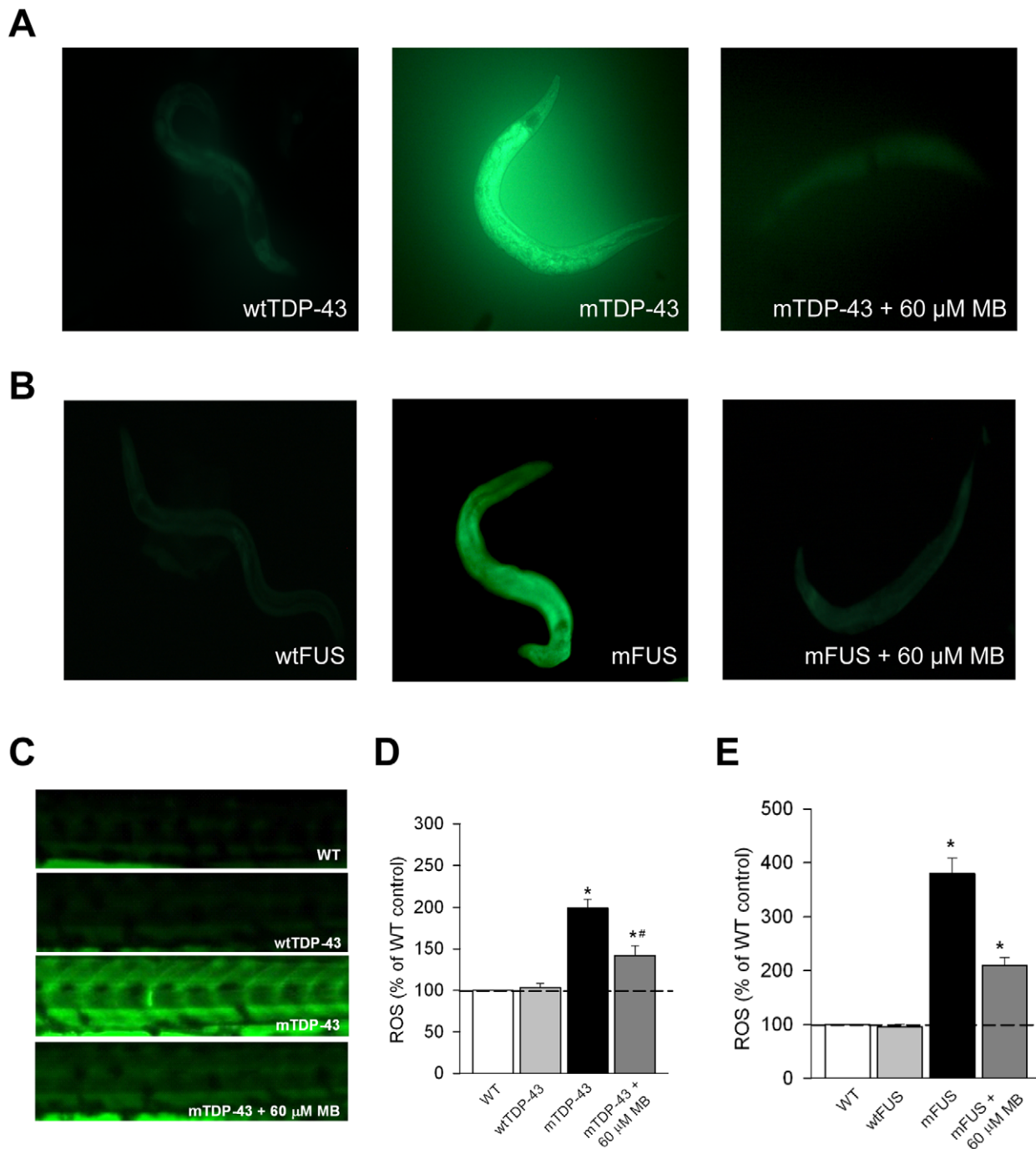


Figure 6. Methylene blue reduces oxidative stress in *C. elegans* and zebrafish transgenics. Oxidative stress was measured in transgenic worms and zebrafish with the dihydrofluorescein diacetate (DHF) that fluoresces when exposed to intracellular peroxide. (A) mTDP-43 worms, but not wtTDP-43 transgenics have a higher level of oxidative stress when stained with DHF. mTDP-43 worms treated with MB and then stained with DHF show a remarkable reduction in fluorescence. (B) wtFUS worms show no fluorescence when stained with DHF compared to mFUS worms. mFUS worms treated with MB and then stained with DHF showed reduced fluorescence. (C) Wild type (WT) zebrafish and zebrafish expressing wtTDP-43 show very low levels of fluorescence when stained with DHF compared to mTDP-43 fish. Treatment with MB reduced fluorescence in DHF stained fish. (D) Quantification of fluorescence of DHF stained fish shows that MB treatment significantly reduced fluorescence in mTDP-43 fish (* P <0.001, *# P <0.01). (E) MB significantly reduced fluorescence in DHF stained mFUS zebrafish (* P <0.001). doi:10.1371/journal.pone.0042117.g006

this project relating to animal care and treatment, certified that the care and treatment of animals was in accordance with the guidelines and principles of the Canadian Council on Animal Care. Further, all matters arising from this proposal that related to

animal care and treatment, and all experimental procedures proposed for use with animals were reviewed and approved by the CDEA before they were initiated or undertaken. This review process was ongoing on a regular basis during the entire period

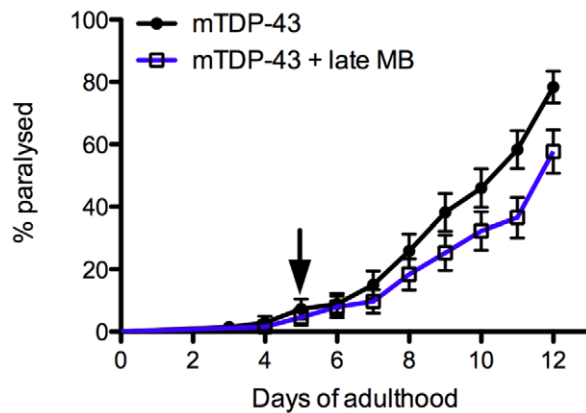


Figure 7. Diminished neuroprotection from late administration of methylene blue. mTDP-43 worms grown on normal plates and switched to plates supplemented with 60 μ M MB at day 5 (indicated by the arrow) of adulthood (late MB) showed a modest but significant reduction in paralysis compared to untreated worms ($P < 0.05$). doi:10.1371/journal.pone.0042117.g007

that the research was being undertaken. Zebrafish embryos (no adults were used) are insensitive to pain. Fish embryos were incubated overnight in each compound and examined the next day and then disposed. Zebrafish embryos were used over a two-day period then terminated.

In-vitro mRNA synthesis and embryo microinjection. Human FUS wild type and mutant [R521H], human TDP-43 wild type and mutant [G348C] mRNAs were transcribed from NotI-linearized pCS2+ using SP6 polymerase with the mMESSAGE Machine Kit (Ambion). This was followed by a phenol:chloroform extraction and isopropanol precipitation, and diluted in nuclease-free water (Ambion). The mRNAs were diluted in nuclease free water (Ambion) with 0.05% Fast Green vital dye (Sigma-Aldrich) at a concentration of 60 ng/ μ l (FUS), 25 ng/ μ l (TDP-43) and were pulse-injected into 1–2 cell stage embryos using a Picospritzer III pressure ejector.

Chemical treatments. Transient transgenics for TDP-43 [G348C] and FUS [R521H] embryos at 24 hpf were placed in individual wells in a 24 well plate and were treated overnight with methylene blue diluted in Evans solution (in mM): 134 NaCl, 2.9 KCl, 2.1 CaCl_2 , 1.2 MgCl_2 , 10 HEPES, 10 glucose, pH 7.8, 290 mOsm, with 0.1% DMSO. Behavioural touch responses were then assessed at 52–56 hpf as described in the following section.

Touch-evoked escape response. Zebrafish larvae were touched lightly at the level of the tail with a pair of blunt forceps and their locomotor behavior was recorded with a Grasshopper 2 Camera (Point Grey Research) at 30 Hz. The movies were then analyzed using the manual tracking plugin of ImageJ 1.45r software (NIH) and the swim duration, swim distance and maximum swim velocity of the fish were calculated.

Unbranched axonal length measurements. For immunohistochemical analysis of axonal projections of motor neurons, monoclonal antibody anti-SV2 (Developmental Studies Hybridoma) were used to assess the motor neuron morphology at 48 and 72 hpf. Fluorescent images of fixed embryos were taken using a Quorum Technologies spinning-disk confocal microscope mounted on an upright Olympus BX61WI fluorescence microscope equipped with an Hamamatsu ORCA-ER camera. Image acquisition was performed with Velocity software (PerkinElmer). As previously described [16], axonal projections from primary and secondary motor neurons at a defined location in the inter somitic segments were determined. Analysis of Z-stacks by confocal

microscopy was performed in three to four axonal projections per animal. The axonal length to the first branching (UAL) was determined by tracing the labeled axon from the spinal cord to the point where it branches using ImageJ (NIH). These values were averaged for each of the animal analyzed (10–30 zebrafish per condition) for the various conditions in our study.

Reactive Oxygen Species measurements. For *in vivo* detection of reactive oxygen species, live 2 day old embryos (2 dpf) were incubated in 5 μ M 2',7'-dichlorofluorescein diacetate (Sigma-Aldrich) for 20 minutes at 28.5°C and washed three times for 5 min with embryo media. Fluorescence was observed under a 488 nm wavelength excitation. The generation of reactive oxygen species in the larvae exposed to the chemicals was also quantitatively assessed as described elsewhere [35]. Briefly, 15 embryos were washed with cold Phosphate Buffer solution (PBS; pH 7.4) twice and then homogenized in cold buffer (0.32 mM of sucrose, 20 mM of HEPES, 1 mM of MgCl_2 , and 0.5 mM of phenylmethyl sulfonylfluoride (PMSF), pH 7.4). The homogenate was centrifuged at 15,000 \times g at 4°C for 20 min, and the supernatant was transferred to new tubes for further experimentation. Twenty microliters of the homogenate was added to a 96-well plate and incubated at room temperature for 5 min, after which 100 μ l of PBS (pH 7.4) and 8.3 μ l of DFH stock solution (10 mg/ml) were added to each well. The plate was incubated at 37°C for 30 minutes. The fluorescence intensity was measured using a microplate reader (SpectraMax M2, Molecular Device, Union City, CA, USA) with excitation and emission at 485 and 530 nm, respectively. The reactive oxygen species concentration was expressed as arbitrary emission units per mg protein.

Statistical analysis. All data values are given as means \pm SEM. Significance was determined using one-way ANOVAs and Fisher LSD tests for normally distributed and equal variance data, Kruskal–Wallis ANOVA and Dunn's method of comparison were used for non-normal distributions.

Supporting Information

Figure S1 Methylene blue has no effect on wild type motility phenotypes in worms or zebrafish. (A) MB had no significant effect on the motility phenotype of wild type (WT) non-transgenic N2 worms. (B) Representative traces of TEER phenotypes in WT zebrafish with and without MB treatment. MB did not affect the swim duration (C), distance swam (D) or maximum swimming velocity (E) of WT zebrafish. (TIF)

Table S1 Lifespan analysis for all experiments. Related to Figure 5A. Animals that died prematurely (ruptured, internal hatching) or were lost (crawled off the plate) were censored at the time of scoring. All control and experimental animals were scored and transferred to new plates at the same time. ns: not significant. (PDF)

Acknowledgments

We would like to thank M. Drits and G. Laliberte for help with zebrafish. P.D. holds a Canada Research Chair in Neuroscience, E.K. holds a MDA Development Grant as well as an AVENIR and Jeune Chercheur contracts with INSERM, J.A.P. is a CIHR New Investigator.

Author Contributions

Conceived and designed the experiments: EK PD JAP MT. Performed the experiments: AV SAP CM EK SC MT. Analyzed the data: AV SAP EK JAP MT. Wrote the paper: AV SAP PD EK JAP MT.

References

- Boillee S, Vande Velde C, Cleveland DW (2006) ALS: a disease of motor neurons and their nonneuronal neighbors. *Neuron* 52: 39–59.
- Lomen-Hoerth C (2008) Amyotrophic lateral sclerosis from bench to bedside. *Semin Neurol* 28: 205–211.
- Neumann M, Sampathu DM, Kwong LK, Truax AC, Micsenyi MC, et al. (2006) Ubiquitinated TDP-43 in frontotemporal lobar degeneration and amyotrophic lateral sclerosis. *Science* 314: 130–133.
- Gitcho MA, Baloh RH, Chakraverty S, Mayo K, Norton JB, et al. (2008) TDP-43 A315T mutation in familial motor neuron disease. *Ann Neurol*.
- Kabashi E, Valdmanis PN, Dion P, Spiegelman D, McConkey BJ, et al. (2008) TARDBP mutations in individuals with sporadic and familial amyotrophic lateral sclerosis. *Nat Genet*.
- Sreedharan J, Blair IP, Tripathi VB, Hu X, Vance C, et al. (2008) TDP-43 mutations in familial and sporadic amyotrophic lateral sclerosis. *Science* 319: 1668–1672.
- Kwiatkowski TJ Jr, Bosco DA, Leclerc AL, Tamrazian E, Vanderburg CR, et al. (2009) Mutations in the FUS/TLS gene on chromosome 16 cause familial amyotrophic lateral sclerosis. *Science* 323: 1205–1208.
- Lagier-Tourenne C, Polymenidou M, Cleveland DW (2010) TDP-43 and FUS/TLS: emerging roles in RNA processing and neurodegeneration. *Hum Mol Genet* 19: R46–64.
- Kabashi E, Bercier V, Lissouba A, Liao M, Brustein E, et al. (2011) FUS and TARDBP but not SOD1 interact in genetic models of Amyotrophic Lateral Sclerosis. *PLoS Genet* in press.
- Wang JW, Brent JR, Tomlinson A, Shneider NA, McCabe BD (2011) The ALS-associated proteins FUS and TDP-43 function together to affect *Drosophila* locomotion and life span. *J Clin Invest*.
- Owens KN, Santos F, Roberts B, Linbo T, Coffin AB, et al. (2008) Identification of genetic and chemical modulators of zebrafish mechanosensory hair cell death. *PLoS Genet* 4: e1000020.
- Peterson RT, Link BA, Dowling JE, Schreiber SL (2000) Small molecule developmental screens reveal the logic and timing of vertebrate development. *Proc Natl Acad Sci U S A* 97: 12965–12969.
- Jones AK, Buckingham SD, Sattelle DB (2005) Chemistry-to-gene screens in *Caenorhabditis elegans*. *Nat Rev Drug Discov* 4: 321–330.
- Kwok TC, Ricker N, Fraser R, Chan AW, Burns A, et al. (2006) A small-molecule screen in *C. elegans* yields a new calcium channel antagonist. *Nature* 441: 91–95.
- Vaccaro A, Tauffenberger A, Aggad D, Rouleau G, Drapeau P, et al. (2012) Mutant TDP-43 and FUS cause age-dependent paralysis and neurodegeneration in *C. elegans*. *PLoS ONE* 7: e31321.
- Kabashi E, Lin L, Tradewell ML, Dion PA, Bercier V, et al. (2009) Gain and loss of function of ALS-related mutations of TARDBP (TDP-43) cause motor deficits in vivo. *Hum Mol Genet* 19: 671–683.
- Kabashi E, Bercier V, Lissouba A, Liao M, Brustein E, et al. (2011) FUS and TARDBP but not SOD1 interact in genetic models of amyotrophic lateral sclerosis. *PLoS Genet* 7: e1002214.
- Schirmer RH, Adler H, Pickhardt M, Mandelkow E (2011) “Lest we forget you - methylene blue ...”. *Neurobiol Aging*.
- Cheah BC, Vucic S, Krishnan AV, Kiernan MC (2010) Riluzole, neuroprotection and amyotrophic lateral sclerosis. *Curr Med Chem* 17: 1942–1999.
- Van Raamsdonk JM, Hekimi S (2009) Deletion of the mitochondrial superoxide dismutase sod-2 extends lifespan in *Caenorhabditis elegans*. *PLoS Genet* 5: e1000361.
- Harding HP, Zhang Y, Zeng H, Novoa I, Lu PD, et al. (2003) An integrated stress response regulates amino acid metabolism and resistance to oxidative stress. *Mol Cell* 11: 619–633.
- Necula M, Breydo L, Milton S, Kaye R, van der Veer WE, et al. (2007) Methylene blue inhibits amyloid Abeta oligomerization by promoting fibrillization. *Biochemistry* 46: 8850–8860.
- Wischik CM, Edwards PC, Lai RY, Roth M, Harrington CR (1996) Selective inhibition of Alzheimer disease-like tau aggregation by phenothiazines. *Proc Natl Acad Sci U S A* 93: 11213–11218.
- Yamashita M, Nonaka T, Arai T, Kametani F, Buchman VL, et al. (2009) Methylene blue and dimebon inhibit aggregation of TDP-43 in cellular models. *FEBS Lett* 583: 2419–2424.
- Arai T, Hasegawa M, Nonaka T, Kametani F, Yamashita M, et al. (2010) Phosphorylated and cleaved TDP-43 in ALS, FTL and other neurodegenerative disorders and in cellular models of TDP-43 proteinopathy. *Neuropathology* 30: 170–181.
- Audet JN, Soucy G, Julien JP (2012) Methylene blue administration fails to confer neuroprotection in two amyotrophic lateral sclerosis mouse models. *Neuroscience*.
- Medina DX, Caccamo A, Oddo S (2011) Methylene blue reduces abeta levels and rescues early cognitive deficit by increasing proteasome activity. *Brain Pathol* 21: 140–149.
- van Bebber F, Paquet D, Hruscha A, Schmid B, Haass C (2010) Methylene blue fails to inhibit Tau and polyglutamine protein dependent toxicity in zebrafish. *Neurobiol Dis* 39: 265–271.
- Simpson EP, Yen AA, Appel SH (2003) Oxidative Stress: a common denominator in the pathogenesis of amyotrophic lateral sclerosis. *Curr Opin Rheumatol* 15: 730–736.
- Lin MT, Beal MF (2006) Mitochondrial dysfunction and oxidative stress in neurodegenerative diseases. *Nature* 443: 787–795.
- Naganska E, Matyja E (2011) Amyotrophic lateral sclerosis - looking for pathogenesis and effective therapy. *Folia Neuropathol* 49: 1–13.
- Rojas JC, Bruchey AK, Gonzalez-Lima F (2012) Neurometabolic mechanisms for memory enhancement and neuroprotection of methylene blue. *Prog Neurobiol* 96: 32–45.
- Rojas JC, Simola N, Kermath BA, Kane JR, Schallert T, et al. (2009) Striatal neuroprotection with methylene blue. *Neuroscience* 163: 877–889.
- Kimmel CB, Ballard WW, Kimmel SR, Ullmann B, Schilling TF (1995) Stages of embryonic development of the zebrafish. *Dev Dyn* 203: 253–310.
- Deng J, Yu L, Liu C, Yu K, Shi X, et al. (2009) Hexabromocyclododecane-induced developmental toxicity and apoptosis in zebrafish embryos. *Aquat Toxicol* 93: 29–36.

METHYLENE BLUE ADMINISTRATION FAILS TO CONFER NEUROPROTECTION IN TWO AMYOTROPHIC LATERAL SCLEROSIS MOUSE MODELS

J.-N. AUDET, G. SOUCY AND J.-P. JULIEN*

Research Centre of CHUQ and Department of Psychiatry and Neurosciences, Laval University, 2705 Laurier Boulevard, QC, Canada G1V 4G2

Abstract—Approximately 20% cases of familial amyotrophic lateral sclerosis (ALS) are caused by mutations in the gene encoding Cu/Zn superoxide dismutase (SOD1). Recent studies have shown that methylene blue (MB) was efficient in conferring protection in several neurological disorders. MB was found to improve mitochondrial function, to reduce reactive oxygen species, to clear aggregates of toxic proteins, and to act as a nitric oxide synthase inhibitor. These pleiotropic effects of relevance to ALS pathogenesis led us to test MB in two models of ALS, SOD1^{G93A} mice and TDP-43^{G348C} transgenic mice. Intraperitoneal administration of MB at two different doses was initiated at the beginning of disease onset, at 90 days of age in SOD1^{G93A} and at 6 months of age in TDP-43^{G348C} mice. Despite its established neuroprotective properties, MB failed to confer protection in both mouse models of ALS. The lifespan of SOD1^{G93A} mice was not affected by MB treatment. The declines in motor function, reflex score, and body weight of SOD1^{G93A} mice remained unchanged. MB treatment had no effect on motor neuron loss and aggregation or misfolding of SOD1. A combination of MB with lithium also failed to provide benefits in SOD1^{G93A} mice. In TDP-43^{G348C} mice, MB failed to improve motor function. Cytosolic translocation of TDP-43, ubiquitination and inflammation remained also unchanged after MB treatment of TDP-43^{G348C} mice. © 2012 IBRO. Published by Elsevier Ltd. All rights reserved.

Key words: methylene blue, superoxide dismutase, TDP-43, ALS, neuroinflammation.

Amyotrophic lateral sclerosis (ALS) is the most common adult-onset motor neuron disease, leading to progressive paralysis and death. Ninety percent of the cases are sporadic (sALS), and the remaining are familial (fALS), but the two forms are clinically and pathologically undistinguishable. Twenty percent of the familial cases are related to mutations in the Cu/Zn superoxide dismutase gene (SOD1) gene, although the mechanisms leading to pathology remain unclear (Boillee et al., 2006). Transgenic mice expressing several SOD1 mutants have been widely used to understand the ALS pathology because they were found to develop motor neuron disease very similar to the human disease (Turner and Talbot, 2008). Various hypotheses

have been proposed to explain the toxicity of SOD1 mutant protein including aggregation (reviewed in Chattopadhyay and Valentine, 2009; Ticozzi et al., 2010), oxidative stress (reviewed in Barber and Shaw, 2010) and mitochondrial dysfunction (reviewed in Pizzuti and Petrucci, 2011), excitotoxicity (reviewed in Bogaert et al., 2010), and more recently RNA processing through TDP-43 and FUS/TLS abnormalities (reviewed in Baumer et al., 2010; Lagier-Tourenne et al., 2010). Although pathological pathways leading to ALS seem to differ between SOD1 and TDP-43 cases, a common hallmark resides in toxic protein aggregation (Chattopadhyay and Valentine, 2009; Johnson et al., 2009).

Although numerous compounds have been tested to treat ALS, most of them were proven ineffective, except riluzole, which slightly prolongs survival of patients (Miller et al., 2007). Methylene blue (MB), a monoamine oxidase inhibitor, has been used for more than a century to treat several diseases and infections. It acts as an inhibitor of NO synthase, whose upregulation occurs in motoneurons and reactive astrocytes of ALS patients (Anneser et al., 2001; Sasaki et al., 2001), as well as in SOD1^{G93A} mice (Cha et al., 1998; Almer et al., 1999; Sasaki et al., 2002). MB can also improve mitochondrial function and be an effective electron carrier, thus acting on reactive oxygen species (Atamna et al., 2008; Wen et al., 2011), which can also be linked to ALS. Increasing evidence shows that methylene blue has strong neuroprotective effects in a growing list of neurological disorders, including Alzheimer's disease (Wischik et al., 1996; Atamna and Kumar, 2010; Medina et al., 2011), Parkinson's disease (Wen et al., 2011), cerebral ischemia (Wiklund et al., 2007; Miclescu et al., 2010; Wen et al., 2011), amnesia (Riha et al., 2011), and bipolar disorder (Naylor et al., 1981; Narasapur and Naylor, 1983; Eroglu and Caglayan, 1997). Furthermore, MB has already been proposed as a potential treatment for ALS, as it clears TDP-43 aggregates in cellular models (Yamashita et al., 2009). Moreover, MB has been shown to prolong survival of normal mice and rats (National Toxicology Program, 2008). The latter may also be relevant to ALS, as a premature senescence of motoneurons may be a cause of ALS (McComas et al., 1973).

During the last years, lithium has also raised a lot of attention as a potential treatment for ALS. Positive results were reported from mouse studies and a clinical trial (Shin et al., 2007; Feng et al., 2008; Fornai et al., 2008), but this was followed more recently by negative results with mice (Gill et al., 2009; Pizzasegola et al., 2009) and humans (Aggarwal et al., 2010; Chio et al., 2010). Various hypoth-

*Corresponding author. Tel: +1-418-654-2296; fax: +1-418-654-2761. E-mail address: jean-pierre.julien@crchul.ulaval.ca (J.-P. Julien). Abbreviations: ALS, amyotrophic lateral sclerosis; DRG, dorsal root ganglia; IR, immunoreactivity; MB, methylene blue; SOD1, Cu/Zn superoxide dismutase; VR, ventral root.

esizes were formulated to explain those divergent outcomes. However it seems that paradigms combining lithium treatment with other compounds often result in improvement of the disease (Shin et al., 2007; Feng et al., 2008). Besides, in an attempt to diminish seizures in an epilepsy model in mice, a combination of lithium with MB produced a significant decrease of seizures when compared with lithium alone (Bahremand et al., 2010). Thus, it may be relevant to assess the synergic potential of lithium with MB.

Here, we evaluated the efficiency of MB alone or in combination with lithium in mouse SOD1^{G93A}, a well-established and characterized model of ALS. Because there is growing evidence that sporadic ALS cases with TDP-43 abnormalities have a different etiology than familial ALS caused by SOD1 (Neumann et al., 2006; Orrell, 2010), we also tested the effectiveness of MB in the new TDP-43^{G348C} model of ALS (Swarup et al., 2011). These TDP-43 transgenic mice recapitulate well pathological hallmarks of ALS/FTD, making it a good model to further validate the efficiency of MB. In contrast to many other neurological disorders, we report that administration of MB, alone or in combination with lithium, conferred no protection in ALS pathogenesis caused by mutant SOD1 or by mutant TDP-43.

EXPERIMENTAL PROCEDURES

Animals

SOD1^{G93A} mice [stock number 002726] were acquired from the Jackson Laboratory (Bar Harbor, ME, USA) and enriched in C57BL/6Hsd strain ($n > 20$). SOD1^{G93A} mice were genotyped in accordance with Jackson Laboratory protocols. SOD1^{G93A} mice were injected at the beginning of the symptomatic stage (90 days) every 2 days until their death. TDP-43^{G348C} mice were generated in C3B6 background (described in Swarup et al., 2011) and backcrossed in C57BL/6 background for at least 10 generations. TDP-43^{G348C} mice were injected at the beginning of the symptomatic stage (6 months) every 2 days until 12 months. Methylene blue (Sigma, St-Louis, MO, USA) was dissolved in 0.9% saline, and mice were given 1 mg/kg (SOD1^{G93A} and TDP-43^{G348C} mice) or 10 mg/kg (SOD1^{G93A} mice) intraperitoneally. Lithium (Sigma) was dissolved in 0.9% saline and injected intraperitoneally at a dose of 10 mg/kg (SOD1^{G93A} mice). The use and maintenance of the mice described in this article were performed in accordance to the Guide of Care and Use of Experimental Animals of the Canadian Council on Animal Care. The number of animals and their suffering has been minimized.

Analysis of disease progression

Measurements of body weight, hind limb reflex and rotarod performance were used to score the clinical effects of SOD1^{G93A} mice. The extensibility and postural reflex of the hind limbs when mice were held up with their tails were scored as described previously (Urushitani et al., 2006). The SOD1^{G93A} reflex score and body weight were measured every 2 days, beginning at 90 days. Scoring was performed in a blind manner by animal technicians who had no information about the genotype but had experience in grading SOD1 mice paralysis. Analysis of TDP-43^{G348C} and SOD1^{G93A} mice disease progression was performed with an accelerated rotarod, starting at 4 rpm with a 0.25 rpm/s acceleration, and time was noted when the mice fell off the roll. Three trials were done per animal, and the mean value was calculated for statistics and graphs. Rotarod tests for SOD1^{G93A} and TDP-43^{G348C} mice were performed once a week.

Tissue collection and immunohistochemical analyses

Mice were anesthetized and transcardially perfused with NaCl 0.9% and fixed with 4% paraformaldehyde. Dissected spinal cord tissues were postfixed for 24 h in 4% paraformaldehyde and equilibrated in a solution of PBS-sucrose (20%) for 48 h. Spinal cord tissues were cut in 25 μ m thick sections with a Leica frozen microtome and kept in a cryoprotective solution at -20°C . For SOD1^{G93A} mice, sections were incubated with anti-misfolded SOD1 antibody A5C3 (Gros-Louis et al., 2010) (Medimabs, Montreal, Canada), stained with the fluorophore-coupled secondary antibody Alexa-488 (Invitrogen, Carlsbad, CA, USA), and counterstained with DAPI. For TDP-43^{G348C} mice, sections were incubated with monoclonal anti-human TDP-43 (Abnova, Taipei, Taiwan), anti-ubiquitin (Abcam, Cambridge, MA, USA), anti-GFAP (formerly Chemicon—Millipore, Billerica, MA, USA), or anti-Iba1 (Wako, Osaka, Japan) antibodies stained with the fluorophore coupled secondary antibody Alexa-488 or Alexa-594 (Invitrogen). Dissected dorsal root ganglia (DRG) were postfixed in a solution of 3% glutaraldehyde for a period of 48 h, washed in PBS, treated with 1% osmium tetroxide for 2 h, and dehydrated through graded alcohol solutions. Before Epon plastic embedding, DRG were further dissected to ensure that all ventral root (VR) axons would be sampled at a distance of 3 mm from the DRG cell body. Semi-thin cross sections (1 μ m) were stained with Toluidine Blue, rinsed, and coverslipped. To quantify the immunoreactivity (IR) score on immunohistochemistries, we measured the optical densities of each staining with ImageJ software (NIH). For A5C3, Iba1, and GFAP immunofluorescences the whole signal intensity was read. To quantify cytoplasmic TDP-43, we surrounded all motoneurons in the spinal cord slices based on their morphology and removed from selection the nucleus for the cytoplasmic measurement. We then read the whole cell intensity and divided the cytoplasm on the whole cell signal to obtain a percentage of cytoplasmic TDP-43 translocation. For ubiquitin quantification we measured the amount of ubiquitin-positive inclusions exclusively in the cytoplasmic part of motoneurons.

Western blotting

Total spinal cord lysates from SOD1^{G93A} transgenic mice and from non-transgenic littermates were prepared by homogenization in 1 mL of TNG-T buffer consisting of 50 mM Tris-HCl, pH 7.4; 150 mM NaCl; 10% glycerol; 1% Triton X-100; protease inhibitor mixture (Roche, Indianapolis, IN, USA). After homogenization, the tissue suspension was centrifuged for 15 min at 1000 g at 4°C . The supernatant (soluble fraction) and the pellet (insoluble fraction) were denatured in the sampling buffer containing 2-mercaptoethanol and SDS with boiling. After migration on standard SDS-PAGE gels, the proteins were blotted on PVDF (PerkinElmer, Waltham, MA, USA) membrane. The membranes were labeled with commercially available anti-SOD1 (Stressgen, Ann Arbor, MI, USA). The amount of loaded protein was verified by stripping the same membranes and incubating with anti-actin antibody (Chemicon). The blots were detected using IgG conjugated with peroxidase and chemiluminescent assay (PerkinElmer). The Western bands were scanned and analyzed by densitometry using ImageJ software (National Institutes of Health, Bethesda, MD, USA).

Statistical analyses

Data were analyzed using Prism 5.0 software (GraphPad Software, LaJolla, CA, USA). Behavioral data were computed by performing two-way ANOVAs (except when specified followed by Bonferroni post-tests and survival data using Mantel-Cox log-rank tests. VR axon counts were compared using two-tailed Student's t -tests. Data are expressed as mean \pm SEM; $P < 0.05$ was considered statistically significant. One-way ANOVA followed by Bonfer-

roni post-test was performed on A5C3 IR scores (SOD1^{G93A} mice) and unpaired *t*-tests were performed on all other IR scores (TDP-43^{G348C} mice).

RESULTS

Methylene blue treatment, alone or in combination with lithium, did not affect lifespan or phenotype of SOD1^{G93A} mice

Following injection of SOD1^{G93A} mice with methylene blue, lithium, or both drugs starting at 90 days of age, we analyzed the lifespan of transgenic mice (Fig. 1A). Mice treated with methylene blue (1 mg/kg) had a lifespan of 141 days, those treated with a combination of methylene blue (1 mg/kg) and lithium (10 mg/kg) had a lifespan of 141.5, those treated with lithium (10 mg/kg) alone lived 139 days; whereas saline injected mice had a median survival of 141 days. The difference was not significant between any of the groups ($P=0.7337$; $n=10$, $n=8$, $n=9$, and $n=18$, respectively). Moreover, analysis of phenotype by

reflex scores and rotarod scores showed no difference between any of the groups ($P=0.3173$ and $P=0.8366$, respectively) (Fig. 1B, C). Correspondingly, body weight measures revealed no difference in disease progression of transgenic mice following any of the treatment ($P=0.5070$) (Fig. 1D). To make sure that the dose of methylene blue was sufficient to induce an effect, we also treated SOD1^{G93A} mice with a 10 mg/kg dose of methylene blue under the same parameters (data not shown). The treated animal had a lifespan of 137.5 days compared with 141 days for the saline treated mice, and again this difference was not statistically significant ($P=0.3268$, $n=8$ and $n=18$, respectively).

MB administration had no effect on motor function of TDP-43^{G348C} mice

As expected, TDP-43^{G348C} transgenic mice performed less well on rotarod assessment than wild-type (WT) mice during all the tested period ($P<0.0001$, $n=9$ and $n=6$,

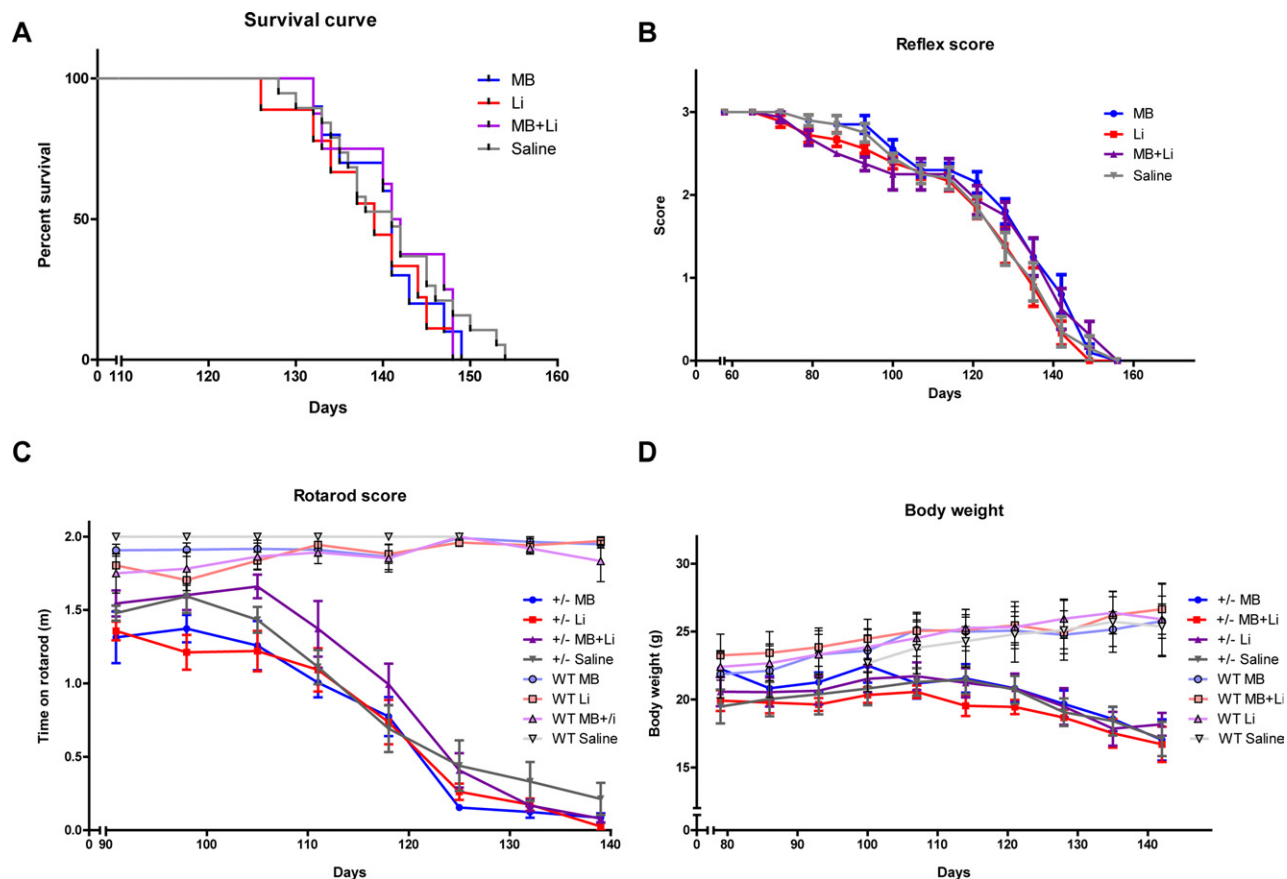


Fig. 1. Treatment with MB, lithium, or both drugs simultaneously does not affect survival or phenotypes of SOD1^{G93A} mice. (A) Survival: Kaplan–Meier survival curve shows that saline treated transgenic mice Sod1^{G93A} ($n=19$) had a mean survival of 141.0 d, whereas MB ($n=10$), Li ($n=9$), or MB+Li ($n=8$) treated mice lived for 141.0, 139.0, and 141.5 d, respectively. Log-rank test shows no significant ($P=0.7337$). (B) Reflex score: two-way ANOVA revealed that the treatment had no effect on the reflex score throughout the time points ($P=0.3173$). (C) Rotarod score: Regardless of the treatment, the performance of the transgenic mice (\pm) was similar on the rotarod until the end of the measurements ($P=0.8366$). Wild-type (WT) mice almost always perform at maximum value (2 min) irrespective of the treatment. (D) Body weight. WT mice consistently gain weight with age unrelatedly of the treatment, whereas transgenic mice lose weight as the paralysis progresses. However, the progressive decrease in the bodyweight of transgenic mice after the onset was comparable between all the groups ($P=0.5070$). For interpretation of the references to color in this figure legend, the reader is referred to the Web version of this article.

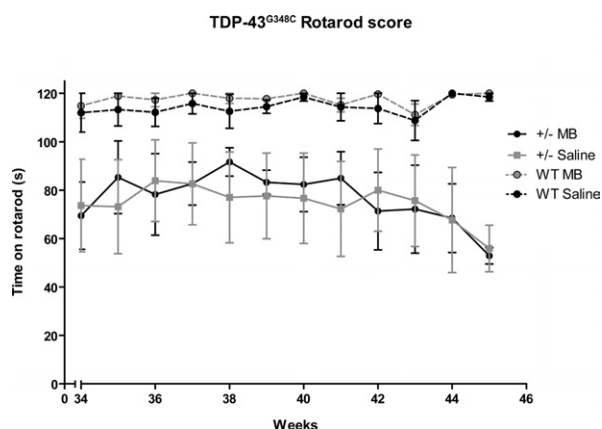


Fig. 2. MB did not improve motor function of TDP-43^{G348C} mice. Rotarod tests were assessed in three consecutive trials every week and the mean value is plotted. WT mice perform significantly better than TDP-43^{G348C} transgenic mice (\pm) ($P < 0.0001$, $n = 6$ and $n = 9$, respectively). There was no difference between MB treated transgenic mice and saline treated transgenic mice neither in any of the time points nor in the overall curve ($P = 0.8801$, $n = 4$ and $n = 5$, respectively).

respectively) (Fig. 2). However, there was no difference between the performances of saline-treated transgenic (\pm) animals versus MB-treated transgenic (\pm) animals ($P = 0.8801$, $n = 5$ and $n = 4$, respectively).

Cellular hallmarks of ALS were unchanged after MB treatment

Misfolded SOD1 is a pathological hallmark of ALS, even in sporadic cases (Bosco et al., 2010; Forsberg et al., 2010). For this reason, we examined its presence with a monoclonal antibody (A5C3) that is specific to misfolded SOD1 (Fig. 3A). However, following any of the treatments, the amount of misfolded SOD1 found in the spinal cord of SOD1^{G93A} mice was not diminished. Comparison of IR scores showed no difference in A5C3 signal for all treatments ($P = 0.4593$, $n = 3$) (Fig. 3C). In TDP-43 transgenic mice as well as in ALS patients, cytosolic TDP-43 translocation is a well-known pathological hallmark of ALS (Arai et al., 2006; Neumann et al., 2006; Swarup et al., 2011). Monoclonal antibody against human TDP-43 revealed no observable difference in the amount of translocated TDP-43 between treated transgenic animal versus transgenic controls (Fig. 3B), and this was confirmed by quantification of the percentage of TDP-43 found in cytoplasm ($P = 0.8662$, $n = 3$, see figure legend for details) (Fig. 3D). Similarly, the extent of ubiquitination was not diminished by MB treatment in transgenic mice ($P = 0.5467$, $n = 3$). Microgliosis and astrogliosis, also associated ALS pathology, were not reduced nor aggravated as revealed by Iba1 and GFAP antibodies in immunofluorescence (Fig. 3B) and their quantification (respectively: $P = 0.9644$, $n = 4$; $P = 0.8263$, $n = 5$) (Fig. 3D).

MB does not affect the number of surviving axons in the dorsal root ganglia of SOD1^{G93A} mice

Axonal degeneration correlates with the disease severity in SOD1 mutant mice (Gurney et al., 1994; Wong et al., 1995;

Bruijn et al., 1997). Therefore, we performed transversal sections of the dorsal root ganglia and assessed the axonal degeneration in the VR (Fig. 4A). While the non-transgenic mice had nearly a thousand motoneurons in the VR, SOD1^{G93A} mice had more or less 35% of their axons remaining (Fig. 4B). However, there was no difference in the number of axons of mice treated with MB, lithium, or both drugs together (MB: 357, Li: 357.5, MB+Li: 346.5, Saline: 378.0; $P = 0.5157$).

Accumulation of insoluble SOD1 is not diminished by MB treatment

It has been proposed that MB may play a role in clearance of a variety of toxic insoluble aggregates. In fact, it was demonstrated that MB can inhibit aggregate formation of a variety of proteins (Wischnik et al., 1996; Taniguchi et al., 2005; Yamashita et al., 2009). To verify this hypothesis in SOD1^{G93A} mice, we compared the ratio of soluble versus insoluble fractions of SOD1 in the spinal cord of SOD1^{G93A} mice, treated or not (Fig. 5). In the non-transgenic (WT) mice we mostly detected soluble SOD1, whereas transgenic SOD1^{G93A} mice had a considerable amount insoluble SOD1, as expected. However, the extent of aggregation was not lessened by MB treatment, lithium, or both treatments together.

DISCUSSION

Here we demonstrate that MB, Li, or both drugs administered jointly had no effect on the disease caused by SOD1^{G93A} in mice. MB also failed to alleviate disease caused by TDP-43^{G348C} in mice. Our analyses demonstrated that MB was unable to attenuate pathological hallmarks of ALS in either SOD1^{G93A} mice or TDP-43^{G348C} mice.

An earlier study concluded of MB ineffectiveness in conferring protection by oral administration at a dose of 25 mg/kg, which is much higher than the safe working dose already used in mice and in humans for other pathologies (Loughheed and Turnbull, 2011). This could have led to a toxic outcome, masking potential beneficial effects of MB. In another paradigm, a low dose of MB was efficient whereas the high dose was not able to induce any beneficial effects (Callaway et al., 2004). Actually, toxicity of MB generally occurs at a dosage above 6–12.5 mg/kg (depending on the studies), and the recommended dosage is 1–2 mg/kg (Wiklund et al., 2007; National Toxicology Program, 2008). In this study we treated all mice with a dose of 1 mg/kg of MB, which is within the mean working dose range used in most other paradigms in mice and humans when injected (0.5–2.5 mg/kg) (Clifton and Leikin, 2003; Callaway et al., 2004; Wiklund et al., 2007; Miculescu et al., 2010; Wen et al., 2011). Moreover, it has been demonstrated that MB crosses easily the blood–brain barrier, resulting in high concentrations in the CNS even at low dose administration (Peter et al., 2000). Nevertheless, to make sure that this dose was not too low, we repeated the experiment in SOD1^{G93A} mice with a dose of 10 mg/kg. Upon measuring the lifespan of this high-dose cohort of

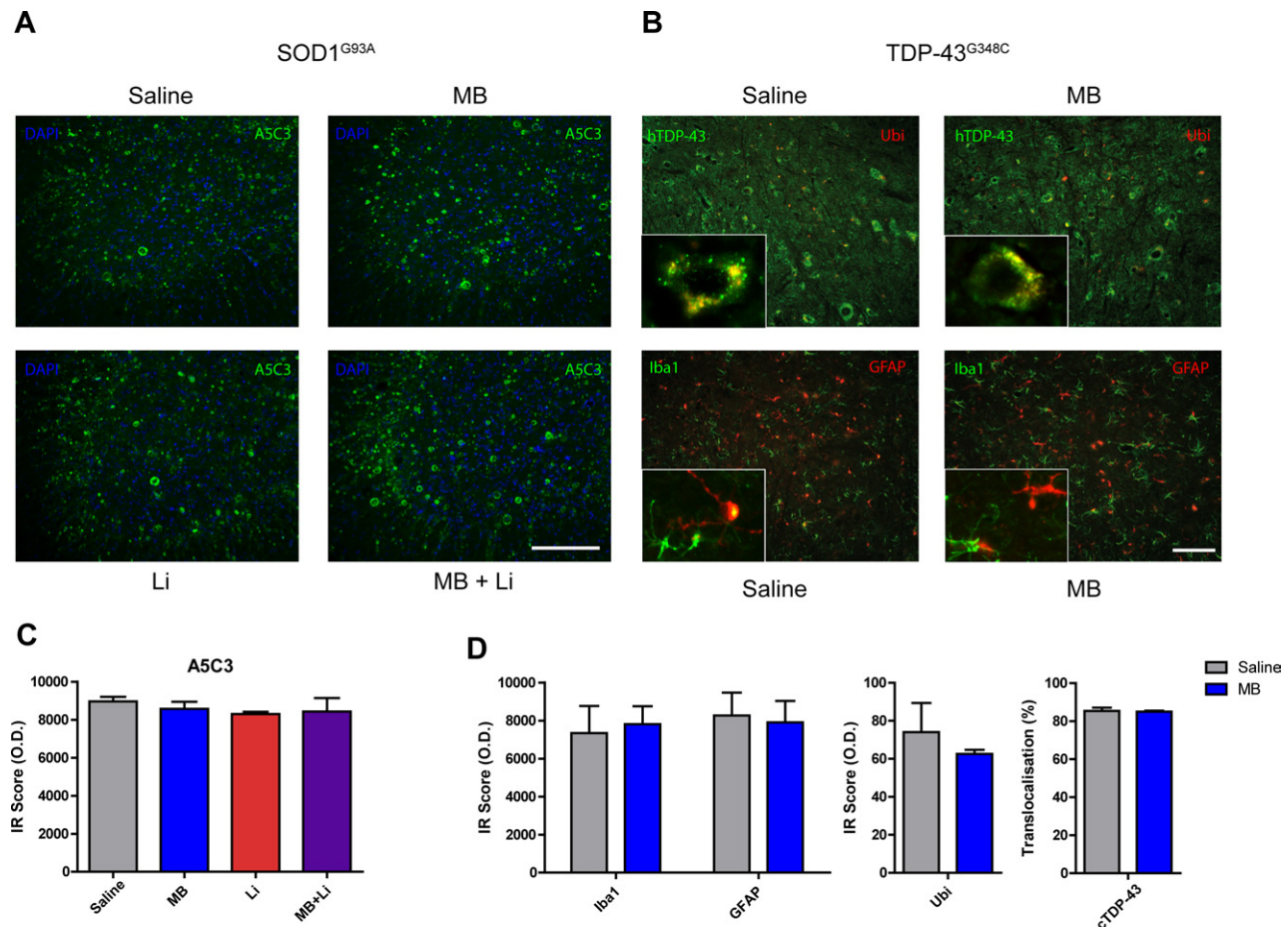


Fig. 3. Cellular pathological hallmarks of ALS are not diminished by MB and/or Li in SOD1^{G93A} or by MB in TDP-43^{G348C} mice. (A) Misfolded SOD1, detected by the A5C3 antibody, is found abundantly in spinal cords of SOD1^{G93A} mice. However, the intensity of the signal is very similar following any of the treatments. Scale bar=50 μ m. (B) Abnormal cytoplasmic hTDP-43 is found plentifully in spinal cord motoneurons of TDP-43^{G348C} mice, and aggregates are sometimes found ubiquitinated (hTDP-43 and Ubi colocalization is shown in inlay magnification of a representative cell). Still, there is no reduction of cytoplasmic TDP-43 or ubiquitination extent by MB treatment. GFAP and Iba1 immunofluorescence are also similar after MB treatment. Scale bar=10 μ m. (C) Quantification of A5C3 immunoreactivity (IR) in SOD1^{G93A} mice reveals no difference among the different treatments ($P=0.4593$, $n=3$) [OD: optical density arbitrary units]. (D) There was no difference in the immunoreactivity scores of MB and saline-treated TDP-43^{G348C} mice for Iba1, GFAP, and ubiquitin (respectively: $P=0.9644$, $n=4$; $P=0.8263$, $n=5$; $P=0.5467$, $n=3$). The amount of hTDP-43 cellular translocation (cTDP-43, calculated as the percentage of cellular TDP-43 divided by the total cell TDP-43 in motoneurons) was also very comparable in both treatments ($P=0.8662$, $n=3$). For interpretation of the references to color in this figure legend, the reader is referred to the Web version of this article.

animals, we consistently saw no difference in the MB-treated animals compared with saline-treated animals (MB: mean=137.5, saline: mean=141.0, $P=0.3268$).

Lougheed and Turnbull (2011) did not report the physiological outcomes of the treatment. Hence, the possibility that MB could have ameliorated some aspects of the disease has not been addressed in that study. Here, we have examined the major pathological hallmarks of ALS in SOD1^{G93A} and in TDP-43^{G348C} mice. First, the number of motor neurons remained unchanged in SOD1^{G93A} (Fig. 4) after MB treatments. Besides, the extent of misfolding and aggregation of SOD1 proteins correlates with the disease in mutant SOD1 mice (Gurney, 1997; Bruijn et al., 1998; Wang et al., 2005; Prudencio et al., 2009). Accordingly, we investigated that feature and we showed that treatment with MB does not reduce aggregation/misfolding of SOD1 (Figs. 3A and 5).

There is evidence that misfolded SOD1 may be a common feature of most ALS patient, familial or even sporadic (Bosco et al., 2010; Forsberg et al., 2010). However, it has been proposed that sporadic ALS cases with TDP-43 abnormalities have a different etiology than familial ALS caused by SOD1 (Neumann et al., 2006; Orrell, 2010). Consequently, the possibility that MB may have protective effects in ALS of other etiologies than mutant SOD1 could not be excluded. For instance, MB was able to clear aggregates of TDP-43 in a cellular model of ALS (Yamashita et al., 2009). In contrast, we report that MB had no effect on disease symptoms or on formation of cytoplasmic TDP-43 inclusions in transgenic mice expressing TDP-43^{G348C}.

The TDP-43^{G348C} mice develop during aging motor dysfunction, a main feature of ALS disease (Swarup et al., 2011). The TDP-43^{G348C} mice treated with MB for 6 months exhib-

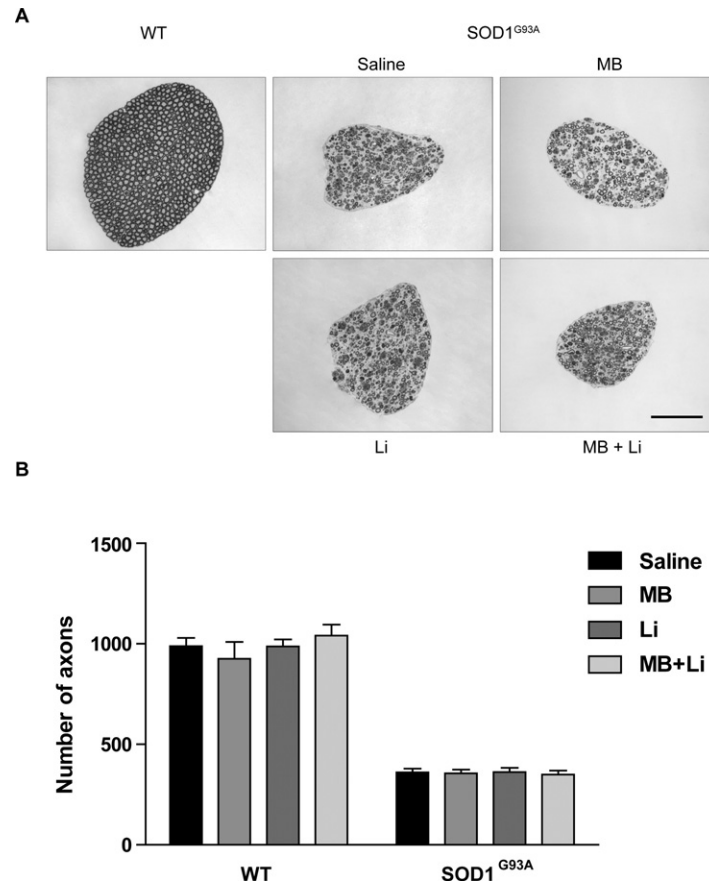


Fig. 4. No change in motor axons of SOD1^{G93A} mice. (A) Although the vast majority of axons appear intact in WT mice, transgenic SOD1^{G93A} mice exhibit massive degeneration of axons in the transversally sliced L5 ventral roots. (B) Quantification of the number of surviving axons in the ventral root shows that SOD1^{G93A} mice had 2.76 times less axons than the WT mice ($P < 0.0001$, $n = 19$ and $n = 13$, respectively). However, the number of axons in the ventral root is similar in all the SOD1^{G93A} mice either for the saline (mean = 361.0, $n = 6$), MB (mean = 356.2, $n = 5$), Li (mean = 362.3, $n = 4$), or MB+Li (mean = 349.0, $n = 4$) treatments ($P = 0.9672$). Scale bar = 50 μ m.

ited the same motor performance as saline-treated TDP-43^{G348C} mice (Fig. 2). Moreover, immunodetection of cytoplasmic TDP-43, of ubiquitin and of inflammation remained unchanged by the MB treatment (Fig. 3B, D).

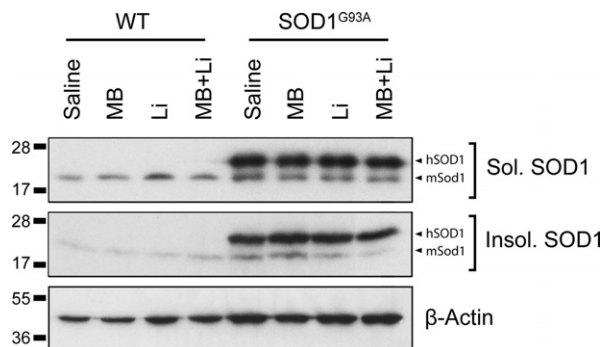


Fig. 5. Insoluble SOD1 is not cleared by MB and/or Li in SOD1^{G93A} mice. Insoluble SOD1 is predominantly found in SOD1^{G93A} mice and is mainly formed of human mutant SOD1 (hSOD1, upper bands in SOD1 panels). However, the ratio insoluble/soluble is consistent for any of the treatments (Saline, MB, Li, or MB+Li). Endogenous mouse SOD1 (mSOD1, lower bands in SOD1 panels) is relatively constant among all the mice.

The fact that lithium did not alleviate ALS symptoms in SOD1^{G93A} mice is concordant with recent negative results by independent groups (Gill et al., 2009; Pizzasegola et al., 2009; Aggarwal et al., 2010; Chio et al., 2010). These negative results were based on studies with larger cohorts of mice than earlier positive studies (Shin et al., 2007; Feng et al., 2008; Fornai et al., 2008). The scope of our experiments was mainly to investigate the possible synergic effect of MB with Li, because both were shown to achieve such effects in other paradigms (Shin et al., 2007; Feng et al., 2008; Bahreman et al., 2010). Based on our results we concluded that this was not the case in G93A mice and consequently we did not pursue further lithium tests in another ALS mouse model, the TDP-43 transgenic mice.

It is surprising that despite the existence of potential therapeutic targets for MB in ALS pathology, this compound could not improve the disease phenotypes in two different mouse models, the G93A mice and TDP-43 mice. There are still much uncertainties about pathogenic mechanisms that contribute directly to neurodegeneration process (Chattopadhyay and Valentine, 2009; Barber and Shaw, 2010; Baumer et al., 2010; Bogaert et al., 2010;

Lagier-Tourenne et al., 2010; Ticozzi et al., 2010; Pizzuti and Petrucci, 2011). Therefore, a possible explanation for the MB failure to alleviate ALS features could be that MB targets such as NOs, oxidative stress, mitochondria deficits, and protein aggregation are not the key contributors of motor neuron loss in these mouse models.

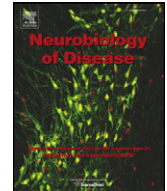
In summary, our results suggest that, despite its recognized protective properties (Schirmer et al., 2011), MB is inappropriate for treatment of ALS associated with either SOD1 mutations or TDP-43 abnormalities.

Acknowledgments—We gratefully thank Mélanie Couture, Christine Bareil, Marie-Ève Boulanger, Mélanie Simard, Caroline Genest, and Sophie Vachon for their technical help. This work was supported by the Canadian Institutes of Health Research. J.-P.J. holds a Canada Research Chair Tier 1 on Mechanisms of Neurodegeneration.

REFERENCES

- Aggarwal SP, Zinman L, Simpson E, McKinley J, Jackson KE, Pinto H, Kaufman P, Conwit RA, Schoenfeld D, Shefner J, Cudkowicz M (2010) Safety and efficacy of lithium in combination with riluzole for treatment of amyotrophic lateral sclerosis: a randomised, double-blind, placebo-controlled trial. *Lancet Neurol* 9:481–488.
- Almer G, Vukosavic S, Romero N, Przedborski S (1999) Inducible nitric oxide synthase up-regulation in a transgenic mouse model of familial amyotrophic lateral sclerosis. *J Neurochem* 72:2415–2425.
- Anneser JM, Cookson MR, Ince PG, Shaw PJ, Borasio GD (2001) Glial cells of the spinal cord and subcortical white matter up-regulate neuronal nitric oxide synthase in sporadic amyotrophic lateral sclerosis. *Exp Neurol* 171:418–421.
- Arai T, Hasegawa M, Akiyama H, Ikeda K, Nonaka T, Mori H, Mann D, Tsuchiya K, Yoshida M, Hashizume Y, Oda T (2006) TDP-43 is a component of ubiquitin-positive tau-negative inclusions in frontotemporal lobar degeneration and amyotrophic lateral sclerosis. *Biochem Biophys Res Commun* 351:602–611.
- Atamna H, Kumar R (2010) Protective role of methylene blue in Alzheimer's disease via mitochondria and cytochrome c oxidase. *J Alzheimers Dis* 20 (Suppl 2):S439–S452.
- Atamna H, Nguyen A, Schultz C, Boyle K, Newberry J, Kato H, Ames BN (2008) Methylene blue delays cellular senescence and enhances key mitochondrial biochemical pathways. *FASEB J* 22:703–712.
- Bahremand A, Nasrabad SE, Ziai P, Rahimian R, Hedayat T, Payandemehr B, Dehpour AR (2010) Involvement of nitric oxide-cGMP pathway in the anticonvulsant effects of lithium chloride on PTZ-induced seizure in mice. *Epilepsy Res* 89:295–302.
- Barber SC, Shaw PJ (2010) Oxidative stress in ALS: key role in motor neuron injury and therapeutic target. *Free Radic Biol Med* 48:629–641.
- Baumer D, Ansorge O, Almeida M, Talbot K (2010) The role of RNA processing in the pathogenesis of motor neuron degeneration. *Expert Rev Mol Med* 12:e21.
- Bogaert E, d'Ydewalle C, Van Den Bosch L (2010) Amyotrophic lateral sclerosis and excitotoxicity: from pathological mechanism to therapeutic target. *CNS Neurol Disord Drug Targets* 9:297–304.
- Boillee S, Vande Velde C, Cleveland DW (2006) ALS: a disease of motor neurons and their nonneuronal neighbors. *Neuron* 52:39–59.
- Bosco DA, Morfin G, Karabacak NM, Song Y, Gros-Louis F, Pasinelli P, Goolsby H, Fontaine BA, Lemay N, McKenna-Yasek D, Frosch MP, Agar JN, Julien JP, Brady ST, Brown RH Jr (2010) Wild-type and mutant SOD1 share an aberrant conformation and a common pathogenic pathway in ALS. *Nat Neurosci* 13:1396–1403.
- Buijn LI, Becher MW, Lee MK, Anderson KL, Jenkins NA, Copeland NG, Sisodia SS, Rothstein JD, Borchelt DR, Price DL, Cleveland DW (1997) ALS-linked SOD1 mutant G85R mediates damage to astrocytes and promotes rapidly progressive disease with SOD1-containing inclusions. *Neuron* 18:327–338.
- Buijn LI, Houseweart MK, Kato S, Anderson KL, Anderson SD, Ohama E, Reaume AG, Scott RW, Cleveland DW (1998) Aggregation and motor neuron toxicity of an ALS-linked SOD1 mutant independent from wild-type SOD1. *Science* 281:1851–1854.
- Callaway NL, Riha PD, Bruchey AK, Munshi Z, Gonzalez-Lima F (2004) Methylene blue improves brain oxidative metabolism and memory retention in rats. *Pharmacol Biochem Behav* 77:175–181.
- Cha CI, Kim JM, Shin DH, Kim YS, Kim J, Gurney ME, Lee KW (1998) Reactive astrocytes express nitric oxide synthase in the spinal cord of transgenic mice expressing a human Cu/Zn SOD mutation. *Neuroreport* 9:1503–1506.
- Chattopadhyay M, Valentine JS (2009) Aggregation of copper-zinc superoxide dismutase in familial and sporadic ALS. *Antioxid Redox Signal* 11:1603–1614.
- Chio A, Borghero G, Calvo A, Capasso M, Caponnetto C, Corbo M, Giannini F, Logroscino G, Mandrioli J, Marcello N, Mazzini L, Moglia C, Monsurro MR, Mora G, Patti F, Perini M, Pietrini V, Pisano F, Pupillo E, Sabatelli M, Salvi F, Silani V, Simone IL, Sorarù G, Tola MR, Volanti P, Beghi E (2010) Lithium carbonate in amyotrophic lateral sclerosis: lack of efficacy in a dose-finding trial. *Neurology* 75:619–625.
- Clifton J, Leikin JB (2003) Methylene blue. *Am J of Ther* 10:289–291.
- Eroglu L, Caglayan B (1997) Anxiolytic and antidepressant properties of methylene blue in animal models. *Pharmacol Res* 36:381–385.
- Feng HL, Leng Y, Ma CH, Zhang J, Ren M, Chuang DM (2008) Combined lithium and valproate treatment delays disease onset, reduces neurological deficit and prolongs survival in an amyotrophic lateral sclerosis mouse model. *Neuroscience* 155:567–572.
- Fornai F, Longone P, Cafaro L, Kastsiuchenka O, Ferrucci M, Manca ML, Lazzeri G, Spalloni A, Bellio N, Lenzi P, Modugno N, Siciliano G, Isidoro C, Murri L, Ruggieri S, Paparelli A (2008) Lithium delays progression of amyotrophic lateral sclerosis. *Proc Natl Acad Sci U S A* 105:2052–2057.
- Forsberg K, Jonsson PA, Andersen PM, Bergemalm D, Graffmo KS, Hultdin M, Jacobsson J, Rosquist R, Marklund SL, Brännström T (2010) Novel antibodies reveal inclusions containing non-native SOD1 in sporadic ALS patients. *PLoS One* 5:e11552.
- Gill A, Kidd J, Vieira F, Thompson K, Perrin S (2009) No benefit from chronic lithium dosing in a sibling-matched, gender balanced, investigator-blinded trial using a standard mouse model of familial ALS. *PLoS One* 4:e6489.
- Gros-Louis F, Soucy G, Larivière R, Julien JP (2010) Intracerebroventricular infusion of monoclonal antibody or its derived Fab fragment against misfolded forms of SOD1 mutant delays mortality in a mouse model of ALS. *J Neurochem* 113:1188–1199.
- Gurney ME (1997) The use of transgenic mouse models of amyotrophic lateral sclerosis in preclinical drug studies. *J Neurol Sci* 152 (Suppl 1):S67–S73.
- Gurney ME, Pu H, Chiu AY, Dal Canto MC, Polchow CY, Alexander DD, Caliendo J, Hentati A, Kwon YW, Deng HX, et al. (1994) Motor neuron degeneration in mice that express a human Cu,Zn superoxide dismutase mutation. *Science* 264:1772–1775.
- Johnson BS, Snead D, Lee JJ, McCaffery JM, Shorter J, Gitler AD (2009) TDP-43 is intrinsically aggregation-prone, and amyotrophic lateral sclerosis-linked mutations accelerate aggregation and increase toxicity. *J Biol Chem* 284:20329–20339.
- Lagier-Tourenne C, Polymenidou M, Cleveland DW (2010) TDP-43 and FUS/TLS: emerging roles in RNA processing and neurodegeneration. *Hum Mol Genet* 19:R46–R64.
- Lougheed R, Turnbull J (2011) Lack of effect of methylene blue in the SOD1 G93A mouse model of amyotrophic lateral sclerosis. *PLoS One* 6:e23141.

- McComas AJ, Upton AR, Sica RE (1973) Motoneuron disease and ageing. *Lancet* 2:1477–1480.
- Medina DX, Caccamo A, Oddo S (2011) Methylene blue reduces abeta levels and rescues early cognitive deficit by increasing proteasome activity. *Brain Pathol* 21:140–149.
- Miclescu A, Sharma HS, Martijn C, Wiklund L (2010) Methylene blue protects the cortical blood-brain barrier against ischemia/reperfusion-induced disruptions. *Crit Care Med* 38:2199–2206.
- Miller RG, Mitchell JD, Lyon M, Moore DH (2007) Riluzole for amyotrophic lateral sclerosis (ALS)/motor neuron disease (MND). *Cochrane Database Syst Rev*:CD001447.
- Narsapur SL, Naylor GJ (1983) Methylene blue. A possible treatment for manic depressive psychosis. *J Affect Disord* 5:155–161.
- National Toxicology Program (2008) Toxicology and carcinogenesis studies of methylene blue trihydrate (cas no. 7220-79-3) in F344/N rats and B6C3F1 mice (gavage studies). *Natl Toxicol Program Tech Rep Ser*:1–224.
- Naylor GJ, Dick DA, Johnston BB, Hopwood SE, Dick EG, Smith AH, Kay D (1981) Possible explanation for therapeutic action of lithium, and a possible substitute (methylene-blue). *Lancet* 2:1175–1176.
- Neumann M, Sampathu DM, Kwong LK, Truax AC, Micsenyi MC, Chou TT, Bruce J, Schuck T, Grossman M, Clark CM, McCluskey LF, Miller BL, Masliah E, Mackenzie IR, Feldman H, Feiden W, Kretzschmar HA, Trojanowski JQ, Lee VM (2006) Ubiquitinated TDP-43 in frontotemporal lobar degeneration and amyotrophic lateral sclerosis. *Science* 314:130–133.
- Orrell RW (2010) Motor neuron disease: systematic reviews of treatment for ALS and SMA. *Br Med Bull* 93:145–159.
- Peter C, Hongwan D, Küpfer A, Lauterburg BH (2000) Pharmacokinetics and organ distribution of intravenous and oral methylene blue. *Eur J Clin Pharmacol* 56:247–250.
- Pizzasegola C, Caron I, Daleno C, Ronchi A, Minoia C, Carri MT, Bendotti C (2009) Treatment with lithium carbonate does not improve disease progression in two different strains of SOD1 mutant mice. *Amyotroph Lateral Scler* 10:221–228.
- Pizzuti A, Petrucci S (2011) Mitochondrial dysfunction as a cause of ALS. *Arch Ital Biol* 149:113–119.
- Prudencio M, Hart PJ, Borchelt DR, Andersen PM (2009) Variation in aggregation propensities among ALS-associated variants of SOD1: correlation to human disease. *Hum Mol Genet* 18:3217–3226.
- Riha PD, Rojas JC, Gonzalez-Lima F (2011) Beneficial network effects of methylene blue in an amnesic model. *Neuroimage* 54:2623–2634.
- Sasaki S, Shibata N, Iwata M (2001) Neuronal nitric oxide synthase immunoreactivity in the spinal cord in amyotrophic lateral sclerosis. *Acta Neuropathol* 101:351–357.
- Sasaki S, Warita H, Abe K, Iwata M (2002) Neuronal nitric oxide synthase (nNOS) immunoreactivity in the spinal cord of transgenic mice with G93A mutant SOD1 gene. *Acta Neuropathol* 103:421–427.
- Schirmer RH, Adler H, Pickhardt M, Mandelkow E (2011) Lest we forget you—methylene blue. *Neurobiol Aging* 32(2325):e2327–2316.
- Shin JH, Cho SI, Lim HR, Lee JK, Lee YA, Noh JS, Joo IS, Kim KW, Gwag BJ (2007) Concurrent administration of Neu2000 and lithium produces marked improvement of motor neuron survival, motor function, and mortality in a mouse model of amyotrophic lateral sclerosis. *Mol Pharmacol* 71:965–975.
- Swarup V, Phaneuf D, Bareil C, Robertson J, Rouleau GA, Kriz J, Julien JP (2011) Pathological hallmarks of amyotrophic lateral sclerosis/frontotemporal lobar degeneration in transgenic mice produced with TDP-43 genomic fragments. *Brain* 134:2610–2626.
- Taniguchi S, Suzuki N, Masuda M, Hisanaga S, Iwatsubo T, Goedert M, Hasegawa M (2005) Inhibition of heparin-induced tau filament formation by phenothiazines, polyphenols, and porphyrins. *J Biol Chem* 280:7614–7623.
- Ticozzi N, Ratti A, Silani V (2010) Protein aggregation and defective RNA metabolism as mechanisms for motor neuron damage. *CNS Neurol Disord Drug Targets* 9:285–296.
- Turner BJ, Talbot K (2008) Transgenics, toxicity and therapeutics in rodent models of mutant SOD1-mediated familial ALS. *Prog Neurobiol* 85:94–134.
- Urushitani M, Sik A, Sakurai T, Nukina N, Takahashi R, Julien JP (2006) Chromogranin-mediated secretion of mutant superoxide dismutase proteins linked to amyotrophic lateral sclerosis. *Nat Neurosci* 9:108–118.
- Wang J, Xu G, Li H, Gonzales V, Fromholt D, Karch C, Copeland NG, Jenkins NA, Borchelt DR (2005) Somatodendritic accumulation of misfolded SOD1-L126Z in motor neurons mediates degeneration: alphaB-crystallin modulates aggregation. *Hum Mol Genet* 14:2335–2347.
- Wen Y, Li W, Poteet EC, Xie L, Tan C, Yan LJ, Ju X, Liu R, Qian H, Marvin MA, Goldberg MS, She H, Mao Z, Simpkins JW, Yang SH (2011) Alternative mitochondrial electron transfer as a novel strategy for neuroprotection. *J Biol Chem* 286:16504–16515.
- Wiklund L, Basu S, Miclescu A, Wiklund P, Ronquist G, Sharma HS (2007) Neuro- and cardioprotective effects of blockade of nitric oxide action by administration of methylene blue. *Ann N Y Acad Sci* 1122:231–244.
- Wischik CM, Edwards PC, Lai RY, Roth M, Harrington CR (1996) Selective inhibition of Alzheimer disease-like tau aggregation by phenothiazines. *Proc Natl Acad Sci U S A* 93:11213–11218.
- Wong PC, Pardo CA, Borchelt DR, Lee MK, Copeland NG, Jenkins NA, Sisodia SS, Cleveland DW, Price DL (1995) An adverse property of a familial ALS-linked SOD1 mutation causes motor neuron disease characterized by vacuolar degeneration of mitochondria. *Neuron* 14:1105–1116.
- Yamashita M, Nonaka T, Arai T, Kametani F, Buchman VL, Ninkina N, Bachurin SO, Akiyama H, Goedert M, Hasegawa M (2009) Methylene blue and dimebon inhibit aggregation of TDP-43 in cellular models. *FEBS Lett* 583:2419–2424.



Pharmacological reduction of ER stress protects against TDP-43 neuronal toxicity *in vivo*

Alexandra Vaccaro^{a,b,c,1}, Shunmoogum A. Patten^{b,c,1}, Dina Aggad^{a,b,c}, Carl Julien^{a,b,c}, Claudia Maios^b, Edor Kabashi^{b,2}, Pierre Drapeau^{b,c}, J. Alex Parker^{a,b,c,*}

^a CRCHUM, Université de Montréal, Montréal, QC, Canada

^b Department of Pathology and Cell Biology and Groupe de recherche sur le système nerveux central, Université de Montréal, Montréal, QC, Canada

^c Centre of Excellence in Neuromics, Université de Montréal, Montréal, QC, Canada

ARTICLE INFO

Article history:

Received 28 December 2012

Revised 20 February 2013

Accepted 26 March 2013

Available online 5 April 2013

Keywords:

TDP-43

ALS

Genetic models

Small molecules

ER stress

Neurodegeneration

C. elegans

Zebrafish

ABSTRACT

C. elegans and *D. rerio* expressing mutant TAR DNA Binding Protein 43 (TDP-43) are powerful *in vivo* animal models for the genetics and pharmacology of amyotrophic lateral sclerosis (ALS). Using these small-animal models of ALS, we previously identified methylene blue (MB) as a potent suppressor of TDP-43 toxicity. Consequently here we investigated how MB might exert its neuroprotective properties and found that it acts through reduction of the endoplasmic reticulum (ER) stress response. We tested other compounds known to be active in the ER unfolded protein response in worms and zebrafish expressing mutant human TDP-43 (mTDP-43). We identified three compounds: salubrinal, guanabenz and a new structurally related compound phenazine, which also reduced paralysis, neurodegeneration and oxidative stress in our mTDP-43 models. Using *C. elegans* genetics, we showed that all four compounds act as potent suppressors of mTDP-43 toxicity through reduction of the ER stress response. Interestingly, these compounds operate through different branches of the ER unfolded protein pathway to achieve a common neuroprotective action. Our results indicate that protein-folding homeostasis in the ER is an important target for therapeutic development in ALS and other TDP-43-related neurodegenerative diseases.

Crown Copyright © 2013 Published by Elsevier Inc. All rights reserved.

Introduction

Amyotrophic lateral sclerosis (ALS) is an adult onset neurodegenerative disorder characterized by a progressive and selective loss of motor neurons in the motor cortex, the brainstem, and the spinal cord (Al-Chalabi et al., 2012). The disease affects about 1–3 people in 100,000. The major pathogenic mechanism of ALS remains unclear but multiple cellular processes have been implicated including RNA processing deficiencies, oxidative stress, protein aggregation, mitochondrial dysfunction and potentially endoplasmic reticulum (ER) stress (Barber and Shaw, 2010; Boillee et al., 2006). Dysregulation of these cellular processes leads to neuronal dysfunction ultimately contributing to cell death and has been implicated in a number of neurological disorders including Alzheimer's disease, Parkinson's disease, Huntington's disease and stroke in addition to ALS (Lagier-Tourenne et al., 2010).

The etiology of ALS is composed of both genetic and environmental factors (Al-Chalabi et al., 2012; Andersen and Al-Chalabi, 2011) and its origins remain unknown for most cases and its clinical development is extremely variable (Bruijn et al., 2004; van Blitterswijk and Landers, 2010). The majority of cases are sporadic but ~10% of patients have an inherited familial form of the disease. Dominant mutations in SOD1 (copper/zinc superoxide dismutase 1) account for ~20% of familial ALS cases and ~1% of sporadic cases (Boillee et al., 2006). Recently, the identification of mutations in two DNA/RNA binding proteins, Transactive Response DNA-binding protein 43 (TDP-43) (Neumann et al., 2006) and Fused in Sarcoma (FUS) (Kwiatkowski et al., 2009; Vance et al., 2009) as causing familial and sporadic ALS, has oriented research interests toward RNA processing as a common pathogenic pathway leading to the development of motor neuron diseases (Bruijn et al., 2004; Lagier-Tourenne and Cleveland, 2009). Recently, hexanucleotide expansions in the first intron of the C9orf72 gene of unknown function have been discovered to be a major cause of familial ALS and a significant cause of sporadic ALS (DeJesus-Hernandez et al., 2011; Renton et al., 2011). As ALS is a complex and multifactorial disorder, strategies to discover new effective therapies remain challenging. Despite numerous attempts to find effective treatments, riluzole is currently the only FDA approved compound but it slows disease progression only modestly (Lacomblez et al., 1996; Riviere et al., 1998).

* Corresponding author at: CRCHUM, Hôpital Notre Dame, 1560 rue Sherbrooke Est, M-5226, Montreal, QC, H2L 4M1, Canada.

E-mail address: ja.parker@umontreal.ca (J.A. Parker).

Available online on ScienceDirect (www.sciencedirect.com).

¹ Equal contribution.

² Current address: Institut du Cerveau et de la Moelle Épinrière, Centre de Recherche, CHU Pitié-Salpêtrière, Paris, France.

In a previous study (Vaccaro et al., 2012a) we identified methylene blue (MB) as a potent suppressor of mutant TDP-43 (mTDP-43) and mutant FUS (mFUS) neuronal toxicity using *C. elegans* that express mTDP-43 and mFUS in motor neurons (Vaccaro et al., 2012b); and also zebrafish ubiquitously expressing mTDP-43 that show shortened and hyperbranched motoneuron axons (Kabashi et al., 2009) and mFUS (Kabashi et al., 2011). Using a variety of approaches we discovered that MB acts in our models through reduction of the endoplasmic reticulum (ER) stress response. We then looked for additional compounds that could reduce mTDP-43 proteotoxicity in worms and zebrafish following a similar mechanism of action and report here that the compounds salubrinal and guanabenz, known to act on ER stress (Boyce et al., 2005; Tsaytler et al., 2011) protected against mTDP-43 toxicity in both our models via the ER unfolded protein response (UPR^{ER}). We also found that the novel, structurally related compound phenazine was effective. Together these results indicate that the ER stress pathway may be an important target for therapeutic development in ALS and related neurodegenerative diseases.

Materials and methods

C. elegans experiments

Transgenics and strains

Strains and mutants used in this study include: *atf-6(ok551)*, *gpls1[hsp-16.2::GFP]*, *ire-1(zc14)*, *N2*, *pek-1(ok275)*, *xqls133[unc-47::TDP-43[A315T];unc-119(+)]*, *zcls4[hsp-4::GFP]*, *zcls9[hsp-60::GFP]*, and *zcls13[hsp-6::GFP]*.

Fluorescence microscopy

For visualization of *hsp-4::GFP*, *hsp-6::GFP*, *hsp-16.2::GFP* and *hsp-60::GFP* animals, M9 buffer with 5 mM levamisole was used for immobilization. Animals were mounted on slides with 2% agarose pads and examined for fluorescence. A Leica CTR 6000 and a Leica DFC 480 camera were used to visualize the worms. L4 animals were grown

on NGM plates and transferred to NGM plates + 60 μ M methylene blue, or NGM plates + 50 μ M salubrinal, or NGM plates + 50 μ M guanabenz, or NGM plates + 50 μ M phenazine (see Table 1 for compounds details), and examined for fluorescence with the Leica system described above. A minimum of 60 animals was examined per treatment over 3 trials. For scoring axons from transgenic mTDP-43 worms, synchronized animals were selected at days 1, 5 and 9 of adulthood for visualization of motor neurons *in vivo*. Animals were immobilized in M9 with 5 mM levamisole and mounted on slides with 2% agarose pads. Motor neurons were visualized with the Leica system described above. A minimum of 100 animals was scored per treatment over 4–6 trials. The mean and SEM were calculated for each trial and two-tailed t-tests were used for statistical analysis. For visualization of fluorescence after treatment with dihydrofluorescein diacetate, L4 animals were grown on NGM plates or NGM plates with methylene blue, salubrinal, guanabenz, or phenazine.

C. elegans drug testing on plates

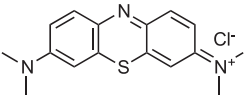
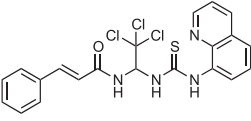
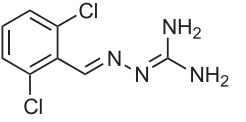
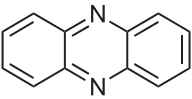
Worms were grown on standard NGM plates with or without compounds. For worms expressing mTDP-43, animals were counted as paralyzed if they failed to move upon prodding with a worm pick. Worms were scored as dead if they were immotile, showed no pharyngeal pumping and failed to move their head after being prodded on the nose.

Protein solubility

For TDP-43 transgenics, soluble and insoluble fractions were obtained using methods previously described (Liachko et al., 2010; Neumann et al., 2006), with modifications. Briefly, worms were homogenized with a pellet mixer (Disposable Pellet Mixer and Cordless Motor, VWR) in one volume (w/v) of low-salt buffer (LS) (10 mM Tris, 5 mM EDTA, 10% sucrose, pH 7.5) and centrifuged at 25,000 \times g for 30 min at 4 °C. The supernatant represents the LS fraction, containing the soluble proteins. The pellet was washed with the same volume of LS, centrifuged again and the supernatant was discarded. The remaining pellet was re-extracted with the same

Table 1

Structures, known biological functions, UPR^{ER}-related actions, and therapeutic uses of the compounds used in this study.

Compound	Chemical structure	Known biological functions	Action within the UPR ^{ER} reported in this study	Therapeutic use
Methylene blue		Interacts with nitric oxide synthase and has an antioxidant potential by decreasing the generation of reactive oxygen species (Rojas et al., 2012).	More specific to the IRE-1 pathway in the context of mTDP-43	Protective against several forms of neurodegeneration: <ul style="list-style-type: none"> - mutant TDP-43 (Vaccaro et al., 2012a; Yamashita et al., 2009) - mutant FUS (Vaccaro et al., 2012a) - mutant SOD1 (Dibaj et al., 2012) - mutant polyglutamine (Sontag et al., 2012) Phase II clinical trial for Alzheimer's disease (Gura, 2008)
Salubrinal		<ul style="list-style-type: none"> - Inhibits eIF2α phosphatases in the UPR^{ER} pathway (Boyce et al., 2005). - Disrupts the PP1 complex to increase phosphorylation of eIF2α (Jousse et al., 2003) 	Functions inside the PERK pathway but seems not restricted to the UPR: continues to reduce mTDP-43 paralysis when PERK absent	Effective in reducing mutant SOD1 toxicity in a mouse model of ALS (Saxena et al., 2009).
Guanabenz		<ul style="list-style-type: none"> - α2 adrenergic receptor agonist (Holmes et al., 1983). - Selectively binds GADD34, disrupting its association with PP1 (Tsaytler et al., 2011). - Protects against misfolded proteins in human cells: interferes with dephosphorylation of eIF2α (Tsaytler et al., 2011). 	Action dependent on PERK and ATF6 to rescue mTDP-43 paralysis	<ul style="list-style-type: none"> - Effective for the treatment of hypertension (Holmes et al., 1983). - Anti-prion activity: yeast and mammalian prions (Tribouillard-Tanvier et al., 2008a, 2008b).
Phenazine			Uses both the IRE-1 and PERK pathways to rescue mTDP-43 toxicity.	We report for the first time potential therapeutic properties of phenazine against mTDP-43 neuronal toxicity.

volume of Triton buffer (TX) (LS + 1% Triton X-100 + 0.5 M NaCl), centrifuged at 180,000 $\times g$ for 30 min at 4 °C. The resulting pellet was re-extracted with the same volume of myelin floatation buffer (TX buffer containing 30% sucrose) and centrifuged at 180,000 $\times g$ for 30 min at 4 °C. The remaining pellet was re-extracted in the same volume of Sarkosyl (SARK) buffer (LS + 1% N-Lauroyl-sarcosine + 0.5 M NaCl), incubated with agitation for 1 h at 22 °C and centrifuged at 180,000 $\times g$ for 30 min at 22 °C. The detergent-insoluble pellet was weighted and solubilized in 5 volumes (w/v) of urea buffer (UREA) (30 mM Tris, 7 M urea, 2 M thiourea, 4% CHAPS (3-[(3-cholamidopropyl)dimethylammonio]-1-propanesulfonate), pH 8.5) and sonicated 5 min. All buffers contained 1 mM DTT and protease inhibitors (LPC; 1/1000). The soluble LS and the insoluble UREA fractions were quantified with the Bradford Protein Assay Kit (Bio-Rad) following the manufacturer's instructions.

Immunoblotting

Worm LS and UREA samples (50 μg /well) were resuspended directly in 1 \times Laemmli sample buffer, boiled for 5 min and migrated in 10% polyacrylamide gels, transferred to nitrocellulose membranes (BioRad) and immunoblotted. The following antibodies were used: rabbit anti-TDP-43 (1:1000, Proteintech), and mouse anti-actin (1:5000, MP Biomedicals). Blots were visualized with peroxidase-conjugated secondary antibodies and ECL Western Blotting Substrate (Thermo Scientific).

Dihydrofluorescein diacetate assay

For visualization of oxidative damage in the transgenic strains the worms were incubated on a slide for 30 min with 5 μM dihydrofluorescein diacetate dye and then washed with PBS 1 \times

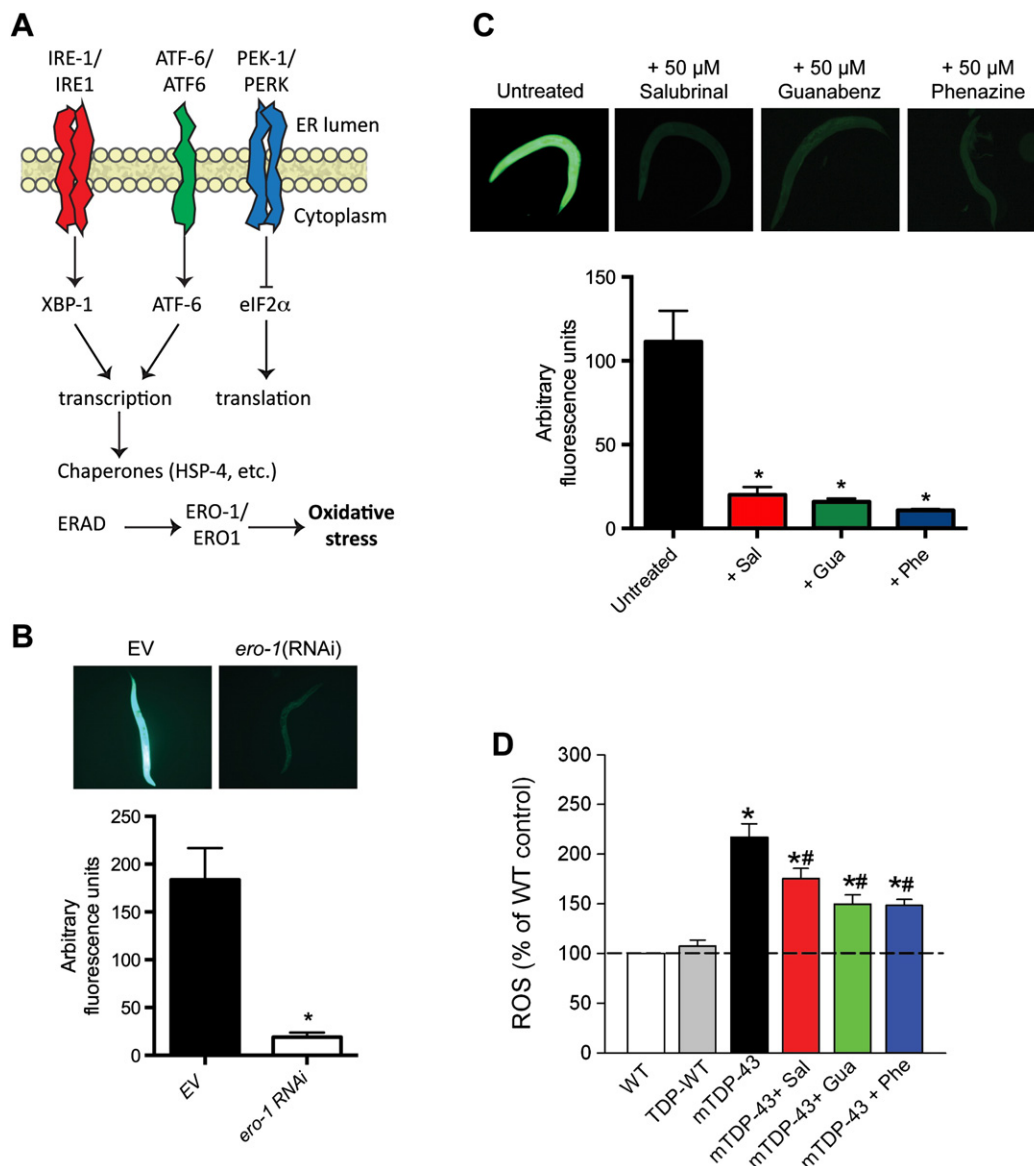


Fig. 1. Salubrinal, guanabenz and phenazine reduce oxidative stress caused by mutant TDP-43. (A) Overview of the three main UPR^{ER} pathways conserved between worms and mammals (based on Mao and Crowder, 2010). ER stress activates three main UPR pathways: ER transmembrane inositol-requiring kinase (IRE-1/IRE1), activating transcription factor 6 (ATF-6/ATF6), and protein kinase RNA-activated (PKR)-like ER kinase (PEK-1/PERK). Misfolded proteins in the ER can directly activate IRE1 and PERK, and the coordinated activation of all three branches is known as the integrated stress response. The activation of the UPR^{ER} leads to up-regulation of chaperones (like HSP-4/BiP) and ER-associated degradation (ERAD) leading to oxidative stress. (B) Dihydrofluorescein fluorescent photos of mTDP-43 worms subjected to either empty vector RNAi controls or *ero-1(RNAi)*. Quantification of fluorescent signals revealed a significant reduction in signal intensity by *ero-1(RNAi)* compared to empty vector controls, **P* < 0.001. (C) Photos and quantification of fluorescence of mTDP-43 worms stained with dihydrofluorescein after treatment with salubrinal, guanabenz or phenazine. mTDP-43 worms treated with any of the compounds had significantly less fluorescence than untreated mTDP-43 transgenics, **P* < 0.001. (D) Quantification of dihydrofluorescein fluorescence in zebrafish expressing mTDP-43 after treatment with salubrinal, guanabenz or phenazine. **P* < 0.001 versus wtTDP43 fish. *#*P* < 0.001 versus mTDP-43.

three times. After the slide was fixed, fluorescence was observed with the Leica system described above.

Statistics

For paralysis and stress-resistance tests, survival curves were generated and compared using the Log-rank (Mantel–Cox) test, and 60–100 animals were tested per genotype and repeated at least three times.

Zebrafish experiments

In-vitro mRNA synthesis and embryo microinjection

Human TDP-43 wild-type and mutant [G348C] (mTDP-43) mRNAs were transcribed from NotI-linearized pCS2+ using SP6 polymerase with the mMESSAGE Machine Kit (Ambion). Wild-type and mutant TDP-43 mRNAs (25 ng/μl) were pulse-injected into 1–2 cell stage embryos using a Picospritzer III pressure ejector.

Chemical treatments

Transient transgenics for TDP-43 [G348C] (mTDP-43) embryos at 24 hpf were placed in individual wells in a 24 well plate and were treated overnight with methylene blue, salubrinal, guanabenz or phenazine diluted in Evans solution (in mM): 134 NaCl, 2.9 KCl, 2.1 CaCl₂, 1.2 MgCl₂, 10 HEPES, 10 glucose, pH 7.8, 290 mOsm, with 0.1% DMSO. Behavioral touch responses were then assessed at 52–56 hpf as described in the following section.

Touch-evoked escape response

Zebrafish larvae were touched lightly at the level of the tail with a pair of blunt forceps and their locomotor behavior was recorded with a Grasshopper 2 Camera (Point Grey Research) at 30 Hz. The movies were then analyzed using the manual tracking plugin of ImageJ 1.45r software (NIH) and the swim duration, swim distance and maximum swim velocity of the fish were calculated.

Immunohistochemistry

Zebrafish larvae (48 hpf) were fixed in 4% paraformaldehyde overnight at 4 °C. After fixation, the larvae were rinsed and washed several times in PBS and permeabilized first for 30 min in 4% Triton-X 100 containing 2% bovine serum albumin (BSA) and 10% goat serum then for 20 min in PBS containing 1 mg/ml of collagenase. Following permeabilization, the larvae were incubated in the primary antibody znp-1 (Developmental Studies Hybridoma Bank; 1:200) for 48 h at 4 °C on a shaker. Tissue sections were washed several times in PBS over a 24 h period, and then incubated in the secondary antibody conjugated with Alexa Fluor 488 (Molecular Probes, Carlsbad, CA, 1:1000) for 4–6 h at room temperature. Animals were washed in PBS several times, cleared in 70% glycerol and mounted. Z-stack images were photographed using a Quorum Technologies spinning disk confocal microscope with a CSU10B (Yokogawa) spinning head mounted on an Olympus BX61W1 microscope. Images were acquired and were compiled using Volocity software (Improvision).

Reactive oxygen species (ROS) measurements

The generation of ROS in the larvae exposed to the chemicals was quantitatively assessed as previously described (Vaccaro et al., 2012a). Briefly, 15 embryos were washed with cold phosphate buffer solution (PBS; pH 7.4) twice and then homogenized in cold buffer (0.32 mM of sucrose, 20 mM of HEPES, 1 mM of MgCl₂, and 0.5 mM of phenylmethyl sulfonylfluoride (PMSF), pH 7.4). The homogenate was centrifuged at 15,000 ×g at 4 °C for 20 min, and the supernatant was transferred to new tubes for further experimentation. Then 20 μl of the homogenate was added to a 96-well plate and incubated at room temperature for 5 min, after which 100 μl of PBS (pH 7.4) and 8.3 μl of 2',7'-dichlorofluorescein diacetate (DFH) (Sigma-Aldrich) stock solution (10 mg/ml) were added to each well. The plate was incubated at 37 °C for 30 min. The fluorescence intensity was measured

using a microplate reader (SpectraMax M2, Molecular Device, Union City, CA, USA) with excitation and emission at 485 and 530 nm, respectively. The ROS concentration was expressed as arbitrary emission units per mg protein.

Statistical analysis

All data values are given as means ± S.E.M. Significance was determined using one-way ANOVAs and Fisher LSD tests for normally distributed and equal variance data, Kruskal–Wallis ANOVA and Dunn's method of comparison were used for non-normal distributions.

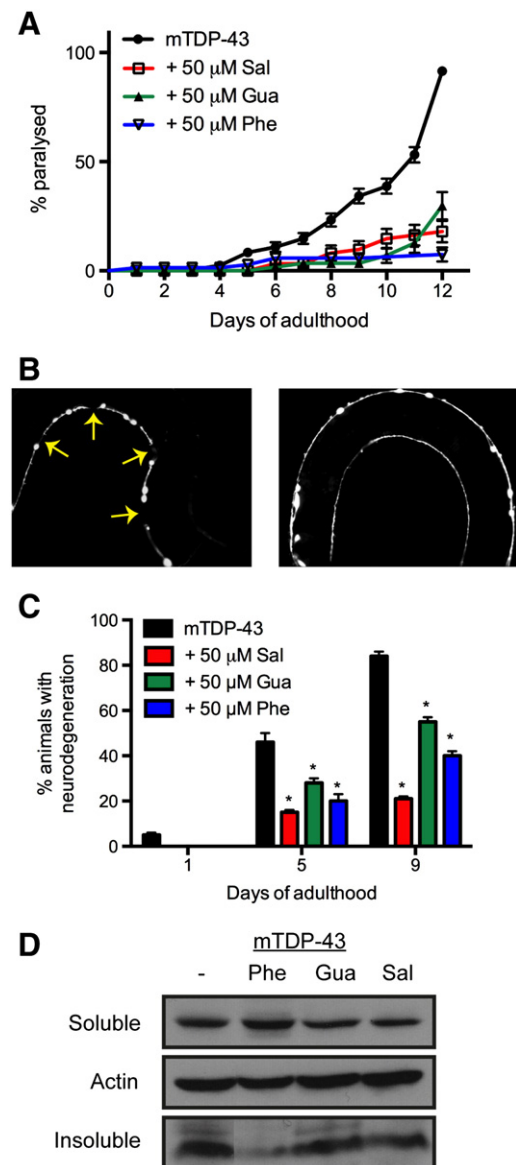


Fig. 2. Salubrinal, guanabenz and phenazine reduce mutant TDP-43 toxicity in *C. elegans*. (A) Salubrinal (Sal), guanabenz (Gua), and phenazine (Phe) reduced age-dependent paralysis on mTDP-43 worms compared to untreated transgenics. Please see Supplemental Table 1 for statistics. (B) Shown are representative photos of living, adult mTDP-43 transgenic worms. Visualization of motor neurons in mTDP-43 with the *unc-47p::GFP* reporter showed gaps and breaks (yellow arrows) along neuronal processes (left panel) that were significantly reduced in animals treated with salubrinal, guanabenz or phenazine (right panel). (C) Quantification of neurodegeneration in mTDP-43 worms at days 1, 5 and 9 of adulthood. Neurodegeneration of motor neurons in mTDP-43 transgenics was reduced by administration of salubrinal, guanabenz or phenazine. **P* < 0.001 versus untreated control mTDP-43 worms. (D) Phenazine, guanabenz, and salubrinal all reduced the amount of insoluble mTDP-43 protein compared to untreated control mTDP-43 transgenics.

Results

Reduction of global oxidative stress in mutant TDP-43 animals after treatment with salubrinal, guanabenz or phenazine

We previously described increased levels of oxidative stress in *C. elegans* and zebrafish expressing mutant TDP-43 proteins (Vaccaro et al., 2012a). We hypothesized that a portion of this oxidative stress may originate within the ER in response to the accumulation of unfolded mutant proteins (UPR^{ER}) as part of the integrated stress response (Harding et al., 2003). Early on the UPR^{ER} is protective but prolonged ER stress stimulates the clearance of misfolded proteins from the ER through ER-associated degradation (ERAD) by transporting misfolded proteins from the ER lumen to the cytoplasm for degradation by the ubiquitin–proteasome (Walker and Atkin, 2011) (Fig. 1A). Cell death may occur if the ER stress is not resolved. The processing of misfolded proteins for ERAD is redox intensive and central to this activity is the ER oxidoreductase *ero-1*/ERO1. Disruption of *ero-1*/ERO1 activity blocks the processing of proteins and the concomitant generation of endogenous peroxides and hence oxidative stress (Harding et al., 2003). As previously reported (Vaccaro et al., 2012a) the expression of mTDP-43 in worms and fish leads to a global increase in oxidative stress that can be detected by staining the animals with the fluorescent dye dichlorofluorescein diacetate (DHF) (Harding et al., 2003). We observed that mTDP-43 worms stained with DHF were highly fluorescent and this fluorescence was extinguished when the animals were subjected to *ero-1* RNAi (Fig. 1B). This is consistent with a previous report showing that *ero-1* is essential for ERAD (Harding et al., 2003) and suggests that the oxidative stress observed in our mTDP-43 worms originates within the ER.

To explore the notion that protection from ER-based proteotoxicity may reduce motor neuron deficits, we further examined whether pharmacological manipulation of the ER stress response would likewise be neuroprotective. ER stress activates three main UPR pathways: ER transmembrane inositol-requiring kinase (IRE1), activating transcription

factor 6 (ATF6), and protein kinase RNA-activated (PKR)-like ER kinase (PERK) (Walker and Atkin, 2011). Following the hypothesis that the ER stress response plays a central role in mTDP-43 toxicity, we selected other compounds known to be active in the UPR^{ER} and tested them against our mTDP-43 worms and zebrafish. A specific target of PERK is the eIF2 α phosphatase, and the compound salubrinal inhibits eIF2 α phosphatase. Sal is effective in reducing mutant superoxide dismutase-1 toxicity in a mouse model of familial ALS, demonstrating that it can protect the ER against misfolded protein stress (Saxena et al., 2009). Guanabenz is an α 2-adrenergic receptor agonist used in the treatment of hypertension (Holmes et al., 1983). This compound shows anti-prion activity (Tribouillard-Tanvier et al., 2008a, 2008b) and protects against misfolded proteins in human cells by interfering with the stress-induced dephosphorylation of eIF2 α (Tsaytler et al., 2011). Phenazine shows structural similarities to MB, salubrinal and guanabenz, so we hypothesized that it may have neuroprotective properties as well. See Table 1 for the structures, known biological functions, UPR^{ER}-related actions, and therapeutic uses of the compounds used in this study. Also, the Maximum Common Subgraph (MCS) scores for assessing the similarity of the compounds are depicted in Supplemental Table 2 (Rahman et al., 2009). We observed that 50 μ M salubrinal, guanabenz and phenazine all significantly reduced oxidative stress in mTDP-43 transgenics stained with DHF (Fig. 1C). Likewise, also using the DHF assay, we observed that all three compounds reduced oxidative stress of zebrafish expressing mTDP-43 compared to untreated controls (Fig. 1D). These data indicate that these compounds can reduce oxidative stress associated with ER proteotoxicity.

Salubrinal, guanabenz and phenazine reduce mTDP-43 toxicity in *C. elegans*

Transgenic worms expressing mTDP-43 show adult onset, age-dependent motility defects leading to paralysis and neurodegeneration accompanied by protein aggregation (Vaccaro et al., 2012b). mTDP-43 worms grown on plates containing salubrinal, guanabenz or phenazine

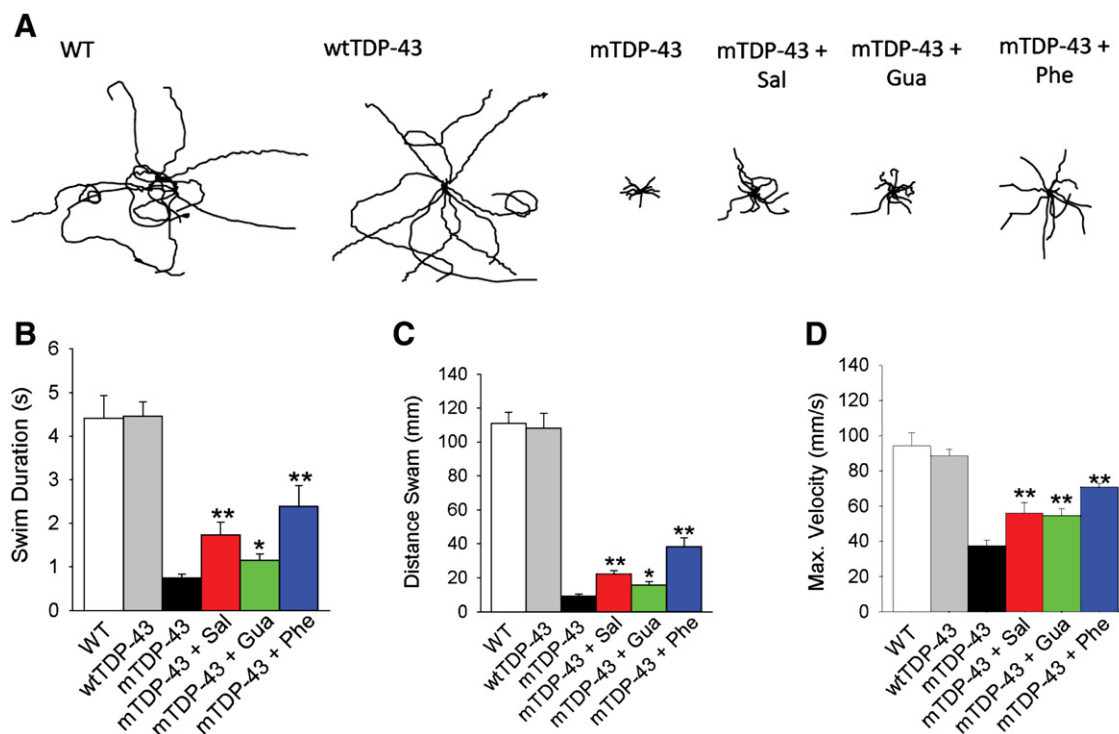


Fig. 3. Salubrinal, guanabenz and phenazine reduce motor deficits in zebrafish expressing mutant TDP-43. (A) Representative traces of touch-evoked escape response phenotypes in wild-type (WT), wtTDP-43, mTDP-43, mTDP-43 + Sal, mTDP-43 + Gua and mTDP-43 + Phe. Application of salubrinal, guanabenz or phenazine led to a significant improvement in the swim duration (B), distance swam (C), and maximum swimming velocity (D) of mTDP-43 fish. **Denotes significant difference from mutant fish $P < 0.001$; *significantly different from mutant fish $P < 0.05$.

had significantly reduced rates of paralysis compared to untreated transgenics (Fig. 2A, Supplemental Table 1). mTDP-43 worms show age-dependent neurodegeneration typically observed as gaps or breaks along neuronal processes (Vaccaro et al., 2012b). Treatment with any of the three compounds also reduced age-dependent neurodegeneration of motor neurons in mTDP-43 transgenics (Figs. 2B and C). Unlike wild type TDP-43, mTDP-43 proteins expressed in our transgenic worms are susceptible to misfolding leading to insolubility and aggregation that may contribute to motor neuron dysfunction and degeneration (Vaccaro et al., 2012b). We observed that mTDP-43 worms treated with salubrinal, guanabenz or phenazine had decreased amounts of insoluble mTDP-43 protein suggesting enhanced clearance of mutant proteins (Fig. 2D). Thus, these compounds share the ability to reduce the load of misfolded mutant proteins as perhaps at least one common mechanism in reducing proteotoxicity and neurodegeneration associated with mTDP-43.

Salubrinal, guanabenz and phenazine reduce mTDP-43 toxicity in zebrafish

To determine if the neuroprotective properties of salubrinal, guanabenz and phenazine extended beyond *C. elegans* we tested these compounds in our zebrafish models of mTDP-43 toxicity, which show characteristic behavioral and motor neuron axon deficits (Kabashi et al., 2009). Zebrafish expressing mTDP-43 [G348C] showed a greatly reduced touch-evoked escape response compared to non-transgenic or

wtTDP-43 fish (Fig. 3A). Interestingly, mTDP-43 fish treated with salubrinal, guanabenz or phenazine showed improved swimming response as assessed by the swim duration, distance swam and maximum swim velocity (Figs. 3A–D).

Besides behavioral defects, immunohistochemical analyses show that transgenic zebrafish expressing mTDP-43 exhibited shortened spinal motor axon length (Figs. 4A and B) and abnormal branching (Figs. 4A–C). These motor phenotypes were rescued by incubation with salubrinal, guanabenz or phenazine (Figs. 4A–C). These results demonstrate that salubrinal, guanabenz and phenazine can significantly reduce the motor neuron phenotypes elicited by expression of mTDP-43 in our zebrafish genetic model of ALS.

Methylene blue, salubrinal, guanabenz and phenazine specifically induce hsp-4/BiP expression in *C. elegans*

Having shown that methylene blue (Vaccaro et al., 2012a), salubrinal, guanabenz, and phenazine all reduce oxidative stress and neurodegeneration phenotypes in our ALS models, we next sought to further explore the mechanism of action of these compounds. Capitalizing on the strength of *C. elegans* genetics, we investigated whether neuroprotection by these compounds involved the upregulation of general compensatory cellular stress response pathways or were more specific to the ER stress response. We used a number of transgenic *C. elegans* reporter strains expressing GFP under specific stress

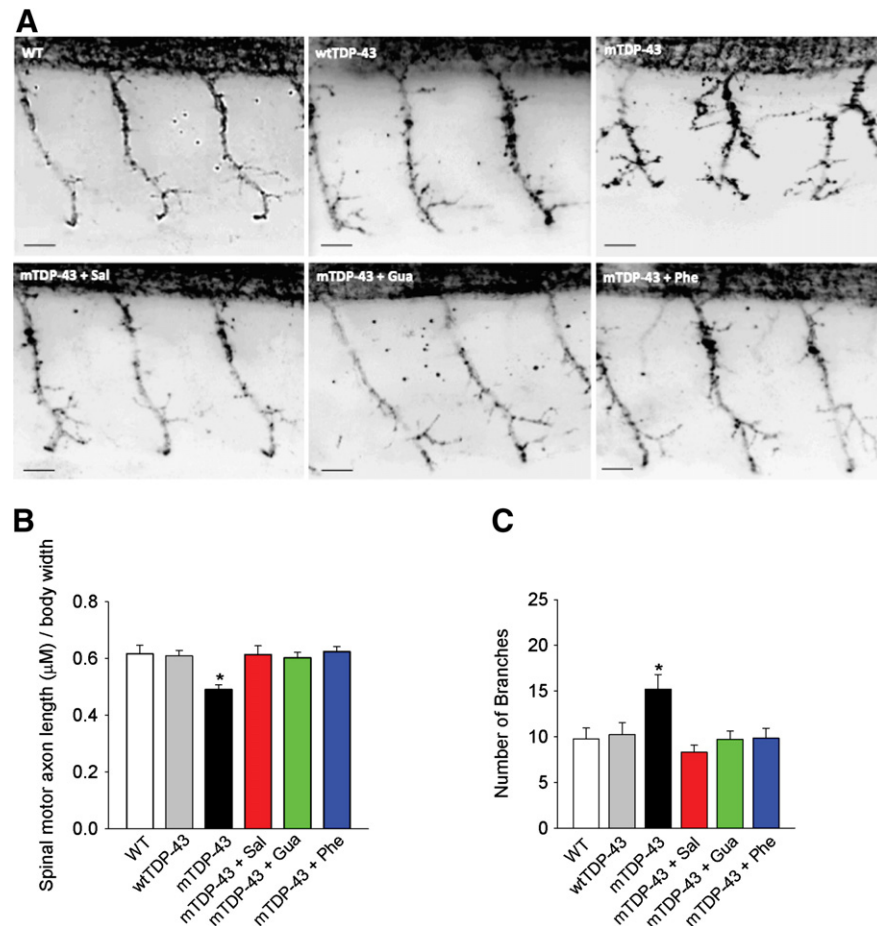


Fig. 4. Salubrinal, guanabenz and phenazine reduce axon defects in zebrafish expressing mutant TDP-43. (A) Appearance of motor neurons in WT, wtTDP-43 and mTDP-43 transgenic zebrafish with and without drug treatments. (B) The primary spinal motor axon length (normalized to body width) phenotype of motor neurons in mTDP-43 transgenic zebrafish is significantly shorter compared to WT and wtTDP-43 (* $P < 0.001$) and this abnormal phenotype is rescued in mTDP-43 fish treated with salubrinal, guanabenz or phenazine. (C) The spinal motor axon of mTDP-43 consists of a significantly larger number of primary and secondary branches compared to WT and wtTDP-43 (* $P < 0.001$) and this overbranching phenotype is rescued in mTDP-43 fish treated with salubrinal, guanabenz or phenazine.

conditions including: *hsp-4*, a protective Hsp70/BiP protein induced by ER-stress (Urano et al., 2002), *hsp-6*, a mitochondrial Hsp70 protein (Yoneda et al., 2004), *hsp-60*, a mitochondrial Hsp10/60 protein (Yoneda et al., 2004), and *hsp-16.2*, a Hsp16 heat shock protein (Link et al., 1999). We observed that all four compounds specifically and significantly induced the expression of *hsp-4::GFP* but did not affect *hsp-6*, *hsp-60* or *hsp-16.2* expression (Fig. 5). These data suggest that the four compounds may function within the integrated stress response since induction of chaperones like HSP-4 is a downstream consequence of sustained ER stress (Fig. 1A).

Chemical genetic analysis of the UPR^{ER}

ER stress activates three different pathways of the UPR leading to upregulation of chaperones for some and to arrest general protein translation for others (Walker and Atkin, 2011) (Fig. 1A). Consequently, we investigated if our compounds required any specific branch of the UPR^{ER} for their neuroprotective activities. To determine the molecular mechanisms of each compound, we took a genetic approach using mutants against key components of the three branches of the UPR^{ER} including *ire-1*/IRE1, *atf-6*/ATF6 and *pek-1*/PERK.

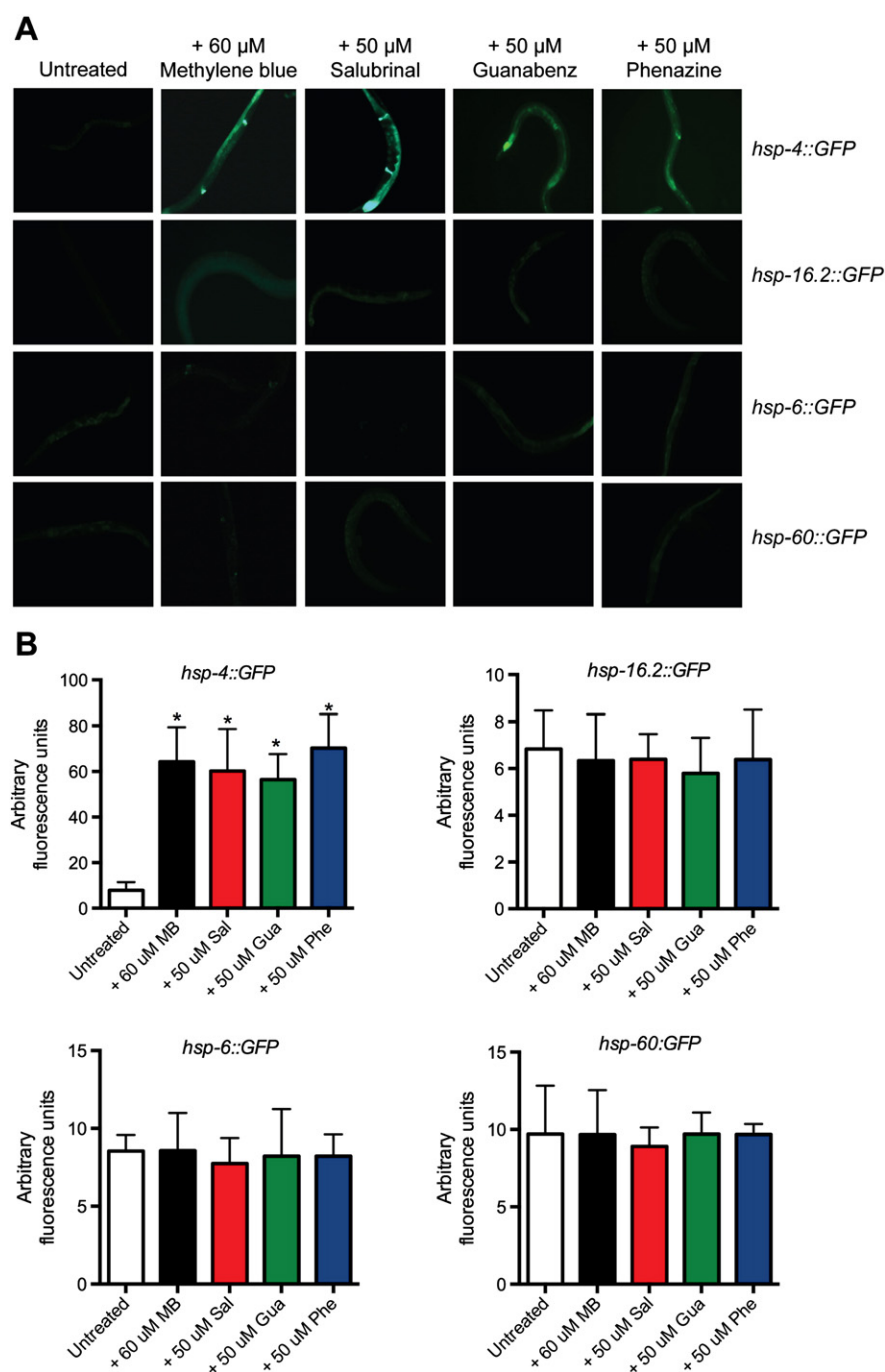


Fig. 5. All four compounds induce *hsp-4* expression. (A) Photographs of GFP reporter strains for several chaperones. Methylene blue, salubrinal, guanabenz and phenazine induce expression of the ER chaperone reporter *hsp-4::GFP* but do not induce expression heat shock reporter *hsp-16.2::GFP* or the mitochondrial chaperones *hsp-6::GFP* and *hsp-60::GFP*. (B) Quantification of fluorescence for each GFP reporter strain treated or untreated with compounds. *P < 0.001 versus untreated *hsp-4::GFP* worms.

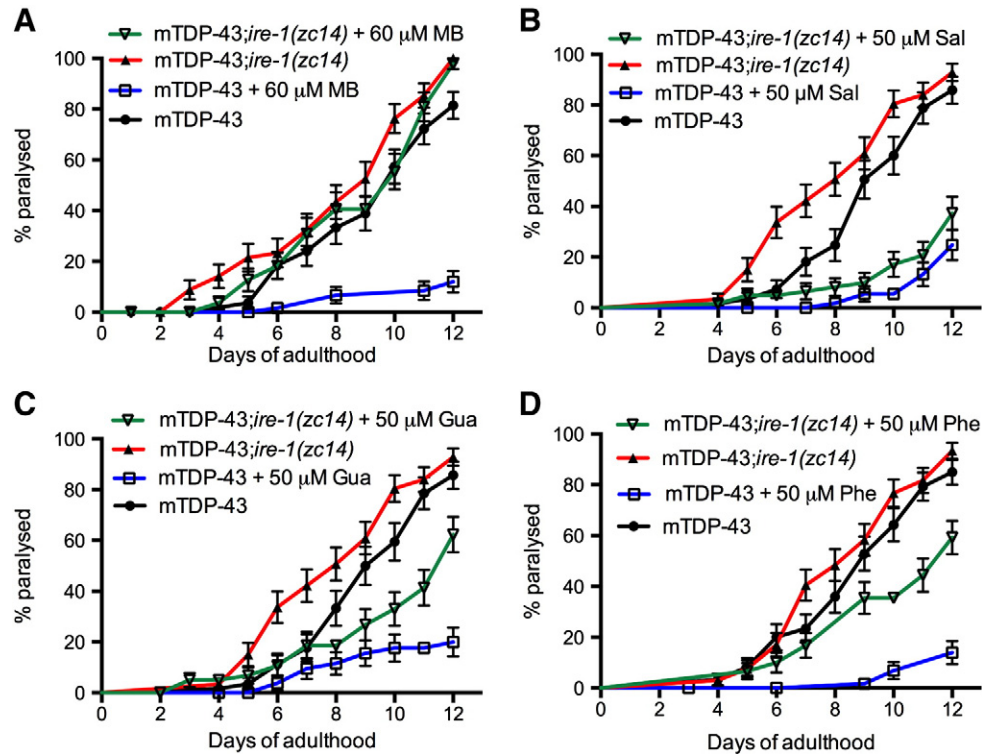


Fig. 6. Chemical genetic analysis of *ire-1* in mutant TDP-43 toxicity. Paralysis assays for MB, Sal, Gua and Phe against mTDP-43 worms and mTDP-43;*ire-1*(zc14) mutants. (A) MB failed to rescue paralysis in mTDP-43;*ire-1*(zc14) mutants. (B) Sal suppressed paralysis in mTDP-43;*ire-1*(zc14) mutants. (C) Gua partially suppressed paralysis in mTDP-43;*ire-1*(zc14) mutants. (D) Phe partially suppressed paralysis in mTDP-43;*ire-1*(zc14) mutants. Please see Supplemental Table 1 for statistics.

To invalidate IRE-1 function in worms, we used *ire-1*(zc14) mutants that have a missense mutation in a conserved residue in the kinase domain (Calfon et al., 2002) and generated a mTDP-43;*ire-1*(zc14) strain.

We noticed that the introduction of the *ire-1*(zc14) point mutation into the mTDP-43 worms somewhat exacerbated the paralysis phenotype when compared to mTDP-43 alone (Fig. 6, Supplemental Table 1)

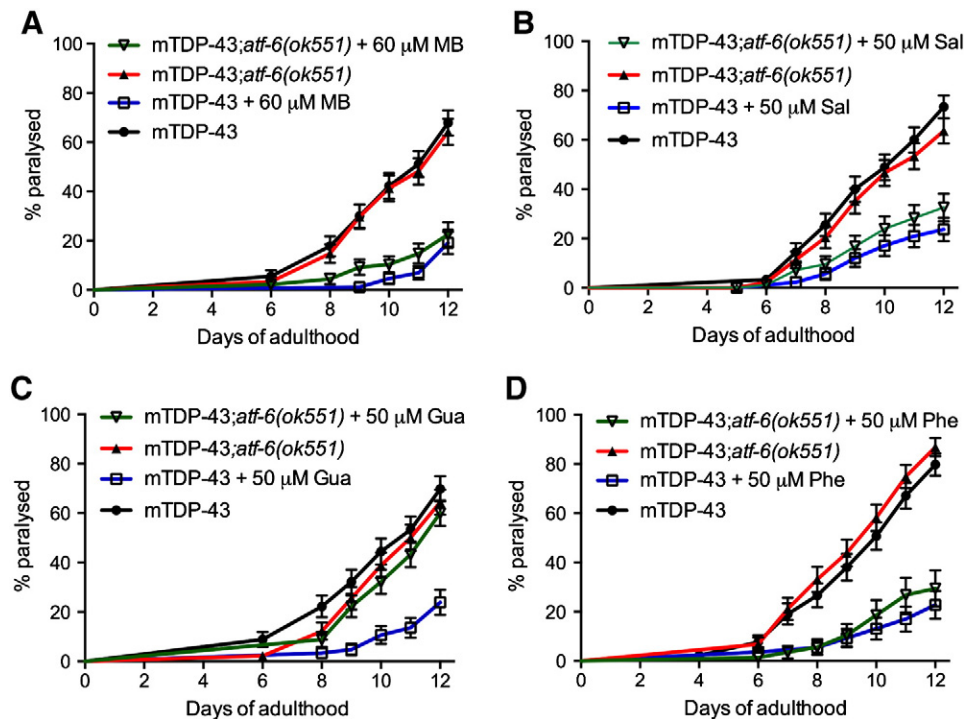


Fig. 7. Chemical genetic analysis of *atf-6* in mutant TDP-43 toxicity. Paralysis assays for MB, Sal, Gua and Phe against mTDP-43 worms and mTDP-43;*atf-6*(ok551) mutants. (A) MB suppressed paralysis in mTDP-43;*atf-6*(ok551) mutants. (B) Sal suppressed paralysis in mTDP-43;*atf-6*(ok551) mutants. (C) Gua failed to suppress paralysis in mTDP-43;*atf-6*(ok551) mutants. (D) Phe suppressed paralysis in mTDP-43;*atf-6*(ok551) mutants. Please see Supplemental Table 1 for statistics.

suggesting that *ire-1* is generally protective against mTDP-43 toxicity. We observed that the rescuing activity of methylene blue was completely dependent on *ire-1* (Fig. 6A). Salubrinal continued to suppress paralysis in the absence of *ire-1* suggesting that salubrinal does not require the *ire-1*/IRE1 branch of the UPR^{ER} (Fig. 6B). In contrast, guanabenz and phenazine were partially dependent on *ire-1* as these compounds had a reduced ability to suppress paralysis (Figs. 6C and D). These data suggest that the four compounds utilize different or possibly overlapping branches of the UPR^{ER} to achieve neuroprotection.

We examined the contribution of the *atf-6*/ATF6 branch with the deletion mutant *atf-6(ok551)*. We observed that *atf-6* was not required for the protective activities of methylene blue, salubrinal or phenazine since these compounds suppressed paralysis in mTDP-43;*atf-6(ok551)* mutants (Figs. 7A, B and D, Supplemental Table 1). However, the protective effect of guanabenz against mTDP-43 induced paralysis was abolished by *atf-6(ok551)* (Fig. 7C), indicating an off-target effect independent of its action on eIF2 α .

The requirement for *pek-1* in neuroprotection was assayed with the deletion mutant *pek-1(ok275)*. Looking at suppression of paralysis by the four compounds we observed that *pek-1* was not required for suppression of paralysis by either methylene blue or salubrinal (Figs. 8A and B). However, neuroprotection from guanabenz treatment was completely dependent on *pek-1*, while phenazine's protective activity was partially reduced in mTDP-43;*pek-1(ok275)* mutants (Figs. 7C and D).

Improved protection from combined compound administration

Our chemical genetic experiments demonstrated that the four compounds showed distinct profiles but had overlapping requirements of the three branches of the UPR^{ER} to protect against mTDP-43 toxicity (Fig. 9A). Given that the compounds affected different aspects of the UPR^{ER}, we reasoned that testing them in combination at reduced concentrations might be more effective than any one compound alone. To explore this notion we tested all paired combinations of methylene

blue, salubrinal, guanabenz and phenazine. We tested each compound at the lower concentration of 25 μ M instead of the usual 50 μ M (or 60 μ M for methylene blue). All compounds continued to rescue mTDP-43 paralysis at 25 μ M (Figs. 9B–G, Supplementary Table 1) albeit less effectively than at 50 μ M (Figs. 6–8). We then examined for combinations of compounds that were more effective than either compound alone. We observed that methylene blue in combination with salubrinal, guanabenz or phenazine was more effective than any compound alone (Figs. 9B–D). In contrast, dual combinations of salubrinal, guanabenz or phenazine were no better than any compound alone (Figs. 9E–G). These data suggest that methylene blue may act in a pathway somewhat distinct from the other compounds and that more effective neuroprotection may be achieved by combining drugs that work in distinct or overlapping UPR^{ER} pathways.

Discussion

Various types of stress can impair or overload ER function leading to the accumulation of unfolded or misfolded proteins. Interestingly, a common feature of many neurodegenerative disorders is the accumulation of misfolded proteins and the expression of ER stress markers has been observed in post-mortem brain tissues from patients with various neurodegenerative diseases (Matus et al., 2008). ER stress triggers the activation of the UPR^{ER} that acts to alleviate stress by increasing protein folding capacity, inhibiting general protein translation and promoting the degradation of misfolded proteins (Ron and Walter, 2007). However, if the response is unable to rescue the cell it will eventually lead to cell death (Ilieva et al., 2007). Although a strong correlation between ER stress, motor neuron loss and ALS progression has been observed (Atkin et al., 2008; Ilieva et al., 2007), the actual role of the UPR^{ER} in the disease process has not yet been clearly established. In this study, we identified methylene blue, salubrinal, guanabenz and a novel compound phenazine as potent suppressors of mTDP-43 proteotoxicity. We observed neuroprotective properties for each compound through a reduction of paralysis and neurodegeneration, and also a decrease in

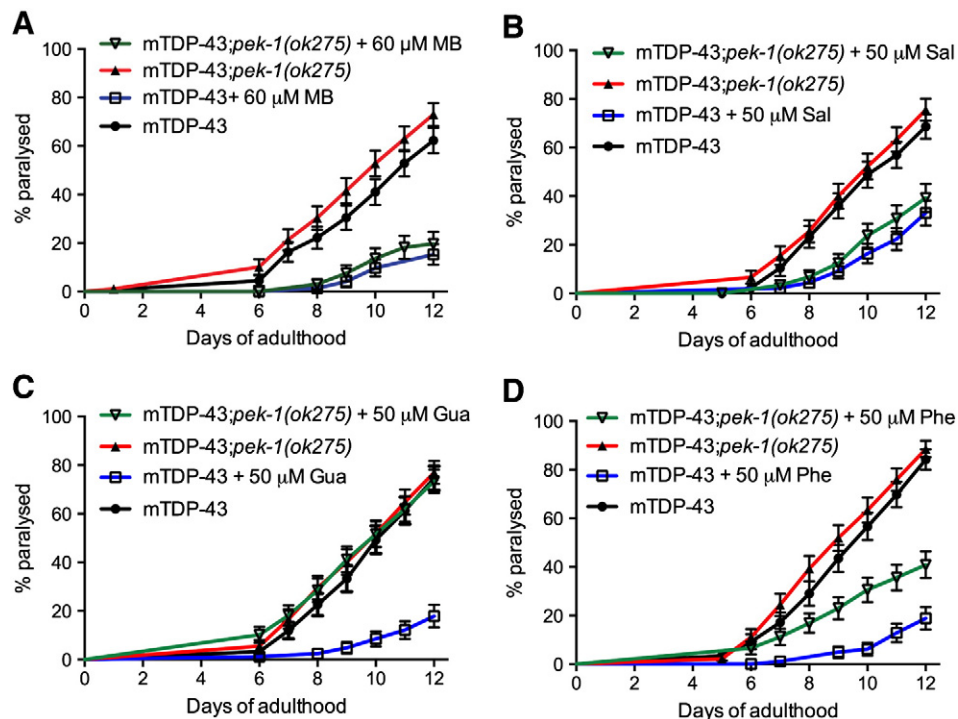


Fig. 8. Chemical genetic analysis of *pek-1* in mutant TDP-43 toxicity. Paralysis assays for MB, Sal, Gua and Phe against mTDP-43 worms and mTDP-43;*pek-1(ok275)* mutants. (A) MB suppressed paralysis in mTDP-43;*pek-1(ok275)* mutants. (B) Sal suppressed paralysis in mTDP-43;*pek-1(ok275)* mutants. (C) Gua failed to suppress paralysis in mTDP-43;*pek-1(ok275)* mutants. (D) Phe partially suppressed paralysis in mTDP-43;*pek-1(ok275)* mutants. Please see Supplemental Table 1 for statistics.

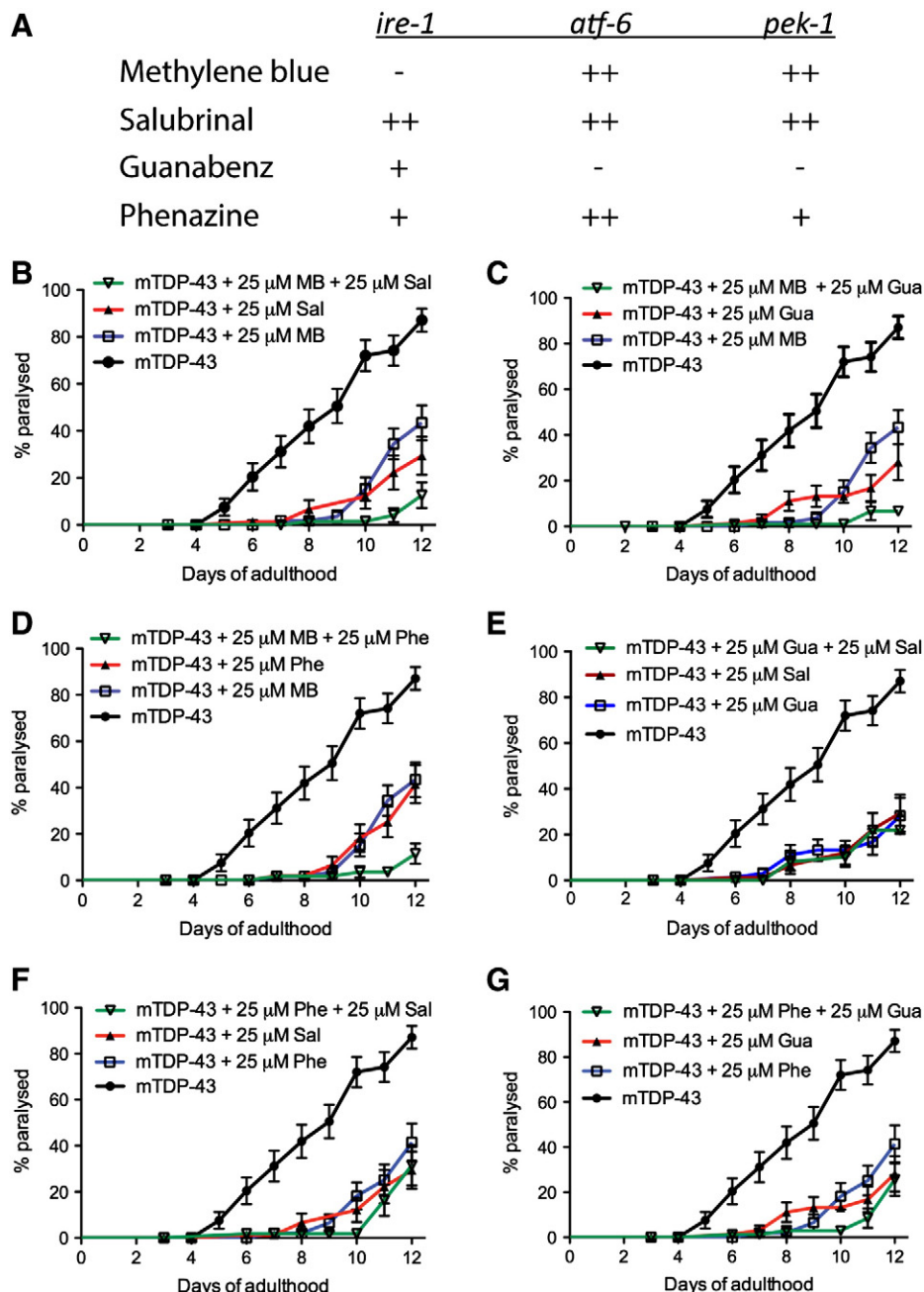


Fig. 9. Methylene blue is additive for neuroprotection. (A) Summary of whether UPR^{ER} genes were required for neuroprotection by the four compounds, -: no activity, +: partial suppression of paralysis, ++: strong suppression of paralysis. Paralysis curves for mTDP-43 transgenics tested with dual combinations of MB, Sal, Gua and Phe including (B) MB and Sal, (C) MB and Gua, (D) MB and Phe, (E) Sal and Gua, (F) Sal and Phe and (G) Gua and Phe. Please see Supplemental Table 1 for statistics.

both protein insolubility and oxidative stress. Our experiments demonstrated that although these four compounds function within the UPR^{ER} they operate through different branches of this pathway to achieve neuroprotection.

There is growing evidence for a protective role of methylene blue against multiple forms of neurodegeneration including mTDP-43 (Vaccaro et al., 2012a; Yamashita et al., 2009), mFUS (Vaccaro et al., 2012a), mutant SOD1 (Dibaj et al., 2012) mutant polyglutamine proteins (Sontag et al., 2012), and MB has shown promising effects in a Phase II clinical trial for AD (Gura, 2008). MB is not protective in adult SOD1 (Lougheed and Turnbull, 2011) or TDP-43 mice (Audet et al., 2012) and we found diminished effect on worms (Vaccaro et al., 2012a), and no activity in zebrafish (data not shown) after the phenotypes have been established, indicating that these compounds

may not be useful for treating the disorder. However young mice have not been tested for the protective effect we observed in our similar models, which would be of interest for pre-clinical relevance. Here we show that MB protects against mTDP-43 through the UPR^{ER} , and more specifically through the IRE1 pathway.

Salubrinal (Boyce et al., 2005) and guanabenz (Tsaytler et al., 2011) are well-characterized compounds and here we attempted to determine which branches of the UPR^{ER} were essential for their protective activity against mTDP-43. During the ER stress response PERK auto-phosphorylates and in turn phosphorylates eIF2 α . eIF2 α is subsequently dephosphorylated by a complex consisting of the phosphatase PP1 and its cofactor GADD34 (Novoa et al., 2001). Salubrinal and guanabenz are inhibitors of eIF2 α phosphatases and they both target eIF2 α phosphatases composed of PP1 bound to GADD34 or CreP (a GADD34

homologue) (Boyce et al., 2005; Jousse et al., 2003; Tsaytler et al., 2011). Salubrinal disrupts the PP1 complex containing both GADD34 and CREP, while guanabenz selectively binds GADD34 disrupting its association with PP1. In this manner both drugs elevate the phosphorylation of eIF2 α in response to ER stress. In *pek-1* mutants we observe increased paralysis in mTDP-43 worms treated with guanabenz but not salubrinal; that is, salubrinal continues to rescue mTDP-43 toxicity in the absence of *pek-1*/PERK. If *pek-1*/PERK is eliminated technically there should be reduced phosphorylation of eIF2 α , which is consistent with the notion that the net effect of guanabenz is to promote phosphorylation of eIF2 α and that *pek-1* is essential for neuroprotection by guanabenz. However, we observed that salubrinal still has a protective effect when *pek-1*/PERK is eliminated, suggesting that salubrinal has actions independent of the phosphorylation activity of PERK on eIF2 α . It has been reported that salubrinal induces phosphorylation of eIF2 α independent of PERK or any other known eIF2 α kinase (Boyce et al., 2005) consistent with our observation of reduced paralysis in mTDP-43;*pek-1(ok275)* worms treated with salubrinal. Furthermore it should be kept in mind that eIF2 α phosphorylation is not exclusive to ER stress but also occurs in response to oxidative and thermal stress among others, and that these compounds may function within the integrated stress response and not just the UPR^{ER} (Harding et al., 2003).

Phenazine is structurally similar to the other compounds we tested in this study (Table 1, Supplementary Table 2) and we show that in our models phenazine rescues toxic phenotypes associated with mTDP-43. Phenazine appeared to act through the *ire-1*/IRE1 and the *pek-1*/PERK branches of the ER stress pathway, but does not require *atf-6*/ATF6 to reduce mTDP-43 proteotoxicity. Nothing is known about phenazine and its properties in neurodegeneration, aging or stress, and we report for the first time new therapeutic properties for phenazine in overcoming neuronal toxicity associated with mTDP-43 in both worms and fish.

As we age, damage to proteins progressively accumulates and protein homeostasis deteriorates (Feder and Hofmann, 1999). Although cellular mechanisms like the UPR^{ER} combat protein misfolding there is a link between the duration of UPR signaling and cell fate under ER stress (Hosoi and Ozawa, 2010). The main goal of our study was to better characterize the mechanism of action of several potent chemical suppressors of mTDP-43 neuronal toxicity to determine if they operate through conserved mechanisms in *C. elegans* and *D. rerio*. The data collected here suggest that our four compounds showed overlapping function within the UPR^{ER} pathway to reduce mTDP-43 proteotoxicity. Indeed, depending on the branch of the UPR^{ER} the compounds follow they will preferentially act on chaperone expression and activity, on translation arrest, and/or cell death. The further benefit of combining any drug with MB suggests that drug combinations might be the best approach to collectively reduce protein misfolding, oxidative stress, and neurodegeneration. Finally, these data and previous reports using mutant SOD1 *in vivo* (Saxena et al., 2009) and *in vitro* (Kosuge et al., 2009) models suggest that compounds reducing ER stress may be an attractive therapeutic avenue to be explored in ALS (Atkin et al., 2008).

Acknowledgments

We would like to thank Marina Drits and Guy Laliberte for help with zebrafish and Dr. Louis Provencher for suggesting that we test phenazine. Some strains were provided by the CGC, which is funded by NIH Office of Research Infrastructure Programs (P40 OD010440). S.A.P. is supported by a CIHR fellowship. E.K. holds a MDA Development Grant as well as an AVENIR and Jeune Chercheur contracts with INSERM. J.A.P. is a CIHR New Investigator and P.D. holds a Canada Research Chair in Neuroscience. This research was supported by the CHUM Foundation, the Bernice Ramsay Discovery Grant program from the ALS Society of Canada, and the Muscular Dystrophy

Association to J.A.P., the Frick Foundation for ALS Research, and Genome Québec to E.K., P.D., and J.A.P.

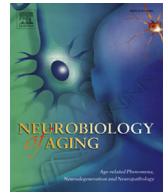
Appendix A. Supplementary data

Supplementary data to this article can be found online at <http://dx.doi.org/10.1016/j.nbd.2013.03.015>.

References

- Al-Chalabi, A., et al., 2012. The genetics and neuropathology of amyotrophic lateral sclerosis. *Acta Neuropathol.* 124, 339–352.
- Andersen, P.M., Al-Chalabi, A., 2011. Clinical genetics of amyotrophic lateral sclerosis: what do we really know? *Nat. Rev. Neurol.* 7, 603–615.
- Atkin, J.D., et al., 2008. Endoplasmic reticulum stress and induction of the unfolded protein response in human sporadic amyotrophic lateral sclerosis. *Neurobiol. Dis.* 30, 400–407.
- Audet, J.N., et al., 2012. Methylene blue administration fails to confer neuroprotection in two amyotrophic lateral sclerosis mouse models. *Neuroscience* 209, 136–143.
- Barber, S.C., Shaw, P.J., 2010. Oxidative stress in ALS: key role in motor neuron injury and therapeutic target. *Free Radic. Biol. Med.* 48, 629–641.
- Boillee, S., et al., 2006. ALS: a disease of motor neurons and their nonneuronal neighbors. *Neuron* 52, 39–59.
- Boyce, M., et al., 2005. A selective inhibitor of eIF2 α dephosphorylation protects cells from ER stress. *Science* 307, 935–939.
- Bruijn, L.I., et al., 2004. Unraveling the mechanisms involved in motor neuron degeneration in ALS. *Annu. Rev. Neurosci.* 27, 723–749.
- Calfon, M., et al., 2002. IRE1 couples endoplasmic reticulum load to secretory capacity by processing the XBP-1 mRNA. *Nature* 415, 92–96.
- DeJesus-Hernandez, M., et al., 2011. Expanded GGGGCC hexanucleotide repeat in non-coding region of C9ORF72 causes chromosome 9p-linked FTD and ALS. *Neuron* 72, 245–256.
- Dibaj, P., et al., 2012. Influence of methylene blue on microglia-induced inflammation and motor neuron degeneration in the SOD1(G93A) model for ALS. *PLoS One* 7, e43963.
- Feder, M.E., Hofmann, G.E., 1999. Heat-shock proteins, molecular chaperones, and the stress response: evolutionary and ecological physiology. *Annu. Rev. Physiol.* 61, 243–282.
- Gura, T., 2008. Hope in Alzheimer's fight emerges from unexpected places. *Nat. Med.* 14, 894.
- Harding, H.P., et al., 2003. An integrated stress response regulates amino acid metabolism and resistance to oxidative stress. *Mol. Cell* 11, 619–633.
- Holmes, B., et al., 1983. Guanabenz. A review of its pharmacodynamic properties and therapeutic efficacy in hypertension. *Drugs* 26, 212–229.
- Hosoi, T., Ozawa, K., 2010. Endoplasmic reticulum stress in disease: mechanisms and therapeutic opportunities. *Clin. Sci. (Lond.)* 118, 19–29.
- Iliev, E.V., et al., 2007. Oxidative and endoplasmic reticulum stress interplay in sporadic amyotrophic lateral sclerosis. *Brain* 130, 3111–3123.
- Jousse, C., et al., 2003. Inhibition of a constitutive translation initiation factor 2 α phosphatase, CREP, promotes survival of stressed cells. *J. Cell Biol.* 163, 767–775.
- Kabashi, E., et al., 2009. Gain and loss of function of ALS-related mutations of TARDBP (TDP-43) cause motor deficits *in vivo*. *Hum. Mol. Genet.* 19, 671–683.
- Kabashi, E., et al., 2011. FUS and TARDBP but not SOD1 interact in genetic models of Amyotrophic Lateral Sclerosis. *PLoS Genet.* 7, e1002214.
- Kosuge, Y., et al., 2009. Characterization of chronic glutamate-mediated motor neuron toxicity in organotypic spinal cord culture prepared from ALS model mice. *Neurosci. Lett.* 454, 165–169.
- Kwiatkowski Jr., T.J., et al., 2009. Mutations in the FUS/TLS gene on chromosome 16 cause familial amyotrophic lateral sclerosis. *Science* 323, 1205–1208.
- Lacomblez, L., et al., 1996. Dose-ranging study of riluzole in amyotrophic lateral sclerosis. Amyotrophic Lateral Sclerosis/Riluzole Study Group II. *Lancet* 347, 1425–1431.
- Lagier-Tourenne, C., Cleveland, D.W., 2009. Rethinking ALS: the FUS about TDP-43. *Cell* 136, 1001–1004.
- Lagier-Tourenne, C., et al., 2010. TDP-43 and FUS/TLS: emerging roles in RNA processing and neurodegeneration. *Hum. Mol. Genet.* 19, R46–R64.
- Liachko, N.F., et al., 2010. Phosphorylation promotes neurotoxicity in a *Caenorhabditis elegans* model of TDP-43 proteinopathy. *J. Neurosci.* 30, 16208–16219.
- Link, C.D., et al., 1999. Direct observation of stress response in *Caenorhabditis elegans* using a reporter transgene. *Cell Stress Chaperones* 4, 235–242.
- Lougheed, R., Turnbull, J., 2011. Lack of effect of methylene blue in the SOD1 G93A mouse model of amyotrophic lateral sclerosis. *PLoS One* 6, e23141.
- Mao, X.R., Crowder, C.M., 2010. Protein misfolding induces hypoxic preconditioning via a subset of the unfolded protein response machinery. *Mol. Cell Biol.* 30, 5033–5042.
- Matus, S., et al., 2008. The stress rheostat: an interplay between the unfolded protein response (UPR) and autophagy in neurodegeneration. *Curr. Mol. Med.* 8, 157–172.
- Neumann, M., et al., 2006. Ubiquitinated TDP-43 in frontotemporal lobar degeneration and amyotrophic lateral sclerosis. *Science* 314, 130–133.
- Novoa, I., et al., 2001. Feedback inhibition of the unfolded protein response by GADD34-mediated dephosphorylation of eIF2 α . *J. Cell Biol.* 153, 1011–1022.
- Rahman, S.A., et al., 2009. Small Molecule Subgraph Detector (SMSD) toolkit. *J. Chem. Inf.* 1, 12.
- Renton, A.E., et al., 2011. A hexanucleotide repeat expansion in C9ORF72 is the cause of chromosome 9p21-linked ALS-FTD. *Neuron* 72, 257–268.

- Riviere, M., et al., 1998. An analysis of extended survival in patients with amyotrophic lateral sclerosis treated with riluzole. *Arch. Neurol.* 55, 526–528.
- Rojas, J.C., et al., 2012. Neurometabolic mechanisms for memory enhancement and neuroprotection of methylene blue. *Prog. Neurobiol.* 96, 32–45.
- Ron, D., Walter, P., 2007. Signal integration in the endoplasmic reticulum unfolded protein response. *Nat. Rev. Mol. Cell Biol.* 8, 519–529.
- Saxena, S., et al., 2009. A role for motoneuron subtype-selective ER stress in disease manifestations of FALS mice. *Nat. Neurosci.* 12, 627–636.
- Sontag, E.M., et al., 2012. Methylene blue modulates huntingtin aggregation intermediates and is protective in Huntington's disease models. *J. Neurosci.* 32, 11109–11119.
- Tribouillard-Tanvier, D., et al., 2008a. Antihypertensive drug guanabenz is active *in vivo* against both yeast and mammalian prions. *PLoS One* 3, e1981.
- Tribouillard-Tanvier, D., et al., 2008b. Protein folding activity of ribosomal RNA is a selective target of two unrelated antiprion drugs. *PLoS One* 3, e2174.
- Tsaytler, P., et al., 2011. Selective inhibition of a regulatory subunit of protein phosphatase 1 restores proteostasis. *Science* 332, 91–94.
- Urano, F., et al., 2002. A survival pathway for *Caenorhabditis elegans* with a blocked unfolded protein response. *J. Cell Biol.* 158, 639–646.
- Vaccaro, A., et al., 2012a. Methylene blue protects against TDP-43 and FUS neuronal toxicity in *C. elegans* and *D. rerio*. *PLoS One* 7, e42117.
- Vaccaro, A., et al., 2012b. Mutant TDP-43 and FUS cause age-dependent paralysis and neurodegeneration in *C. elegans*. *PLoS One* 7, e31321.
- van Blitterswijk, M., Landers, J.E., 2010. RNA processing pathways in amyotrophic lateral sclerosis. *Neurogenetics* 11, 275–290.
- Vance, C., et al., 2009. Mutations in FUS, an RNA processing protein, cause familial amyotrophic lateral sclerosis type 6. *Science* 323, 1208–1211.
- Walker, A.K., Atkin, J.D., 2011. Stress signaling from the endoplasmic reticulum: a central player in the pathogenesis of amyotrophic lateral sclerosis. *IUBMB Life* 63, 754–763.
- Yamashita, M., et al., 2009. Methylene blue and dimebon inhibit aggregation of TDP-43 in cellular models. *FEBS Lett.* 583, 2419–2424.
- Yoneda, T., et al., 2004. Compartment-specific perturbation of protein handling activates genes encoding mitochondrial chaperones. *J. Cell Sci.* 117, 4055–4066.



Evaluation of longevity enhancing compounds against transactive response DNA-binding protein-43 neuronal toxicity

Arnaud Tauffenberger^{a,b,c}, Carl Julien^{a,b,c}, J. Alex Parker^{a,b,c,*}

^a CRCHUM, Montréal, Québec, Canada

^b Center of Excellence in Neuromics, Université de Montréal, Montréal, Québec, Canada

^c Département de Pathologie et Biologie Cellulaire, Université de Montréal, Montréal, Québec, Canada

ARTICLE INFO

Article history:

Received 21 September 2012

Received in revised form 2 March 2013

Accepted 11 March 2013

Available online 13 April 2013

Keywords:

TDP-43

Amyotrophic lateral sclerosis

C. elegans

Neurodegeneration

Longevity

Proteotoxicity

ABSTRACT

In simple systems, lifespan can be extended by various methods including dietary restriction, mutations in the insulin/insulin-like growth factor (IGF) pathway or mitochondria among other processes. It is widely held that the mechanisms that extend lifespan may be adapted for diminishing age-associated pathologies. We tested whether a number of compounds reported to extend lifespan in *C. elegans* could reduce age-dependent toxicity caused by mutant TAR DNA-binding protein-43 in *C. elegans* motor neurons. Only half of the compounds tested show protective properties against neurodegeneration, suggesting that extended lifespan is not a strong predictor for neuroprotective properties. We report here that resveratrol, rolipram, reserpine, trolox, propyl gallate, and ethosuximide protect against mutant TAR DNA-binding protein-43 neuronal toxicity. Finally, of all the compounds tested, only resveratrol required *daf-16* and *sir-2.1* for protection, and ethosuximide showed dependence on *daf-16* for its activity.

Crown Copyright © 2013 Published by Elsevier Inc. All rights reserved.

1. Introduction

For more than 75 years, people have been fascinated by the discovery that rats living on a restricted diet (dietary restriction) showed increased lifespan (McCay et al., 1989), a phenomenon that is under investigation in primates (Colman et al., 2009; Mattison et al., 2012). Of great interest is the fact that not only do many organisms show increased lifespan under dietary restriction conditions but they also show decreased incidences of age-related pathologies (Anderson and Weindruch, 2012). Additional mechanisms that regulate longevity have been discovered including mitochondrial function and the insulin/insulin-like growth factor (IGF) signaling pathway. Molecular and genetic approaches have begun to decipher the cellular mechanisms of lifespan extension and this has led to the development of an industry hoping to find and develop longevity mimetics as potential therapeutic agents against age-related disease (Mercken et al., 2012). Work from model organisms like *C. elegans* has identified numerous compounds that extend lifespan by influencing conserved longevity mechanisms and we wondered if these compounds would be effective against age-dependent proteotoxicity. To evaluate these compounds we turned to a *C. elegans* model of age-dependent motor neuron

toxicity (Vaccaro et al., 2012a) and tested 11 compounds reported to extend lifespan. We identified 6 compounds that reduced mutant transactive response (TAR) DNA-binding protein-43 (TDP-43) neuronal toxicity and might be useful as candidates for testing and drug development in mammalian models of neurodegeneration.

2. Methods

2.1. *C. elegans* strains and genetics

Standard methods of culturing and handling worms were used. Worms were maintained on standard nematode growth media plates streaked with OP50 *E. coli*. All strains were scored at 20 °C. Mutations and transgenes used in this study were: *daf-16(mu86)*, *hsf-1(sy441)*, *rrf-3(pk1426)*, *sir-2.1(ok434)*, and *xqls133[unc-47::TDP-43(A315T);unc-119(+)]*. Most of the strains were obtained from the *C. elegans* Genetics Center (University of Minnesota, Minneapolis, MN, USA). Mutants or transgenic worms were verified by visible phenotypes, polymerase chain reaction analysis for deletion mutants, sequencing for point mutations, or a combination thereof. Deletion mutants were outcrossed a minimum of 3 times to wild type N2 worms before use.

2.2. Paralysis assays

Worms were counted as paralyzed if they failed to move when prodded with a worm pick. Worms were scored as dead if they

* Corresponding author at: CRCHUM, Hôpital Notre Dame, 1560 rue Sherbrooke Est, M-5226, Montréal, Québec H2L 4M1, Canada. Tel.: +1 514 890 8000 x28826; fax: +1 514 412-7602.

E-mail address: ja.parker@umontreal.ca (J.A. Parker).

failed to move their head after being prodded in the nose and showed no pharyngeal pumping. For the paralysis tests worms grown on the specific compound from hatching were transferred to the appropriate experimental plate for scoring.

2.3. Neurodegeneration assays

For scoring of neuronal processes, TDP-43 transgenic animals were selected at day 9 of adulthood for visualization of motor neurons processes in vivo. Animals were immobilized in M9 with 5 mM levamisole and mounted on slides with 2% agarose pads. Neurons were visualized using a Leica DM6000 microscope and a Leica DFC 480 camera. A minimum of 100 animals were scored per treatment over 4–6 trials. The mean and standard error of the mean were calculated for each trial and 2-tailed *t* tests were used for statistical analysis.

2.4. RNAi experiments

RNA interference (RNAi)-treated strains were fed *E. coli* (HT115) containing an empty vector or *skn-1* (T19E7.2) RNAi clones from the ORFeome RNAi library (Open Biosystems). RNAi experiments were performed at 20 °C. Worms were grown on Nematode Growth Media enriched with 1 mM isopropyl- β -D-thiogalactopyranoside. All RNAi paralysis tests were performed using a TDP-43

[A315T];*rrf-3(pk1426)* strain. To minimize developmental effects, L4 worms were grown on plates with either *skn-1*(RNAi) or empty vector and assayed for paralysis as adults. *skn-1*(RNAi) activity was confirmed by the observation of lethal and sterile phenotypes in the progeny of treated animals.

2.5. Protein extraction

Worms were lysed in radioimmunoprecipitation assay buffer (150 mM NaCl, 50 mM Tris pH 7.4, 1% Triton X-100, 0.1% sodium dodecyl sulfate, 1% sodium deoxycholate) plus 0.1% protease inhibitors (10 mg/mL leupeptin, 10 mg/mL pepstatin A, 10 mg/mL chymostatin). Nematodes were lysed with a 27 $\frac{1}{2}$ syringe 10–15 times, incubated on ice for 10 minutes then moved at room temperature for 10 minutes and finally centrifuged at 16,000g for 10 minutes. Protein quantification was performed using a BCA protein assay kit (Thermo Scientific). For TDP-43 transgenic worms, soluble and insoluble fractions were obtained using methods previously described (Liachko et al., 2010; Neumann et al., 2006), with modifications. Briefly, worms pellets were homogenized with a pellet mixer (Disposable Pellet Mixer and Cordless Motor, VWR) in 1 volume (wt/vol) of low-salt buffer (Benedetti et al., 2008) (10 mM Tris, 5 mM Ethylene Diamine Triacetic Acid (EDTA), 10% sucrose, pH 7.5) and centrifuged at 25,000g for 30 minutes at 4 °C. The supernatant represents the low salt (LS) fraction, containing the soluble proteins.

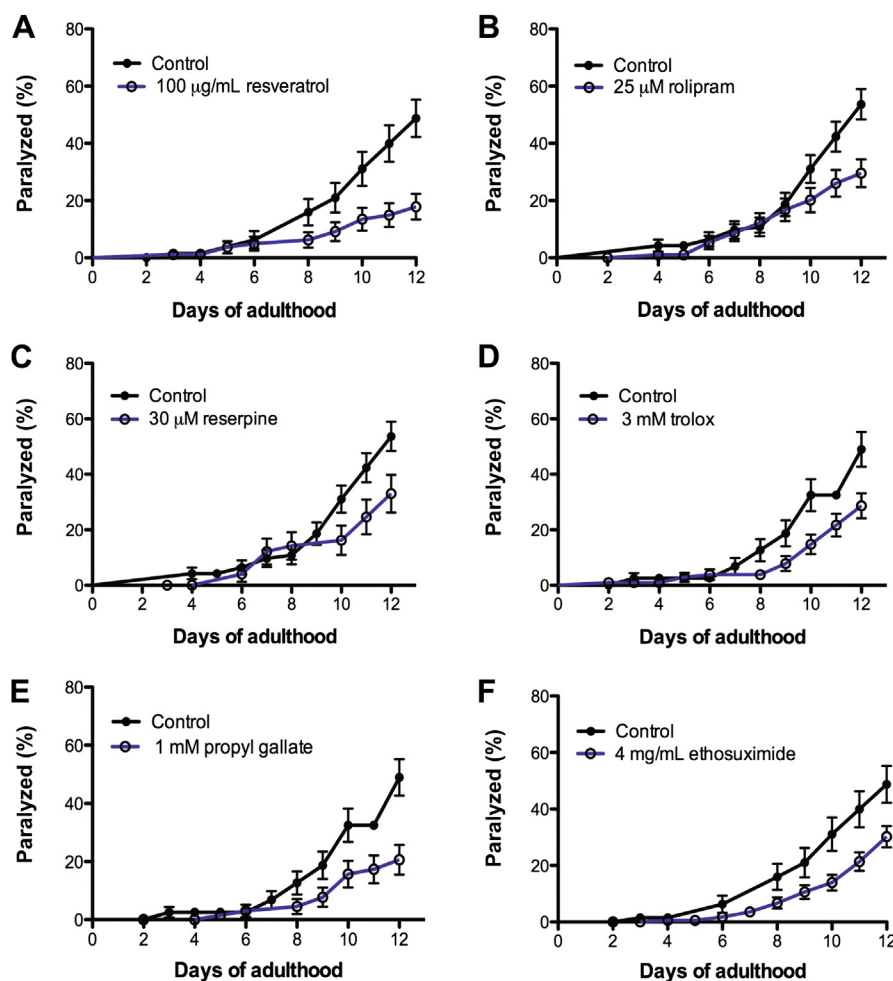


Fig. 1. Lifespan-extending compounds reduce mutant TAR DNA-binding protein-43-induced paralysis. Compounds that reduced mutant TAR DNA-binding protein-43-induced motility defects and paralysis compared with untreated control animals included: (A) 100 μ M resveratrol ($p < 0.001$); (B) 25 μ M rolipram ($p < 0.001$); (C) 30 μ M reserpine ($p < 0.05$); (D) 3 mM trolox ($p < 0.01$); (E) 1 mM propyl gallate ($p < 0.01$); (F) 4 mg/mL ethosuximide ($p < 0.01$). See also Supplementary Table 1.

The pellet was washed with the same volume of LS, centrifuged again, and the supernatant was discarded. The remaining pellet was re-extracted with the same volume of Triton buffer (LS with 1% Triton X-100 and 0.5 M NaCl), centrifuged at 180,000g for 30 minutes at 4 °C. The resulting pellet was re-extracted with the same volume of myelin floatation buffer (Triton buffer containing 30% sucrose) and centrifuged at 180,000g for 30 minutes at 4 °C. The remaining pellet was re-extracted in the same volume of Sarkosyl buffer (LS with 1% N-Lauroyl-sarcosine and 0.5 M NaCl), incubated with agitation for 1 hour at 22 °C and centrifuged at 180,000g for 30 minutes at 22 °C. The detergent-insoluble pellet was weighted and solubilized in 5 volumes (wt/vol) of urea buffer (30 mM Tris, 7 M urea, 2 M thiourea, 4% 3-[(3-cholamidopropyl) dimethylammonio]-1-propanesulfonate, pH 8.5) and sonicated for 5 minutes. All buffers contained 1 mM Dithiothreitol DTT and protease inhibitors (LPC; 1/1000). The soluble LS and the insoluble urea fractions were quantified with the Bradford Protein Assay Kit (Bio-Rad) according to the manufacturer's instructions.

3. Results

3.1. Neuroprotection from select longevity-enhancing compounds

We investigated neurodegeneration with a well-characterized transgenic *C. elegans* strain that expresses the full-length human TDP-43 with the A315T mutation associated with amyotrophic lateral sclerosis in the worm's GABAergic motor neurons (Vaccaro et al., 2012a). These animals display adult-onset motility problems leading to progressive paralysis and neuronal degeneration that can be assessed over a period of 9 to 12 days (Vaccaro et al., 2012a). With this model, we then tested 11 compounds reported to increase lifespan in *C. elegans* for whether they could suppress the progressive paralysis caused by mutant TDP-43 (mTDP-43). The compounds tested included: the antioxidants propyl gallate (PG), trolox (TRO), and α -lipoic acid (Benedetti et al., 2008), the polyphenols resveratrol (RSV) (Morselli et al., 2010) and quercetin (Kampkotter et al., 2008), the anticonvulsant ethosuximide (ETX)

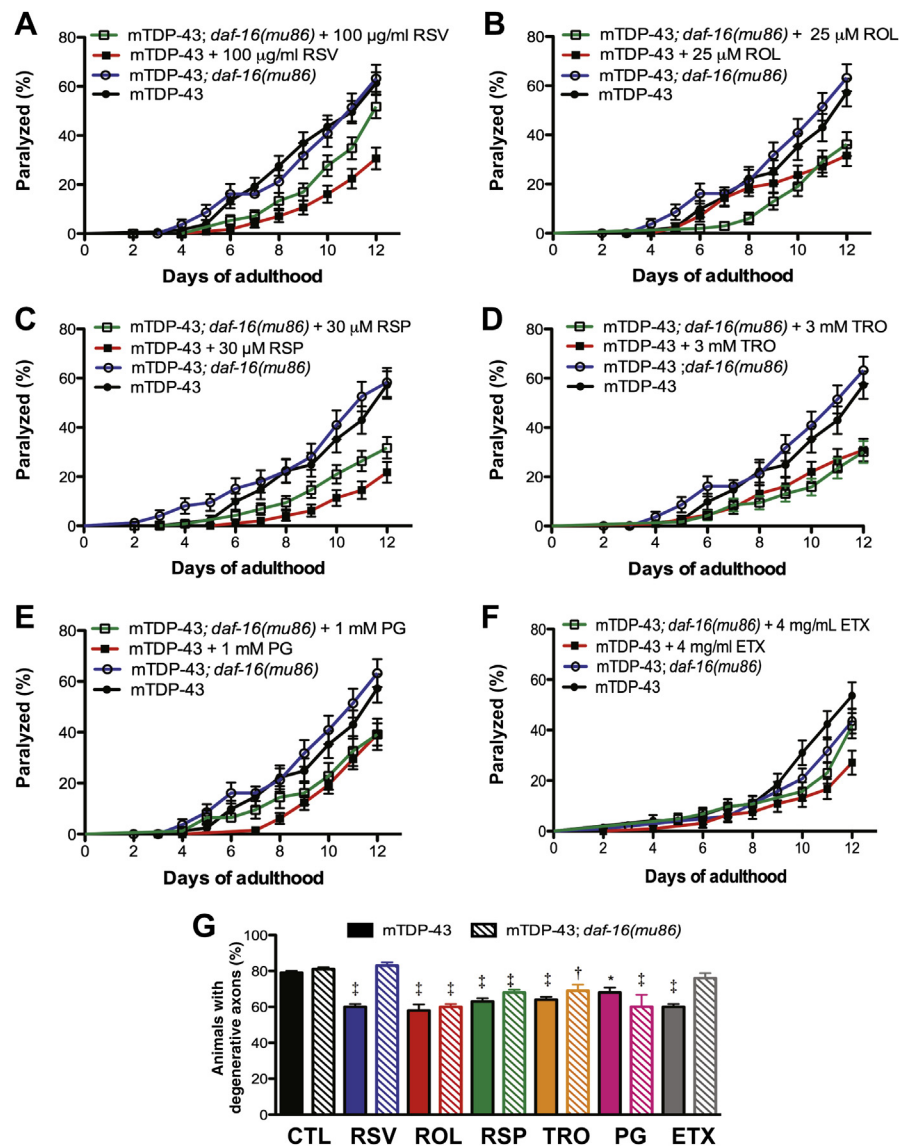


Fig. 2. Transcription factor *daf-16*/Forkhead box O (FOXO) mediates RSV and ETX neuroprotection. (A) RSV delayed mutant TAR DNA-binding protein-43 (mTDP-43) paralysis and this effect was dependent on *daf-16*. (B–E) ROL, RSP, TRO, and PG all reduced mTDP-43 paralysis compared with untreated control animals independent of *daf-16*. See [Supplementary Table 1](#) for statistical information. (F) ETX delayed mTDP-43 paralysis and this was dependent on *daf-16*. (G) RSV and ETX failed to rescue neuronal degeneration in *daf-16* mutant animals but all other compounds reduced neuronal degeneration at adult day 9 in *daf-16* mutant animals compared with untreated transgenic animals. * $p < 0.05$; † $p < 0.001$; ‡ $p < 0.0001$. Abbreviations: ETX, ethosuximide; PG, propyl gallate; ROL, rolipram; RSP, reserpine; RSV, resveratrol; TRO, trolox.

(Collins et al., 2008), reserpine (RSP) (Srivastava et al., 2008), spermidine (Eisenberg et al., 2009), valproic acid (Evason et al., 2008), and thioflavin (Alavez et al., 2011), and rolipram (ROL), a Phosphodiesterase 4 inhibitor that mimics the effects of RSV on mitochondrial function and glucose tolerance (Park et al., 2012) (please see Supplementary Table 1 for official names and suppliers). Interestingly, only 6 compounds rescued TDP-43 toxicity: RSV, ROL, RSP, TRO, PG, and ETX (Fig. 1, Supplementary Table 2) rescued mTDP-43 proteotoxicity at dosages previously used to increase lifespan. The 5 remaining compounds did not delay paralysis in the transgenic mTDP-43 worms (Supplementary Fig. 1, Supplementary Table 2). We also tested whether these 6 neuroprotective compounds extended lifespan in our worms and found that all compounds except for RSV increased lifespan (Supplementary Fig. 2, Supplementary Table 3). We also tested whether the reported effects were dependent on changes on protein expression. We found no differences in global protein expression after treatment with the 6 compounds in our transgenic worms

(Supplementary Fig. 3). Interestingly, we also observed a reduction in mTDP-43 insolubility in animals treated with TRO, PG, and ETX suggesting these compounds might aid the cellular clearance of toxic protein species (Supplementary Fig. 3). Our data reveal an imperfect correlation between the ability of a compound to extend lifespan and reduce neuronal proteotoxicity.

3.2. Involvement of *daf-16*, *hsf-1*, *sir-2.1*, and *skn-1* pathways in compound-mediated neuroprotection

Some of the key regulators of aging and stress signaling in *C. elegans* include the forkhead transcription factor *daf-16*, the heat shock factor transcription factor *hsf-1*, the sirtuin deacetylase *sir-2.1* (Kenyon, 2010), and the Nuclear respiratory factor transcription factor *skn-1* (An and Blackwell, 2003; Bishop and Guarente, 2007). To test if the 6 active compounds functioned within these pathways, we crossed our mTDP-43 transgenic animals with

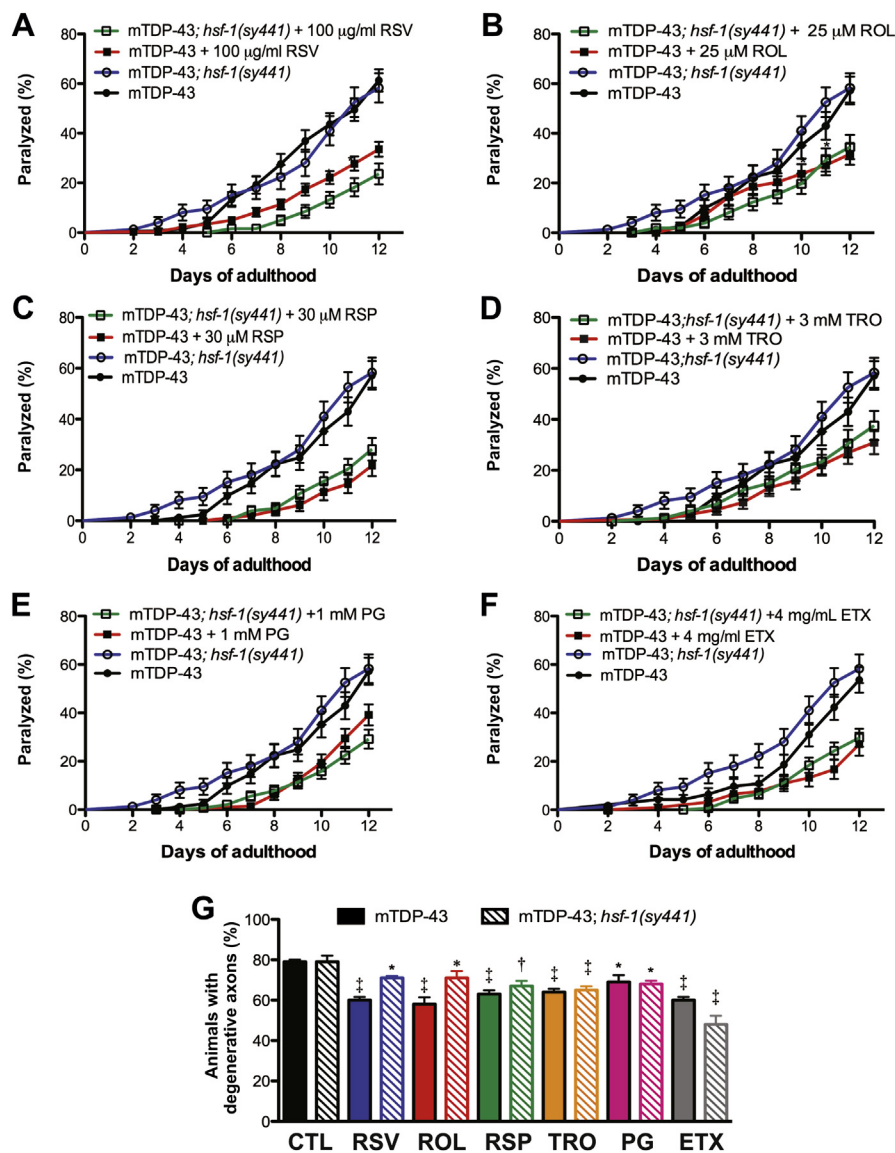


Fig. 3. Neuroprotective effects by the compounds are independent of *hsf-1*. (A–F) All compounds reduced mutant TAR DNA-binding protein-43 (mTDP-43) paralysis compared with untreated control animals independently of *hsf-1*. See Supplementary Table 1 for statistical information. (G) All compounds reduced neuronal degeneration in mTDP-43 animals compared with untreated control animals. * $p < 0.05$; † $p < 0.001$; ‡ $p < 0.0001$. Abbreviations: ETX, ethosuximide; PG, propyl gallate; ROL, rolipram; RSP, reserpine; RSV, resveratrol; TRO, trolox.

loss-of-function mutations or RNAi for each gene and tested if the compounds maintained neuroprotective activity.

3.2.1. Transcription factor *daf-16* mediates resveratrol and ETX neuroprotection

Reduced insulin/IGF pathway signaling has been implicated in aging and stress resistance (Kenyon, 2005; Kenyon et al., 1993). The downstream effector *daf-16*/Forkhead box O has been identified as a key target of RSV neuroprotective effects in polyglutamine toxicity (Parker et al., 2005), and consistently, RSV was less effective at reducing mTDP-43-induced paralysis and axonal degeneration (Fig. 2A and G). Of the remaining compounds we observed that ETX was less effective at suppressing paralysis and neurodegeneration in mTDP-43;*daf-16* mutants suggesting that part of this compound's neuroprotective activity might rest within the insulin/IGF signaling pathway (Fig. 2F and G).

3.2.2. Neuroprotective effects by compounds are independent of *hsf-1*

Chaperones are key regulators of the cellular stress response and the heat shock factor *hsf-1*/Heat shock factor 1 (HSF1) has been implicated in dietary restriction and proteotoxicity (Cohen et al., 2006; Teixeira-Castro et al., 2011). We tested the different compounds in mTDP-43;*hsf-1*(*sy441*) mutants and observed no differences in the rates of paralysis or neurodegeneration compared with untreated mTDP-43 control animals (Fig. 3 and Supplementary Table 2). Thus, although *hsf-1* is important for proteotoxicity modification, it seems that neuroprotection by the 6 compounds tested here is independent of *hsf-1*.

3.2.3. Resveratrol reduces neurotoxicity in a *sir-2.1*-dependent manner

The polyphenol RSV is naturally produced by certain plant species in response to environmental stress (Signorelli and Ghidoni,

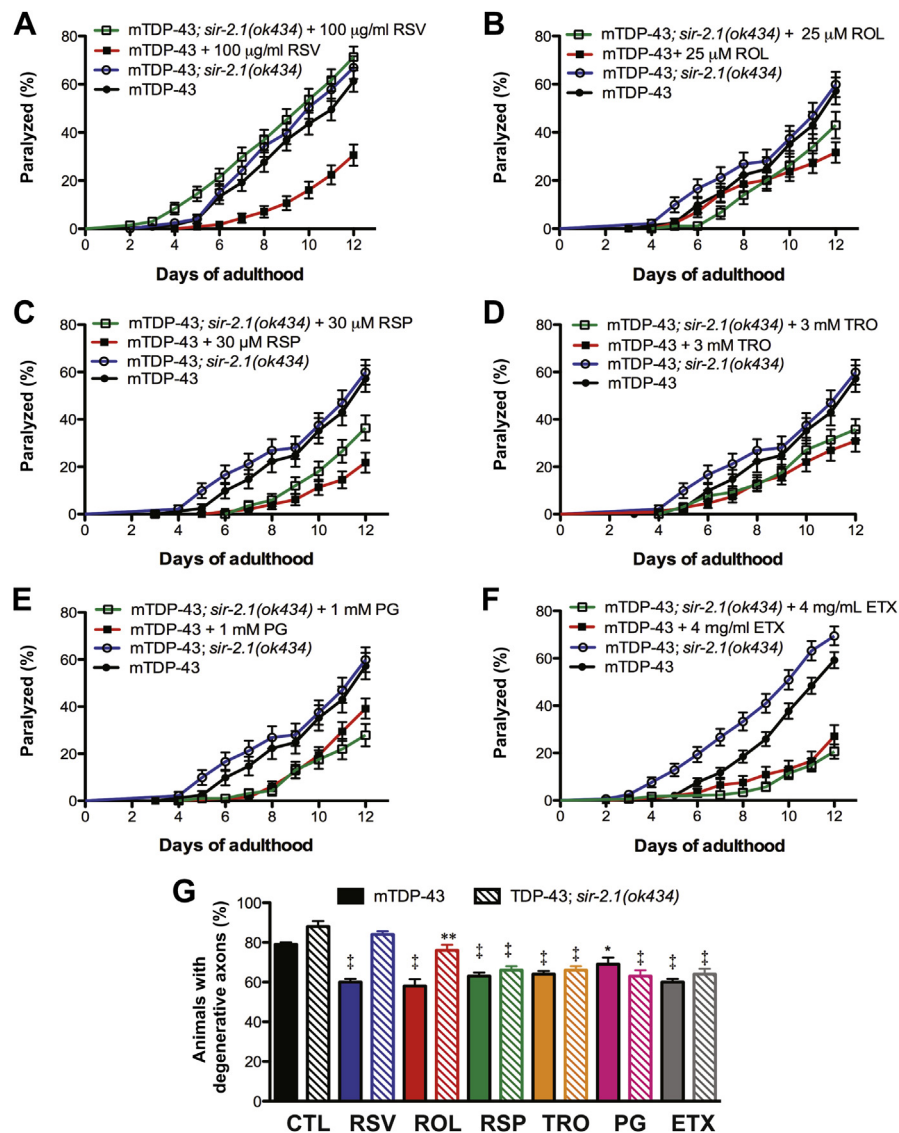


Fig. 4. Resveratrol reduces neurotoxicity in a *sir-2.1*-dependent manner. (A) RSV delayed mutant TAR DNA-binding protein-43 (mTDP-43) paralysis and this was dependent on *sir-2.1*. (B–F) ROL, RSP, TRO, PG, and ETX all reduced mTDP-43 paralysis compared with untreated animals independently of *sir-2.1*. See Supplementary Table 1 for statistical information. (G) RSV failed to rescue axonal degeneration in *sir-2.1* mutant animals but all other compounds reduced neuronal degeneration in mTDP-43 animals compared with untreated control animals. * $p < 0.05$; ** $p < 0.01$; † $p < 0.0001$. Abbreviations: ETX, ethosuximide; PG, propyl gallate; ROL, rolipram; RSP, reserpine; RSV, resveratrol; TRO, trolox.

2005). Subsequent studies have shown that RSV requires sirtuins, a class of nicotinamide adenine dinucleotide-dependent deacetylases, for lifespan extension using dietary restriction (Lin et al., 2000), and was able to rescue neurodegeneration in different late age of onset disease in a Sirtuin 1-dependent manner (Kim et al., 2007; Parker et al., 2005). Thus, consistent with previous studies, RSV failed to rescue paralysis and neurodegeneration in mTDP-43; *sir-2.1(ok434)* mutants (Figs. 4A, 2G and Supplementary Table 2). However, the remaining 5 compounds continued to suppress paralysis and neurodegeneration phenotypes in the absence of *sir-2.1* (Figs. 4B–F and 2G), suggesting they function through alternative pathways.

3.2.4. Neuroprotective effects by compounds are independent of *skn-1*

Many genes involved in aging modulation and stress resistance overlap. We investigated whether the transcription factor *skn-1*, an Nuclear respiratory factor-like response factor that regulates stress

resistance and longevity (Tullet et al., 2008; Wang et al., 2010), was required for rescue of neuronal phenotypes in mTDP-43 transgenic worms after treatment with the 6 compounds. However, all the compounds continued to rescue paralysis and axonal degeneration in the absence of *skn-1* (Fig. 5 and Supplementary Table 2).

4. Discussion

Understanding the cellular mechanisms of lifespan extension is an active area of research, as are efforts to apply these findings to age-related pathologies. Because extending lifespan by genetic or dietary methods delays age-associated negative phenotypes from worms to primates, the quest to identify chemicals replicating these effects is a promising area of therapeutic investigation. Supporting this notion are studies from *C. elegans* demonstrating that dietary restriction (Steinkraus et al., 2008), insulin/IGF signaling (Cohen et al., 2006; Morley et al., 2002), *hsf-1* (Cohen et al., 2006; Hsu et al., 2003), *sir-2.1* (Parker et al., 2005), or *skn-1* (Wang et al.,

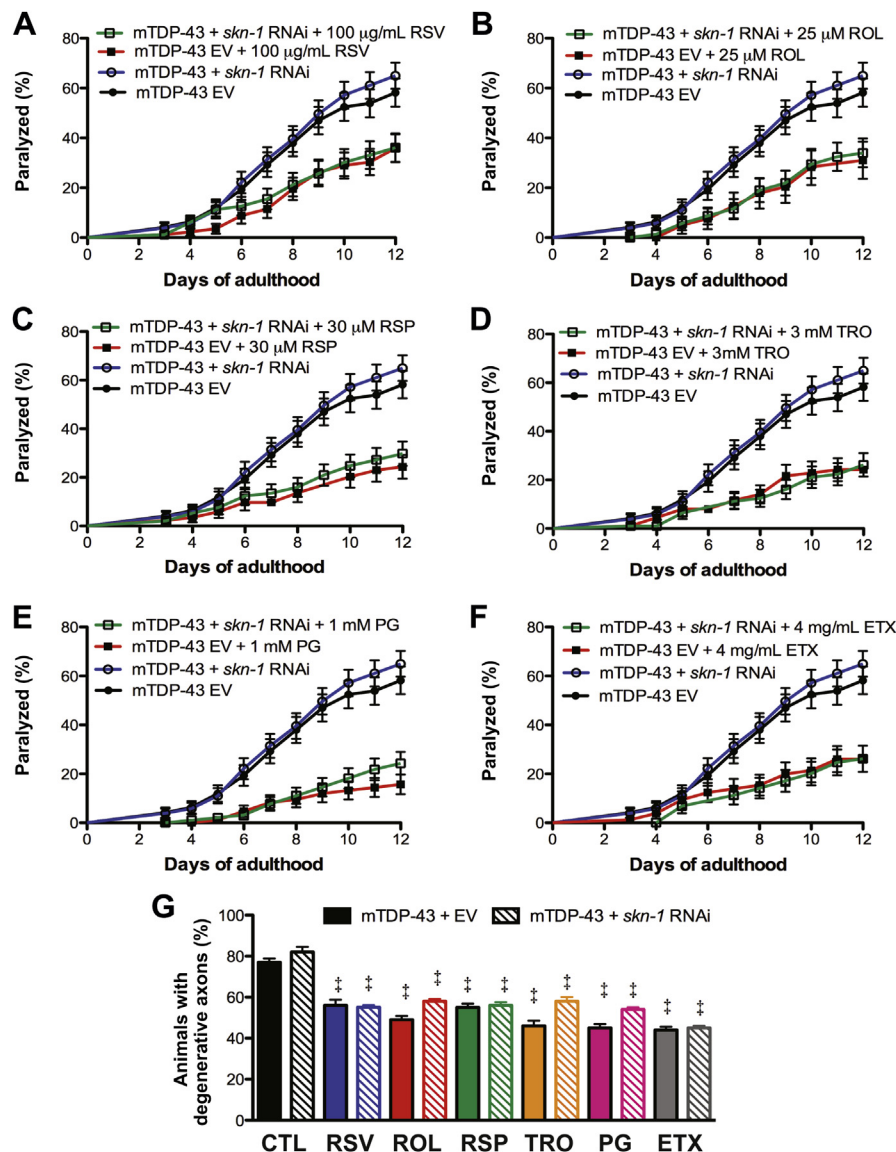


Fig. 5. Neuroprotective effects by compounds are independent of *skn-1*. (A–F) All compounds reduced mutant TAR DNA-binding protein-43 (mTDP-43) paralysis compared with untreated control animals independently of *skn-1*. See Supplementary Table 1 for statistical information. (G) All compounds reduced neuronal degeneration in mTDP-43 animals compared with untreated control animals. † $p < 0.0001$. Abbreviations: ETX, ethosuximide; EV, Empty Vector; PG, propyl gallate; RNAi, RNA interference; ROL, rolipram; RSP, reserpine; RSV, resveratrol; TRO, trolox.

2010) modify proteotoxicity. With this goal in mind, we examined a number of compounds shown to extend lifespan, or in some cases, to reduce polyglutamine or amyloid- β proteotoxicity in *C. elegans*, and investigated if they could suppress neuronal mTDP-43 toxicity. We identified 6 compounds that suppressed neuronal toxicity, but of these only RSV and ETX showed dependence on the aging genes *daf-16* and *sir-2.1*.

Our data suggest that lifespan extension might not be a strong predictor for neuroprotection. Indeed, recent work has shown that dietary restriction is ineffective against delaying neurodegeneration caused by mTDP-43 or polyglutamine in worms (Tauffenberger et al., 2012), amyloid- β or tau toxicity in flies (Kerr et al., 2011), or mutant superoxide dismutase 1 in mice (Patel et al., 2010). Regarding the insulin/IGF pathway, reduced signaling has been shown to rescue (Cohen et al., 2006) or enhance proteotoxicity (Vaccaro et al., 2012b), suggesting this pathway might be difficult to manipulate for therapeutic benefit. Part of the discrepancy might be that earlier studies investigating longevity and proteotoxicity relied on models expressing mutant proteins in *C. elegans* body wall muscle cells. Similar results have been observed for *sir-2.1*, where deletion of *sir-2.1* exacerbates polyglutamine toxicity in neurons (Bates et al., 2006; Parker et al., 2005), but rescues polyalanine and α -synuclein toxicity in muscle cells (Catoire et al., 2008; van Ham et al., 2008). The disparity between muscle and neuronal models might apply to drug screening as well, where compounds like thioflavin have been shown to reduce amyloid- β and polyglutamine toxicity in muscle cells (Alavez et al., 2011), but we observed no activity in our neuronal TDP-43 model. Neurons and muscle cells have different functions and metabolic requirements so it might not be surprising that they respond differently to manipulations promoting overall lifespan extensions in the context of proteotoxicity. Indeed, neurons and muscle cells appear to have different capabilities in responding to protein misfolding during aging (Kern et al., 2010). Thus, the predictive value of muscle-based models for neurodegenerative disorders needs to be interpreted with caution.

Although we describe an imperfect correlation between longevity and neuroprotection, we have identified 6 compounds that protect against mTDP-43 toxicity in motor neurons. Further investigation and validation in vertebrate systems will be required to gauge the effectiveness of these compounds as early leads for drug discovery and development in amyotrophic lateral sclerosis and other late-onset proteinopathies.

Disclosure statement

All authors have no conflicts of interest to disclose.

No approvals were required for the work described in this report.

Acknowledgements

The authors thank S. Peyrard for technical support. A.T. is supported by a CIHR and Huntington's Society of Canada fellowship. J.A.P. is a CIHR New Investigator. The CHUM Foundation, a CIHR Catalyst Grant, the Bernice Ramsay Discovery Grant from the ALS Society of Canada, and the Congressionally Directed Medical Research Program (CDMRP) Amyotrophic Lateral Sclerosis Research Program (USA) supported this work.

Appendix A. Supplementary data

Supplementary data associated with this article can be found, in the online version, at <http://dx.doi.org/10.1016/j.neurobiolaging.2013.03.014>.

References

- Alavez, S., Vantipalli, M.C., Zucker, D.J., Klang, I.M., Lithgow, G.J., 2011. Amyloid-binding compounds maintain protein homeostasis during ageing and extend lifespan. *Nature* 472, 226–229.
- An, J.H., Blackwell, T.K., 2003. SKN-1 links *C. elegans* mesodermal specification to a conserved oxidative stress response. *Genes Dev.* 17, 1882–1893.
- Anderson, R.M., Weindruch, R., 2012. The caloric restriction paradigm: implications for healthy human aging. *Am. J. Hum. Biol.* 24, 101–106.
- Bates, E.A., Victor, M., Jones, A.K., Shi, Y., Hart, A.C., 2006. Differential contributions of Caenorhabditis elegans histone deacetylases to huntingtin polyglutamine toxicity. *J. Neurosci.* 26, 2830–2838.
- Benedetti, M.G., Foster, A.L., Vantipalli, M.C., White, M.P., Sampayo, J.N., Gill, M.S., Olsen, A., Lithgow, G.J., 2008. Compounds that confer thermal stress resistance and extended lifespan. *Exp. Gerontol.* 43, 882–891.
- Bishop, N.A., Guarente, L., 2007. Two neurons mediate diet-restriction-induced longevity in *C. elegans*. *Nature* 447, 545–549.
- Catoire, H., Pasco, M.Y., Abu-Baker, A., Holbert, S., Tourette, C., Brais, B., Rouleau, G.A., Parker, J.A., Neri, C., 2008. Sirtuin inhibition protects from the polyalanine muscular dystrophy protein PABPN1. *Hum. Mol. Genet.* 17, 2108–2117.
- Cohen, E., Bieschke, J., Perciavalle, R.M., Kelly, J.W., Dillin, A., 2006. Opposing activities protect against age-onset proteotoxicity. *Science* 313, 1604–1610.
- Collins, J.J., Evason, K., Pickett, C.L., Schneider, D.L., Kornfeld, K., 2008. The anti-convulsant ethosuximide disrupts sensory function to extend *C. elegans* lifespan. *PLoS Genet.* 4, e1000230.
- Colman, R.J., Anderson, R.M., Johnson, S.C., Kastman, E.K., Kosmatka, K.J., Beasley, T.M., Allison, D.B., Cruzen, C., Simmons, H.A., Kemnitz, J.W., Weindruch, R., 2009. Caloric restriction delays disease onset and mortality in rhesus monkeys. *Science* 325, 201–204.
- Eisenberg, T., Knauer, H., Schauer, A., Buttner, S., Ruckenstein, C., Carmona-Gutierrez, D., Ring, J., Schroeder, S., Magnes, C., Antonacci, L., Fussi, H., Deszcz, L., Hartl, R., Schraml, E., Criollo, A., Megalou, E., Weiskopf, D., Laun, P., Heeren, G., Breitenbach, M., Grubeck-Lobenstein, B., Herker, E., Fahrenkrog, B., Frohlich, K.U., Sinner, F., Tavernarakis, N., Minois, N., Kroemer, G., Madeo, F., 2009. Induction of autophagy by spermidine promotes longevity. *Nature Cell Biol.* 11, 1305–1314.
- Evason, K., Collins, J.J., Huang, C., Hughes, S., Kornfeld, K., 2008. Valproic acid extends Caenorhabditis elegans lifespan. *Aging Cell* 7, 305–317.
- Hsu, A.L., Murphy, C.T., Kenyon, C., 2003. Regulation of aging and age-related disease by DAF-16 and heat-shock factor. *Science* 300, 1142–1145.
- Kampkotter, A., Timpel, C., Zurawski, R.F., Ruhl, S., Chovolou, Y., Proksch, P., Watjen, W., 2008. Increase of stress resistance and lifespan of Caenorhabditis elegans by quercetin. *Comp. Biochem. Physiol. B Biochem. Mol. Biol.* 149, 314–323.
- Kenyon, C., 2005. The plasticity of aging: insights from long-lived mutants. *Cell* 120, 449–460.
- Kenyon, C., Chang, J., Gensch, E., Rudner, A., Tabtiang, R., 1993. A *C. elegans* mutant that lives twice as long as wild type. *Nature* 366, 461–464.
- Kenyon, C.J., 2010. The genetics of ageing. *Nature* 464, 504–512.
- Kern, A., Ackermann, B., Clement, A.M., Duerk, H., Behl, C., 2010. HSF1-controlled and age-associated chaperone capacity in neurons and muscle cells of *C. elegans*. *PLoS One* 5, e8568.
- Kerr, F., Augustin, H., Piper, M.D., Gandy, C., Allen, M.J., Lovestone, S., Partridge, L., 2011. Dietary restriction delays aging, but not neuronal dysfunction, in Drosophila models of Alzheimer's disease. *Neurobiol. Aging* 32, 1977–1989.
- Kim, D., Nguyen, M.D., Dobbin, M.M., Fischer, A., Sananbenesi, F., Rodgers, J.T., Delalle, I., Baur, J.A., Sui, G., Armour, S.M., Puigserver, P., Sinclair, D.A., Tsai, L.H., 2007. SIRT1 deacetylase protects against neurodegeneration in models for Alzheimer's disease and amyotrophic lateral sclerosis. *EMBO J.* 26, 3169–3179.
- Liachko, N.F., Guthrie, C.R., Kraemer, B.C., 2010. Phosphorylation promotes neurotoxicity in a Caenorhabditis elegans model of TDP-43 proteinopathy. *J. Neurosci.* 30, 16208–16219.
- Lin, S.J., Defossez, P.A., Guarente, L., 2000. Requirement of NAD and SIR2 for lifespan extension by calorie restriction in *Saccharomyces cerevisiae*. *Science* 289, 2126–2128.
- Mattison, J.A., Roth, G.S., Beasley, T.M., Tilmont, E.M., Handy, A.M., Herbert, R.L., Longo, D.L., Allison, D.B., Young, J.E., Bryant, M., Barnard, D., Ward, W.F., Qi, W., Ingram, D.K., de Cabo, R., 2012. Impact of caloric restriction on health and survival in rhesus monkeys from the NIA study. *Nature* 489, 318–321.
- McCay, C.M., Crowell, M.F., Maynard, L.A., 1989. The effect of retarded growth upon the length of life span and upon the ultimate body size. 1935. *Nutrition* 5, 155–171; discussion, 172.
- Mercken, E.M., Carboneau, B.A., Krzysik-Walker, S.M., de Cabo, R., 2012. Of mice and men: the benefits of caloric restriction, exercise, and mimetics. *Ageing Res. Rev.* 11, 390–398.
- Morley, J.F., Brignull, H.R., Weyers, J.J., Morimoto, R.I., 2002. The threshold for polyglutamine-expansion protein aggregation and cellular toxicity is dynamic and influenced by aging in *Caenorhabditis elegans*. *Proc. Natl. Acad. Sci. U. S. A.* 99, 10417–10422.
- Morselli, E., Maiuri, M.C., Markaki, M., Megalou, E., Pasparaki, A., Palikaras, K., Criollo, A., Galluzzi, L., Malik, S.A., Vitale, I., Michaud, M., Madeo, F., Tavernarakis, N., Kroemer, G., 2010. Caloric restriction and resveratrol promote longevity through the Sirtuin-1-dependent induction of autophagy. *Cell Death Dis.* 1, e10.

- Neumann, M., Sampathu, D.M., Kwong, L.K., Truax, A.C., Micsenyi, M.C., Chou, T.T., Bruce, J., Schuck, T., Grossman, M., Clark, C.M., McCluskey, L.F., Miller, B.L., Masliah, E., Mackenzie, I.R., Feldman, H., Feiden, W., Kretschmar, H.A., Trojanowski, J.Q., Lee, V.M., 2006. Ubiquitinated TDP-43 in frontotemporal lobar degeneration and amyotrophic lateral sclerosis. *Science* 314, 130–133.
- Park, S.J., Ahmad, F., Philp, A., Baar, K., Williams, T., Luo, H., Ke, H., Rehmann, H., Taussig, R., Brown, A.L., Kim, M.K., Beaven, M.A., Burgin, A.B., Manganiello, V., Chung, J.H., 2012. Resveratrol ameliorates aging-related metabolic phenotypes by inhibiting cAMP phosphodiesterases. *Cell* 148, 421–433.
- Parker, J.A., Arango, M., Abderrahmane, S., Lambert, E., Tourette, C., Catoire, H., Neri, C., 2005. Resveratrol rescues mutant polyglutamine cytotoxicity in nematode and mammalian neurons. *Nat. Genet.* 37, 349–350.
- Patel, B.P., Safdar, A., Raha, S., Tarnopolsky, M.A., Hamadeh, M.J., 2010. Caloric restriction shortens lifespan through an increase in lipid peroxidation, inflammation and apoptosis in the G93A mouse, an animal model of ALS. *PLoS One* 5, e9386.
- Signorelli, P., Ghidoni, R., 2005. Resveratrol as an anticancer nutrient: molecular basis, open questions and promises. *J. Nutr. Biochem.* 16, 449–466.
- Srivastava, D., Arya, U., SoundaraRajan, T., Dwivedi, H., Kumar, S., Subramaniam, J.R., 2008. Reserpine can confer stress tolerance and lifespan extension in the nematode *C. elegans*. *Biogerontology* 9, 309–316.
- Steinkraus, K.A., Smith, E.D., Davis, C., Carr, D., Pendergrass, W.R., Sutphin, G.L., Kennedy, B.K., Kaeberlein, M., 2008. Dietary restriction suppresses proteotoxicity and enhances longevity by an hsf-1-dependent mechanism in *Caenorhabditis elegans*. *Aging Cell* 7, 394–404.
- Tauffenberger, A., Vaccaro, A., Aulas, A., Vande Velde, C., Parker, J.A., 2012. Glucose delays age-dependent proteotoxicity. *Aging Cell* 11, 856–866.
- Teixeira-Castro, A., Ailion, M., Jalles, A., Brignull, H.R., Vilaca, J.L., Dias, N., Rodrigues, P., Oliveira, J.F., Neves-Carvalho, A., Morimoto, R.I., Maciel, P., 2011. Neuron-specific proteotoxicity of mutant ataxin-3 in *C. elegans*: rescue by the DAF-16 and HSF-1 pathways. *Hum. Mol. Genet.* 20, 2996–3009.
- Tullet, J.M., Hertweck, M., An, J.H., Baker, J., Hwang, J.Y., Liu, S., Oliveira, R.P., Baumeister, R., Blackwell, T.K., 2008. Direct inhibition of the longevity-promoting factor SKN-1 by insulin-like signaling in *C. elegans*. *Cell* 132, 1025–1038.
- Vaccaro, A., Tauffenberger, A., Aggad, D., Rouleau, G., Drapeau, P., Parker, J.A., 2012a. Mutant TDP-43 and FUS cause age-dependent paralysis and neurodegeneration in *C. elegans*. *PLoS One* 7, e31321.
- Vaccaro, A., Tauffenberger, A., Ash, P.E., Carlomagno, Y., Petrucelli, L., Parker, J.A., 2012b. TDP-1/TDP-43 regulates stress signaling and age-dependent proteotoxicity in *Caenorhabditis elegans*. *PLoS Genet.* 8, e1002806.
- van Ham, T.J., Thijssen, K.L., Breitling, R., Hofstra, R.M., Plasterk, R.H., Nollen, E.A., 2008. *C. elegans* model identifies genetic modifiers of alpha-synuclein inclusion formation during aging. *PLoS Genet.* 4, e1000027.
- Wang, J., Robida-Stubbs, S., Tullet, J.M., Rual, J.F., Vidal, M., Blackwell, T.K., 2010. RNAi screening implicates a SKN-1-dependent transcriptional response in stress resistance and longevity deriving from translation inhibition. *PLoS Genet.* 6, e1001048.



Worming forward: amyotrophic lateral sclerosis toxicity mechanisms and genetic interactions in *Caenorhabditis elegans*

Martine Therrien¹ and J. Alex Parker^{2*}

¹ Département de Pathologie et Biologie Cellulaire, CRCHUM-Centre Hospitalier de l'Université de Montréal, Université de Montréal, Montréal, QC, Canada

² Département de Pathologie et Biologie Cellulaire, Département de Neurosciences, CRCHUM-Centre Hospitalier de l'Université de Montréal, Université de Montréal, Montréal, QC, Canada

Edited by:

Shin Murakami, Touro
University-California, USA

Reviewed by:

Eirini Lionaki, Foundation for
Research and Technology-Hellas,
Greece

Maria Markaki, Foundation for
Research and Technology-Hellas,
Greece

Marta Artal Sanz, Pablo de Olavide
University, Spain

*Correspondence:

J. Alex Parker, CRCHUM- Centre
Hospitalier de l'Université de
Montréal, Université de Montréal,
900 St-Denis, Tour Viger, R09.440,
Montréal, QC H2X 0A9, Canada
e-mail: ja.parker@umontreal.ca

Neurodegenerative diseases share pathogenic mechanisms at the cellular level including protein misfolding, excitotoxicity and altered RNA homeostasis among others. Recent advances have shown that the genetic causes underlying these pathologies overlap, hinting at the existence of a genetic network for neurodegeneration. This is perhaps best illustrated by the recent discoveries of causative mutations for amyotrophic lateral sclerosis (ALS) and frontotemporal degeneration (FTD). Once thought to be distinct entities, it is now recognized that these diseases exist along a genetic spectrum. With this wealth of discoveries comes the need to develop new genetic models of ALS and FTD to investigate not only pathogenic mechanisms linked to causative mutations, but to uncover potential genetic interactions that may point to new therapeutic targets. Given the conservation of many disease genes across evolution, *Caenorhabditis elegans* is an ideal system to investigate genetic interactions amongst these genes. Here we review the use of *C. elegans* to model ALS and investigate a putative genetic network for ALS/FTD that may extend to other neurological disorders.

Keywords: *C. elegans*, ALS (Amyotrophic lateral sclerosis), TDP-43, FUS, C9orf72, SOD1, genetic networks, motor neuron disease

INTRODUCTION

Amyotrophic lateral sclerosis (ALS) is a neurodegenerative disorder affecting 1–2/100,000 individuals. Most cases of ALS are sporadic, but 10% of cases are familial (Turner et al., 2013b). Mutations in the gene *superoxide dismutase 1* (SOD1) were identified in 1993 (Rosen et al., 1993) as the first cause of familial ALS. Thanks to the recent advances in genetics, more than 20 genes are now linked to ALS (Chen et al., 2013) (Table 1). Genes recently shown to be mutated in ALS include the DNA/RNA binding proteins TAR DNA binding protein 43 (TARDBP) and Fused-in-sarcoma (FUS) (Kabashi et al., 2008; Sreedharan et al., 2008; Vance et al., 2009). More recently, mutations in C9ORF72 have turned out to be a major cause of familial and sporadic ALS (DeJesus-Hernandez et al., 2011; Renton et al., 2011).

ALS is characterized by the selective loss of motor neurons in the motor cortex, the brainstem and the spinal cord, the loss of myelin in the spinal cord, and the presence of neuroinflammation (Robberecht and Philips, 2013). Onset of the disease usually begins in the lower limb and spreads toward the upper motor neurons leading to muscle weakness, fasciculation, and wasting. Death occurs 3–5 years after the beginning of the symptoms (Kiernan et al., 2011) and is caused by respiratory failure due to denervation of the respiratory muscles.

50% of ALS patients show cognitive impairment, of which 15% met the criteria of frontotemporal dementia (FTD) (Ringholz et al., 2005). FTD is a group of non-Alzheimer

dementias characterized by atrophy of the frontal and/or temporal lobes causing mid-life behavioral changes or language impairment (Warren et al., 2013). Over the past few years, the identification of TDP-43, C9ORF72 and UBQLN2 as genes causing ALS and FTD has suggested a similarity for both diseases (Morris et al., 2012). Similar pathogenic mechanisms have been suggested for ALS and FTD (Van Langenhove et al., 2012; Ling et al., 2013) but so far it is unclear how patients with the same genetic mutations can have either ALS, FTD or both.

The genes involved in ALS have diverse functions and we still do not know how they interact to cause motor neuron degeneration. Most of the research over the past 20 years has focused on the toxicity caused by mutant SOD1. Among the proposed mechanisms of toxicity are mitochondrial dysfunction, axonal dysfunction, excitotoxicity and neuroinflammation (Turner et al., 2013b). However, TDP-43, FUS, and C9ORF72 proteins seem to point toward RNA toxicity (Ling et al., 2013). Most importantly, only one drug, riluzole, is used to slow disease progression and has only modest effects (Kiernan et al., 2011). Diagnosis is difficult and requires an experienced neurologist to differentiate between ALS and other neurological diseases (Turner et al., 2013a). It is thought that the clinical manifestations of ALS are downstream events that occur much later after the initial insult to the nervous system (Turner et al., 2013a). Therefore, the identification of biomarkers is essential for the rapid, early diagnosis of ALS, and the identification of new drugs limiting the degeneration of motor neuron is an essential unmet need for ALS patients.

Table 1 | ALS genes and their *C. elegans* orthologs.

Human gene	Function	<i>C. elegans</i> gene
MOST COMMON ALS GENES		
<i>SOD1</i>	Superoxide metabolism	<i>sod-1</i>
<i>TARDBP</i>	RNA metabolism	<i>tdp-1</i>
<i>FUS</i>	RNA metabolism	<i>fust-1</i>
<i>OPTN</i>	Vesicular transport	–
<i>VCP</i>	Vesicular transport	<i>cdc-48.1/2</i>
<i>UBQLN2</i>	Proteasome	<i>ubqnl-1</i>
<i>C9ORF72</i>	Unknown, DENN protein	<i>alfa-1</i>
<i>SQSTM1</i>	Autophagy	<i>sqst-2</i>
<i>PFN1</i>	Cytoskeleton dynamics	<i>pfn-1</i>
OTHER GENES INVOLVED IN ALS		
<i>DCTN1</i>	Cytoskeleton dynamics	<i>dnc-1</i>
<i>ALS2</i>	Endocytosis	–
<i>CHMP2B</i>	Vesicular transport	–
<i>FIG4</i>	Vesicular transport	<i>C34B7.2</i>
<i>HNRNPA2B1</i>	RNA metabolism	<i>hrp-1</i>
<i>ELP3</i>	–	–
<i>SETX</i>	RNA processing	–
<i>HNRNPA1</i>	RNA processing	<i>hrp-1</i>
<i>ATXN2</i>	–	<i>atx-2</i>
<i>ANG</i>	Blood vessels formation	–
<i>SPG11</i>	DNA damage	–
<i>VAPB</i>	Vesicular transport	<i>vpr-1</i>
<i>NEFH</i>	Cytoskeleton dynamics	<i>H39E23.3</i>
<i>ARHGEF28</i>	RNA metabolism	<i>rhgf-1</i>

To understand better the impact of the genetic mutations on the function of the different proteins involved in ALS, *in vivo* models have proved to be essential. Ever since the first SOD1 mouse was developed in 1994 (Gurney et al., 1994), several groups have tried to investigate ALS pathogenesis by expressing different ALS related mutations in mice, an approach that has recently been extended to other genes including TDP-43 and FUS for example. While the over expression of wild type SOD1 causes a mild denervation of neurons (Epstein et al., 1987), the over expression of SOD1^{G93A} causes a loss of motor neurons, neuroinflammation, and reduces life span (Gurney et al., 1994; Guo et al., 2009). One model expressing mutant TDP-43Q^{331K} or M337V in the mouse central nervous system has shown selectivity for large caliber motor neuron neurodegeneration (Arnold et al., 2013), while others over expressing mutant TDP-43^{G348C, A315T} and FUS^{R512C, 14Δ} have limited neuronal loss (Swarup et al., 2011; Verbeeck et al., 2012). Some rodent models display relevant ALS pathology, but given the time and expense to develop models for many of the recently discovered ALS genes, not to mention the difficulty of manipulating several genes at once, some laboratories have turned to simpler organisms to model ALS toxicity.

One model showing increasing popularity is the nematode *Caenorhabditis elegans*. This 1 mm long worm has a painstakingly characterized, invariant cell lineage that includes 302 neurons. The nervous system, its interconnections and its synapses are well studied which makes it an ideal model to study mechanisms of

neuronal toxicity. The *C. elegans* genome was the first to be fully sequenced in 1998 and includes more than 19,000 genes on 6 chromosomes (*C. elegans* Sequencing Consortium, 1998). Since then, deletion mutants have been produced for many *C. elegans* genes and approximately 80% of *C. elegans* genes have a human homolog (Lai et al., 2000) (Shaye and Greenwald, 2011). *C. elegans* behavior is well studied and many experimental assays are available, including for worm locomotion. Worms initiate movement by bending their body to advance forward in a sinusoidal pattern, a process that is orchestrated by GABAergic and cholinergic neurons. Cholinergic neurons initiate the contraction along the dorsal or ventral body wall muscles while the GABAergic neurons send an inhibitory signal on the opposite side (Jorgensen, 2005).

C. elegans has been an important tool for the characterization of many neurodegenerative disorders (Li and Le, 2013). Many protein-misfolding disorders have been modeled in worms including Alzheimer's disease, Parkinson's disease, Huntington's disease and different spinocerebellar ataxias. Also, the toxicity of non-coding mutations in *C. elegans* resemble the toxicity in mammalian tissues (Wang et al., 2011b). Since many cellular stress and survival pathways are conserved in worms, our group and others have used *C. elegans* to model ALS. This review aims to summarize the work done modeling ALS in *C. elegans* and highlights the future possibilities and applications.

USE OF *C. elegans* TO MODEL SOD1 TOXICITY

SOD1 is an enzyme that catalyzes the conversion of O₂⁻ into O₂ and H₂O₂. More than 160 mutations causative for ALS have been found in *SOD1* since 1993 (Al-Chalabi et al., 2012). Phenotypic heterogeneity is observed among *SOD1* mutation carriers where *SOD1*^{A4V} seems to cause an aggressive form of ALS while *SOD1*^{D90A} causes a milder, long duration ALS (Renton et al., 2014). It is hypothesized that *SOD1* mutations cause toxicity through a gain of function, even though a loss of enzyme activity have been observed in patients and some models (Saccon et al., 2013). Many pathogenic mechanisms have been hypothesized but no consensus has been reached, although it is thought that the misfolding of mutant SOD1, and sometimes wild type SOD1, may be an important first step of the pathogenesis observed in patients (Pickles and Vande Velde, 2012). Based on pathological evidence, it is now acknowledged that ALS caused by mutations in *SOD1* is a distinctive form of ALS (Mackenzie et al., 2007).

Several groups have used *C. elegans* to model SOD1 toxicity (Table 2) starting with Oeda and colleagues who showed that the ubiquitous expression of human mutant SOD1 impairs the worm's response to oxidative stress and causes protein aggregates (Oeda et al., 2001). It was later shown that expression of mutant SOD1 throughout the worm's entire nervous system resulted in locomotion defects and impaired neuronal transmission (Wang et al., 2009). Interestingly, the formation of aggregates seemed to be restricted to certain mechanosensory neurons despite the pan neuronal expression of SOD1. Other models are non-neuronal in nature and have relied on the expression of SOD1 proteins in the body wall muscles where it was observed that distinct SOD1 mutations have varying propensities to aggregate (Gidalevitz et al., 2009). More recently a *C. elegans* model was generated

Table 2 | Summary of transgenic SOD1 models.

Study	Promoter	Gene	Motor phenotype	Aggregation	Neuro-degeneration	Synaptic dysfunction
Oeda et al., 2001	<i>hsp-16.2</i> : all tissues except the germline	SOD1 ^{A4V}	n.d.	n.d.	n.d.	n.d.
		SOD1 ^{G37R}	n.d.	n.d.	n.d.	n.d.
		SOD1 ^{G93R}	n.d.	n.d.	n.d.	n.d.
	<i>myo-3</i> : muscle cells	SOD1 ^{A4V}	n.d.	yes	n.a.	n.a.
Wang et al., 2009	<i>snb-1</i> : entire nervous system	SOD1 ^{WT}	No	No	n.d.	Normal
		SOD1 ^{G83R}	Yes	Yes	n.d.	Impaired
Gidalevitz et al., 2009	<i>unc-54</i> : muscle cells	SOD1 ^{WT}	No	No	n.a.	n.a.
		SOD1 ^{G85R}	Yes	Yes	n.a.	n.a.
		SOD1 ^{G93A}	Yes	Yes	n.a.	n.a.
		SOD1 ^{127X}	Yes	Yes	n.a.	n.a.
Li et al., 2013a	<i>unc-25</i> : GABAergic motor neurons	SOD1 ^{WT}	Yes	Yes	Yes	n.d.
		SOD1 ^{G93A}	Yes	Yes	Yes	n.d.

n.d., not determined; n.a., not applicable.

based on the expression of SOD1 in the worm's motor neurons showing neurodegeneration in the absence of caspases (Li et al., 2013a), an intriguing finding since the motor neuron loss observed in mouse models is associated with caspase activation (Pasinelli et al., 2000). Whether this reflects a difference between invertebrate and vertebrate systems, or reflects a novel mechanism of neurodegeneration remains to be determined.

The *C. elegans sod-1* gene has a similar function to human SOD1. *sod-1* loss of function mutants have increased O₂⁻ levels, shorter lifespan and are sensitive to some environmental stresses (Yanase et al., 2009). Inversely, overexpression of the worm *sod-1* increases lifespan and increases the level of H₂O₂, the by-product of the catalase reaction of SOD1. However, the increased lifespan seems to be independent of SOD-1 catalase activity, but may be due to altered endoplasmic reticulum (ER) stress signaling (Cabreiro et al., 2011). Interestingly, Van Raamsdonk et al. have generated a *sod* null worm, where all five *C. elegans sod* genes have been mutated and these worms have a normal lifespan and response to oxidative damage but are sensitive to many acute environmental stresses (Van Raamsdonk and Hekimi, 2012).

In summary, many aspects of SOD1 function and toxicity are conserved in worms, but some questions remain. It is known that mutant SOD1 is found in association with the mitochondria in SOD1 mouse model and ALS patients (Pickles and Vande Velde, 2012). To our knowledge, no group has yet investigated the effects of human mutant SOD1 in worm mitochondria. However, it was recently shown that a cleavage product of *vpr-1*, the ortholog of VAPB also involved in ALS, affects mitochondrial organization in muscle cells (Han et al., 2013). A similar analysis of the different SOD1 transgenic models would be interesting and could help identify pathways and drugs that act specifically on this important aspect of ALS pathogenesis.

USE OF *C. elegans* TO MODEL TDP-43 TOXICITY

TDP-43 is a protein encoded by the *TARDBP* gene on chromosome 1. The protein contains two RNA binding domains, a glycine rich domain and nuclear export and import signals.

TDP-43 is similar to the members of the ribonucleoprotein family. TDP-43 was identified in 2006 as the main constituents of sporadic and familial ALS/FTD aggregates (Neumann et al., 2006). In patients, the ubiquitinated aggregates are present in the most affected regions of the brain and spinal cord. These aggregates contain a hyperphosphorylated form of TDP-43 and the C terminus cleaved fragment (Neumann et al., 2006). In 2008, mutations in the *TARDBP* gene were linked to familial and sporadic ALS/FTD cases (Kabashi et al., 2008; Sreedharan et al., 2008; Sreedharan and Brown, 2013). So far, more than 40 mutations in *TARDBP* have been linked to ALS/FTD and most of them are found in the C terminus region of the protein, a region involved in protein-protein interactions (Al-Chalabi et al., 2012).

Under normal cellular conditions, TDP-43 protein shuttles from the nucleus to the cytoplasm. The normal function of TDP-43 is still unclear but the protein participates in transcription, miRNA processing, mRNA splicing, RNA transport and stress granule formation (Ling et al., 2013). The pathogenic effect of the mutant proteins is not well understood and it is still unclear if the toxicity is a gain of function, a loss of function, or both (Ling et al., 2013; Vanden Broeck et al., 2014). An important aspect of TDP-43 toxicity was discovered when characterizing TDP-43 wild type mice. Mice with elevated expression of wild type TDP-43 also have characteristics of TDP-43 mutant proteins (Xu et al., 2010). Therefore, expression level is important and should be considered when generating different transgenic models.

To clarify the toxicity caused by the expression of mutant TDP-43, several groups have developed *C. elegans* models (Table 3). In 2010, Ash and colleagues developed the first TDP-43 overexpression model in *C. elegans*. The pan neuronal expression of human TDP-43 and *C. elegans* TDP-1 resulted in worms with uncoordinated, slow movements and defasciculation of the GABAergic motor neurons (Ash et al., 2010). The results regarding the expression of human TDP-43 were confirmed by Liachko and colleagues who also observed motility defects and degeneration phenotypes from the expression of mutant TDP-43 proteins throughout the worms nervous system (Liachko et al., 2010).

Table 3 | Summary of transgenic TDP-43 models.

Study	Promoter	Gene	Motor phenotype	Aggregation	Neuro-degeneration	Synaptic dysfunction
Ash et al., 2010	<i>snb-1</i> : entire nervous system	TDP-1	Yes	n.d.	n.d.	n.d.
		TDP-43 ^{WT}	Yes	n.d.	GABAergic	n.d.
		TDP-43 ^{ΔRRM1}	No	n.d.	n.d.	n.d.
		TDP-43 ^{ΔRRM2}	No	n.d.	n.d.	n.d.
		TDP-43 ^{ΔC terminus}	No	n.d.	n.d.	n.d.
		TDP-43 ^{no caspase}	Yes	n.d.	n.d.	n.d.
		TDP-43 ^{no NLS}	No	n.d.	n.d.	n.d.
Liachko et al., 2010	<i>snb-1</i> : entire nervous system	TDP-43 ^{WT}	Yes	Yes	No	n.d.
		TDP-43 ^{G290A}	Yes	Yes	GABAergic and dopaminergic	n.d.
		TDP-43 ^{A315T}	Yes	Yes	GABAergic and dopaminergic	n.d.
		TDP-43 ^{M337V}	Yes	Yes	GABAergic and dopaminergic	n.d.
Zhang et al., 2012b	<i>snb-1</i> : entire nervous system	TDP-43 ^{WT}	Yes	Yes	No	Impaired
		TDP-43 ^{G331K}	Yes	n.d.	No	Impaired
		TDP-43 ^{M337V}	Yes	n.d.	No	Impaired
		TDP-43 ^{C terminus}	Yes	Yes	No	Impaired
Vaccaro et al., 2012c	<i>unc-47</i> : GABAergic neurons	TDP-43 ^{WT}	No	No	No	No
		TDP-43 ^{A315T}	Yes	Yes	GABAergic	Impaired

n.d., not determined; NLS, nuclear localization signal; ΔRRM, deletion of RNA recognition motif; ΔC terminus, deletion of C terminus; no caspase, mutations in TDP-43 that block caspase cleavage.

These phenotypes also highly correlated with protein phosphorylation levels where hyperphosphorylation increased the toxicity of mutant TDP-43 proteins similarly to what is observed in ALS patients (Liachko et al., 2010). The TDP-43 C terminus fragment shows another similarity with patients. Zhang and colleagues showed that the pan neuronal expression of human TDP-43 C' fragment caused a phenotype similar to the expression of wild type or mutant TDP-43 (Zhang et al., 2011). Even though no neuronal loss was observed in the latter model, all strains displayed synaptic transmission abnormalities. In worms, GABAergic neurons seem to be particularly sensitive to the expression of TDP-43 (Liachko et al., 2010). To evaluate if the effect of TDP-43 expression in these neurons could cause locomotor defects, our group developed models in which human wild type or mutant TDP-43 were expressed specifically in GABAergic motor neurons as directed by an *unc-47* promoter (McIntire et al., 1997). Interestingly, the overexpression of mutant TDP-43, but not wild type TDP-43, caused an adult-onset, progressive paralysis phenotype accompanied by GABAergic neurodegeneration and synaptic transmission impairment (Vaccaro et al., 2012b). Finally, some of these models showed aggravation of the phenotypes during aging recapitulating an important feature of ALS and neurodegeneration (Liachko et al., 2010; Vaccaro et al., 2012b).

It is still unclear if the toxicity of mutant TDP-43 proteins in ALS patients arises from a gain of function, a loss of function or if both mechanisms are employed. The transgenic *C. elegans* models of TDP-43 are based on the overexpression of TDP-43 in worms and likely represent a gain of function rather than a loss of function. However, the *C. elegans* genome has an ortholog of TDP-43 called TDP-1. TDP-1 is a primarily nuclear protein expressed in

most tissues including body wall muscles, pharynx and neurons (Vaccaro et al., 2012c; Zhang et al., 2012b). TDP-1 contains two RNA binding motifs, a nuclear localization signal and an export signal but lacks the glycine rich domain found in human TDP-43. TDP-1 seems to be functionally conserved because the expression of human TDP-43 can rescue the toxicity of a loss of function of a *tdp-1* mutant (Zhang et al., 2012b).

Mutant *tdp-1* animals show numerous phenotypes including slow development, and locomotion defects (Liachko et al., 2010; Zhang et al., 2012b). TDP-1 was also shown to be involved in lifespan and the cellular stress response. Somewhat paradoxically, worms lacking *tdp-1* have a longer lifespan but are more sensitive to oxidative and osmotic stresses (Vaccaro et al., 2012c; Zhang et al., 2012b). The expression of *tdp-1* can be induced by oxidative stress, either chemically or from activation of the ER stress response, and it is thought that chronic induction of *tdp-1* by stress is ultimately cytotoxic and reduces the worms lifespan (Vaccaro et al., 2012c). Furthermore, several studies have shown that wild type TDP-1 protein may contribute to the neurodegeneration elicited by mutant protein in *C. elegans*. Neurodegeneration was suppressed by deleting *tdp-1* from worms in several ALS models (Vaccaro et al., 2012c; Zhang et al., 2012b) as well as in a *C. elegans* model of Huntington's disease (Tauffenberger et al., 2013a) suggesting there may be genetic interactions amongst genes linked to neurodegeneration. Interestingly, a transcriptome analysis of *tdp-1(ok803)* showed that one of the biological process that was highly affected in the mutant worms was the ER unfolded protein response (Zhang et al., 2012b). ER stress and proteostasis have been a recurrent theme in ALS research (Matus et al., 2013; Musarò, 2013) which

is of interest since sporadic and familial cases of ALS are known to have an abnormal ER stress response (Ilieva et al., 2007; Atkin et al., 2008; Hetz et al., 2009; Ito et al., 2009).

USE OF *C. elegans* TO MODEL FUS TOXICITY

After the identification of TDP-43, several groups examined related RNA-binding proteins for their potential contributions to ALS. In 2009, a protein with a similar function, FUS, was identified as causative of ALS (Kwiatkowski et al., 2009; Vance et al., 2009). Similar to TDP-43, FUS contains a RNA binding domain and a glycine rich domain but also has a two arginine glycine rich regions and one large glutamine, glycine, serine, tyrosine domain in N terminus. Because of their high degree of structural similarity, it was hypothesized that FUS and TDP-43 share common functions. It is known that FUS can bind DNA and RNA and is involved in many of the same RNA processing activities of TDP-43 (Ling et al., 2013). FUS transgenic models are relatively recent additions to the research field and much remains to be learned about the function of FUS and the implication of the mutant protein in neurodegeneration.

Two transgenic models have been developed in *C. elegans* for FUS (Table 4). Murakami et al. (2012) expressed several FUS mutations and two truncated FUS proteins throughout the worm's nervous system. Interestingly, only the mutations that caused aggregation resulted in motor phenotypes in worms. The motor phenotype could not be rescued by the expression of wild type FUS suggesting a gain of function mechanism. Our group confirmed a similar toxicity mechanism in models expressing FUS in the worm motor neurons. Expression of FUS wild type did not cause aggregation but expression of mutant FUS caused aggregation accompanied by paralysis, neuronal synaptic impairment and neurodegeneration (Vaccaro et al., 2012b).

FUS is well conserved and the *C. elegans* ortholog is named *fus-1*. In contrast to *tdp-1*, a *fus-1* deletion mutant could not alleviate the toxicity induced by the expression of C' TDP-43 fragment (Zhang et al., 2012b), suggesting a different role in proteotoxicity. In *Drosophila*, *Cabeza* (Caz), the *Drosophila* ortholog of FUS, is expressed in motor neurons and a decreased expression of Caz causes a motor phenotype and motor neuron degeneration

(Wang et al., 2011a; Sasayama et al., 2012). These results suggest a link between the expression and function of FUS, and the specificity of ALS neurodegeneration and we await further investigations of *fus-1* in *C. elegans*.

USE OF *C. elegans* TO MODEL C9ORF72 TOXICITY

A region of chromosome 9 had been linked to ALS for several years (Morita et al., 2006; Vance et al., 2006; van Es et al., 2009; Shatunov et al., 2010) but the gene was only identified in 2011 (DeJesus-Hernandez et al., 2011; Renton et al., 2011) and has since been shown to be a major cause of sporadic and familial ALS (Turner et al., 2013b). The basis of the mutation is a GGGGCC repeat expansion within the first intron of C9ORF72. Many questions remain to be answered about the role of C9ORF72 in the pathogenesis of ALS. It is still not clear whether the GGGGCC repeat expansion results in a loss of function, a gain of function or both, or if the size of the repeat has differential effects on these potential mechanisms. Recent reports have observed decreased expression of C9ORF72 when the GGGGCC repeat reaches pathogenic length (DeJesus-Hernandez et al., 2011; Ciura et al., 2013; Xi et al., 2013). Whether decreased expression contributes to ALS pathogenesis is unknown since very little is known about the biological role of C9ORF72 other than its sequence similarity to the GDP/GTP exchange factor "Differentially Expressed in Normal and Neoplasia" (DENN) (Zhang et al., 2012a; Levine et al., 2013). DENN proteins are involved in the regulation of Rab-GTPases and endocytosis. Recently, C9ORF72 was shown to be implicated in endosomal trafficking (Farg et al., 2014), confirming its role as a DENN protein. In *C. elegans*, work has been previously done regarding some Rab proteins using deletion mutants and GFP reporters (Sato et al., 2008) to investigate endocytosis (Fares and Grant, 2002). *C. elegans* would be an ideal model to confirm the involvement of C9ORF72 in this pathway. The *C. elegans* homolog of C9ORF72 is named *alfa-1* (ALS/FTD associated gene homolog). Our group characterized the loss of function mutant *alfa-1(ok3062)* where we observed that decreased expression of *alfa-1* causes a motility defect, neurodegeneration specifically of the motor neurons and sensitivity to osmotic stress (Therrien et al., 2013). Further characterization still remains to be done but it is interesting that loss of *alfa-1* is linked

Table 4 | Summary of transgenic FUS models.

Study	Promoter	Gene	Motor phenotype	Aggregation	Neuro-degeneration	Synaptic dysfunction
Murakami et al., 2012	<i>rgef-1</i> : entire nervous system	FUS ^{WT}	No	No	n.d.	n.d.
		FUS ^{R514G}	No	No	n.d.	n.d.
		FUS ^{R521G}	No	No	n.d.	n.d.
		FUS ^{R522G}	Yes	Yes	n.d.	n.d.
		FUS ^{P525L}	Yes	Yes	n.d.	n.d.
		FUS ^{501trunc}	Yes	Yes	n.d.	n.d.
		FUS ^{513trunc}	Yes	Yes	n.d.	n.d.
Vaccaro et al., 2012c	<i>unc-47</i> : GABAergic neurons	FUS ^{WT}	No	No	No	Normal
		FUS ^{S57Δ}	Yes	Yes	GABAergic neurons	Impaired

n.d., not determined; trunc, truncation.

to neuronal integrity specifically for GABAergic motor neurons in worm.

GGGGCC repeat expansions are found in the first intron of *C9ORF72* and the presence of such long non-coding repeats is suggestive of a toxic gain of function mechanism driving neurodegeneration as seen in many of the trinucleotide repeat expansion diseases. In patients, the repeat was shown to induce abnormal translation (non-ATG translation of the repeat, also called RAN translation) leading to the production of different dipeptides (Ash et al., 2013; Mori et al., 2013b). Also of interest were the presence of RNA foci containing the expanded GGGGCC repeat in patients (DeJesus-Hernandez et al., 2011). It is unknown whether a toxic gain of function is caused by the presence of toxic RNA or the presence of toxic protein, or both. So far, no groups have generated transgenic worms to model this aspect of the toxicity however the expression of the non-coding GGGGCC repeat in *Drosophila* causes neurodegeneration (Xu et al., 2013). *C. elegans* may be useful to model non-coding repeats based on previous efforts studying the expression of non-coding CUG repeats that were toxic to worms (Chen et al., 2007) and recapitulated aspects of RNA foci toxicity (Wang et al., 2011b).

STRESS RESPONSE AND AGE-DEPENDENT NEURODEGENERATION IN *C. elegans*

With the identification of TDP-43 in most ALS aggregates and later the identification of mutations affecting *TARDBP* and *FUS* genes, RNA metabolism has become an important area of investigation in ALS research. Under normal conditions, both proteins are mainly observed in the nucleus but the mutant proteins are also found in the cytoplasm. FUS and TDP-43 contain a low-complexity prion-like domain and a RNA binding domain suggesting a role in RNA metabolism (Li et al., 2013b). High throughput RNA-sequencing experiments have been used to identify targets of TDP-43 and FUS in normal or disease states. In worms, the transcriptome of the *tdp-1(ok803)* mutant has been studied (Zhang et al., 2012b) and showed the involvement of TDP-1 in various aspects of development.

Under cellular stress, wild type and mutant TDP-43 and FUS proteins form RNA granules (Bosco et al., 2010; Dormann et al., 2010; Liu-Yesucevitz et al., 2010; Gal et al., 2011; McDonald et al., 2011). These granules are usually formed in order to protect RNA from degradation under stress conditions. In worms, a variety of different RNA granules exist: P granules, P bodies and stress granules. P granules are the most characterized RNA granules in worms and are highly involved in cellular development (Updike and Strome, 2010). However, human proteins found in P bodies and stress granules, such as TIA1, the decapping enzymes and polyA binding proteins, have *C. elegans* ortholog and their role seem conserved regarding RNA granules (Jud et al., 2008; Sun et al., 2011). An active area of research concerns whether mutant TDP-43 and/or FUS proteins interfere with stress granule homeostasis. In a transgenic model of FUS, wild type and mutant FUS were shown to colocalize to stress granules after a heat shock but only the recruitment of mutant FUS to the stress granules caused persistent motility defects in the worms (Murakami et al., 2012). Most work done in *C. elegans* to study stress granules have used thermal stress as an inducer of the granule (Sun et al., 2011). In

cells, formation of granules containing FUS is also initiated by other environmental stresses such as osmotic stress (Baron et al., 2013) and oxidative stress (Vance et al., 2013), thus the effect of these other stresses would be interesting to evaluate. Since most of the components of the granules are conserved in worms, *C. elegans* could be a powerful system to investigate stress biology in the context of aging, an aspect not easily studied in cellular systems.

Since TDP-43 and FUS are components of stress granules, this has led to the hypothesis that both proteins may be involved in the cellular stress response. The genetic pathways governing cellular stress signaling have been studied to great success in *C. elegans*. The different stress response pathways are highly characterized in worms with the insulin/IGF-1 pathway being a major, conserved signaling axis (Lau and Chalasani, 2014). In worms, the insulin/IGF-1 pathway has a sole insulin/IGF-1 receptor, DAF-2, that acts through the kinases AGE-1, PDK and AKT to phosphorylate the FOXO transcription factor DAF-16, and regulate stress resistance and longevity (Lapierre and Hansen, 2012). The most common stresses applied to worms in laboratory settings include exposure to thermal, oxidative, osmotic or hypoxic stresses (Rodriguez et al., 2013). While each is a damaging stress, they can elicit distinct genetic signaling pathways with diverse outcomes. An open question in the field of late-onset neurodegeneration is whether environmental components exist to account for the range in disease onset and progression for what are many highly penetrant, monogenic, dominantly acting disorders. A stress intrinsic to ALS and many neurodegenerative diseases is proteotoxicity. Here mutant proteins misfold leading to a diverse range of proteotoxic consequences. Thus, cells maintain an extensive network of mechanisms, including the insulin/IGF-1 pathway, to maintain protein homeostasis in the face of environmentally derived damage or genetically encoded misfolded proteins.

Work from *C. elegans* directly linked *tdp-1* to the insulin/IGF-1 pathway and proteotoxicity. In *C. elegans* *tdp-1* is required for the stress resistance of *daf-2* mutants and the stress-induced expression of *tdp-1* was dependent on *daf-16*. These data suggest a role for TDP-1/TDP-43 in the insulin/IGF-1 pathway and it remains to see if insulin/IGF-1 signaling is altered by disease-associated TDP-43 mutations.

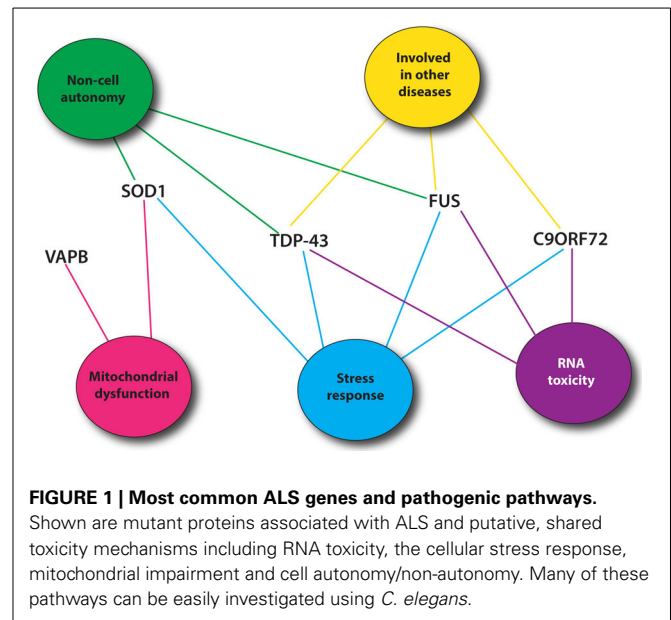
Interestingly, in Vaccaro et al., mutant TDP-43 and mutant FUS proteins were only expressed in the 26 GABAergic motor neurons but activated the ER unfolded protein response chaperone HSP-4 in intestinal tissue (Vaccaro et al., 2012c). This observation suggests that proteotoxic insults can induce stress-signaling pathways in other tissues. It is not known if this is due to a diffusible signaling molecule, or if the mutant proteins make their way from the nervous system to adjacent tissue. TDP-43, FUS, HNRNPA1, HNRNAP2B and TAF15 all contain a prion-like domain (Couthouis et al., 2011; Polymenidou and Cleveland, 2011; Kim et al., 2013) and misfolded SOD1 protein may be able to self propagate (Grad and Cashman, 2014). Thus, these proteins could share properties with toxic prion protein (PrPsc) that misfolds, become infectious, and spreads from cell to cell (Kabir and Safar, 2014). The development of ALS symptoms, starting usually in the lower limb and spreading upward, also suggests a propagation mechanism. Little is known about

the propagation potential of the ALS associated misfolded proteins in *C. elegans* transgenic models. Mutant TDP-43 and FUS proteins in the worm's motor neurons were shown to induce the expression of HSP-4 in the intestine, but the proteins were not visualized outside of the neurons where they were expressed (Vaccaro et al., 2012c). A prion model was however characterized expressing Sup35NM, a yeast prion protein, in the body wall muscle of the worm. The most toxic form of the protein was shown between muscle cells, in the intestine and the coelomocytes, and the toxic fibrils were able to induce protein misfolding (Nussbaum-Krammer et al., 2013). Also, proteostasis, ER stress resistance and longevity, all major ALS research topics, have been recently shown to have important cell-non-autonomous components (Taylor and Dillin, 2013; van Oosten-Hawle et al., 2013). Since *C. elegans* is transparent, direct visualization of tagged proteins during development and aging is possible. The development of additional tools should help establish if a propagation mechanism exists for mutant TDP-43, FUS and SOD1 proteins.

IDENTIFICATION OF GENETIC INTERACTIONS

Recent genetic advances have identified many new causative genes for familial cases of ALS (Table 1). Moreover, genome-wide association studies (GWAS) have also been done in sporadic ALS cohorts to identify potential genes (Renton et al., 2014). With the increasing number of genes linked to ALS along with the diverse functions of these genes, it is essential to identify common pathological pathways relevant to ALS. Genetic interactions amongst genes can refer to functional relationships amongst a group of genes (Boucher and Jenna, 2013). However, genetic interactions are not always easy to interpret and do not necessarily point toward genes that function in the same pathway but rather identify functional similarity between genes that could be in the same pathway or in compensatory pathways (Boucher and Jenna, 2013). Therefore, identification of genetic interactions between ALS genes could point toward potential therapeutic avenues for ALS patients (Figure 1).

Among the proteins identified, TDP-43, SOD1, FUS, OPTN, UBQLN2, and NEFH proteins are found in familial and sporadic ALS inclusions (Al-Chalabi et al., 2012). In zebrafish and *Drosophila*, FUS, and TDP-43 were shown to interact genetically together but independently of SOD1 (Kabashi et al., 2011; Lanson et al., 2011; Wang et al., 2011a). The rapid development of phenotypes and the availability of multiple mutants or RNAi clones make *C. elegans* an expedient model to study genetic interactions. In worms, TDP-1 was shown to participate in the neurotoxicity observed in motor neuron caused by human TDP-43 and human FUS (Vaccaro et al., 2012c). However, FUS and TDP-43 seem to interact differently with PGRN, a gene involved in FTD, and C9ORF72/ALFA-1 (Taufenberg et al., 2013a; Therrien et al., 2013). Those results provide an interesting start to the identification of common pathological pathways in ALS. Finally, the characterization of the loss of function mutant of *pgrn-1*, the *C. elegans* ortholog of progranulin, showed that PGRN-1 is involved in apoptotic cell clearance (Kao et al., 2011). Understanding how *pgrn-1* interacts with the different genes involved in ALS/FTD could help to better understand the



variation observed along ALS/FTD continuum (Mackenzie et al., 2011).

At a broader level, screening for potential genetic modifiers using RNAi has brought a new understanding of the pathogenesis. For example, SOD1 aggregation was linked to motor dysfunction in worms, but upon decreasing the expression of chaperone proteins, the worms exhibited larger aggregates and increased locomotion deficits (Wang et al., 2009). A non-biased screening approach has recently demonstrated that targeting proteins that affect the phosphorylation levels of TDP-43 greatly affects its neuronal toxicity, setting the stage for novel therapeutic approaches (Liachko et al., 2013). Thus far, only a handful of genetic screens have been described for *C. elegans* ALS models but future studies may help uncover pathogenic mechanisms and therapeutic strategies.

TDP-43 aggregates were shown to be the main protein found in non-SOD1 ALS cases (Neumann et al., 2006). However, the presence of TDP-43 aggregates is not exclusive to ALS. TDP-43 aggregates are observed in other neurodegenerative diseases such as Huntington's disease, Parkinson's disease, Alzheimer's disease, and FTD (Mackenzie et al., 2010). FUS is also found in the aggregates of polyglutamine disorders (Woulfe et al., 2010) and mutations in *FUS* were linked to essential tremor (Merner et al., 2012). Recently, FIG4 and VCP were also identified in different neurodegenerative aggregates (Mori et al., 2013a; Kon et al., 2014). Uncovering specific genetic interactions that involve these proteins could also help our understanding of their recruitment to the aggregates of so many neurodegenerative disorders. Using other models, groups have shown that intermediate polyglutamine repeat of *ATXN2* gene and *EPHA4* are potent modulators of ALS toxicity (Elden et al., 2010; Van Hoecke et al., 2012). Therefore, a genetic interaction map may extend the role of these genes beyond ALS and perhaps into other neurodegenerative disorders.

USING *C. elegans* MODEL FOR ALS DRUG DISCOVERY

The small size of *C. elegans*, its rapid life cycle, its ease of cultivation and ability to obtain large numbers of animals makes it an attractive model for drug discovery. Furthermore, worms can be grown on solid media or in liquid culture, the latter being relatively easy to adapt for drug screening purposes often through use of multiwell plates and/or automated screening methods (O'Reilly et al., 2013). The transparency of *C. elegans* makes it an ideal model for neurodegeneration applications since protein aggregation and neuronal morphology can be easily assayed as a complement to behavioral phenotypes.

Boyd and colleagues have shown that drugs identified from cell based systems often have relevance in *C. elegans* (Boyd et al., 2013). A screen to identify compounds that decrease TDP-43 aggregation was performed in cell lines and many of the molecules identified were able to suppress the impaired motility phenotype of worms expressing mutant human TDP-43 (Boyd et al., 2013).

Our group has also developed a high-throughput drug-screening assay. We observed that the paralysis phenotype that typically manifests over 5–12 days on solid media can be observed after just hours when the worms are placed in liquid culture (Vaccaro et al., 2012b; Therrien et al., 2013). Using this technique, more than 4000 FDA approved compounds were screened in our laboratory. From this screen, we identified a number of molecules including methylene blue and others acting on the ER stress response that decrease the toxicity of TDP-43 (Vaccaro et al., 2012a, 2013). Interestingly, these drugs were also confirmed in zebrafish ALS models confirming that these compounds can be effective across species. These compounds are therefore promising leads for testing in mammalian models.

Even though in the disease state, aging and neurodegeneration seem to go hand in hand, we have shown that the drugs that act on neurodegeneration can be separated from those that broadly affect lifespan (Tauffenberger et al., 2013b) suggesting that lifespan extension is not a strong predictor of neuroprotection.

OTHER MOTOR NEURON DISEASES

ALS is part of the neurological group of disorders called motor neuron diseases. This group also includes spinal muscular atrophy (SMA), primary lateral sclerosis (PLS), hereditary spastic paraplegia (HSP) and many others affecting the upper and/or lower motor neurons. The causative genes of these diseases are involved in many cellular functions, however they all share a common toxic pathways since they mainly affect motor neurons. Finding similarities and differences among those diseases could highly increase our understanding of motor neuron toxicity. *C. elegans* has been used to study two of these, SMA and HSP.

HSP is a group of disorders affecting mainly the lower motor neurons. More than 40 loci have been linked to HSP and the genes identified are involved in axon pathfinding and myelination, mitochondrial maintenance and membrane trafficking (Blackstone, 2012). Recently, a large network including many of these genes have been identified and this network is highly similar to Parkinson's, ALS and Alzheimer's diseases (Novarino et al., 2014). Using *C. elegans*, the function and toxicity of two HSP genes have been investigated. First, *spas-1*, the *C. elegans*

ortholog of *spastin*, also called *SPG4*, was shown to be involved in the development of microtubules. SPAS-1 is expressed in the cytoskeleton and is involved specifically in the disassembly of microtubules (Matsushita-Ishiodori et al., 2007). Then, the pan neuronal expression of *NIPA-1* associated mutations led to motor deficits and shortened the lifespan of transgenic worms probably through the activation of caspases and increased ER toxicity (Zhao et al., 2008). With the rapid discovery of new HSP genes, more models are surely to come and will help unravel similarities between these diseases.

SMA is a rare autosomal recessive disorder and a leading genetic cause of infant death. All genetic causes of SMA lead to a decreased expression of the proteins survival of motor neuron (SMN) 1 and 2 (Arnold and Burghes, 2013). It mainly affects the lower motor neurons, but recent evidences suggest that it can be a systemic disease affecting the vascular, cardiac and hepatic functions as well as affecting bone formation (Hamilton and Gillingwater, 2013). *C. elegans* possesses one ortholog of the SMN gene, *smn-1*. In 1999, Miguel-Aliaga and colleagues showed that decreased expression of *smn-1* in worms resulted in severe locomotion defects and sterility (Miguel-Aliaga et al., 1999). Then SMN-1 was shown to interact with SMI-1, a known interactor of SMN in humans (Burt et al., 2006). Briese and colleagues characterized the first *smn-1* deletion mutant observing that the mutants displayed early developmental arrest, which could be rescued by reintroducing expression of *smn-1* in the nervous system, while expression in muscle cells was ineffective (Briese et al., 2009). Little is known about any downstream targets of SMN and no drugs are available. Thus, several groups have used *C. elegans* to identify modifiers of the *smn-1* phenotypes. In a cross-species study, it was shown that proteins involved in endocytosis and mRNA regulation could modify the toxicity (Dimitriadis et al., 2010). Also, knowing that the ubiquitin-proteasome pathway degrades SMN, decreased expression of *Mib1*, an E3 ligase, was shown to ameliorate *smn-1* phenotypes (Kwon et al., 2013). Since the *smn-1* deletion allele *ok355* is an early larval lethal phenotype, to aid the development of drug screening Sleight and colleagues identified a less severe mutant allele that more closely resembles the severity of SMA (Sleight et al., 2011). Using this mutant, they identified several small molecules that alleviate *smn-1* phenotypes of the worms, therefore, being highly promising compounds for SMA drug development (Sleight et al., 2011).

PERSPECTIVES

With the discovery of many new ALS genes comes the need to better understand their functions, expression patterns and their modes of toxicity. *C. elegans* has proven to be an informative model to study neurodegeneration mechanisms arising from multiple ALS related proteins. We envision that the introduction of new transgenic and genetic models will help unravel important questions about the normal and pathogenic roles of these proteins.

Most models explained here recapitulate some if not many, important features of ALS, however, phenotypic variations are seen amongst the different models, for a number of reasons. First, the models do not all use the same mutations, thus the resulting mutant proteins may not all be equally toxic, or display the

same interactions with other proteins. Also, the level of expression is important to consider as for example, there is considerable evidence that TDP-43 levels are tightly regulated (Budini and Buratti, 2011), and elevated expression is toxic in nearly every system studied (Ash et al., 2010; Xu et al., 2010; Estes et al., 2011). The most common method to generate transgenic worms is by microinjection to create stable lines followed by radiation to integrate the transgene in the genome. This procedure typically produces transgenics with multiple copies of the gene inserted in the genome, thus some of the toxicity observed may be due to overexpression. Aware of this issue, a new generation of ALS transgenic worms should be constructed based on single copy integration (Frøkjær-Jensen et al., 2008) or with the CRISPR-Cas9 method (Friedland et al., 2013) instead to ensure that transgenic lines have a similar level of expression from the same genomic location. Finally, the phenotypic variance may also be due to the promoter used. Some models have used pan neuronal expression constructs, while others have targeted transgenic expression to specific neuronal populations. In humans, most of these proteins are expressed ubiquitously but only specific neuronal populations are sensitive to degeneration. Thus, worm models based on motor neuron transgenics could be ideal model to uncover conserved mechanisms of motor neuron degeneration. To confirm the specificity of each phenotype, mutant and wild type proteins should be carefully compared and similar changes should be confirmed in higher eukaryotes. For example, mutant TDP-43 and FUS proteins induce an ER stress response in worms which is not observed when the wild type proteins are expressed (Vaccaro et al., 2012b). Also, the ER stress response was shown to be activated in other ALS models and in patients (see section above).

These models are setting the stage for novel toxicity hypothesis. The immune system seems to play an important role in the neurodegeneration observed in ALS. Protein aggregation could activate the immune response and neuroinflammation actively contributes to disease progression (McCombe and Henderson, 2011). *C. elegans* relies on an evolutionary conserved, innate immune response (Engelmann and Pujol, 2010) that coordinates its activity with the insulin/IGF-1 pathway (Singh and Aballay, 2009) suggesting these may be pathways worth investigating. Also, in the past year, a convergence of data has suggested a role for glial cells in ALS neurodegeneration (Parisi et al., 2013; Valori et al., 2013; Chiu et al., 2014). The worm has 56 glial cells and some are found at the neuromuscular junction (Oikonomou and Shaham, 2011). Characterization of the cross talk between the neurons and the glial cells would also be an interesting area of investigation.

An important topic related to ALS and to other neurodegenerative disorders is aging. The risk of ALS increases with age, peaking between 70 and 80 years old (Gordon, 2013). Aging pathways are well characterized in worms and among others, include the insulin/IGF-1, the target of rapamycin (TOR) and germline signaling pathways. There is a strong overlap between proteotoxicity and aging where autophagy and lipid metabolism are major targets (Lapierre and Hansen, 2012). Evaluating the toxic impact of mutant proteins during aging is not feasible in many models, but is easily accomplished using *C. elegans*. The development

of models with age-related toxicity is essential and could help understand the link between the proteotoxicity and aging.

When using *C. elegans* or other animal models, most studies have focused on the toxicity of known ALS genes. It is important to note that almost 90% of ALS cases are sporadic ALS with no link to known genetic abnormalities. Therefore, we still do not know how most patients develop ALS. However, it is important to know that sporadic and familial cases of ALS are clinically indistinguishable (Al-Chalabi and Hardiman, 2013). Given that ALS patients can live between 6 months and 6 years after diagnosis, it has been hypothesized that environmental factors may influence disease onset and progression (Al-Chalabi and Hardiman, 2013). Many environmental factors have been examined in relation to ALS but there is no consensus for their contribution to the disease (Al-Chalabi and Hardiman, 2013). *C. elegans* could be useful to study some of the environmental risks hypothesized. In fact, several groups have identified compounds that could cause specific degeneration of motor neurons (Du and Wang, 2009; Negga et al., 2012; Estevez et al., 2014) opening the door to identifying environmental modifiers of degeneration in ALS models.

However, how relevant are any of these findings to humans? Will any of the drugs identified in *C. elegans* translate to mammalian models let alone ALS patients? So far, many drugs identified using rodent models focusing mainly on protein aggregation and cell death mechanisms have failed in subsequent clinical trials. Using *C. elegans* to identify drugs acting on early neuronal dysfunction mechanisms could be an effective way to prevent ensuing cellular decline and death. From a liquid culture screen, our group has identified a compound with this property (unpublished results). The compound is effective in vertebrate ALS animal models and is now being tested in ALS patients. Therefore, large screens using *C. elegans* targeting specific early aspects of neurodegeneration seem promising and show relevance in higher organisms.

ACKNOWLEDGMENTS

Funding from ALS Canada, the Canadian Institutes of Health Research, the Congressionally Directed Medical Research Program (CDMRP) Amyotrophic Lateral Sclerosis Research Program (USA), and the Muscular Dystrophy Association (USA) supported this work.

REFERENCES

- Al-Chalabi, A., and Hardiman, O. (2013). The epidemiology of ALS: a conspiracy of genes, environment and time. *Nat. Rev. Neurol.* 9, 617–628. doi: 10.1038/nrneurol.2013.203
- Al-Chalabi, A., Jones, A., Troakes, C., King, A., Al-Sarraj, S., and van den Berg, L. H., (2012). The genetics and neuropathology of amyotrophic lateral sclerosis. *Acta Neuropathol.* 124, 339–352. doi: 10.1007/s00401-012-1022-4
- Arnold, E. S., Ling, S.-C., Huelga, S. C., Lagier-Tourenne, C., Polymenidou, M., Ditsworth, D., et al. (2013). ALS-linked TDP-43 mutations produce aberrant RNA splicing and adult-onset motor neuron disease without aggregation or loss of nuclear TDP-43. *Proc. Natl. Acad. Sci. U.S.A.* 110, E736–E745. doi: 10.1073/pnas.1222809110
- Arnold, W. D., and Burghes, A. H. M. (2013). Spinal muscular atrophy: development and implementation of potential treatments. *Ann. Neurol.* 74, 348–362. doi: 10.1002/ana.23995
- Ash, P. E. A., Bieniek, K. F., Gendron, T. F., Caulfield, T., Lin, W.-L., DeJesus-Hernandez, M., et al. (2013). Unconventional translation of C9orf72 GGGGCC expansion generates insoluble polypeptides

- specific to c9FTD/ALS. *Neuron* 77, 639–646. doi: 10.1016/j.neuron.2013.02.004
- Ash, P. E. A., Zhang, Y. J., Roberts, C. M., Saldi, T., Hutter, H., Buratti, E., et al. (2010). Neurotoxic effects of TDP-43 overexpression in *C. elegans*. *Hum. Mol. Genet.* 19, 3206–3218. doi: 10.1093/hmg/ddq230
- Atkin, J. D., Farg, M. A., Walker, A. K., McLean, C., Tomas, D., and Horne, M. K. (2008). Endoplasmic reticulum stress and induction of the unfolded protein response in human sporadic amyotrophic lateral sclerosis. *Neurobiol. Dis.* 30, 400–407. doi: 10.1016/j.nbd.2008.02.009
- Baron, D. M., Kaushansky, L. J., Ward, C. L., Sama, R. R. K., Chian, R.-J., Boggio, K. J., et al. (2013). Amyotrophic lateral sclerosis-linked FUS/TLS alters stress granule assembly and dynamics. *Mol. Neurodegener.* 8:30. doi: 10.1186/1750-1326-8-30
- Blackstone, C. (2012). Cellular pathways of hereditary spastic paraplegia. *Annu. Rev. Neurosci.* 35, 25–47. doi: 10.1146/annurev-neuro-062111-150400
- Bosco, D. A., Lemay, N., Ko, H. K., Zhou, H., Burke, C., Kwiatkowski, T. J., et al. (2010). Mutant FUS proteins that cause amyotrophic lateral sclerosis incorporate into stress granules. *Hum. Mol. Genet.* 19, 4160–4175. doi: 10.1093/hmg/ddq335
- Boucher, B., and Jenna, S. (2013). Genetic interaction networks: better understand to better predict. *Front. Genet.* 4:290. doi: 10.3389/fgene.2013.00290
- Boyd, J. D., Lee-Armandt, J. P., Feiler, M. S., Zauur, N., Liu, M., Kraemer, B., et al. (2013). A high-content screen identifies novel compounds that inhibit stress-induced TDP-43 cellular aggregation and associated cytotoxicity. *J. Biomol. Screen.* 19, 44–56. doi: 10.1177/1087057113501553
- Briese, M., Esmaili, B., Fraboulet, S., Burt, E. C., Christodoulou, S., Towers, P. R., et al. (2009). Deletion of smn-1, the *Caenorhabditis elegans* ortholog of the spinal muscular atrophy gene, results in locomotor dysfunction and reduced lifespan. *Hum. Mol. Genet.* 18, 97–104. doi: 10.1093/hmg/ddn320
- Budini, M., and Buratti, E. (2011). TDP-43 autoregulation: implications for disease. *J. Mol. Neurosci.* 45, 473–479. doi: 10.1007/s12031-011-9573-8
- Burt, E. C., Towers, P. R., and Sattelle, D. B. (2006). *Caenorhabditis elegans* in the study of SMN-interacting proteins: a role for SMI-1, an orthologue of human Gemin2 and the identification of novel components of the SMN complex. *Invert. Neurosci.* 6, 145–159. doi: 10.1007/s10158-006-0027-x
- C. elegans Sequencing Consortium. (1998). Genome sequence of the nematode *C. elegans*: a platform for investigating biology. *Science* 282, 2012–2018. doi: 10.1126/science.282.5396.2012
- Cabreiro, F., Ackerman, D., Doonan, R., Araiz, C., Back, P., Papp, D., et al. (2011). Increased life span from overexpression of superoxide dismutase in *Caenorhabditis elegans* is not caused by decreased oxidative damage. *Free Radic. Biol. Med.* 51, 1575–1582. doi: 10.1016/j.freeradbiomed.2011.07.020
- Chen, K.-Y., Pan, H., Lin, M.-J., Li, Y.-Y., Wang, L.-C., Wu, Y.-C., et al. (2007). Length-dependent toxicity of untranslated CUG repeats on *Caenorhabditis elegans*. *Biochem. Biophys. Res. Commun.* 352, 774–779. doi: 10.1016/j.bbrc.2006.11.102
- Chen, S., Sayana, P., Zhang, X., and Le, W. (2013). Genetics of amyotrophic lateral sclerosis: an update. *Mol. Neurodegener.* 8:28. doi: 10.1186/1750-1326-8-28
- Chiu, H., Alqadah, A., and Chang, C. (2014). The role of microRNAs in regulating neuronal connectivity. *Front. Cell. Neurosci.* 7:283. doi: 10.3389/fncel.2013.00283
- Ciura, S., Lattante, S., Le Ber, I., Latouche, M., Tostivint, H., Brice, A., et al. (2013). Loss of function of C9orf72 causes motor deficits in a zebrafish model of Amyotrophic Lateral Sclerosis. *Ann Neurol.* 74, 180–187. doi: 10.1002/ana.23946
- Couthouis, J., Hart, M. P., Shorter, J., DeJesus-Hernandez, M., Erion, R., Oristano, R., et al. (2011). A yeast functional screen predicts new candidate ALS disease genes. *Proc. Natl. Acad. Sci. U.S.A.* 108, 20881–20890. doi: 10.1073/pnas.1109434108
- DeJesus-Hernandez, M., Mackenzie, I. R., Boeve, B. F., Boxer, A. L., Baker, M., Rutherford, N. J., et al. (2011). Expanded GGGGCC hexanucleotide repeat in noncoding region of C9orf72 causes chromosome 9p-linked FTD and ALS. *Neuron* 72, 245–256. doi: 10.1016/j.neuron.2011.09.011
- Dimitriadis, M., Sleight, J. N., Walker, A., Chang, H. C., Sen, A., Kalloo, G., et al. (2010). Conserved genes act as modifiers of invertebrate SMN loss of function defects. *PLoS Genet.* 6:e1001172. doi: 10.1371/journal.pgen.1001172
- Dormann, D., Rodde, R., Edbauer, D., Bentmann, E., Fischer, I., Hruscha, A., et al. (2010). ALS-associated fused in sarcoma (FUS) mutations disrupt Transportin-mediated nuclear import. *EMBO J.* 29, 2841–2857. doi: 10.1038/emboj.2010.143
- Du, M., and Wang, D. (2009). The neurotoxic effects of heavy metal exposure on GABAergic nervous system in nematode *Caenorhabditis elegans*. *Environ. Toxicol. Pharmacol.* 27, 314–320. doi: 10.1016/j.etap.2008.11.011
- Elden, A. C., Kim, H.-J., Hart, M. P., Chen-Plotkin, A. S., Johnson, B. S., Fang, X., et al. (2010). Ataxin-2 intermediate-length polyglutamine expansions are associated with increased risk for ALS. *Nature* 466, 1069–1075. doi: 10.1038/nature09320
- Engelmann, I., and Pujol, N. (2010). Innate immunity in *C. elegans*. *Adv. Exp. Med. Biol.* 708, 105–121. doi: 10.1007/978-1-4419-8059-5_6
- Epstein, C. J., Avraham, K. B., Lovett, M., Smith, S., Elroy-Stein, O., Rotman, G., et al. (1987). Transgenic mice with increased Cu/Zn-superoxide dismutase activity: animal model of dosage effects in Down syndrome. *Proc. Natl. Acad. Sci. U.S.A.* 84, 8044–8048. doi: 10.1073/pnas.84.22.8044
- Estes, P. S., Boehringer, A., Zwick, R., Tang, J. E., Grigsby, B., and Zarnescu, D. C. (2011). Wild-type and A315T mutant TDP-43 exert differential neurotoxicity in a Drosophila model of ALS. *Hum. Mol. Genet.* 20, 2308–2321. doi: 10.1093/hmg/ddr124
- Estevez, A. O., Morgan, K. L., Szewczyk, N. J., Gems, D., and Estevez, M. (2014). The neurodegenerative effects of selenium are inhibited by FOXO and PINK1/PTEN regulation of insulin/insulin-like growth factor signaling in *Caenorhabditis elegans*. *Neurotoxicology* 41, 28–43. doi: 10.1016/j.neuro.2013.12.012
- Fares, H., and Grant, B. (2002). Deciphering endocytosis in *Caenorhabditis elegans*. *Traffic* 3, 11–19. doi: 10.1034/j.1600-0854.2002.30103.x
- Farg, M. A., Sundaramoorthy, V., Sultana, J. M., Yang, S., Atkinson, R. A. K., Levina, V., et al. (2014). C9orf72, implicated in amyotrophic lateral sclerosis and frontotemporal dementia, regulates endosomal trafficking. *Hum. Mol. Genet.* doi: 10.1093/hmg/ddu068. [Epub ahead of print].
- Friedland, A. E., Tzur, Y. B., Esvelt, K. M., Colaiácovo, M. P., Church, G. M., and Calarco, J. A. (2013). Heritable genome editing in *C. elegans* via a CRISPR-Cas9 system. *Nat. Meth.* 10, 741–743. doi: 10.1038/nmeth.2532
- Froekjaer-Jensen, C., Davis, M. W., Hopkins, C. E., Newman, B. J., Thummel, J. M., Olesen, S.-P., et al. (2008). Single-copy insertion of transgenes in *Caenorhabditis elegans*. *Nat. Genet.* 40, 1375–1383. doi: 10.1038/ng.248
- Gal, J., Zhang, J., Kwinter, D. M., Zhai, J., Jia, H., Jia, J., et al. (2011). Nuclear localization sequence of FUS and induction of stress granules by ALS mutants. *Neurobiol. Aging* 32, 2323.e27–e40. doi: 10.1016/j.neurobiolaging.2010.06.010
- Gidalevitz, T., Krupinski, T., Garcia, S., and Morimoto, R. I. (2009). Destabilizing protein polymorphisms in the genetic background direct phenotypic expression of mutant SOD1 toxicity. *PLoS Genet.* 5:e1000399. doi: 10.1371/journal.pgen.1000399
- Gordon, P. H. (2013). Amyotrophic lateral sclerosis: an update for 2013 clinical features, pathophysiology, management and therapeutic trials. *Aging Dis.* 4, 295–310. doi: 10.14336/AD.2013.0400295
- Grad, L. I., and Cashman, N. R. (2014). Prion-like activity of Cu/Zn superoxide dismutase: implications for amyotrophic lateral sclerosis. *Prion* 8, 35–43. doi: 10.4161/pri.27602
- Guo, Y.-S., Wu, D.-X., Wu, H.-R., Wu, S.-Y., Yang, C., Li, B., et al. (2009). Sensory involvement in the SOD1-G93A mouse model of amyotrophic lateral sclerosis. *Exp. Mol. Med.* 41, 140–150. doi: 10.3858/emmm.2009.41.3.017
- Gurney, M. E., Pu, H., Chiu, A. Y., Dal Canto, M. C., Polchow, C. Y., Alexander, D. D., et al. (1994). Motor neuron degeneration in mice that express a human Cu,Zn superoxide dismutase mutation. *Science* 264, 1772–1775. doi: 10.1126/science.8209258
- Hamilton, G., and Gillingwater, T. H. (2013). Spinal muscular atrophy: going beyond the motor neuron. *Trends Mol. Med.* 19, 40–50. doi: 10.1016/j.molmed.2012.11.002
- Han, S. M., Oussini, E. L. H., Scekcic-Zahirovic, J., Vibbert, J., Cottee, P., and Miller, M. A. (2013). VAPB/ALS8 MSP ligands regulate striated muscle energy metabolism critical for adult survival in *Caenorhabditis elegans*. *PLoS Genet.* 9:e1003738. doi: 10.1371/journal.pgen.1003738
- Hetz, C., Thielen, P., Matus, S., Nassif, M., Court, F., Kiffin, R., et al. (2009). XBP-1 deficiency in the nervous system protects against amyotrophic lateral sclerosis by increasing autophagy. *Genes Dev.* 23, 2294–2306. doi: 10.1101/gad.1830709
- Ilieva, E. V., Ayala, V., Jové, M., Dalfó, E., Cacabelos, D., Povedano, M., et al. (2007). Oxidative and endoplasmic reticulum stress interplay in sporadic amyotrophic lateral sclerosis. *Brain* 130, 3111–3123. doi: 10.1093/brain/awm190

- Ito, Y., Yamada, M., Tanaka, H., Aida, K., Tsuruma, K., Shimazawa, M., et al. (2009). Involvement of CHOP, an ER-stress apoptotic mediator, in both human sporadic ALS and ALS model mice. *Neurobiol. Dis.* 36, 470–476. doi: 10.1016/j.nbd.2009.08.013
- Jorgensen, E. M. (2005). GABA. *WormBook* 1–13. doi: 10.1895/wormbook.1.14.1
- Jud, M. C., Czerwinski, M. J., Wood, M. P., Young, R. A., Gallo, C. M., Bickel, J. S., et al. (2008). Large P body-like RNPs form in *C. elegans* oocytes in response to arrested ovulation, heat shock, osmotic stress, and anoxia and are regulated by the major sperm protein pathway. *Dev. Biol.* 318, 38–51. doi: 10.1016/j.ydbio.2008.02.059
- Kabashi, E., Bercier, V., Lissouba, A., Liao, M., Bruste, E., Rouleau, G. A., et al. (2011). FUS and TARDBP but not SOD1 interact in genetic models of amyotrophic lateral sclerosis. *PLoS Genet.* 7:e1002214. doi: 10.1371/journal.pgen.1002214
- Kabashi, E., Valdmanis, P. N., Dion, P., Spiegelman, D., McConkey, B. J., Vande Velde, C., et al. (2008). TARDBP mutations in individuals with sporadic and familial amyotrophic lateral sclerosis. *Nat. Genet.* 40, 572–574. doi: 10.1038/ng.132
- Kabir, M. E., and Safar, J. G. (2014). Implications of prion adaptation and evolution paradigm for human neurodegenerative diseases. *Prion* 8, 113–118. doi: 10.4161/pri.27661
- Kao, A. W., Eisenhut, R. J., Martens, L. H., Nakamura, A., Huang, A., Bagley, J. A., et al. (2011). A neurodegenerative disease mutation that accelerates the clearance of apoptotic cells. *Proc. Natl. Acad. Sci.* 108, 4441–4446. doi: 10.1073/pnas.1100650108
- Kiernan, M. C., Vucic, S., Cheah, B. C., Turner, M. R., Eisen, A., Hardiman, O., et al. (2011). Amyotrophic lateral sclerosis. *Lancet* 377, 942–955. doi: 10.1016/S0140-6736(10)61156-7
- Kim, H. J., Kim, N. C., Wang, Y.-D., Scarborough, E. A., Moore, J., Diaz, Z., et al. (2013). Mutations in prion-like domains in hnRNPA2B1 and hnRNPA1 cause multisystem proteinopathy and ALS. *Nature* 495, 467–473. doi: 10.1038/nature11922
- Kon, T., Mori, F., Tanji, K., Miki, Y., Toyoshima, Y., Yoshida, M., et al. (2014). ALS-associated protein FIG4 is localized in Pick and Lewy bodies, and also neuronal nuclear inclusions, in polyglutamine and intranuclear inclusion body diseases. *Neuropathology* 34, 19–26. doi: 10.1111/neup.12056
- Kwiatkowski, T. J., Bosco, D. A., LeClerc, A. L., Tamrazian, E., Vandenberg, C. R., Russ, C., et al. (2009). Mutations in the FUS/TLS gene on chromosome 16 cause familial amyotrophic lateral sclerosis. *Science* 323, 1205–1208. doi: 10.1126/science.1166066
- Kwon, D. Y., Dimitriadis, M., Terzic, B., Cable, C., Hart, A. C., Chitnis, A., et al. (2013). The E3 ubiquitin ligase mind bomb 1 ubiquitinates and promotes the degradation of survival of motor neuron protein. *Mol. Biol. Cell* 24, 1863–1871. doi: 10.1091/mbc.E13-01-0042
- Lai, C. H., Chou, C. Y., Ch'ang, L. Y., Liu, C. S., and Lin, W. (2000). Identification of novel human genes evolutionarily conserved in *Caenorhabditis elegans* by comparative proteomics. *Genome Res.* 10, 703–713. doi: 10.1101/gr.10.5.703
- Lanson, N. A., Maltare, A., King, H., Smith, R., Kim, J. H., Taylor, J. P., et al. (2011). A Drosophila model of FUS-related neurodegeneration reveals genetic interaction between FUS and TDP-43. *Hum. Mol. Genet.* 20, 2510–2523. doi: 10.1093/hmg/ddr150
- Lapierre, L. R., and Hansen, M. (2012). Lessons from *C. elegans*: signaling pathways for longevity. *Trends Endocrinol. Metab.* 23, 637–644. doi: 10.1016/j.tem.2012.07.007
- Lau, H. E., and Chalasani, S. H. (2014). Divergent and convergent roles for insulin-like peptides in the worm, fly and mammalian nervous systems. *Invert. Neurosci.* doi: 10.1007/s10158-013-0166-9. [Epub ahead of print].
- Levine, T. P., Daniels, R. D., Gatta, A. T., Wong, L. H., and Hayes, M. J. (2013). The product of C9orf72, a gene strongly implicated in neurodegeneration, is structurally related to DENN Rab-GEFs. *Bioinformatics* 29, 499–503. doi: 10.1093/bioinformatics/bts725
- Li, J., and Le, W. (2013). Modeling neurodegenerative diseases in *Caenorhabditis elegans*. *Exp. Neurol.* 250, 94–103. doi: 10.1016/j.expneurol.2013.09.024
- Li, J., Li, T., Zhang, X., Tang, Y., Yang, J., and Le, W. (2013a). Human superoxide dismutase 1 overexpression in motor neurons of *Caenorhabditis elegans* causes axon guidance defect and neurodegeneration. *Neurobiol. Aging* 35, 837–846. doi: 10.1016/j.neurobiolaging.2013.09.003
- Li, Y. R., King, O. D., Shorter, J., and Gitler, A. D. (2013b). Stress granules as crucibles of ALS pathogenesis. *J. Cell Biol.* 201, 361–372. doi: 10.1083/jcb.201302044
- Liachko, N. F., Guthrie, C. R., and Kraemer, B. C. (2010). Phosphorylation promotes neurotoxicity in a *Caenorhabditis elegans* Model of TDP-43 proteinopathy. *J. Neurosci.* 30, 16208–16219. doi: 10.1523/JNEUROSCI.2911-10.2010
- Liachko, N. F., McMillan, P. J., Guthrie, C. R., Bird, T. D., Leverenz, J. B., and Kraemer, B. C. (2013). CDC7 inhibition blocks pathological TDP-43 phosphorylation and neurodegeneration. *Ann. Neurol.* 74, 39–52. doi: 10.1002/ana.23870
- Ling, S.-C., Polymenidou, M., and Cleveland, D. W. (2013). Converging mechanisms in ALS and FTD: disrupted RNA and protein homeostasis. *Neuron* 79, 416–438. doi: 10.1016/j.neuron.2013.07.033
- Liu-Yesucevitz, L., Bilgutay, A., Zhang, Y.-J., Vanderweyde, T., Vanderweyde, T., Citro, A., et al. (2010). Tar DNA binding protein-43 (TDP-43) associates with stress granules: analysis of cultured cells and pathological brain tissue. *PLoS ONE* 5:e13250. doi: 10.1371/journal.pone.0013250
- Mackenzie, I. R. A., Ansorge, O., Strong, M., Bilbao, J., Zinman, L., Ang, L. C., et al. (2011). Pathological heterogeneity in amyotrophic lateral sclerosis with FUS mutations: two distinct patterns correlating with disease severity and mutation. *Acta Neuropathol.* 122, 87–98. doi: 10.1007/s00401-011-0838-7
- Mackenzie, I. R. A., Bigio, E. H., Ince, P. G., Geser, F., Neumann, M., Cairns, N. J., et al. (2007). Pathological TDP-43 distinguishes sporadic amyotrophic lateral sclerosis from amyotrophic lateral sclerosis with SOD1 mutations. *Ann. Neurol.* 61, 427–434. doi: 10.1002/ana.21147
- Mackenzie, I. R., Rademakers, R., and Neumann, M. (2010). TDP-43 and FUS in amyotrophic lateral sclerosis and frontotemporal dementia. *Lancet Neurol* 9, 995–1007. doi: 10.1016/S1474-4422(10)70195-2
- Matsushita-Ishiodori, Y., Yamanaka, K., and Ogura, T. (2007). The *C. elegans* homologue of the spastic paraplegia protein, spastin, disassembles microtubules. *Biochem. Biophys. Res. Commun.* 359, 157–162. doi: 10.1016/j.bbrc.2007.05.086
- Matus, S., Valenzuela, V., Medinas, D. B., and Hetz, C. (2013). ER dysfunction and protein folding stress in ALS. *Int. J. Cell Biol.* 2013, 674751. doi: 10.1155/2013/674751
- McCombe, P. A., and Henderson, R. D. (2011). The role of immune and inflammatory mechanisms in ALS. *Curr. Mol. Med.* 11, 246–254. doi: 10.2174/156652411795243450
- McDonald, K. K., Aulas, A., Destrois, L., Pickles, S., Beale, E., Camu, W., et al. (2011). TAR DNA-binding protein 43 (TDP-43) regulates stress granule dynamics via differential regulation of G3BP and TIA-1. *Hum. Mol. Genet.* 20, 1400–1410. doi: 10.1093/hmg/ddr021
- McIntire, S. L., Reimer, R. J., Schuske, K., Edwards, R. H., and Jorgensen, E. M. (1997). Identification and characterization of the vesicular GABA transporter. *Nature* 389, 870–876. doi: 10.1038/39908
- Merner, N. D., Girard, S. L., Catoire, H., Bourassa, C. V., Belzil, V. V., Rivière, J.-B., et al. (2012). Exome sequencing identifies FUS mutations as a cause of essential tremor. *Am. J. Hum. Genet.* 91, 313–319. doi: 10.1016/j.ajhg.2012.07.002
- Miguel-Aliaga, I., Culetto, E., Walker, D. S., Baylis, H. A., Sattelle, D. B., and Davies, K. E. (1999). The *Caenorhabditis elegans* orthologue of the human gene responsible for spinal muscular atrophy is a maternal product critical for germline maturation and embryonic viability. *Hum. Mol. Genet.* 8, 2133–2143. doi: 10.1093/hmg/8.12.2133
- Mori, F., Tanji, K., Toyoshima, Y., Sasaki, H., Yoshida, M., Kakita, A., et al. (2013a). Valosin-containing protein immunoreactivity in tauopathies, synucleinopathies, polyglutamine diseases and intranuclear inclusion body disease. *Neuropathology* 33, 637–644. doi: 10.1111/neup.12050
- Mori, K., Weng, S.-M., Arzberger, T., May, S., Rentzsch, K., Kremmer, E., et al. (2013b). The C9orf72 GGGGCC repeat is translated into aggregating dipeptide-repeat proteins in FTL/ALS. *Science* 339, 1335–1338. doi: 10.1126/science.1232927
- Morita, M., Al-Chalabi, A., Andersen, P. M., Hosler, B., Sapp, P., Englund, E., et al. (2006). A locus on chromosome 9p confers susceptibility to ALS and frontotemporal dementia. *Neurology* 66, 839–844. doi: 10.1212/01.wnl.0000200048.53766.b4
- Morris, H. R., Waite, A. J., Williams, N. M., Neal, J. W., and Blake, D. J. (2012). Recent advances in the genetics of the ALS-FTLD complex. *Curr. Neurol. Neurosci. Rep.* 12, 243–250. doi: 10.1007/s11910-012-0268-5
- Murakami, T., Yang, S.-P., Xie, L., Kawano, T., Fu, D., Mukai, A., et al. (2012). ALS mutations in FUS cause neuronal dysfunction and death in *Caenorhabditis*

- elegans* by a dominant gain-of-function mechanism. *Hum. Mol. Genet.* 21, 1–9. doi: 10.1093/hmg/ddr417
- Musarò, A. (2013). Understanding ALS: new therapeutic approaches. *FEBS J.* 280, 4315–4322. doi: 10.1111/febs.12087
- Negga, R., Stuart, J. A., Machen, M. L., Salva, J., Lizek, A. J., Richardson, S. J., et al. (2012). Exposure to glyphosate- and/or Mn/Zn-ethylene-bis-dithiocarbamate-containing pesticides leads to degeneration of γ -aminobutyric acid and dopamine neurons in *Caenorhabditis elegans*. *Neurotox. Res.* 21, 281–290. doi: 10.1007/s12640-011-9274-7
- Neumann, M., Sampathu, D. M., Kwong, L. K., Truax, A. C., Micsenyi, M. C., Chou, T. T., et al. (2006). Ubiquitinated TDP-43 in frontotemporal lobar degeneration and amyotrophic lateral sclerosis. *Science* 314, 130–133. doi: 10.1126/science.1134108
- Novarino, G., Fenstermaker, A. G., Zaki, M. S., Hofree, M., Silhavy, J. L., Heiberg, A. D., et al. (2014). Exome sequencing links corticospinal motor neuron disease to common neurodegenerative disorders. *Science* 343, 506–511. doi: 10.1126/science.1247363
- Nussbaum-Krammer, C. I., Park, K.-W., Li, L., Melki, R., and Morimoto, R. I. (2013). Spreading of a prion domain from cell-to-cell by vesicular transport in *Caenorhabditis elegans*. *PLoS Genet.* 9:e1003351. doi: 10.1371/journal.pgen.1003351
- Oeda, T., Shimohama, S., Kitagawa, N., Kohno, R., Imura, T., Shibasaki, H., et al. (2001). Oxidative stress causes abnormal accumulation of familial amyotrophic lateral sclerosis-related mutant SOD1 in transgenic *Caenorhabditis elegans*. *Hum. Mol. Genet.* 10, 2013–2023. doi: 10.1093/hmg/10.19.2013
- Oikonomou, G., and Shaham, S. (2011). The glia of *Caenorhabditis elegans*. *Glia* 59, 1253–1263. doi: 10.1002/glia.21084
- O'Reilly, L. P., Luke, C. J., Perlmutter, D. H., Silverman, G. A., and Pak, S. C. (2013). *C. elegans* in high-throughput drug discovery. *Adv. Drug Deliv. Rev.* doi: 10.1016/j.addr.2013.12.001. [Epub ahead of print].
- Parisi, C., Arisi, I., D'Ambrosi, N., Storti, A. E., Brandi, R., D'Onofrio, M., et al. (2013). Dysregulated microRNAs in amyotrophic lateral sclerosis microglia modulate genes linked to neuroinflammation. *Cell Death Dis.* 4, e959. doi: 10.1038/cddis.2013.491
- Pasinelli, P., Houseweart, M. K., Brown, R. H., and Cleveland, D. W. (2000). Caspase-1 and -3 are sequentially activated in motor neuron death in Cu,Zn superoxide dismutase-mediated familial amyotrophic lateral sclerosis. *Proc. Natl. Acad. Sci. U.S.A.* 97, 13901–13906. doi: 10.1073/pnas.240305897
- Pickles, S., and Vande Velde, C. (2012). Misfolded SOD1 and ALS: zeroing in on mitochondria. *Amyotroph. Lateral Scler.* 13, 333–340. doi: 10.3109/17482968.2012.648645
- Polymenidou, M., and Cleveland, D. W. (2011). The seeds of neurodegeneration: prion-like spreading in ALS. *Cell* 147, 498–508. doi: 10.1016/j.cell.2011.10.011
- Renton, A. E., Chiò, A., and Traynor, B. J. (2014). State of play in amyotrophic lateral sclerosis genetics. *Nat. Neurosci.* 17, 17–23. doi: 10.1038/nn.3584
- Renton, A. E., Majounie, E., Waite, A., Simón-Sánchez, J., Rollinson, S., Gibbs, J. R., et al. (2011). A hexanucleotide repeat expansion in C9ORF72 is the cause of chromosome 9p21-linked ALS-FTD. *Neuron* 72, 257–268. doi: 10.1016/j.neuron.2011.09.010
- Ringholz, G. M., Appel, S. H., Bradshaw, M., Cooke, N. A., Mosnik, D. M., and Schulz, P. E. (2005). Prevalence and patterns of cognitive impairment in sporadic ALS. *Neurology* 65, 586–590. doi: 10.1212/01.wnl.0000172911.39167.b6
- Robberecht, W., and Philips, T. (2013). The changing scene of amyotrophic lateral sclerosis. *Nat. Rev. Neurosci.* 14, 248–264. doi: 10.1038/nrn3430
- Rodriguez, M., Snoek, L. B., De Bono, M., and Kammenga, J. E. (2013). Worms under stress: *C. elegans* stress response and its relevance to complex human disease and aging. *Trends Genet.* 29, 367–374. doi: 10.1016/j.tig.2013.01.010
- Rosen, D. R., Siddique, T., Patterson, D., Figlewicz, D. A., Sapp, P., Hentati, A., et al. (1993). Mutations in Cu/Zn superoxide dismutase gene are associated with familial amyotrophic lateral sclerosis. *Nature* 362, 59–62. doi: 10.1038/362059a0
- Saccon, R. A., Bunton-Stasyshyn, R. K. A., Fisher, E. M. C., and Fratta, P. (2013). Is SOD1 loss of function involved in amyotrophic lateral sclerosis? *Brain* 136, 2342–2358. doi: 10.1093/brain/awt097
- Sasayama, H., Shimamura, M., Tokuda, T., Azuma, Y., Yoshida, T., Mizuno, T., et al. (2012). Knockdown of the Drosophila fused in sarcoma (FUS) homologue causes deficient locomotive behavior and shortening of motoneuron terminal branches. *PLoS ONE* 7:e39483. doi: 10.1371/journal.pone.0039483
- Sato, M., Sato, K., Liou, W., Pant, S., Harada, A., and Grant, B. D. (2008). Regulation of endocytic recycling by *C. elegans* Rab35 and its regulator RME-4, a coated-pit protein. *EMBO J.* 27, 1183–1196. doi: 10.1038/emboj.2008.54
- Shatunov, A., Mok, K., Newhouse, S., Weale, M. E., Smith, B., Vance, C., et al. (2010). Chromosome 9p21 in sporadic amyotrophic lateral sclerosis in the UK and seven other countries: a genome-wide association study. *Lancet Neurol.* 9, 986–994. doi: 10.1016/S1474-4422(10)70197-6
- Shaye, D. D., and Greenwald, I. (2011). OrthoList: a compendium of *C. elegans* genes with human orthologs. *PLoS ONE* 6:e20085. doi: 10.1371/journal.pone.0020085
- Singh, V., and Aballay, A. (2009). Regulation of DAF-16-mediated innate immunity in *Caenorhabditis elegans*. *J. Biol. Chem.* 284, 35580–35587. doi: 10.1074/jbc.M109.060905
- Sleigh, J. N., Buckingham, S. D., Esmaeili, B., Viswanathan, M., Cuppen, E., Westlund, B. M., et al. (2011). A novel *Caenorhabditis elegans* allele, smn-1(cb131), mimicking a mild form of spinal muscular atrophy, provides a convenient drug screening platform highlighting new and pre-approved compounds. *Hum. Mol. Genet.* 20, 245–260. doi: 10.1093/hmg/ddq459
- Sreedharan, J., Blair, I. P., Tripathi, V. B., Hu, X., Vance, C., Rogelj, B., et al. (2008). TDP-43 mutations in familial and sporadic amyotrophic lateral sclerosis. *Science* 319, 1668–1672. doi: 10.1126/science.1154584
- Sreedharan, J., and Brown, R. H. (2013). Amyotrophic lateral sclerosis: problems and prospects. *Ann. Neurol.* 74, 309–316. doi: 10.1002/ana.2401
- Sun, Y., Yang, P., Zhang, Y., Bao, X., Li, J., Hou, W., et al. (2011). A genome-wide RNAi screen identifies genes regulating the formation of P bodies in *C. elegans* and their functions in NMD and RNAi. *Protein Cell* 2, 918–939. doi: 10.1007/s13238-011-1119-x
- Swarup, V., Phaneuf, D., Bareil, C., Robertson, J., Rouleau, G. A., Kriz, J., et al. (2011). Pathological hallmarks of amyotrophic lateral sclerosis/frontotemporal lobar degeneration in transgenic mice produced with TDP-43 genomic fragments. *Brain* 134, 2610–2626. doi: 10.1093/brain/awr159
- Tauffmanberger, A., Chitramuthu, B. P., Bateman, A., Bennett, H. P. J., and Parker, J. A. (2013a). Reduction of polyglutamine toxicity by TDP-43, FUS and progranulin in Huntington's disease models. *Hum. Mol. Genet.* 22, 782–794. doi: 10.1093/hmg/ddr485
- Tauffmanberger, A., Julien, C., and Parker, J. A. (2013b). Evaluation of longevity enhancing compounds against transactive response DNA-binding protein-43 neuronal toxicity. *Neurobiol. Aging* 34, 2175–2182. doi: 10.1016/j.neurobiolaging.2013.03.014
- Taylor, R. C., and Dillin, A. (2013). XBP-1 is a cell-nonautonomous regulator of stress resistance and longevity. *Cell* 153, 1435–1447. doi: 10.1016/j.cell.2013.05.042
- Therrien, M., Rouleau, G. A., Dion, P. A., and Parker, J. A. (2013). Deletion of C9ORF72 results in motor neuron degeneration and stress sensitivity in *C. elegans*. *PLoS ONE* 8:e83450. doi: 10.1371/journal.pone.0083450
- Turner, M. R., Bowser, R., Bruijn, L., Dupuis, L., Ludolph, A., McGrath, M., et al. (2013a). Mechanisms, models and biomarkers in amyotrophic lateral sclerosis. *Amyotroph. Lateral Scler. Frontotemporal Degener.* 14(Suppl. 1), 19–32. doi: 10.3109/21678421.2013.778554
- Turner, M. R., Hardiman, O., Benatar, M., Brooks, B. R., Chiò, A., de Carvalho, M., et al. (2013b). Controversies and priorities in amyotrophic lateral sclerosis. *Lancet Neurol.* 12, 310–322. doi: 10.1016/S1474-4422(13)70036-X
- Updike, D., and Strome, S. (2010). P granule assembly and function in *Caenorhabditis elegans* germ cells. *J. Androl.* 31, 53–60. doi: 10.2164/jandrol.109.008292
- Vaccaro, A., Patten, S. A., Aggad, D., Julien, C., Maios, C., Kabashi, E., et al. (2013). Pharmacological reduction of ER stress protects against TDP-43 neuronal toxicity in vivo. *Neurobiol. Dis.* 55, 64–75. doi: 10.1016/j.nbd.2013.03.015
- Vaccaro, A., Patten, S. A., Ciura, S., Maios, C., Therrien, M., Drapeau, P., et al. (2012a). Methylene blue protects against TDP-43 and FUS neuronal toxicity in *C. elegans* and *D. rerio*. *PLoS ONE* 7:e42117. doi: 10.1371/journal.pone.0042117
- Vaccaro, A., Tauffmanberger, A., Aggad, D., Rouleau, G., Drapeau, P., and Parker, J. A. (2012b). Mutant TDP-43 and FUS cause age-dependent paralysis and neurodegeneration in *C. elegans*. *PLoS ONE* 7:e31321. doi: 10.1371/journal.pone.0031321
- Vaccaro, A., Tauffmanberger, A., Ash, P. E. A., Carlomagno, Y., Petrucelli, L., and Parker, J. A. (2012c). TDP-1/TDP-43 regulates stress signaling and age-dependent proteotoxicity in *Caenorhabditis elegans*. *PLoS Genet.* 8:e1002806. doi: 10.1371/journal.pgen.1002806

- Valori, C. F., Brambilla, L., Martorana, F., and Rossi, D. (2013). The multifaceted role of glial cells in amyotrophic lateral sclerosis. *Cell. Mol. Life Sci.* 71, 287–297. doi: 10.1007/s00018-013-1429-7
- Vance, C., Al-Chalabi, A., Ruddy, D., Smith, B. N., Hu, X., Sreedharan, J., et al. (2006). Familial amyotrophic lateral sclerosis with frontotemporal dementia is linked to a locus on chromosome 9p13.2–21.3. *Brain* 129, 868–876. doi: 10.1093/brain/awl030
- Vance, C., Rogelj, B., Hortobágyi, T., De Vos, K. J., Nishimura, A. L., Sreedharan, J., et al. (2009). Mutations in FUS, an RNA processing protein, cause familial amyotrophic lateral sclerosis type 6. *Science* 323, 1208–1211. doi: 10.1126/science.1165942
- Vance, C., Scotter, E. L., Nishimura, A. L., Troakes, C., Mitchell, J. C., Kathe, C., et al. (2013). ALS mutant FUS disrupts nuclear localization and sequesters wild-type FUS within cytoplasmic stress granules. *Hum. Mol. Genet.* 22, 2676–2688. doi: 10.1093/hmg/ddt117
- Vanden Broeck, L., Callaerts, P., and Dermaut, B. (2014). TDP-43-mediated neurodegeneration: towards a loss-of-function hypothesis? *Trends Mol. Med.* 20, 66–71. doi: 10.1016/j.molmed.2013.11.003
- van Es, M. A., Veldink, J. H., Saris, C. G. J., Blauw, H. M., van Vught, P. W. J., Birve, A., et al. (2009). Genome-wide association study identifies 19p13.3 (UNC13A) and 9p21.2 as susceptibility loci for sporadic amyotrophic lateral sclerosis. *Nat. Genet.* 41, 1083–1087. doi: 10.1038/ng.442
- Van Hoecke, A., Schoonaert, L., Lemmens, R., Timmers, M., Staats, K. A., Laird, A. S., et al. (2012). EPHA4 is a disease modifier of amyotrophic lateral sclerosis in animal models and in humans. *Nat. Med.* 18, 1418–1422. doi: 10.1038/nm.2901
- Van Langenhove, T., van der Zee, J., and Van Broeckhoven, C. (2012). The molecular basis of the frontotemporal lobar degeneration-amyotrophic lateral sclerosis spectrum. *Ann. Med.* 44, 817–828. doi: 10.3109/07853890.2012.665471
- van Oosten-Hawle, P., Porter, R. S., and Morimoto, R. I. (2013). Regulation of organismal proteostasis by transcellular chaperone signaling. *Cell* 153, 1366–1378. doi: 10.1016/j.cell.2013.05.015
- Van Raamsdonk, J. M., and Hekimi, S. (2012). Superoxide dismutase is dispensable for normal animal lifespan. *Proc. Natl. Acad. Sci. U.S.A.* 109, 5785–5790. doi: 10.1073/pnas.1116158109
- Verbeeck, C., Deng, Q., DeJesus-Hernandez, M., Taylor, G., Ceballos-Diaz, C., Kocerha, J., et al. (2012). Expression of Fused in sarcoma mutations in mice recapitulates the neuropathology of FUS proteinopathies and provides insight into disease pathogenesis. *Mol. Neurodegener.* 7:53. doi: 10.1186/1750-1326-7-53
- Wang, J., Farr, G. W., Hall, D. H., Li, F., Furtak, K., Dreier, L., et al. (2009). An ALS-linked mutant SOD1 produces a locomotor defect associated with aggregation and synaptic dysfunction when expressed in neurons of *Caenorhabditis elegans*. *PLoS Genet* 5:e1000350. doi: 10.1371/journal.pgen.1000350
- Wang, J.-W., Brent, J. R., Tomlinson, A., Shneider, N. A., and McCabe, B. D. (2011a). The ALS-associated proteins FUS and TDP-43 function together to affect *Drosophila* locomotion and life span. *J. Clin. Invest.* 121, 4118–4126. doi: 10.1172/JCI57883
- Wang, L.-C., Chen, K.-Y., Pan, H., Wu, C.-C., Chen, P.-H., Liao, Y.-T., et al. (2011b). Muscleblind participates in RNA toxicity of expanded CAG and CUG repeats in *Caenorhabditis elegans*. *Cell. Mol. Life Sci.* 68, 1255–1267. doi: 10.1007/s00018-010-0522-4
- Warren, J. D., Rohrer, J. D., and Rossor, M. N. (2013). Clinical review. Frontotemporal dementia. *BMJ* 347, f4827. doi: 10.1136/bmj.f4827
- Woulfe, J., Gray, D. A., and Mackenzie, I. R. A. (2010). FUS-immunoreactive intranuclear inclusions in neurodegenerative disease. *Brain Pathol.* 20, 589–597. doi: 10.1111/j.1750-3639.2009.00337.x
- Xi, Z., Zinman, L., Moreno, D., Schymick, J., Liang, Y., Sato, C., et al. (2013). Hypermethylation of the CpG island near the G4C2 repeat in ALS with a C9orf72 expansion. *Am. J. Hum. Genet.* 92, 981–989. doi: 10.1016/j.ajhg.2013.04.017
- Xu, Y.-F., Gendron, T. F., Zhang, Y.-J., Lin, W.-L., D'Alton, S., Sheng, H., et al. (2010). Wild-type human TDP-43 expression causes TDP-43 phosphorylation, mitochondrial aggregation, motor deficits, and early mortality in transgenic mice. *J. Neurosci.* 30, 10851–10859. doi: 10.1523/JNEUROSCI.1630-10.2010
- Xu, Z., Poidevin, M., Li, X., Li, Y., Shu, L., Nelson, D. L., et al. (2013). Expanded GGGGCC repeat RNA associated with amyotrophic lateral sclerosis and frontotemporal dementia causes neurodegeneration. *Proc. Natl. Acad. Sci. U.S.A.* 110, 7778–7783. doi: 10.1073/pnas.1219643110
- Yanase, S., Onodera, A., Tedesco, P., Johnson, T. E., and Ishii, N. (2009). SOD-1 deletions in *Caenorhabditis elegans* alter the localization of intracellular reactive oxygen species and show molecular compensation. *J. Gerontol. A Bio. Sci. Med. Sci.* 64, 530–539. doi: 10.1093/gerona/glp020
- Zhang, D., Iyer, L. M., He, F., and Aravind, L. (2012a). Discovery of Novel DENN Proteins: implications for the evolution of eukaryotic intracellular membrane structures and human disease. *Front. Genet.* 3:283. doi: 10.3389/fgene.2012.00283
- Zhang, T., Hwang, H. Y., Hao, H., Talbot, C., and Wang, J. (2012b). *Caenorhabditis elegans* RNA-processing protein TDP-1 regulates protein homeostasis and life span. *J. Biol. Chem.* 287, 8371–8382. doi: 10.1074/jbc.M111.311977
- Zhang, T., Mullane, P. C., Periz, G., and Wang, J. (2011). TDP-43 neurotoxicity and protein aggregation modulated by heat shock factor and insulin/IGF-1 signaling. *Hum. Mol. Genet.* 20, 1952–1965. doi: 10.1093/hmg/ddr076
- Zhao, J., Matthies, D. S., Botzolakis, E. J., Macdonald, R. L., Blakely, R. D., and Hedera, P. (2008). Hereditary spastic paraplegia-associated mutations in the NIPA1 gene and its *Caenorhabditis elegans* homolog trigger neural degeneration *in vitro* and *in vivo* through a gain-of-function mechanism. *J. Neurosci.* 28, 13938–13951. doi: 10.1523/JNEUROSCI.4668-08.2008

Conflict of Interest Statement: The authors declare that the research was conducted in the absence of any commercial or financial relationships that could be construed as a potential conflict of interest.

Received: 14 February 2014; paper pending published: 28 February 2014; accepted: 30 March 2014; published online: 17 April 2014.

Citation: Therrien M and Parker JA (2014) Worming forward: amyotrophic lateral sclerosis toxicity mechanisms and genetic interactions in *Caenorhabditis elegans*. *Front. Genet.* 5:85. doi: 10.3389/fgene.2014.00085

This article was submitted to *Genetics of Aging*, a section of the journal *Frontiers in Genetics*.

Copyright © 2014 Therrien and Parker. This is an open-access article distributed under the terms of the Creative Commons Attribution License (CC BY). The use, distribution or reproduction in other forums is permitted, provided the original author(s) or licensor are credited and that the original publication in this journal is cited, in accordance with accepted academic practice. No use, distribution or reproduction is permitted which does not comply with these terms.

TDP-43 Toxicity Proceeds via Calcium Dysregulation and Necrosis in Aging *Caenorhabditis elegans* Motor Neurons

Dina Aggad,¹ Julie Vérièpe,^{1,2} Arnaud Tauffenberger,^{1,2} and  J. Alex Parker^{1,2,3}

¹CRCHUM, Départements de ²Pathologie et Biologie Cellulaire, and ³Neurosciences, Université de Montréal, Montréal, Québec H1Y 3L1, Canada

Amyotrophic lateral sclerosis (ALS) is a heterogeneous disease with either sporadic or genetic origins characterized by the progressive degeneration of motor neurons. At the cellular level, ALS neurons show protein misfolding and aggregation phenotypes. Transactive response DNA-binding protein 43 (TDP-43) has recently been shown to be associated with ALS, but the early pathophysiological deficits causing impairment in motor function are unknown. Here we used *Caenorhabditis elegans* expressing mutant TDP-43^{A315T} in motor neurons and explored the potential influences of calcium (Ca²⁺). Using chemical and genetic approaches to manipulate the release of endoplasmic reticulum (ER) Ca²⁺ stores, we observed that the reduction of intracellular Ca²⁺ ([Ca²⁺]_i) rescued age-dependent paralysis and prevented the neurodegeneration of GABAergic motor neurons. Our data implicate elevated [Ca²⁺]_i as a driver of TDP-43-mediated neuronal toxicity. Furthermore, we discovered that neuronal degeneration is independent of the executioner caspase CED-3, but instead requires the activity of the Ca²⁺-regulated calpain protease TRA-3, and the aspartyl protease ASP-4. Finally, chemically blocking protease activity protected against mutant TDP-43^{A315T}-associated neuronal toxicity. This work both underscores the potential of the *C. elegans* system to identify key targets for therapeutic intervention and suggests that a focused effort to regulate ER Ca²⁺ release and necrosis-like degeneration consequent to neuronal injury may be of clinical importance.

Key words: ALS; *C. elegans*; calcium; ER; necrosis; TDP-43

Introduction

Amyotrophic lateral sclerosis (ALS) is a fatal neurodegenerative disease characterized by the selective loss of both upper and lower motor neurons in the cortex and spinal cord (Wijesekera and Leigh, 2009). ALS is an age-dependent, rapidly progressive disease with life expectancy typically being between 2 and 5 years after onset. Thanks to recent genetic advances, causative mutations for ALS have been discovered in over a dozen genes (Renton et al., 2014), including one encoding transactive response DNA-binding protein 43 (TDP-43; Kabashi et al., 2008) among others.

Evidence is mounting that pathways regulating protein degradation may influence ALS pathogenesis (Blokhuys et al., 2013). We previously reported that mutant TDP-43^{A315T} proteins expressed in *Caenorhabditis elegans* motor neurons are susceptible to misfolding, leading to insolubility, aggregation (Vaccaro et al., 2012a), and activation of the endoplasmic reticulum (ER) unfolded protein response (UPR^{ER}; Vaccaro et al., 2012b, 2013).

Induction of the UPR^{ER} by mutant TDP-43 suggests that the capacity of the ER to properly fold proteins may be exceeded, leading to cellular dysfunction and death (Walker and Atkin, 2011).

The ER constitutes a Ca²⁺ store whose uptake and release are extensively regulated to maintain cellular Ca²⁺ homeostasis, and disrupted ER function can induce Ca²⁺ depletion (Burdakov and Verkhratsky, 2006). Altered Ca²⁺ homeostasis has been investigated as a mechanism to distinguish motor neurons that are vulnerable or resistant to degeneration in ALS (Palecek et al., 1999; Vanselow and Keller, 2000). Indeed, ALS-vulnerable motor neurons in mice display Ca²⁺ buffering capacities that are five to six times lower compared with those found in ALS-resistant oculomotor neurons (Vanselow and Keller, 2000), while a more recent study has shown that altered Ca²⁺ buffering may be a risk factor for SOD-1 toxicity (von Lewinski et al., 2008).

We investigated the role of cellular Ca²⁺ balance in our TDP-43 models to learn more about the mechanisms of Ca²⁺-mediated cellular demise. We report that a null mutation in calreticulin (CRT-1), a central regulator of ER Ca²⁺ homeostasis, suppresses both paralysis and the neurodegeneration caused by mutant TDP-43^{A315T} in motor neurons. Furthermore, deletion of the Ca²⁺ binding ER protein calnexin (CNX-1), the ER Ca²⁺ release channels UNC-68 (ryanodine receptor), or ITR-1 (inositol 1,4,5 triphosphate receptor) suppressed TDP-43 toxicity. Consistently, pharmacological manipulations modulating ER Ca²⁺ release and/or uptake suppressed TDP-43 toxicity. Downstream from perturbed Ca²⁺ homeostasis, we discovered that mutations in the Ca²⁺-regulated calpain protease TRA-3 and aspartyl protease ASP-4 also suppressed TDP-43 toxicity.

Received June 12, 2013; revised July 24, 2014; accepted July 28, 2014.

Author contributions: D.A., J.V., A.T., and J.A.P. designed research; D.A. and J.V. performed research; A.T. contributed unpublished reagents/analytic tools; D.A., J.V., and J.A.P. analyzed data; D.A. and J.A.P. wrote the paper.

Some strains were provided by the *Caenorhabditis* Genetics Center, which is funded by the National Institutes of Health Office of Research Infrastructure Programs (P40 OD010440). This research was supported by the CHUM Foundation, the ALS Society of Canada, the Canadian Institutes of Health Research, the Fonds de Recherche Santé Québec, the Muscular Dystrophy Association (U.S.), and the Congressionally Directed Medical Research Program Amyotrophic Lateral Sclerosis Research Program (U.S.), and a Canadian Institutes of Health Research New Investigator Award to J.A.P. We thank S. Peyrard for technical help.

Correspondence should be addressed to J. Alex Parker, CRCHUM, 900 St-Denis, Tour Viger, R09.440, Montreal, QC H2X 0A9, Canada. E-mail: ja.parker@umontreal.ca.

DOI:10.1523/JNEUROSCI.2495-13.2014

Copyright © 2014 the authors 0270-6474/14/3412093-11\$15.00/0

Our findings suggest that the regulation, and possibly release, of ER Ca^{2+} stores are required for neurotoxicity of TDP-43 in *C. elegans*. It is generally believed that caspase-driven neuronal apoptosis is an underlying pathogenic mechanism in many late-onset neurodegenerative diseases including ALS (Martin, 1999), but the executioner caspase CED-3 is dispensable for neurodegeneration in our TDP-43 model. Instead, the involvement of calpain and aspartyl proteases is more similar to necrosis-mediated cell death (Syntichaki et al., 2002). We propose that misfolded mutant TDP-43 increases $[\text{Ca}^{2+}]_i$ by disrupting ER function and activates calpain proteases, which in turn activates killer aspartyl proteases, leading to cell destruction.

Materials and Methods

C. elegans strains and methods. Standard culturing and genetic methods were used (Stiernagle, 2006). Animals were maintained at 20°C unless otherwise indicated. Unless otherwise stated, the strains used in this study were obtained from the Caenorhabditis Genetics Center (University of Minnesota, Minneapolis, MN) and include the following: *asp-4(ok2693)*, *ced-3(ok2734)*, *cnx-1(nr2009)*, *cnx-1(nr2010)*, *crt-1(bz30)*, *crt-1(jh101)*, *itr-1(sa73)*, *kbIs7 [nhx-2p::rde-1 + rol-6(su1006)]*, *kzIs20[pDM#715(hlh-1p::rde-1) + pTG95(sur-5p::nls::GFP)]*, *oxIs12 [unc-47p::GFP + lin-15(+)]*, *rde-1(ne219)*, *sid-1(pk3321)*, *tra-3(ok2207)*, *uIs69 [pCFJ90(myo-2p::mCherry) + unc-119p::sid-1]*, and *unc-68(e540)*. Genetic crosses generated transgenic/mutant combinations, and the presence of transgenes and mutations was confirmed by PCR, visible markers, sequencing, or a combination thereof.

Transgenic lines expressing mutant TDP-43^{A315T}, wild-type TDP-43 (TDP-43^{WT}), *unc-47p::GFP*; TDP-43^{A315T}, and *unc-47p::GFP*; TDP-43^{WT} were previously described (Vaccaro et al., 2012a) and created as follows: human cDNAs for TDP-43^{WT} and TDP-43^{A315T} (a gift from Dr. Guy Rouleau, McGill University, Montreal, QC, Canada) were amplified by PCR and cloned into the Gateway vector pDONR221 following the manufacturer's protocol (Invitrogen). Multisite Gateway recombination was performed with the pDONR TDP-43 clones along with clones containing the *unc-47* promoter (a gift from Dr. Erik Jorgensen, University of Utah, Salt Lake City, UT; and Dr. Marc Hammarlund, Yale University, New Haven, CT), the *unc-54* 3' UTR plasmid pCM5.37 (Addgene plasmid 17253; a gift from Dr. Geraldine Seydoux, Johns Hopkins University, Baltimore, MD), and the destination vector pCFJ150 (Addgene plasmid 19329; a gift from Dr. Erik Jorgensen, University of Utah) to create *unc-47p::TDP-43* expression vectors. Transgenic lines were created by microinjection of *unc-119(ed3)* worms, multiple lines were generated, and strains behaving similarly were kept for further analysis. Transgenes were integrated by UV irradiation, and lines were outcrossed to wild-type N2 worms five times before use. Several strains showing comparable phenotypes and transgene expression levels were kept and the strains used in this study include the following: *xqIs132[unc-47p::TDP-43^{WT}; unc-119(+)]* and *xqIs133[unc-47p::TDP-43^{A315T}; unc-119(+)]*.

Pharmacological treatment. All chemicals were obtained from Sigma-Aldrich. Dantrolene and thapsigargin were dissolved in DMSO and added to agar plate to final concentrations of 10 μM and 3 $\mu\text{g}/\text{ml}$, respectively. EGTA was dissolved in 1N NaOH and was added to agar plates to a final concentration of 0.5 mM. MDL-28170 was dissolved in DMSO and added to agar plate to a final concentration of 20 μM .

Paralysis assay. Worms were grown at 20°C on standard Nematode Growth Media (NGM) plates with or without compounds (30 animals/plate, by triplicates) and scored daily for movement. Animals were scored as paralyzed if they failed to move upon prodding with a worm pick. Failure to move their head to touch and the absence of pharyngeal pumping was scored as dead. Statistical analysis was performed using GraphPad Prism software (log-rank Mantel–Cox test).

Neurodegeneration assay. Worms (*unc-47p::GFP*; TDP-43^{A315T} or *unc-47p::GFP*; TDP-43^{WT}, with or without additional mutations listed above) were grown at 20°C on standard NGM plates with or without compounds. Young adult worms were transferred onto seeded NGM plates (with or without compounds), and were selected at days 1, 5, and 9 of adulthood (100 animals/treatment). Live worms were placed on a

2% agarose pad containing 5 mM levamisole in M9 medium to immobilize the worms. Worms were observed under fluorescence microscopy (Leica 6000 microscope) and scored for gaps or breaks in the processes of GABAergic neurons. The mean and SEM were calculated, and ANOVA with Bonferroni correction were used for statistical analyses.

RNA interference experiments. RNA interference (RNAi)-treated strains were fed *Escherichia coli* (HT115) containing an empty vector (EV) or an RNAi clone corresponding to the gene of interest indicated above. All RNAi clones were from the ORFeome RNAi library (Open Biosystems). RNAi experiments were performed at 20°C. Worms were grown on NGM enriched with 1 mM isopropyl- β -D-thiogalactopyranoside. All RNAi paralysis tests were performed using a TDP-43^{A315T}; *unc-47p::GFP* in conjunction with the appropriate mutation and transgenes for tissue-specific silencing in neurons, intestine, or muscle cells based on strains TU3401, VP303, or NR350, respectively. To minimize developmental effects, L4 worms were grown on plates with RNAi bacteria and assayed for paralysis as adults. Worms were transferred every 2 d.

Western blot analysis. Synchronized populations of worms expressing TDP-43 were grown at 20°C on standard NGM plates with or without compounds (15 plates/treatment). Immunoblot analysis of protein levels was performed on whole-animal extracts prepared by washing animals in M9 medium to remove adherent bacteria. The pellets were placed at -80°C overnight and homogenized in 1 ml/g RIPA buffer (150 mM NaCl, 50 mM Tris, pH 7.4, 1% Triton X-100, 0.1% SDS, 1% sodium deoxycholate) plus 0.1% protease inhibitors (10 mg/ml leupeptin, 10 mg/ml pepstatin A, 10 mg/ml chymostatin; 1:1000). Pellets were sonicated and centrifuged at $16,000 \times g$. Supernatants were collected and were saved as the total fraction. Protein concentrations were determined by the Quick Start Bradford Protein Assay (Bio-Rad). Supernatants, 50 $\mu\text{g}/\text{well}$, were subjected to SDS-PAGE (10%) and transferred to nitrocellulose membranes (Bio-Rad). The immunoblotting analyses were performed using the following antibodies: rabbit anti-TDP-43 (1:1000; Proteintech) and mouse anti-actin (1:20,000 for worms; MP Biomedicals). Proteins were visualized using peroxidase-conjugated secondary antibodies and ECL Western Blotting Substrate (Thermo Scientific). Densitometry was performed with Photoshop (Adobe).

Results

Genetic manipulation of $[\text{Ca}^{2+}]$ suppresses TDP-43 toxicity in motor neurons

CRT-1 is a Ca^{2+} binding/storing protein of the ER that serves both as a molecular chaperone and as a central regulator of Ca^{2+} homeostasis (Michalak et al., 1999). Worms expressing mutant TDP-43 in their motor neurons show age-dependent motility defects, leading to paralysis and neurodegeneration (Vaccaro et al., 2012a). To investigate the role of Ca^{2+} balance in TDP-43 neuronal toxicity, we constructed *crt-1(bz30)*; TDP-43^{A315T} and *crt-1(jh101)*; TDP-43^{A315T} strains, and scored them for paralysis. We observed a significant reduction in the rate of paralysis for *crt-1(bz30)*; TDP-43^{A315T} and *crt-1(jh101)*; TDP-43^{A315T} animals compared with control TDP-43^{A315T} transgenics (Fig. 1A). Focusing on *crt-1(bz30)*; TDP-43^{A315T}, we also observed a significant rate of motor neuron degeneration compared with control TDP-43^{A315T} transgenics (Fig. 1B).

In the ER, calreticulin works in conjunction with CNX-1 to execute chaperone functions and mediate cellular Ca^{2+} homeostasis (Krause and Michalak, 1997). Given the functional and structural similarities between the two proteins, we tested whether calnexin, encoded by *cnx-1* in *C. elegans*, also influenced TDP-43 toxicity. We observed that introduction of the loss of function mutations *cnx-1(nr2009)* or *cnx-1(nr2010)* into mutant TDP-43^{A315T} transgenics led to a significant decrease in paralysis compared with control TDP-43^{A315T} transgenics (Fig. 1A). Focusing on *cnx-1(nr2010)*; TDP-43^{A315T}, we also observed a sig-

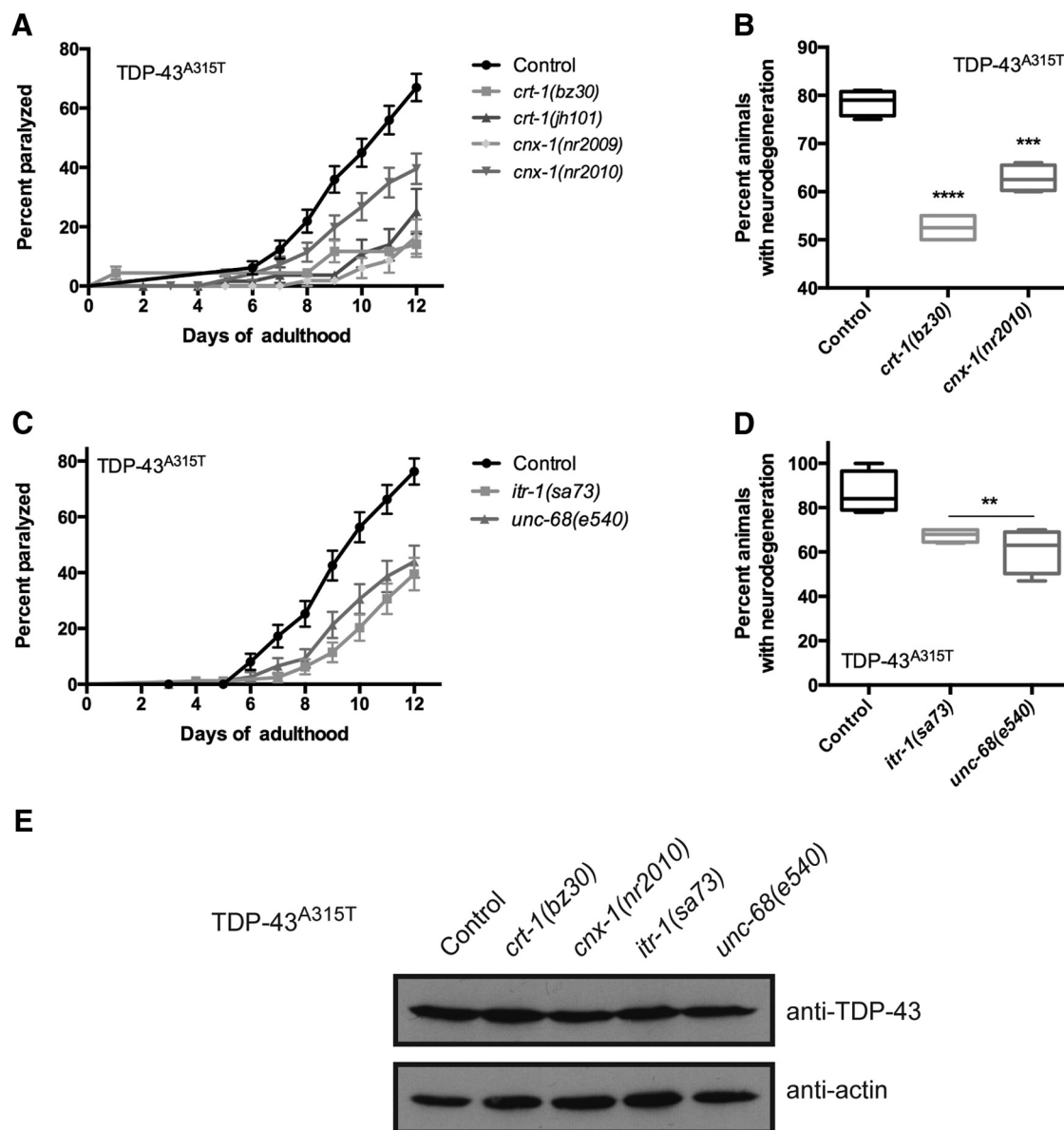


Figure 1. Genes regulating ER calcium release promote TDP-43 neuronal toxicity. **A**, Null mutations in *cnx-1* or *crt-1* suppress age-dependent paralysis caused by TDP-43^{A315T} compared with transgenic TDP-43^{A315T} controls. $p < 0.0001$ for TDP-43^{A315T}; *cnx-1(nr2009)* versus TDP-43^{A315T}; $p = 0.0002$ for TDP-43^{A315T}; *cnx-1(nr2010)* versus TDP-43^{A315T}; $p < 0.0001$ for TDP-43^{A315T}; *crt-1(bz30)* versus TDP-43^{A315T}; $p < 0.0001$ for TDP-43^{A315T}; *crt-1(jh101)* versus TDP-43^{A315T}. TDP-43^{A315T}, $n = 114$; TDP-43^{A315T}; *cnx-1(nr2009)*, $n = 76$; TDP-43^{A315T}; *cnx-1(nr2010)*, $n = 98$; TDP-43^{A315T}; *crt-1(bz30)*, $n = 90$; and TDP-43^{A315T}; *crt-1(jh101)*, $n = 63$. **B**, Mutations in *cnx-1* or *crt-1* reduce age-dependent neurodegeneration in TDP-43^{A315T} transgenics compared with TDP-43^{A315T} control animals. $***p < 0.001$ versus TDP-43^{A315T} at day 9; $****p < 0.0001$ versus TDP-43^{A315T} at day 9. **C**, Null mutations in *unc-68* and *itr-1* reduce TDP-43^{A315T}-mediated paralysis compared with control TDP-43^{A315T} transgenics. $p < 0.0001$ for either for TDP-43^{A315T}; *unc-68(e540)* or for TDP-43^{A315T}; *itr-1(sa73)* versus TDP-43^{A315T}. TDP-43^{A315T}, $n = 90$; TDP-43^{A315T}; *itr-1(sa73)*, $n = 88$; and TDP-43^{A315T}; *unc-68(e540)*, $n = 84$. **D**, Degeneration of motor neurons is reduced in adult day 9 TDP-43^{A315T} transgenics compared with controls. $**p < 0.01$ versus TDP-43^{A315T} at day 9. **E**, Western blotting with a human anti-TDP-43 antibody revealed comparable levels of protein expression in all strains.

nificant decrease of motor neuron degeneration compared with control TDP-43^{A315T} transgenics (Fig. 1B).

To complete the genetic investigation of cellular Ca^{2+} balance, we tested the following two other genes involved in ER regulation of $[Ca^{2+}]_i$: the ER Ca^{2+} release channel inositol triphosphate receptor channel InsP3R, encoded by *itr-1* (Dal Santo et al., 1999), and the ER Ca^{2+} release channel ryanodine receptor channel RyR, encoded by *unc-68* (Maryon et al., 1996). We then investigated the effects of mutations in the InsP3R and RyR genes on TDP-43^{A315T}-mediated paralysis and motor neuron degeneration. Similar to the disruption of calnexin and calreticulin function, *itr-1(sa73)*; TDP-43^{A315T} and *unc-68(e540)*; TDP-43^{A315T} strains displayed significantly reduced paralysis

and motor neuron degeneration phenotypes compared with TDP-43^{A315T} controls (Fig. 1C,D). To confirm that the suppression of TDP-43^{A315T} neuronal toxicity was not due to transgene effects, we quantified the level of TDP-43 protein expression by immunoblotting and observed no difference in protein levels for TDP-43 in combination with any of the mutations (Fig. 1E).

Pharmacological modulation of $[Ca^{2+}]_i$ regulates TDP-43^{A315T} toxicity in motor neurons

To confirm that altering $[Ca^{2+}]_i$ levels in turn regulates TDP-43 toxicity, we turned to a complementary approach by using chemical reagents to manipulate ER Ca^{2+} release and/or uptake. We first treated TDP-43^{A315T} mutants with EGTA, a Ca^{2+} -specific

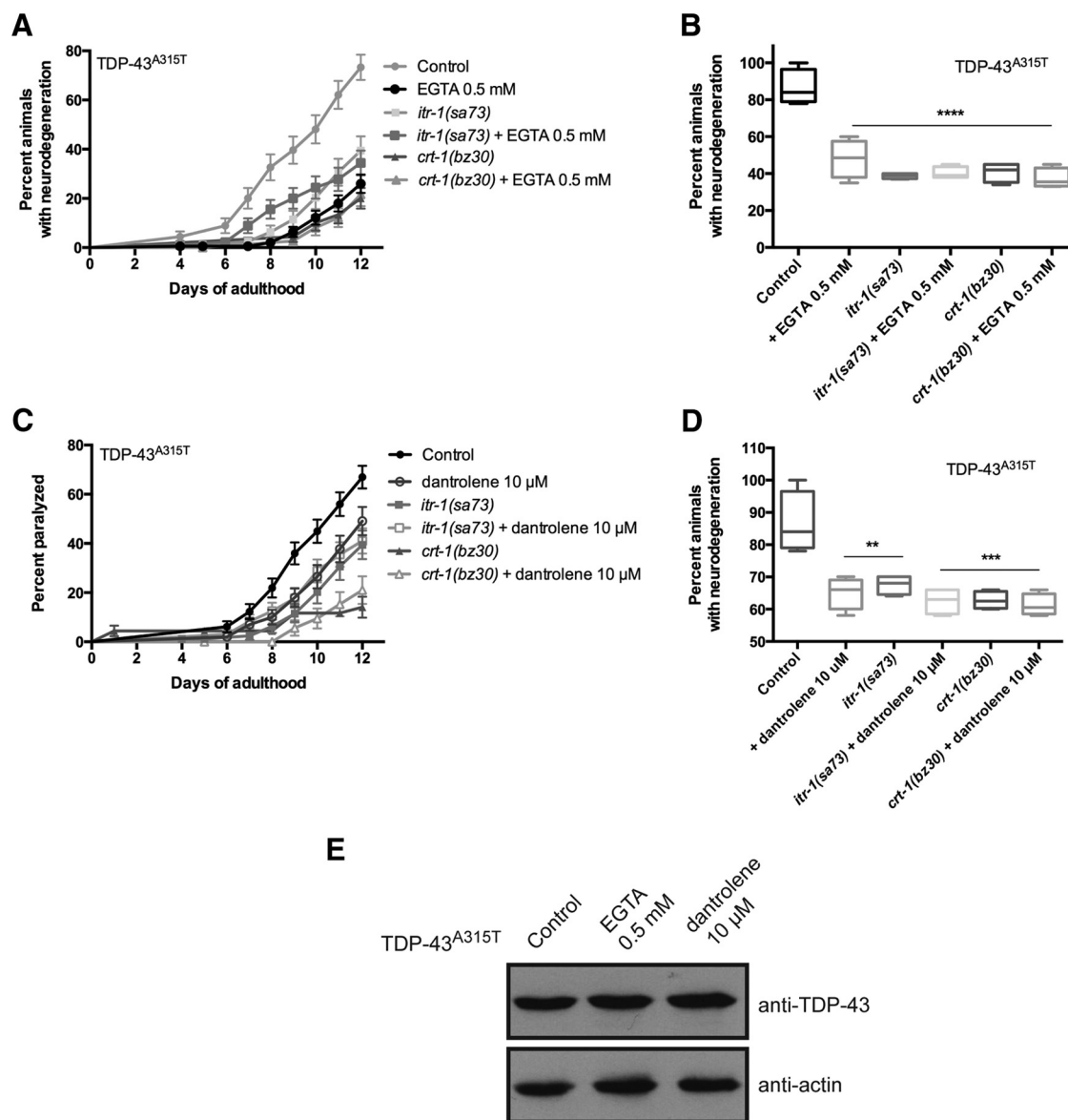


Figure 2. Pharmacological manipulation of $[Ca^{2+}]_i$ reduces TDP-43 neuronal toxicity. **A**, TDP-43^{A315T} transgenics treated with EGTA showed significantly less paralysis compared with untreated controls ($p < 0.0001$ versus TDP-43^{A315T}). The protective effect of EGTA was not additive to the suppression of TDP-43-mediated paralysis by mutation in either *crt-1* or *itr-1*. $p = 0.8470$ versus TDP-43^{A315T}; *crt-1(bz30)*; and $p = 0.7817$ versus TDP-43^{A315T}; *itr-1(sa73)*. TDP-43^{A315T}, $n = 90$; TDP-43^{A315T} + EGTA, $n = 181$; TDP-43^{A315T}; *itr-1(sa73)*, $n = 90$; TDP-43^{A315T}; *itr-1(sa73)* + EGTA, $n = 90$; TDP-43^{A315T}; *crt-1(bz30)*, $n = 90$; TDP-43^{A315T}; *crt-1(bz30)* + EGTA, $n = 90$. **B**, Degeneration of motor neurons in TDP-43^{A315T} animals at day 9 of adulthood was reduced to comparable levels in TDP-43^{A315T} transgenics treated with EGTA alone or in combination with mutations in *crt-1* or *itr-1*. $****p < 0.0001$ versus TDP-43^{A315T} at day 9. **C**, Treatment with dantrolene suppressed TDP-43^{A315T}-mediated paralysis compared with untreated control animals ($p = 0.0031$ versus TDP-43^{A315T}). Suppression of TDP-43^{A315T}-mediated paralysis by *crt-1* or *itr-1* was not significantly different from these same mutant strains treated with dantrolene. TDP-43^{A315T}, $n = 114$; TDP-43^{A315T} + dantrolene, $n = 100$; TDP-43^{A315T}; *itr-1(sa73)*, $n = 88$; TDP-43^{A315T}; *itr-1(sa73)* + dantrolene, $n = 96$; TDP-43^{A315T}; *crt-1(bz30)*, $n = 90$; TDP-43^{A315T}; *crt-1(bz30)* + dantrolene, $n = 90$. **D**, Degeneration of motor neurons, in TDP-43^{A315T} animals at day 9 of adulthood was reduced to similar levels in TDP-43^{A315T} transgenics treated with dantrolene alone or in combination with mutations for *crt-1* or *itr-1*. $**p < 0.01$ versus TDP-43^{A315T} at day 9; $***p < 0.001$ versus TDP-43^{A315T} at day 9. **E**, TDP-43 protein expression was unchanged by culture conditions with EGTA or dantrolene.

chelator, and observed a clear reduction in the rate of paralysis and neurodegeneration compared with untreated TDP-43^{A315T} transgenics (Fig. 2*A,B*). Additionally, EGTA did not further suppress paralysis and neurodegeneration in *crt-1(bz30)*; TDP-43^{A315T} or *itr-1(sa73)*; TDP-43^{A315T} strains (Fig. 2*A,B*), suggesting that *crt-1*, *itr-1*, and EGTA use a common mechanism to reduce TDP-43 toxicity, namely reduced $[Ca^{2+}]_i$.

We next tested whether Ca^{2+} derived from ER stores might contribute to the progressive paralysis caused by mutant TDP-43. We treated TDP-43^{A315T} mutants with dantrolene, a reagent that specifically inhibits Ca^{2+} release from ER stores (Song et al.,

1993). In dantrolene-treated animals, paralysis and neurodegeneration were markedly reduced consistent with the hypothesis that ER Ca^{2+} stores contribute to TDP-43 neuronal toxicity (Fig. 2*C,D*). Dantrolene treatment did not further suppress paralysis and neurodegeneration phenotypes caused by TDP-43^{A315T} in *crt-1(bz30)* and *itr-1(sa73)* mutants, suggesting a shared mechanism of action (Fig. 2*C,D*). The suppression of TDP-43 toxicity by EGTA and dantrolene were not due to reduced transgene expression since similar levels of TDP-43 protein expression were detected by immunoblotting in treated and untreated TDP-43 transgenics (Fig. 2*E*).

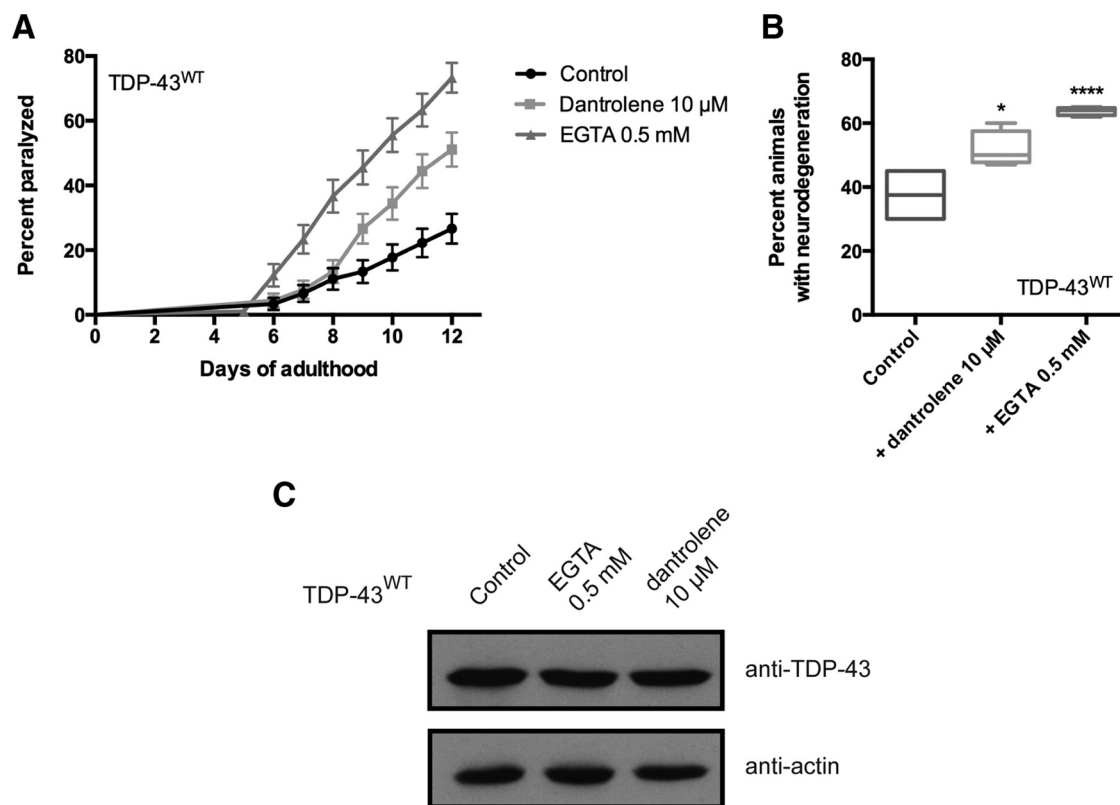


Figure 3. Disrupted Ca^{2+} homeostasis enhances wild-type TDP-43 toxicity. **A**, Transgenic worms expressing TDP-43^{WT} treated with either EGTA or dantrolene had increased rates of paralysis compared with untreated controls ($p < 0.01$ for dantrolene-treated worms versus untreated TDP-43^{WT} controls; $p < 0.0001$ for EGTA-treated worms versus untreated TDP-43^{WT} controls). TDP-43^{WT}, $n = 90$; TDP-43^{WT} + dantrolene, $n = 90$; TDP-43^{WT} + EGTA, $n = 90$. **B**, Treatment with dantrolene or EGTA increased neurodegeneration in adults on day 9; TDP-43^{WT} transgenics compared with untreated TDP-43^{WT} transgenics. * $p < 0.05$ versus TDP-43^{WT} at day 9, **** $p < 0.0001$ versus TDP-43^{WT} at day 9. **C**, Similar levels of TDP-43 proteins were detected by Western blotting in untreated TDP-43^{WT} transgenics compared with animals treated with EGTA or dantrolene.

We previously reported that worms expressing mutant TDP-43, but not wild-type TDP-43, show elevated ER and oxidative stress (Vaccaro et al., 2013). Ca^{2+} release and uptake is essential for normal cellular function, and we hypothesized that chemically manipulating $[\text{Ca}^{2+}]_i$ may only be beneficial to neurons expressing mutant TDP-43 if disrupted Ca^{2+} homeostasis is indeed an underlying mechanism of mutant TDP-43 toxicity. To explore this possibility, we tested transgenics expressing TDP-43^{WT} with EGTA or dantrolene, and observed that exposure to either compound greatly enhanced paralysis and neurodegeneration (Fig. 3). Thus, chemically manipulating $[\text{Ca}^{2+}]_i$ is beneficial only to neurons expressing mutant TDP-43 proteins.

Thapsigargin-induced ER Ca^{2+} release restores TDP-43^{A315T}-dependent cell death in the absence of calreticulin

We next explored whether forced ER Ca^{2+} release might overcome the *crt-1*-induced block on TDP-43-mediated paralysis and neurodegeneration. Here, we sought to reverse *crt-1*-dependent suppression of TDP-43 neuronal toxicity by driving release of the remaining ER Ca^{2+} stores in TDP-43^{A315T}; *crt-1(bz30)* animals. We treated TDP-43^{A315T}; *crt-1(bz30)* animals, which are fully suppressed for paralysis and neurodegeneration, with thapsigargin, a compound that inhibits the sarcoplasmic/endoplasmic reticulum Ca^{2+} ATPase (SERCA) ER Ca^{2+} reuptake pump and induces the release of ER Ca^{2+} via the InsP3 receptor channel (Takemura et al., 1989). We found that thapsigargin treatment significantly restored paralysis and neurodegeneration in TDP-43^{A315T}; *crt-1(bz30)* mutants compared with chemically untreated controls (Fig. 4A,B). As a positive control, we exposed

transgenics expressing TDP-43^{WT} to thapsigargin, and we observed the enhancement of paralysis and neurodegeneration phenotypes (Fig. 4A,B), suggesting that increased $[\text{Ca}^{2+}]_i$ induces cellular damage in *C. elegans*. Finally, using immunoblotting we confirmed that treatment with thapsigargin did not affect the expression of TDP-43 transgenics (Fig. 4C). In summary, these data suggest that the elevation of $[\text{Ca}^{2+}]_i$ itself may be cytotoxic in nematode motor neurons, supporting a model in which a critical rise in $[\text{Ca}^{2+}]_i$ is a causative factor in neurotoxicity, and that CRT-1 is not required for thapsigargin-induced cell death.

Calpain and aspartyl proteases are required for neurodegeneration in a *C. elegans* ALS model

Caspase-dependent apoptosis is a major mechanism promoting cell death in neurodegenerative diseases (Fuchs and Steller, 2011). To determine whether apoptosis was involved in TDP-43 toxicity, we disrupted the main executioner protease, caspase CED-3, which mediates programmed cell death in *C. elegans* (Ellis and Horvitz, 1986). We observed that *ced-3* was not required for paralysis or degenerative phenotypes induced by mutant TDP-43^{A315T} in motor neurons (Fig. 5A,B). Thus, having shown that genetic and pharmacological manipulation of $[\text{Ca}^{2+}]_i$ suppresses neurotoxic effects of TDP-43^{A315T} in motor neurons, and based on the “calpain–cathepsin” hypothesis described previously (Yamashima et al., 1998), we investigated aspartyl and calpain protease function in paralysis and neurodegeneration. There are 17 genes with similarity to calpain, 7 of which show significant identity to mammalian calpains (Syntichaki et al., 2002), and 7 aspartyl protease genes encoded in the *C. elegans*

genome (Tcherepanova et al., 2000). Based on previous work linking some of these genes to neurodegeneration in *C. elegans* (Syntichaki et al., 2002), as well as the availability of viable loss-of-function mutant strains, we focused on the Ca^{2+} -regulated calpain protease TRA-3 and the aspartyl protease ASP-4. Furthermore, *asp-4* has previously been identified as a modifier of α -synuclein toxicity in *C. elegans* (Qiao et al., 2008). Using null mutants for *tra-3* and *asp-4*, we scored for paralysis and neurodegeneration in strains expressing TDP-43^{A315T}. We observed a significant reduction in the rate of paralysis and the progressive degeneration of motor neurons for TDP-43^{A315T}; *tra-3(ok2207)* or TDP-43^{A315T}; *asp-4(ok2693)* animals compared with control TDP-43^{A315T} strains (Fig. 5*A,B*). To confirm that these calpain and aspartyl proteases acted downstream of elevated $[\text{Ca}^{2+}]_i$ to regulate mutant TDP-43 toxicity, we treated TDP-43^{A315T}; *tra-3(ok2207)* and TDP-43^{A315T}; *asp-4(ok2693)* strains with thapsigargin. We observed that thapsigargin treatment failed to restore TDP-43^{A315T}-induced paralysis and neurodegeneration when the calpain or aspartyl proteases were absent (Fig. 5*C,D*). These data suggest that *tra-3* and *asp-4* are essential for calcium-mediated neurotoxicity associated with mutant TDP-43, and that these proteases may be a terminal effector of neurodegeneration. Furthermore, TDP-43 transgene expression was not affected by mutations in *ced-3*, *tra-3*, or *asp-4* (Fig. 5*E*). We next wanted to determine whether the calpain–aspartyl protease pathway could be a target for small-molecule intervention against TDP-43 toxicity. Z-Val-Phe-CHO (MDL-28170) is a calpain inhibitor previously shown to suppress necrosis in *C. elegans* (Syntichaki et al., 2002). We observed a significant reduction of TDP-43^{A315T}-mediated paralysis in worms treated with MDL-28170 (Fig. 5*F*). These data suggest that calpain and aspartyl proteases may be targeted for preventing neurodegeneration associated with mutant ALS proteins.

Cell-autonomous suppression of TDP-43 toxicity by *tra-3* and *asp-4* in motor neurons

We wondered whether the regulation of TDP-43 toxicity was specific to *tra-3* and *asp-4*, or involved additional calpain and aspartyl proteases. Using RNAi, we conducted a blind screen of five calpain (*clp-1*, *clp-2*, *clp-4*, *clp-7*, and *tra-3*) and seven aspartyl (*asp-1*, *asp-3*, *asp-4*, *asp-6*, *asp-7*, *asp-10*, and *asp-13*) protease genes against TDP-43^{A315T} transgenics engineered for RNAi sensitivity only within the nervous system (Calixto et al., 2010). We observed that RNAi against only *tra-3* or *asp-4* significantly suppressed the paralysis phenotype of TDP-43^{A315T} transgenics (Fig.

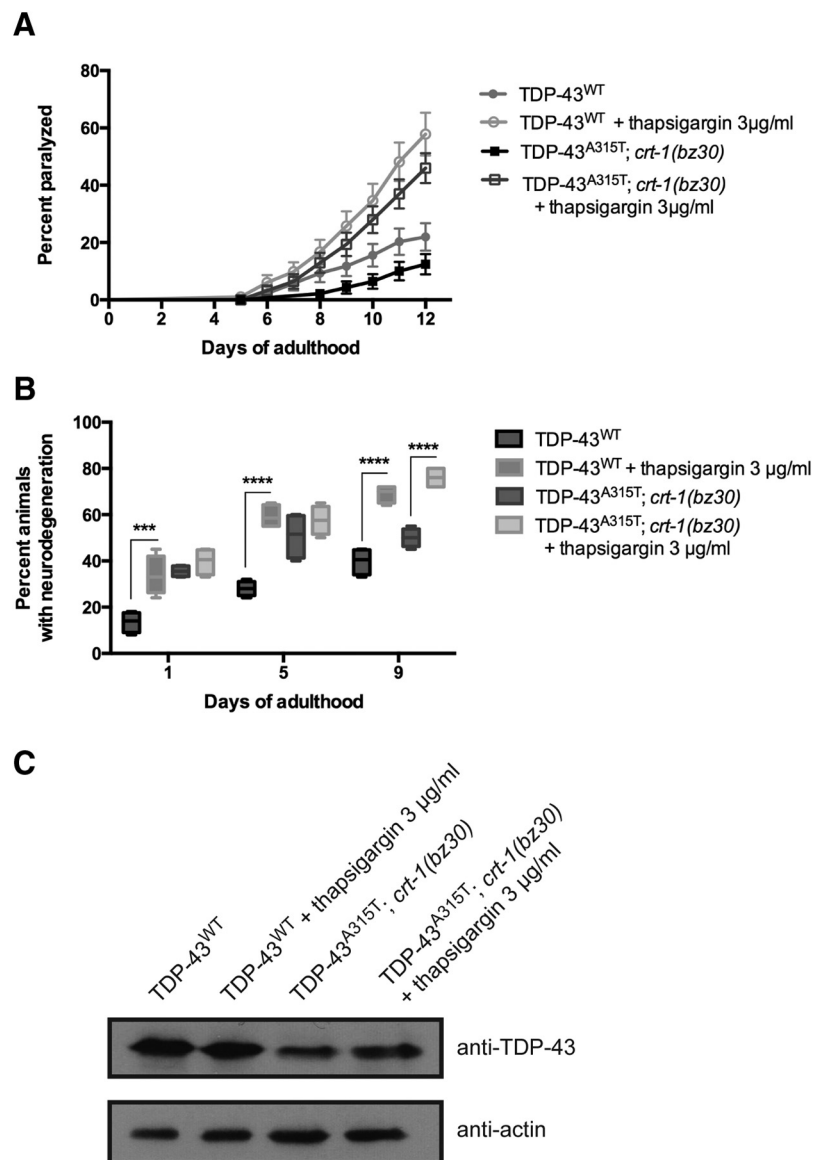


Figure 4. Forced release of ER Ca^{2+} stores enhances TDP-43 neuronal toxicity. **A**, Paralysis was enhanced in TDP-43^{A315T}; *crt-1(bz30)* and TDP-43^{WT} transgenics treated with thapsigargin compared with untreated transgenic controls. $p < 0.001$ for TDP-43^{A315T}; *crt-1(bz30)* animals versus those treated with thapsigargin; $p < 0.001$ for TDP-43^{WT} versus those treated with thapsigargin. TDP-43^{WT}, $n = 98$; TDP-43^{WT} + thapsigargin, $n = 95$; TDP-43^{A315T}; *crt-1(bz30)*, $n = 96$; TDP-43^{A315T}; *crt-1(bz30)* + thapsigargin, $n = 100$. **B**, Thapsigargin enhanced neurodegeneration transgenics expressing TDP-43^{WT} at days 1, 5, and 9 of adulthood compared with untreated controls. The suppression of neurodegeneration in TDP-43^{A315T}; *crt-1(bz30)* animals was lost by thapsigargin treatment in adult day 9 transgenics. *** $p < 0.001$ versus TDP-43^{WT} at day 1; **** $p < 0.0001$ versus TDP-43^{WT} or TDP-43^{A315T}; *crt-1(bz30)*. **C**, Thapsigargin did not affect TDP-43 protein expression in TDP-43^{WT} or TDP-43^{A315T} worms.

6*A,B*). In conjunction with our experiments using null mutants, our RNAi experiments suggest that the regulation of TDP-43^{A315T} toxicity is specific to *tra-3* and *asp-4*. We wondered whether the effects of *tra-3* and *asp-4* in mediating TDP-43^{A315T} motor defects were cell autonomous or cell nonautonomous. We conducted *tra-3* or *asp-4* RNAi experiments in TDP-43^{A315T} transgenics sensitized to RNAi only within intestinal cells or body wall muscle cells. We observed no significant reduction of paralysis by *tra-3* or *asp-4* RNAi targeted to intestinal or body wall muscle cells (Fig. 6*C,D*). These data suggest that motor defects and degenerative phenotypes caused by TDP-43^{A315T} require the activity of *tra-3* and *asp-4* in the nervous system, and are not likely to be influenced by protease activity in other tissues. Unfortun-

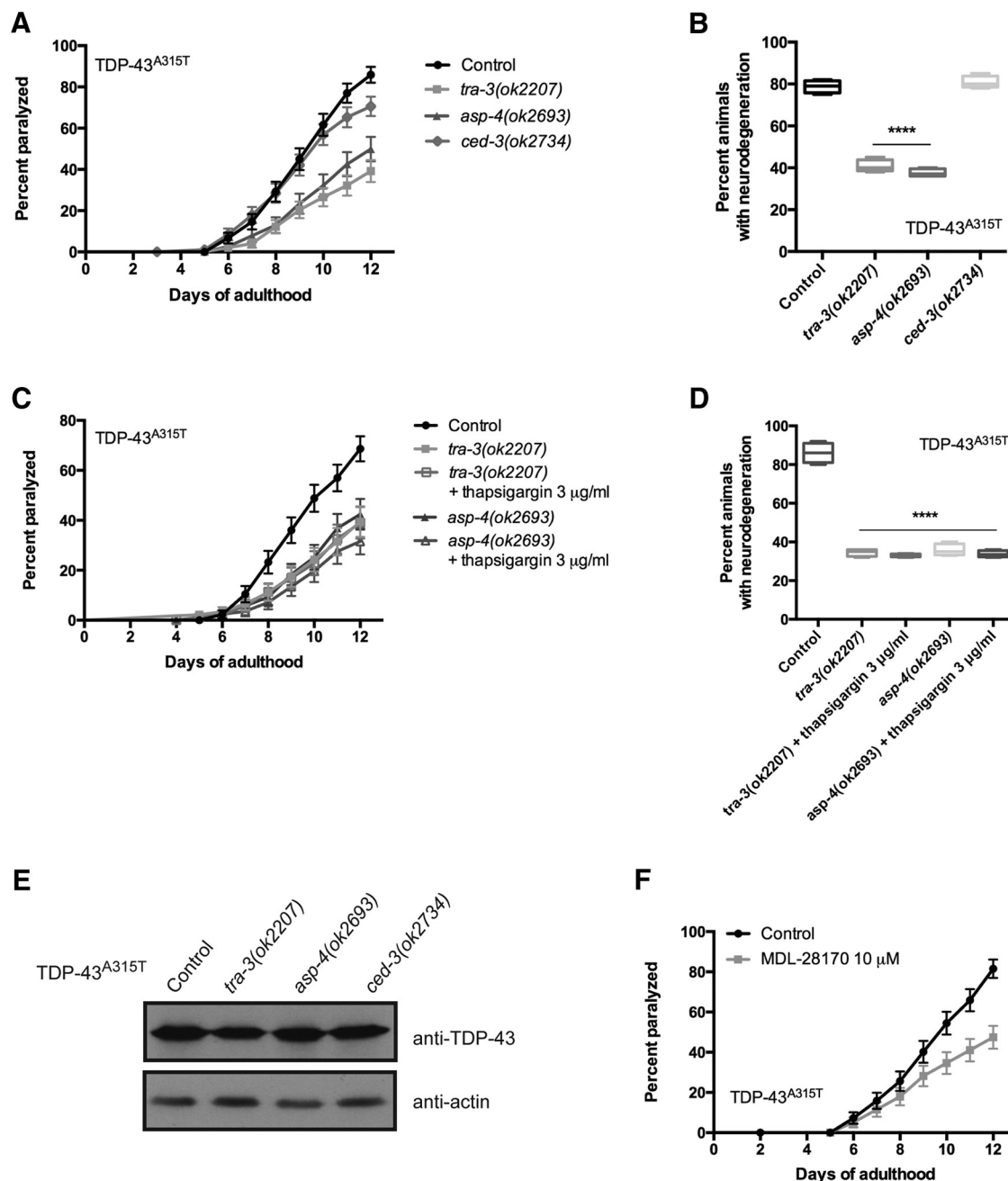


Figure 5. Calpain and aspartyl proteases facilitate TDP-43 neuronal toxicity. **A**, Null mutations in *tra-3* or *asp-4* suppress age-dependent paralysis in TDP-43^{A315T} transgenics compared with TDP-43^{A315T} controls. Mutation in *ced-3* had no significant effect on paralysis phenotypes compared with TDP-43^{A315T}. $p < 0.0001$ for TDP-43^{A315T}; *tra-3(ok2207)* or TDP-43^{A315T}; *asp-4(ok2693)* versus TDP-43^{A315T} transgenic controls. TDP-43^{A315T}, $n = 90$; TDP-43^{A315T}; *tra-3(ok2207)*, $n = 102$; TDP-43^{A315T}; *asp-4(ok2693)*, $n = 79$; TDP-43^{A315T}; *ced-3(ok2734)*, $n = 96$. **B**, Neurodegeneration was significantly reduced in adult, day 9, TDP-43^{A315T} transgenics by *tra-3* or *asp-4* null mutations compared with TDP-43^{A315T} alone. A null mutation of *ced-3* failed to suppress TDP-43^{A315T} neurodegeneration. **** $p < 0.0001$ versus TDP-43^{A315T} at day 9. **C**, The suppression of TDP-43^{A315T}-mediated paralysis by *tra-3* or *asp-4* was unaffected by the addition of thapsigargin. $p < 0.0001$ for TDP-43^{A315T} versus TDP-43^{A315T}; *tra-3(ok2207)* or TDP-43^{A315T}; *asp-4(ok2693)* with or without thapsigargin treatment. TDP-43^{A315T}, $n = 90$; TDP-43^{A315T}; *tra-3(ok2207)*, $n = 90$; TDP-43^{A315T}; *tra-3(ok2207)* + thapsigargin, $n = 90$; TDP-43^{A315T}; *asp-4(ok2693)*, $n = 90$; TDP-43^{A315T}; *asp-4(ok2693)* + thapsigargin, $n = 90$. **D**, Suppression of age-dependent neurodegeneration in TDP-43^{A315T} transgenics by *tra-3* or *asp-4* mutations was unchanged by thapsigargin treatment. **** $p < 0.0001$ versus TDP-43^{A315T} at day 9. **E**, Null mutations of *tra-3*, *asp-4*, or *ced-3* did not affect TDP-43 protein expression. **F**, The calpain inhibitor MDL-28170 reduced paralysis in TDP-43^{A315T} transgenics. $p < 0.001$ for treated versus untreated TDP-43^{A315T} animals. TDP-43^{A315T}, $n = 92$; TDP-43^{A315T} + MDL-28170, $n = 82$.

nately, we could not extend this analysis to Ca²⁺ homeostasis genes since *crt-1* and *itr-1* RNAi were ineffective in our assays.

Ca²⁺ homeostasis and protease genes do not suppress TDP-43^{WT} motor defects

Since our primary assay to identify neuroprotective agents depends on a behavioral assay to detect improved motility of TDP-

43^{A315T} transgenics, there is the possibility that we may have identified mutants that nonspecifically augment motility phenotypes. To rule this out, we turned to our TDP-43^{WT} strains that show limited toxicity, with paralysis phenotypes comparable to the expression of GFP alone (Vaccaro et al., 2012a). We crossed *itr-1(sa73)*, *unc-68(e540)*, *crt-1(bz30)*, *cnx-1(nr2010)*, *tra-3(ok2207)*, or *asp-4(ok2693)* mutations into the

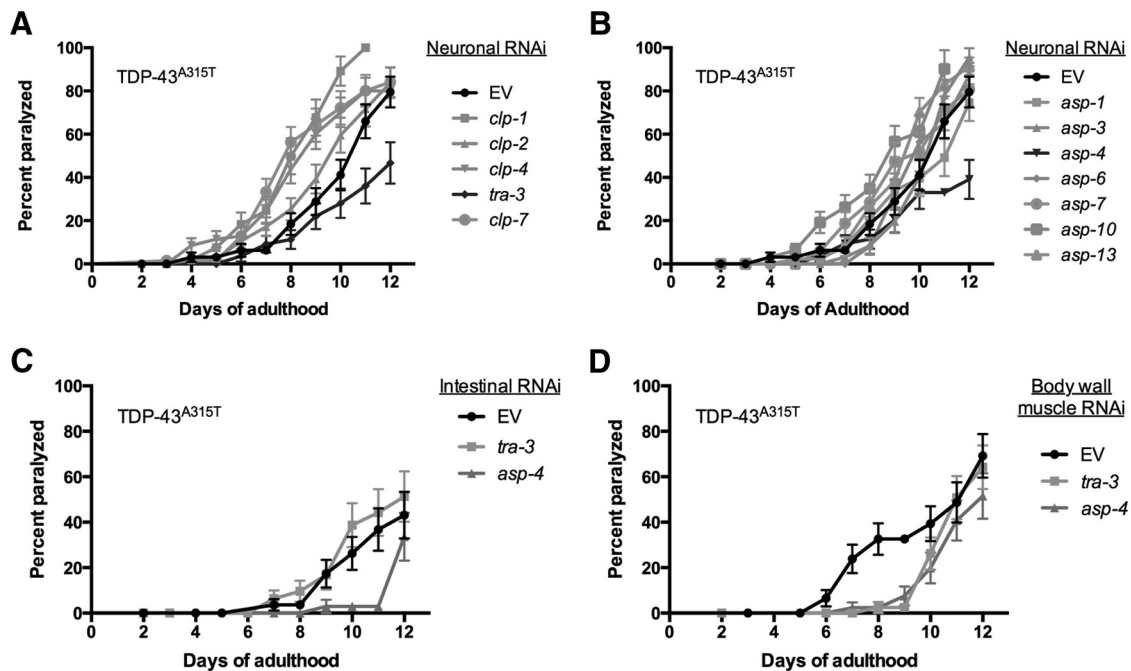


Figure 6. TDP-43-mediated motility defects require *tra-3* and *asp-4* in the nervous system. **A**, RNAi against *tra-3* suppressed TDP-43^{A315T}-mediated paralysis. $p < 0.05$ for TDP-43^{A315T} treated with *tra-3*(RNAi) versus TDP-43^{A315T} treated with EV control RNAi. TDP-43^{A315T} + EV, $n = 71$; TDP-43^{A315T} + *clp-1*(RNAi), $n = 71$; TDP-43^{A315T} + *clp-2*(RNAi), $n = 84$; TDP-43^{A315T} + *clp-4*(RNAi), $n = 79$; TDP-43^{A315T} + *tra-3*(RNAi), $n = 68$; TDP-43^{A315T} + *clp-7*(RNAi), $n = 69$. **B**, RNAi against *asp-4* suppressed TDP-43^{A315T}-mediated paralysis. $p < 0.05$ for TDP-43^{A315T} treated with *asp-4*(RNAi) versus TDP-43^{A315T} treated with EV control RNAi. TDP-43^{A315T} + EV, $n = 71$; TDP-43^{A315T} + *asp-1*(RNAi), $n = 54$; TDP-43^{A315T} + *asp-3*(RNAi), $n = 66$; TDP-43^{A315T} + *asp-4*(RNAi), $n = 67$; TDP-43^{A315T} + *asp-6*(RNAi), $n = 59$; TDP-43^{A315T} + *asp-7*(RNAi), $n = 62$; TDP-43^{A315T} + *asp-10*(RNAi), $n = 68$; TDP-43^{A315T} + *asp-13*(RNAi), $n = 58$. **C**, There were no significant differences in the rates of paralysis for TDP-43^{A315T} sensitized for intestine-specific RNAi by treatment with EV(RNAi), *tra-3*(RNAi), or *asp-4*(RNAi). TDP-43^{A315T} + EV, $n = 77$; TDP-43^{A315T} + *tra-3*(RNAi), $n = 54$; TDP-43^{A315T} + *asp-4*(RNAi), $n = 59$. **D**, There were no significant differences in the rates of paralysis for TDP-43^{A315T} sensitized for body wall muscle-specific RNAi by treatment with EV(RNAi), *tra-3*(RNAi), or *asp-4*(RNAi). TDP-43^{A315T} + EV, $n = 64$; TDP-43^{A315T} + *tra-3*(RNAi), $n = 51$; TDP-43^{A315T} + *asp-4*(RNAi), $n = 60$.

TDP-43^{WT} strain, but none of the mutations suppressed the paralysis phenotype caused by TDP-43^{WT} (Fig. 7). However, TDP-43^{WT}; *unc-68(e540)* animals had a higher rate of paralysis compared with TDP-43^{WT} controls ($p < 0.05$), suggesting that a general impairment of UNC-68 function may negatively impact the neuronal function and motility observed in TDP-43^{WT} worms. Thus, we conclude that neuroprotective effects of these mutants against TDP-43^{A315T} toxicity are not due to a general improvement of motor function.

Discussion

Ca²⁺ homeostasis and ALS

Ca²⁺ is an intracellular signaling molecule that regulates many mechanisms in the nervous system (Nikolopoulou and Tavernarakis, 2012). Cells maintain a tightly controlled resting cytosolic free calcium concentration of ~100 nM by extruding excess Ca²⁺ by pumps and exchangers, and by compartmentalizing Ca²⁺. The ER is involved in many critical processes, including being a specialized Ca²⁺-storing organelle (100–800 μ M range). The ER is closely involved in the regulation of Ca²⁺ flow within cells and is found in all neurons, occupying cell bodies, and extending toward axons, dendrites, and dendritic spines. In the context of ALS, evidence is mounting that the capacity of the cellular machinery of the ER to properly fold proteins is exceeded (Hetz and Mollereau, 2014), leading cells to react with the UPR^{ER} and that a perturbation of the ER function can induce Ca²⁺ depletion. Studies investigating Ca²⁺

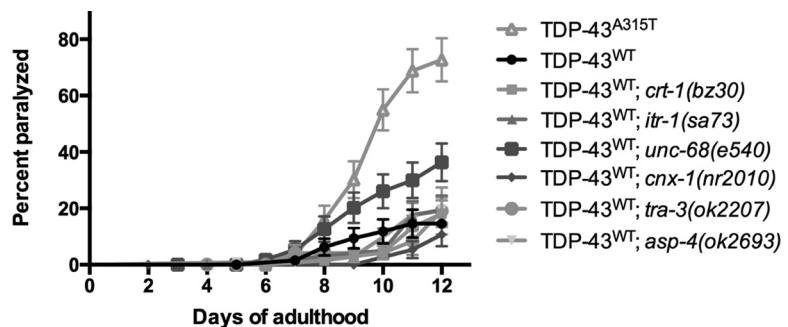


Figure 7. Calcium homeostasis and protease genes do not suppress motility defects in TDP-43^{WT} animals. There was no significant suppression of TDP-43^{WT} motility defects by Ca²⁺ or protease gene mutations. $p < 0.001$ for TDP-43^{A315T} versus TDP-43^{WT}. TDP-43^{A315T}, $n = 81$; TDP-43^{WT}, $n = 65$; TDP-43^{WT}; *crt-1(bz30)*, $n = 71$; TDP-43^{WT}; *itr-1(sa73)*, $n = 71$; TDP-43^{WT}; *unc-68(e540)*, $n = 60$; TDP-43^{WT}; *cnx-1(nr2010)*, $n = 61$; TDP-43^{WT}; *tra-3(ok2207)*, $n = 71$; TDP-43^{WT}; *asp-4(ok2693)*, $n = 115$.

homeostasis in motor neurons have shown that ALS-vulnerable motor neurons in mice display low endogenous Ca²⁺ buffering capacities (Lips and Keller, 1998; Palecek et al., 1999). We hypothesized that dysregulated [Ca²⁺]_i, possibly from the release of ER Ca²⁺ stores, may contribute to mutant TDP-43 neuronal toxicity.

We tested for potential influences of Ca²⁺ in mutant TDP-43^{A315T}-induced degeneration in the following two ways: with genetic mutations that alter release of ER Ca²⁺ stores; and by using chemical reagents to manipulate ER Ca²⁺ release (Fig. 8). We found that null mutations in *crt-1*, a molecular chaperone that plays a critical and complex role in cellular calcium homeostasis as a major site for stored Ca²⁺ (Michalak et al., 1999), suppressed both paralysis and neurodegeneration induced by

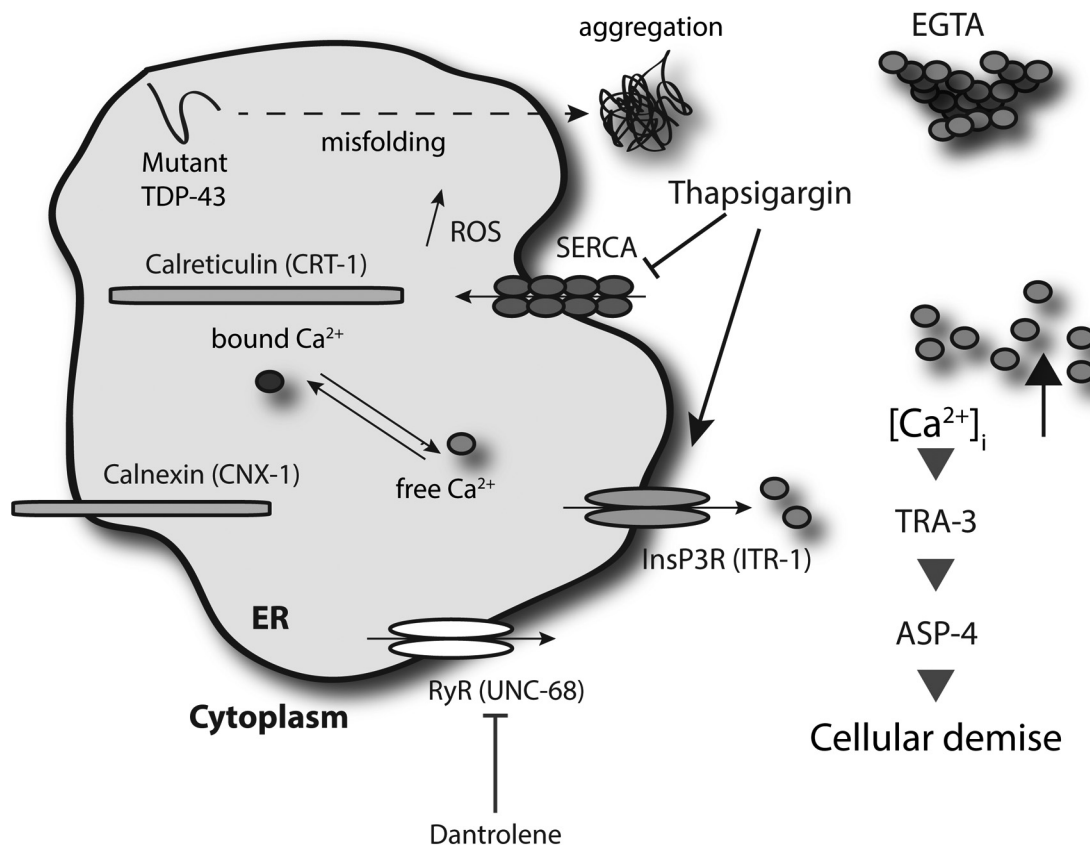


Figure 8. Working model for TDP-43 and Ca^{2+} -dependent necrosis-like neuronal toxicity. The chronic stress induced by protein misfolding and aggregation of mutant TDP-43 proteins may lead to inappropriate release of Ca^{2+} from ER stores into the cytoplasm. The resultant $[\text{Ca}^{2+}]_i$ increase is essential for downstream events, including activation of the Ca^{2+} -regulated TRA-3 calpain protease, which in turn mediates leakage of killer aspartyl proteases (ASP-4), leading to neuronal dysfunction and cell death. Mutations affecting ER Ca^{2+} storage (calreticulin and calnexin) or ER calcium release (InsP3R and RyR calcium release channels) disrupt release and are therefore neuroprotective. Pharmacological reduction of $[\text{Ca}^{2+}]_i$ by EGTA or dantrolene is also neuroprotective, while a forced increase of $[\text{Ca}^{2+}]_i$ by thapsigargin enhances neuronal toxicity. Disabling the activity of calpain or aspartyl proteases also protects against TDP-43-associated neuronal dysfunction and degeneration.

mutant TDP-43. Dysregulation of the ER-resident Ca^{2+} binding protein calreticulin may directly contribute to motor neuron death in ALS models (Bernard-Marissal et al., 2012). Our data showing that calreticulin contributes to neurodegeneration is somewhat at odds with findings for an SOD-1 model showing that reduced calreticulin levels activate the FAS/CD95 pathway to trigger cell death (Bernard-Marissal et al., 2012). However, no clear ortholog of FAS/CD95 exists in the *C. elegans* genome, suggesting that the role of calreticulin in mediating TDP-43 neuronal toxicity in our study may follow different cellular mechanisms. Alternatively, the mechanisms governing the degradation of SOD1 proteins may be distinct from TDP-43 (Mulligan and Chakrabarty, 2013).

However, ER stress has emerged as a mechanism in ALS (Matus et al., 2013; Tadic et al., 2014), and has been linked to the motor neuron vulnerability observed in SOD-1 mouse models (Nishitoh et al., 2008; Saxena et al., 2009), but it remains to be seen whether the ER is a site of action for other ALS mouse models. Furthermore, many aspects of the genetic signaling pathways controlling ER stress response were discovered in *C. elegans* and are conserved in mammalian systems (Mori, 2009). Encouragingly, we previously linked the ER stress response to TDP-43 toxicity (Vaccaro et al., 2013), and identified a number of small molecules that reduce neurodegeneration in *C. elegans* and zebrafish TDP-43 motor neuron models. Further insights into the induction of the ER stress response and neurodegeneration come

from a recent report using a *C. elegans* model of SOD1 neuronal toxicity (Thompson et al., 2014). Linking the model organism studies to mammals are the ER stress-protective compounds salubrinal (Saxena et al., 2009) and guanabenz (Jiang et al., 2014), both of which show neuroprotective activity in mouse SOD-1 models. Thus, work from *C. elegans* models may be predictive for mechanisms of motor neuron degeneration in mammalian systems.

Because luminal calreticulin works in conjunction with calnexin to effectuate chaperone functions and mediate cellular Ca^{2+} homeostasis (Krause and Michalak, 1997), we also disrupted calnexin function using loss-of-function mutations and confirmed the suppression of TDP-43 neuronal toxicity. It is known that Ca^{2+} is released from ER stores into the cytoplasm via the InsP3R and the RyR Ca^{2+} channels. We blocked the RyR function by using a null mutation in *unc-68* or by treatment with dantrolene, a reagent that specifically inhibits Ca^{2+} release from ER stores (Song et al., 1993), and InsP3R by using a null mutation in *itr-1*, and we showed the same suppression of TDP-43 toxicity. Thus, our data extend upon and are consistent with recent work showing that inositol triphosphate receptors regulate neurotoxicity in *Drosophila* and cell culture TDP-43 models (Kim et al., 2012). Further highlighting the role of Ca^{2+} homeostasis, treatment of TDP-43^{A315T} mutants with EGTA, a Ca^{2+} -specific chelator, produced a clear reduction of paralysis and neurodegeneration phenotypes. Importantly, the fact that nei-

ther dantrolene nor EGTA enhanced TDP-43 toxicity in TDP-43^{A315T}; *crt-1* or TDP-43^{A315T}; *itr-1* double mutants suggests that the inappropriate release of Ca²⁺ from ER stores may be a common mechanism of TDP-43-mediated neuronal toxicity. Conversely, thapsigargin-induced ER Ca²⁺ release, by activating the InsP3R function and blocking the Ca²⁺ return to the ER from the cytoplasm via the SERCA Ca²⁺ pump, can restore TDP-43^{A315T}-induced cell death in the absence of calreticulin, indicating that Ca²⁺ release and uptake are essential for TDP-43^{A315T} neuronal toxicity, and can in fact also enhance the toxicity of worms expressing TDP-43^{WT} in motor neurons.

The role of endogenous TDP-1/TDP-43 in neurodegeneration

Our group (Vaccaro et al., 2012b), plus another research team (Zhang et al., 2012), previously reported that endogenous TDP-1 (*C. elegans* ortholog of TDP-43) is required for toxicity caused by the transgenic expression of mutant TDP-43 in the *C. elegans* nervous system. Additionally, we also showed that TDP-1/TDP-43 is required for the toxicity of mutant polyglutamine proteins in *C. elegans* and mammalian cell culture models of Huntington's disease (Tauffenberger et al., 2013). These findings suggest that wild-type TDP-1/TDP-43 may actively contribute to neurodegeneration beyond ALS. Our previous work also showed that *tdp-1* is ubiquitously expressed, and is mainly a nuclear protein. Under stress conditions, including ER stress, TDP-1 expression is increased, and this chronic, elevated expression is cytotoxic, leading to decreased lifespan in worms (Vaccaro et al., 2012b). These observations are consistent with the function of TDP-43 as a stress-inducible protein, as is seen in many systems (Janssens and Van Broeckhoven, 2013). Another conserved phenotype of TDP-43 is its cytotoxicity when overexpressed, suggesting that its expression levels are tightly regulated (Buratti and Baralle, 2011). A caveat of our data interpretation in this current study is that a role for TDP-1 in the necrosis-like degeneration of TDP-43^{A315T} motor neurons was not examined. Part of the cascade of molecular events described here leading to neurodegeneration may involve endogenous TDP-1. The cytotoxicity of TDP-1 itself may depend on Ca²⁺ homeostasis and/or protease genes. Additionally, since TDP-1 is a DNA/RNA binding protein, another possibility is that TDP-1 may regulate the expression of Ca²⁺ and protease genes under stress conditions, including for proteotoxicity and ER stress. Future studies will explore the contribution of TDP-1 to these molecular mechanisms.

Necroptosis as a key mechanism of neurodegeneration in ALS

The perturbation of cytosolic Ca²⁺ homeostasis has been implicated in necrotic cell death both in mammals and in *C. elegans* (Sattler and Tymianski, 2000; Xu et al., 2001), but the mechanism by which Ca²⁺ triggers cellular demise remains unclear; so, we investigated relevant signaling pathways based upon the "calpain–cathepsin hypothesis." In 1998, Yamashima et al. formulated the calpain–cathepsin hypothesis, according to which Ca²⁺-activated cysteine proteases compromise the integrity of the lysosome and cause leakage of acidic hydrolases (Yamashima et al., 1998). We tested the requirement for calpain and aspartyl protease activity in neurodegeneration inflicted by the expression of TDP-43^{A315T} in GABAergic motor neurons, and showed that null mutations in the calcium-regulated *tra-3* calpain protease and aspartyl protease *asp-4* suppress both paralysis and neurodegeneration. Interestingly, TDP-43^{A315T} toxicity was unaffected by a null mutation in the cysteine–aspartate protease CED-3, a protein central to apoptosis in *C. elegans*, and in agreement with previous studies of TDP-43 toxicity in *C. elegans* (Liachko et al.,

2010). Thus, in terms of genetic signaling pathways the neuronal toxicity caused by TDP-43^{A315T} in *C. elegans* more closely resembles necrosis than classic apoptosis (Troulinaki and Tavernarakis, 2012).

Recent work has suggested that motor neuron death in models of both sporadic and familial ALS occurs through necroptosis (Re et al., 2014), a form of programmed necrosis that does not require caspases (Ofengeim and Yuan, 2013). Our work is in agreement with this notion as inactivation of a *C. elegans* key executioner caspase, *ced-3*, had no effect on motor neuron dysfunction in our TDP-43 models. Key molecules regulating necroptosis in ALS models include the receptor-interacting serine/threonine-protein kinase 1 and mixed-lineage kinase domain-like, but whether orthologs of these proteins regulate TDP-43 toxicity in our *C. elegans* ALS models requires further investigation. Importantly, work from *C. elegans* detailing programmed necrosis may shed light on mechanisms relevant to neurodegeneration in mammalian settings and perhaps specifically ALS.

Abnormal Ca²⁺ signaling has been linked to multiple neurological disorders, but the challenge remains in identifying disease-specific mechanisms (Bezprozvanny, 2009). We propose that the chronic stress induced by misfolded mutant TDP-43 proteins induces the inappropriate release of Ca²⁺ from ER stores into the cytoplasm is a trigger for subsequent neurodegeneration (Fig. 8). Disrupted Ca²⁺ homeostasis may have multiple downstream, effector mechanisms promoting neuronal dysfunction and cell death, including the inappropriate activation of the Ca²⁺-dependent proteases identified here, disrupting mitochondrial activity (Tradewell et al., 2011; Parone et al., 2013), or altered Ca²⁺ signaling at the neuromuscular junction (Armstrong and Drapeau, 2013). Thus, restoration of Ca²⁺ homeostasis in ALS motor neurons and/or limiting programmed necrosis may be pursued as potential therapeutic interventions.

References

- Armstrong GA, Drapeau P (2013) Calcium channel agonists protect against neuromuscular dysfunction in a genetic model of TDP-43 mutation in ALS. *J Neurosci* 33:1741–1752. [CrossRef Medline](#)
- Bernard-Marissal N, Moumen A, Sunyach C, Pellegrino C, Dudley K, Henderson CE, Raoul C, Pettmann B (2012) Reduced calreticulin levels link endoplasmic reticulum stress and Fas-triggered cell death in motoneurons vulnerable to ALS. *J Neurosci* 32:4901–4912. [CrossRef Medline](#)
- Bezprozvanny I (2009) Calcium signaling and neurodegenerative diseases. *Trends Mol Med* 15:89–100. [CrossRef Medline](#)
- Blokhuys AM, Groen EJ, Koppers M, van den Berg LH, Pasterkamp RJ (2013) Protein aggregation in amyotrophic lateral sclerosis. *Acta Neuropathol* 125:777–794. [CrossRef Medline](#)
- Buratti E, Baralle FE (2011) TDP-43: new aspects of autoregulation mechanisms in RNA binding proteins and their connection with human disease. *FEBS J* 278:3530–3538. [CrossRef Medline](#)
- Burdakov D, Verkhratsky A (2006) Biophysical re-equilibration of Ca²⁺ fluxes as a simple biologically plausible explanation for complex intracellular Ca²⁺ release patterns. *FEBS Lett* 580:463–468. [CrossRef Medline](#)
- Calixto A, Chelur D, Topalidou I, Chen X, Chalfie M (2010) Enhanced neuronal RNAi in *C. elegans* using SID-1. *Nat Methods* 7:554–559. [CrossRef Medline](#)
- Dal Santo P, Logan MA, Chisholm AD, Jorgensen EM (1999) The inositol trisphosphate receptor regulates a 50-second behavioral rhythm in *C. elegans*. *Cell* 98:757–767. [CrossRef Medline](#)
- Ellis HM, Horvitz HR (1986) Genetic control of programmed cell death in the nematode *C. elegans*. *Cell* 44:817–829. [CrossRef Medline](#)
- Fuchs Y, Steller H (2011) Programmed cell death in animal development and disease. *Cell* 147:742–758. [CrossRef Medline](#)
- Hetz C, Mollereau B (2014) Disturbance of endoplasmic reticulum proteostasis in neurodegenerative diseases. *Nat Rev Neurosci* 15:233–249. [CrossRef Medline](#)
- Janssens J, Van Broeckhoven C (2013) Pathological mechanisms underlying TDP-43 driven neurodegeneration in FTL-ALS spectrum disorders. *Hum Mol Genet* 22:R77–R87. [CrossRef Medline](#)

- Jiang HW, Ren M, Jiang HZ, Wang J, Zhang J, Yin X, Wang SY, Qi Y, Wang XD, Feng HL (2014) Guanabenz delays the onset of disease symptoms, extends lifespan, improves motor performance and attenuates motor neuron loss in the SOD1 G93A mouse model of amyotrophic lateral sclerosis. *Neuroscience* 277C:132–138. [CrossRef Medline](#)
- Kabashi E, Valdmanis PN, Dion P, Spiegelman D, McConkey BJ, Vande Velde C, Bouchard JP, Lacomblez L, Pochigaeva K, Salachas F, Pradat PF, Camu W, Meininger V, Dupre N, Rouleau GA (2008) TARDBP mutations in individuals with sporadic and familial amyotrophic lateral sclerosis. *Nat Genet* 40:572–574. [CrossRef Medline](#)
- Kim SH, Zhan L, Hanson KA, Tibbetts RS (2012) High-content RNAi screening identifies the Type 1 inositol triphosphate receptor as a modifier of TDP-43 localization and neurotoxicity. *Hum Mol Genet* 21:4845–4856. [CrossRef Medline](#)
- Krause KH, Michalak M (1997) Calreticulin. *Cell* 88:439–443. [CrossRef Medline](#)
- Liachko NF, Guthrie CR, Kraemer BC (2010) Phosphorylation promotes neurotoxicity in a *Caenorhabditis elegans* model of TDP-43 proteinopathy. *J Neurosci* 30:16208–16219. [CrossRef Medline](#)
- Lips MB, Keller BU (1998) Endogenous calcium buffering in motoneurons of the nucleus hypoglossus from mouse. *J Physiol* 511:105–117. [CrossRef Medline](#)
- Martin JB (1999) Molecular basis of the neurodegenerative disorders. *N Engl J Med* 340:1970–1980. [CrossRef Medline](#)
- Marion EB, Coronado R, Anderson P (1996) unc-68 encodes a ryanodine receptor involved in regulating *C. elegans* body-wall muscle contraction. *J Cell Biol* 134:885–893. [CrossRef Medline](#)
- Matus S, Valenzuela V, Medinas DB, Hetz C (2013) ER dysfunction and protein folding stress in ALS. *Int J Cell Biol* 2013:674751. [CrossRef Medline](#)
- Michalak M, Corbett EF, Mesaeli N, Nakamura K, Opas M (1999) Calreticulin: one protein, one gene, many functions. *Biochem J* 344:281–292. [CrossRef Medline](#)
- Mori K (2009) Signalling pathways in the unfolded protein response: development from yeast to mammals. *J Biochem* 146:743–750. [CrossRef Medline](#)
- Mulligan VK, Chakrabarty A (2013) Protein misfolding in the late-onset neurodegenerative diseases: common themes and the unique case of amyotrophic lateral sclerosis. *Proteins* 81:1285–1303. [CrossRef Medline](#)
- Nikolotopoulou V, Tavernarakis N (2012) Calcium homeostasis in aging neurons. *Front Genet* 3:200. [CrossRef Medline](#)
- Nishitoh H, Kadowaki H, Nagai A, Maruyama T, Yokota T, Fukutomi H, Noguchi T, Matsuzawa A, Takeda K, Ichijo H (2008) ALS-linked mutant SOD1 induces ER stress- and ASK1-dependent motor neuron death by targeting Delrin-1. *Genes Dev* 22:1451–1464. [CrossRef Medline](#)
- Ofengeim D, Yuan J (2013) Regulation of RIP1 kinase signalling at the crossroads of inflammation and cell death. *Nat Rev Mol Cell Biol* 14:727–736. [CrossRef Medline](#)
- Palecek J, Lips MB, Keller BU (1999) Calcium dynamics and buffering in motoneurons of the mouse spinal cord. *J Physiol* 520:485–502. [CrossRef Medline](#)
- Parone PA, Da Cruz S, Han JS, McAlonis-Downes M, Vetto AP, Lee SK, Tseng E, Cleveland DW (2013) Enhancing mitochondrial calcium buffering capacity reduces aggregation of misfolded SOD1 and motor neuron cell death without extending survival in mouse models of inherited amyotrophic lateral sclerosis. *J Neurosci* 33:4657–4671. [CrossRef Medline](#)
- Qiao L, Hamamichi S, Caldwell KA, Caldwell GA, Yacoubian TA, Wilson S, Xie ZL, Speake LD, Parks R, Crabtree D, Liang Q, Crimmins S, Schneider L, Uchiyama Y, Iwatsubo T, Zhou Y, Peng L, Lu Y, Standaert DG, Walls KC, et al. (2008) Lysosomal enzyme cathepsin D protects against alpha-synuclein aggregation and toxicity. *Mol Brain* 1:17. [CrossRef Medline](#)
- Re DB, Le Verche V, Yu C, Amoroso MW, Politi KA, Phani S, Ikiz B, Hoffmann L, Koolen M, Nagata T, Papadimitriou D, Nagy P, Mitsumoto H, Kariya S, Wichterle H, Henderson CE, Przedborski S (2014) Necroptosis drives motor neuron death in models of both sporadic and familial ALS. *Neuron* 81:1001–1008. [CrossRef Medline](#)
- Renton AE, Chiò A, Traynor BJ (2014) State of play in amyotrophic lateral sclerosis genetics. *Nat Neurosci* 17:17–23. [CrossRef Medline](#)
- Sattler R, Tymianski M (2000) Molecular mechanisms of calcium-dependent excitotoxicity. *J Mol Med* 78:3–13. [CrossRef Medline](#)
- Saxena S, Cabuy E, Caroni P (2009) A role for motoneuron subtype-selective ER stress in disease manifestations of FALS mice. *Nat Neurosci* 12:627–636. [CrossRef Medline](#)
- Song SK, Karl IE, Ackerman JJ, Hotchkiss RS (1993) Increased intracellular Ca²⁺: a critical link in the pathophysiology of sepsis? *Proc Natl Acad Sci U S A* 90:3933–3937. [CrossRef Medline](#)
- Stiernagle T (2006) Maintenance of *C. elegans*. *WormBook*:1–11. [Medline](#)
- Syntichaki P, Xu K, Driscoll M, Tavernarakis N (2002) Specific aspartyl and calpain proteases are required for neurodegeneration in *C. elegans*. *Nature* 419:939–944. [CrossRef Medline](#)
- Tadic V, Prell T, Lautenschlaeger J, Grosskreutz J (2014) The ER mitochondrial calcium cycle and ER stress response as therapeutic targets in amyotrophic lateral sclerosis. *Front Cell Neurosci* 8:147. [CrossRef Medline](#)
- Takemura H, Hughes AR, Thastrup O, Putney JW Jr (1989) Activation of calcium entry by the tumor promoter thapsigargin in parotid acinar cells. Evidence that an intracellular calcium pool and not an inositol phosphate regulates calcium fluxes at the plasma membrane. *J Biol Chem* 264:12266–12271. [Medline](#)
- Tauffenberger A, Chitramuthu BP, Bateman A, Bennett HP, Parker JA (2013) Reduction of polyglutamine toxicity by TDP-43, FUS and progranulin in Huntington's disease models. *Hum Mol Genet* 22:782–794. [CrossRef Medline](#)
- Tcherepanova I, Bhattacharyya L, Rubin CS, Freedman JH (2000) Aspartic proteases from the nematode *Caenorhabditis elegans*. Structural organization and developmental and cell-specific expression of asp-1. *J Biol Chem* 275:26359–26369. [CrossRef Medline](#)
- Thompson ML, Chen P, Yan X, Kim H, Borom AR, Roberts NB, Caldwell KA, Caldwell GA (2014) TorsinA rescues ER-associated stress and locomotive defects in *C. elegans* models of ALS. *Dis Model Mech* 7:233–243. [CrossRef Medline](#)
- Tradewell ML, Cooper LA, Minotti S, Durham HD (2011) Calcium dysregulation, mitochondrial pathology and protein aggregation in a culture model of amyotrophic lateral sclerosis: mechanistic relationship and differential sensitivity to intervention. *Neurobiol Dis* 42:265–275. [CrossRef Medline](#)
- Troulinaki K, Tavernarakis N (2012) Endocytosis and intracellular trafficking contribute to necrotic neurodegeneration in *C. elegans*. *EMBO J* 31:654–666. [CrossRef Medline](#)
- Vaccaro A, Tauffenberger A, Aggad D, Rouleau G, Drapeau P, Parker JA (2012a) Mutant TDP-43 and FUS cause age-dependent paralysis and neurodegeneration in *C. elegans*. *PLoS One* 7:e31321. [CrossRef Medline](#)
- Vaccaro A, Tauffenberger A, Ash PE, Carlomagno Y, Petrucelli L, Parker JA (2012b) TDP-1/TDP-43 regulates stress signaling and age-dependent proteotoxicity in *Caenorhabditis elegans*. *PLoS Genet* 8:e1002806. [CrossRef Medline](#)
- Vaccaro A, Patten SA, Aggad D, Julien C, Maios C, Kabashi E, Drapeau P, Parker JA (2013) Pharmacological reduction of ER stress protects against TDP-43 neuronal toxicity in vivo. *Neurobiol Dis* 55:64–75. [CrossRef Medline](#)
- Vanselow BK, Keller BU (2000) Calcium dynamics and buffering in oculomotor neurons from mouse that are particularly resistant during amyotrophic lateral sclerosis (ALS)-related motoneuron disease. *J Physiol* 525:433–445. [CrossRef Medline](#)
- von Lewinski F, Fuchs J, Vanselow BK, Keller BU (2008) Low Ca²⁺ buffering in hypoglossal motoneurons of mutant SOD1 (G93A) mice. *Neurosci Lett* 445:224–228. [CrossRef Medline](#)
- Walker AK, Atkin JD (2011) Stress signaling from the endoplasmic reticulum: a central player in the pathogenesis of amyotrophic lateral sclerosis. *IUBMB Life* 63:754–763. [CrossRef Medline](#)
- Wijesekera LC, Leigh PN (2009) Amyotrophic lateral sclerosis. *Orphanet J Rare Dis* 4:3. [CrossRef Medline](#)
- Xu K, Tavernarakis N, Driscoll M (2001) Necrotic cell death in *C. elegans* requires the function of calreticulin and regulators of Ca(2+) release from the endoplasmic reticulum. *Neuron* 31:957–971. [CrossRef Medline](#)
- Yamashita T, Kohda Y, Tsuchiya K, Ueno T, Yamashita J, Yoshioka T, Komimami E (1998) Inhibition of ischaemic hippocampal neuronal death in primates with cathepsin B inhibitor CA-074: a novel strategy for neuroprotection based on 'calpain-cathepsin hypothesis'. *Eur J Neurosci* 10:1723–1733. [CrossRef Medline](#)
- Zhang T, Hwang HY, Hao H, Talbot C Jr, Wang J (2012) *Caenorhabditis elegans* RNA-processing protein TDP-1 regulates protein homeostasis and life span. *J Biol Chem* 287:8371–8382. [CrossRef Medline](#)